

Hanno Schmiedt

Molecular Symmetry, Super-Rotation, and Semiclassical Motion

New Ideas for Solving Old Problems



Springer

Springer Series on Atomic, Optical, and Plasma Physics

Volume 97

Editor-in-chief

Gordon W.F. Drake, Windsor, Canada

Series editors

James Babb, Cambridge, USA

Andre D. Bandrauk, Sherbrooke, Canada

Klaus Bartschat, Des Moines, USA

Philip George Burke, Belfast, UK

Robert N. Compton, Knoxville, USA

Tom Gallagher, Charlottesville, USA

Charles J. Joachain, Bruxelles, Belgium

Peter Lambropoulos, Iraklion, Greece

Gerd Leuchs, Erlangen, Germany

Pierre Meystre, Tucson, USA

The Springer Series on Atomic, Optical, and Plasma Physics covers in a comprehensive manner theory and experiment in the entire field of atoms and molecules and their interaction with electromagnetic radiation. Books in the series provide a rich source of new ideas and techniques with wide applications in fields such as chemistry, materials science, astrophysics, surface science, plasma technology, advanced optics, aeronomy, and engineering. Laser physics is a particular connecting theme that has provided much of the continuing impetus for new developments in the field, such as quantum computation and Bose-Einstein condensation. The purpose of the series is to cover the gap between standard undergraduate textbooks and the research literature with emphasis on the fundamental ideas, methods, techniques, and results in the field.

More information about this series at <http://www.springer.com/series/411>

Hanno Schmiedt

Molecular Symmetry, Super-Rotation, and Semiclassical Motion

New Ideas for Solving Old Problems



Springer

Hanno Schmiedt
Institute of Physics I
University of Cologne
Cologne
Germany

ISSN 1615-5653 ISSN 2197-6791 (electronic)
Springer Series on Atomic, Optical, and Plasma Physics
ISBN 978-3-319-66070-7 ISBN 978-3-319-66071-4 (eBook)
DOI 10.1007/978-3-319-66071-4

Library of Congress Control Number: 2017949496

© Springer International Publishing AG 2017

This work is subject to copyright. All rights are reserved by the Publisher, whether the whole or part of the material is concerned, specifically the rights of translation, reprinting, reuse of illustrations, recitation, broadcasting, reproduction on microfilms or in any other physical way, and transmission or information storage and retrieval, electronic adaptation, computer software, or by similar or dissimilar methodology now known or hereafter developed.

The use of general descriptive names, registered names, trademarks, service marks, etc. in this publication does not imply, even in the absence of a specific statement, that such names are exempt from the relevant protective laws and regulations and therefore free for general use.

The publisher, the authors and the editors are safe to assume that the advice and information in this book are believed to be true and accurate at the date of publication. Neither the publisher nor the authors or the editors give a warranty, express or implied, with respect to the material contained herein or for any errors or omissions that may have been made. The publisher remains neutral with regard to jurisdictional claims in published maps and institutional affiliations.

Printed on acid-free paper

This Springer imprint is published by Springer Nature
The registered company is Springer International Publishing AG
The registered company address is: Gewerbestrasse 11, 6330 Cham, Switzerland

Preface

Describing molecules with mathematical methods has fascinated the scientific community for a long time. Nowadays, large computing facilities are available, and they are used for extremely precise calculations of molecular properties that can be investigated in experiments. Nevertheless, developments in experimental techniques are still challenging the theoretical predictions by their overwhelming accuracy. This book is at first place intended to show that away from an extensive use of computational techniques, the reflection onto the most fundamental property of many-body physics, namely symmetry, still leads to new insights into the wide field of molecular dynamics. The beauty of using simple algebraic methods even for the description of some of the most challenging problems in recent molecular research has excited me from the first day on. With this book, I hope to transfer this excitement to the reader and show that the theoretical work also on the foundations of molecular dynamics is still far from being completed.

Recent developments in experimental high-resolution spectroscopy have opened up very many new routes for the study of molecules [1]. For instance, ion-trap spectroscopy has become a versatile tool in studying ion–molecule reactions in a quantum-state resolved manner (see, e.g., [2] and references therein). This is used to analyze the reactions themselves but it also facilitates the characterization of molecular states of single ions, which are inaccessible to traditional spectroscopic methods. With this, the famous protonated methane, an “enfant terrible” ([3], p. 1) of molecular spectroscopy, has been precisely characterized only a few years ago [4]. Traditional theories encounter major problems in describing the respective dynamics since its extreme floppiness even at low temperatures makes it impossible to define any structure, which is traditionally the inevitable starting point for theories of molecular dynamics.

In addition to the above-described techniques, where stored ions are actually cooled to temperatures of a few Kelvin, other technologies have emerged to study molecules at the opposite side of energetic excitation: Optical centrifuges allow to control and study molecules in extremely high excited rotational states. For those states, quantum chemical calculations even with the most advanced algorithms are faced again with serious computing-time problems.

All these improvements brought up the question if using larger and larger computing facilities is in fact the “golden way” to tackle the problems of molecular theory. Or is it possible to step back and use the most fundamental properties of molecular dynamics to answer at least some of the questions arising from modern-day molecular spectroscopy?

This book is intended to review some of these questions and actually presents a clear answer to this question: We can in fact use basic symmetry considerations to achieve new answers to the questions of modern-day molecular spectroscopy. Reviewing and renewing parts of the foundations of molecular physics is worthwhile and can be used to circumvent—at least in a first step—the use of large computing facilities, even though the latter are still needed for more exact studies.

In general, this book has three parts: It aims to show how basic symmetry considerations help in (i) understanding selection rules in molecular reactions but also (ii) in the characterization of exotic molecules. Furthermore, ideas of classical mechanics are reformulated and attached to advanced quantum mechanical models to understand (iii) ultrafast rotating molecules. During the course of this work, various basic ideas of molecular symmetry and semi-classical treatments are presented. And, as a final goal, the book shows these basic concepts to answer some of the challenging problems of molecular spectroscopy. As one example of these answers, it shows the advent of a fundamentally new way of studying molecular rotation, the super-rotor model, which successfully describes the protonated methane molecule, which has been tackled by traditional theories for over 30 years. As a new model, it led to many controversial debates in the past few years, and this book is meant to set the stage for even more such discussions and, hopefully, for future work.

The results presented in this book are based on my Ph.D. work in the group of Stephan Schlemmer and on recent publications together with him, Per Jensen, and some of the people from the ExoMol group in London [5–9]. I want to thank all of them, especially Stephan Schlemmer, who was the most supportive Ph.D. supervisor one could imagine. In addition, I would like to thank his awesome group; without the numerous discussions with, e.g., the experts on ion-trap spectroscopy, this work would have been impossible. A very special thanks also to Anni who supported me at all times and cheered me up whenever I needed it. Indeed, I want to thank Monika, Helmut, and Jacob for everything they did for me in the last twenty-nine years. Not to forget all my friends and former colleagues who are playing an important role in getting me out of science from time to time. I must admit that I enjoy that very much.

The work starts with a general introduction, where also the structure of the rest of the book is outlined. Therefore, I postpone this to the first chapter and hope that the reader can enjoy the problems of molecular dynamics with as much fascination and fun as I had by working on them.

Cologne, Germany

Hanno Schmiedt

Contents

1	New Ideas for Solving Old Problems - An Introduction	1
Part I Group Theory in Molecular Physics		
2	Basic Concepts	9
2.1	Symmetry Groups of the Molecular Hamiltonian	9
2.1.1	General Representation Theory	11
2.1.2	Lie Groups and Permutation Groups	14
2.2	Zero-Order Models in Molecular Theory	18
2.2.1	The Separation of the Molecular Hamiltonian	19
2.2.2	The Zero-Order Models for Nuclear Motion	22
2.3	Connecting Dynamics and Group Theory – Outlook to This Work	25
3	Schur–Weyl Duality in Molecules	27
3.1	Nuclear Spin States in Molecules	27
3.1.1	The Natural Way	31
3.1.2	Unitary Symmetry	35
3.1.3	Permutation Symmetry	37
3.2	Schur–Weyl Duality	39
3.2.1	Application of the Duality Theorem	40
3.3	Conclusion	41
4	Reactive Collisions	45
4.1	Representation Theory in Reactions of Small Molecules	47
4.1.1	Mathematical Preliminaries	47
4.1.2	Single Molecules	49
4.1.3	A First Example	51

4.2	The $\text{H}_3^+ + \text{H}_2$ Reaction	53
4.2.1	A Restricted Symmetry Group for the Intermediate Complex	56
4.2.2	Implications for Experiments	59
4.2.3	The Deuterated Version	59
4.3	Discussion	62
Part II Extremely Floppy Molecules		
5	Introducing Extreme Floppiness	67
6	Symmetry Beyond Perturbation Theory	71
6.1	Representation Theory of Molecular Rotation	71
6.1.1	Example: The H_3^+ ion	81
6.2	The Failure of the Subgroup Picture	82
6.3	Concluding Remarks	86
7	The Molecular Super-Rotor	87
7.1	Large Amplitude Motion	87
7.2	Super-Rotation	91
7.2.1	The Energy Expression	93
7.2.2	Degrees of Freedom	94
8	Super-Rotor States and Their Symmetry	95
8.1	Five-Dimensional Rotor States	95
8.1.1	Parity and Dipole Selection Rules	99
8.2	Permutation-Inversion Symmetry	100
8.2.1	The Permutation Group of Five Identical Particles	102
8.3	Conclusion	105
9	Protonated Methane	107
9.1	The Molecule	107
9.2	The Experiment	109
9.3	The Model	111
9.4	The Discussion	115
10	Refinements and Further Applications	117
10.1	Beyond Zero-Order	117
10.1.1	Generalized Moments of Inertia	117
10.1.2	Higher-Order Terms	120
10.2	Additional Target Molecules	121
10.3	Concluding Remarks	123

Part III	Semi-classical Approach to Rotational Dynamics	
11	Ultrafast Rotation	127
11.1	Introduction	127
11.2	The Gutzwiller Trace Formula	129
11.3	The Rotational Energy Surface	136
11.3.1	The Paths on the Rotational Energy Surface	139
11.3.2	The Quantization Conditions	142
11.3.3	Two Approaches to Generate the Rotational Energy Surface	144
12	Application to Sulfur Dioxide	149
12.1	The Molecule	149
12.2	The Comparison	150
13	Discussion	155
13.1	The TROVE - Generated Rotational Energy Surface	155
13.2	Generalization of the Approach	156
14	New Ideas for Solving Old Problems – A Conclusion	159
References		163
Index		169

Chapter 1

New Ideas for Solving Old Problems - An Introduction

Abstract In this introductory chapter, a general view on the field of molecular dynamics and the main ideas of this book are presented. Furthermore, an outline of the rest of the book is shown by describing the contents of the three different parts.

If one sets up a length scale diagram for objects studied in the different fields of physics, molecules are located somewhere in between the single particle scales of nuclei or elementary particles and the macroscopic length scales of condensed matter (see Fig. 1.1). Correspondingly, this line of objects with increasing size can also be followed in the sense of an evolution: Elementary particles clump together to form nuclei, which together with electrons subsequently can form molecules. An aggregation of molecules can consequently be viewed as either forming liquids or, depending on structural properties, crystalline solids and other macroscopic forms of matter. Zooming into the length scales of single molecules, already there, notifiable differences occur. On the one hand side we find small molecules like the prominent water molecule, H_2O , and on the other hand there are all kinds of sugars, acids, or even DNA and proteins. A detailed understanding of the properties of single molecules of all sizes is obviously of great interest to the research community with influences on very different fields like organic and inorganic chemistry as well as biochemistry.

In this work, the main focus is on small molecules with at most ten nuclei. Apart from being the building blocks also for larger molecules, they are special in many different senses: First, they are found literally everywhere, in the human body, in earth's atmosphere as well as in the surrounding of the center of our galaxy. Secondly and maybe a little surprisingly, even though the number of particles is small, we find an enormous variety of dynamical properties. The latter are nowadays explored by spectroscopic techniques that reach astonishingly high resolutions. Experiments on diatomic molecules have shown that electric dipole transitions between molecular states can be recorded with an accuracy of $\Delta f/f \approx 10^{-9}$ [10, 11]. Therefore, theoretical models for the description of the internal dynamics must be extremely accurate in predicting these transitions and a lot of computational effort is required to accomplish this task.

Such highly precise measurements and accurate models are used not only to predict the dynamics of molecules in the laboratory but also in other environments with very different and even unknown conditions. One prominent respective example is the aforementioned interstellar space, where, e.g., temperature, densities, and

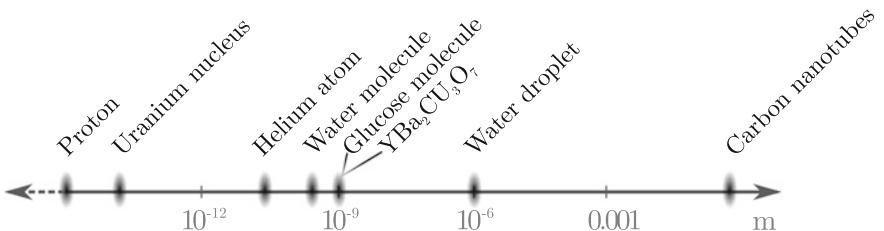


Fig. 1.1 Typical length scales of some of the objects studied in physics. Molecules, the topic of the present book, are located between the single particle scale of nuclei or atoms and the macroscopic length scales of long nanotubes or the unit cell diameter of crystalline superconductors like $\text{YBa}_2\text{Cu}_3\text{O}_7$. Already here, the difference in the dimensions of the water and the glucose molecule indicates the wide variety of objects of molecular spectroscopy

time-scales are much different from those in experiments. Nevertheless, by using observational studies, one tries to unambiguously identify certain molecules in various regions in space, where, e.g., astrochemical networks afterwards are used to explain the evolution of galaxies, planets or even exoplanetary atmospheres. These identification procedures need extremely precise predictions since the observed spectra are mostly extremely dense and slight changes in molecular parameters would lead to large uncertainties in the identification. Due to large efforts in high-resolution spectroscopy in the laboratories, astronomical observations were able to find (to date) about 180 molecules in very different conditions in space. The largest found molecules were recently the fullerenes C_{60} and C_{70} in young planetary nebula [12]. On the way to more complex molecules, molecules like ethanol [13] and, more recently, ether methyl ether, $\text{C}_2\text{H}_5\text{OCH}_3$, have been detected already but the search for larger and more complex molecules is still ongoing and a ‘hot topic’ in the astrophysical community.

In addition to the study of single molecules, molecular spectroscopy is also used to record reactions of molecules. In general, knowing reaction rates for small molecules are of large interest again in the astrochemical community, since respective reaction networks strongly depend on the accuracy of these parameters. Again using high-resolution methods, it is nowadays possible to follow the reaction processes on a quantum state resolved level. In particular, measurements are made to explain features of, e.g., reactive collisions in interstellar space, where very cold molecules collide and at most exchange a small portion of energy. Nevertheless, in this process, the internal properties of the colliding particles can change when concerning, e.g., their intrinsic spins.

In conclusion, studying small molecules with high-resolution experiments is obviously contributing a lot to the understanding of astrochemical processes. This is indeed only one of the various applications of molecular spectroscopy but a review of all possible relevant fields is beyond the scope of this work.

However, away from such implications of molecular spectroscopy to other topics of natural sciences, molecular physics itself represents a paradigmatic example of quantum mechanics. As such, molecular dynamics is a playground for testing

predictions from theories which are formed on a very abstract basis initially. One of the most famous examples is the ‘umbrella flipping’ motion in ammonia, NH_3 , which is predicted and explained by quantum mechanics. Another more recently studied example is protonated methane, where the concept of a classical structure must be abandoned completely since even at zero temperature, its wave function is highly delocalized.

In addition to these examples of how molecular dynamics is influenced by quantum theory, another important issue is the influence of general symmetry properties. The latter is used in both, classical and quantum theories to simplify or explain certain phenomena and again, molecular physics is one of the prototypical examples, where the influence of symmetry is hard to underestimate. In difference to elementary particle and condensed matter theory, molecules are described by the apparatus of representation theory of *finite* groups which is actually itself an active field of study in modern mathematics. Molecules form a formidable testing ground for some of the respective abstract theorems of group theory in general. One very basic example is the ortho- and para-form of molecular hydrogen, H_2 , the most simple molecule one can imagine. These forms are separable by symmetry: While in para hydrogen the two nuclear spins are coupled anti-symmetrically, in ortho-hydrogen they are interchangeable without any sign change of the molecular wave function. This fundamental difference leads to the strict statement from representation theory that both forms cannot be inter-converted by any electromagnetic radiation. This statement is validated by measurements, where exactly defined ratios of these forms are found. In cold reactions, both forms of molecular hydrogen actually behave as distinct chemical species which has large implications on the related reaction dynamics. Indeed, for larger molecules, the concept of separate spin configurations get more complex but with the help of representation theory is still achievable.

In the course of this work, we will discuss some of the aspects of how representation theory and molecular physics are correlated and find more examples, where influences of quantum mechanics and symmetry are not negligible for the description of molecular dynamics. Before going into the details, we start with formulating some of the fundamental assumptions, molecular physics is based on.

In describing inter- and intra-molecular dynamics, the most convenient starting point is actually to consider an almost static molecular structure, where the nuclei appear as the building parts and the electrons as bonds between them. Nuclear vibrations lead to small displacements of the nuclear coordinates and molecular rotation can be described as that of an almost rigid body. This rather intuitive view is extended by a perturbative approach, where non-rigid terms as well as rotation-vibrational (ro-vibrational) couplings are incorporated into the systems Hamiltonian. With this concept, a large number of molecules can be characterized by structural parameters and higher order equivalents. In particular, these constants give rise to a fingerprint spectrum of individual molecules which is used, e.g., to identify them in radio-astronomical observations of interstellar space.

Experimental laboratory spectroscopy is used to find these structural constants and hence to characterize the molecules as nearly static structures with a well-defined set of numbers indicating the higher order terms in the perturbation series.

However, technical developments have always been a trigger for extending traditional models and often led to the rejection of ideas which were thought to be universal. As experimental spectroscopy reaches higher and higher accuracies in frequency, many different deviations from this ball-and-stick picture emerge: For example, molecules are now known to possibly exhibit distinct low-energy structures that are interconvertible by only a small or even a vanishing portion of energy. Therefore, some molecules must be described in a superposition state of various isomeric geometries. The most renown example is the aforementioned ammonia molecule, where the nitrogen nucleus is imagined to be located “above” or “below” the plane of the three protons. These two possibilities are indistinguishable and hence the molecule must be described as a quantum object, where both structures are superimposed.

Although ammonia is treatable by an extended ball-and-stick model, [14] where both geometries are treated simultaneously, other molecules and conditions exist, where established molecular theory reaches limits which cannot be solved even by the power of modern computing facilities. If, e.g., the perturbation series converge very slowly, calculations become very expensive and most likely lack a clear physical interpretation. In this work, we discuss two examples of pathological cases where traditional theories tend to fail in a proper description of molecular dynamics:

- In **Part II** of this work, we discuss *extremely floppy molecules* in which the idea of a fixed geometrical structure must be totally abandoned due to numerous large amplitude vibrations. The latter are defined to exhibit nuclear displacements comparable to the linear dimension of the molecular equilibrium structure. One example is the already mentioned tunneling motion in the ammonia molecule. We start that part by a particular discussion of the symmetry of rotational states in molecules, and show certain limits of conventional rotational theory, when it comes to special but still relatively simple molecules [9]. In the subsequent chapters, we review the development of a fundamentally new model for the dynamics of extremely floppy molecules, where internal rotational motion and the overall rotation of the molecule are combined [6, 7]. We call this collective motion *super-rotation* and, in the tradition of theoretical physics, we find an underlying symmetry principle guiding to the formulation of an approximate model for the respective dynamics. It turns out that in contrast to more traditional studies of this class of molecules, this model provides a simple, analytical energy expression as well as the possibility to symmetry classify the according generalized rotational states in the molecular symmetry group. We furthermore show a comparison of this theory to recent experimental results on the dynamics of the prototypical example of extreme floppiness, protonated methane, CH_5^+ [4, 15]. By fitting a single parameter, our model provides a super-rotational energy spectrum that compares surprisingly well with the experimental results. We retrieve almost all energy levels with an accuracy of a few wave numbers,¹ and find the value of the free parameter close to results of existing ab-initio calculations. These encouraging results are used to outline

¹We use the spectroscopic wave number in units of reciprocal centimeters for the unit of energy throughout the text. 1 cm^{-1} is equivalent to a frequency of about 30 GHz and hence to an energy of approximately $2 \cdot 10^{-23} \text{ J}$, the energy of a single photon with a wavelength of one centimeter.

possible extensions of the model, and we discuss potential applications to various kinds of other molecules, summarized in Chap. 10.

- In **Part III**, we consider again rotational dynamics but on a different energy scale. Whereas protonated methane was measured at temperatures of a few Kelvin, rotational dynamics at high temperatures are posing a considerable challenge to traditional quantum mechanical calculations as well. These *ultrafast rotations* involve molecular states with a very large angular momentum quantum number. We demonstrate that they can be described properly in a semi-classical approach [16], where a path-integral based method is used to predict quantized energies without using expensive matrix diagonalization procedures. Once more symmetry is used to determine the paths which the classical rotation “vector” is allowed to follow under the restriction of quantized energies. Based on ideas from the 1990s (see, e.g., [17]), we further develop the theory of semi-classical rotation by applying it to a full quantum mechanical treatment of underlying nuclear vibrations. This induces an intuitive understanding of the rotational dynamics, even at high speed, in terms of a classical rotation. In addition, it provides a relatively fast method to calculate the respective energy levels. As a proof of principle, we use a relatively simple well-known molecule, namely sulfur dioxide, SO₂, for testing the method. It turns out that the provided energies are not yet accurate enough for spectroscopic needs, nevertheless, future refinements potentially lead to a better applicability and the possibility to study molecules with more peculiar behavior at these large rotational speeds. The latter includes for instance the coupling of the fast rotations to other degrees freedom.

In both parts of this work, symmetry is identified to be *the* combining element. We show it to be of crucial importance when traditional approaches reach their limits. Therefore, we start this work with the more general **Part I** on molecular symmetry, where we introduce the basic concepts for the later chapters. The mathematical details are kept at a minimum but sufficient level. We highlight certain parts in boxes and include examples throughout the work to render the text comprehensible also for readers yet unfamiliar with concepts like representation theory, Lie algebras and other parts of mathematical group theory. The more interested reader is referred to textbooks like [18, 19] for the mathematical part and to [14] for the application of group theory to molecules.

As one result of these general symmetry considerations, we show in Chap. 3 of Part I the application of the Schur–Weyl duality theorem, a well-known result of representation theory, to the nuclear spin states in molecules [8]. It enables us to simplify the calculation of the so-called nuclear spin statistical weights, responsible, e.g., for non-observable energy levels, forbidden by Pauli’s well-known exchange principle. Furthermore, the Schur–Weyl duality introduces a new correlation of spin angular momentum and spin permutation symmetry which were yet thought to exist somehow independently. In addition, we show in Chap. 4 how the symmetry of the nuclear spin states in particular influences reactive collisions. We use the famous H₃⁺ + H₂ → H₂ + H₃⁺ reaction as an illustrative example of formulating selection rules for state-to-state transitions in bi-molecular reactions. They are shown to depend in

particular on the symmetry of an intermediately formed complex. With discussing two respective examples, we are able to show the differences in, e.g., ortho-to-para transition probabilities for the molecular hydrogen under the collisional reaction with H_3^+ . All the calculations related to the Schur–Weyl duality are done energy- and hence model-independent. Consequently, we put this part ahead of the discussions on the dynamical models for extremely floppy or extremely fast rotating molecules.

In conclusion, this work is intended to show how fundamental symmetry properties and their proper mathematical understanding are essential in the description of molecular dynamics. The semi-classical model of ultrafast rotations as well as the super-rotation model for extremely floppy molecules can serve as a basis for further studies on these pathological cases, where all traditional approaches tend to reach their natural limits. Therefore, ‘old problems’ can be solved by using ‘new ideas’ from basic symmetry considerations.

Part I

Group Theory in Molecular Physics

Chapter 2

Basic Concepts

Abstract As in many fields of physics and chemistry, symmetry plays a major role in the discussion of inter- and intra-molecular dynamics. Since we will use fundamental concepts of symmetry throughout the whole present work, this first chapter is intended to introduce some of the basic concepts. We start with a short summary of the symmetry groups of the molecular Hamiltonian. Subsequently, we discuss the general representation theory of the groups we use in this work. In contrast to these two group theory based sections, we introduce the main dynamical models of molecular physics in Sect. 2.2. The connection of these so-called zero-order models and representation theory is done in Sect. 2.3 where we also include a short outlook on the upcoming parts.

As in many fields of physics and chemistry, symmetry plays a major role in the discussion of inter- and intra-molecular dynamics. Since we will use fundamental concepts of symmetry throughout the whole present work, this first chapter is intended to introduce some of the basic concepts. We start with a short summary of the symmetry groups of the molecular Hamiltonian. Subsequently, we discuss the general representation theory of the groups we use in this work. In contrast to these two group theory based sections, we introduce the main dynamical models of molecular physics in Sect. 2.2. The connection of these so-called zero-order models and representation theory is done in Sect. 2.3 where we also include a short outlook on the upcoming parts. The present chapter is not expected to be a complete introduction to the field of molecular symmetry, the interested reader is referred to the textbooks indicated throughout the text.

2.1 Symmetry Groups of the Molecular Hamiltonian

The internal dynamics of a single molecule is described by the time-independent Schrödinger equation $H_{\text{full}}\Psi_{\text{full}} = E\Psi_{\text{full}}$ which provides the energies and eigenstates of the molecule. The full molecular Hamiltonian H_{full} therefore is the central object in the description of molecules. It incorporates all kinds of motions and interactions of the molecular constituents, namely the electrons and nuclei. Since this leads to

a many-body Schrödinger equation, the latter is generally not solvable from first principles.

Graybox Schematically we can write the **full molecular Hamiltonian** as (see [14, p. 127])

$$H_{\text{full}} = \hat{T} + V + \hat{H}_{\text{es}} + \hat{H}_{\text{hfs}}.$$

The first term \hat{T} is the total kinetic energy operator consisting of the kinetic energy operator for all constituents, namely electrons and nuclei. The potential energy term V describes the **electrostatic interaction** of electrons and nuclei. Furthermore, the two last parts include the **spin degrees of freedom**. \hat{H}_{es} describes all kinds of interactions affecting the electronic spin. Moreover, \hat{H}_{hfs} describes the **hyperfine effects**, which is the general term for all interactions involving the nuclear spin.

However, symmetry can be used to reduce its complexity and to find approximations that can give at least a first idea on the molecular dynamics. Before discussing details of some of these dynamical models, we step back for a more generic view on molecular symmetry. From such a general perspective, we can identify five symmetry groups of the molecular Hamiltonian: [14]

- The internal dynamics of a single molecule should not depend on translations along any space-fixed axis, we call the respective symmetry group G_T .
- Space is isotropic, hence there must be a rotational invariance leading to the rotation group K (spatial).
- The electrons in a molecule are indistinguishable, they must be interchangeable without any influence on the physical properties of the molecule. This results in the electron permutation symmetry group $S_n^{(e)}$, where n denotes the number of electrons.¹
- Identical nuclei equivalently are indistinguishable leading to a nuclear permutation group $S_N^{(n)}$, where N is the number of identical nuclei respectively.
- Since the fundamental weak interaction is not observable at usual time scales of spectroscopic experiments, the inversion of all spatial coordinates of nuclei and electrons is a symmetry of the molecular Hamiltonian. We call it the inversion group \mathcal{E} .

We omit here the discussion of time-reversal and charge conjugation symmetry which are of no relevance in the rest of this work.

¹For a more rigorous definition of the group S_n , see Sect. 2.1.2.

A **symmetry group** is defined as a set of operators that all commute with the Hamiltonian of the system and satisfy the well known group axioms. The elements of the group are described in certain basis as matrices defining the so-called **representations** of the group (see Sect. 2.1.1). The number of elements in the group is the **order** of the group. Groups of infinite order are called **continuous**.

The full molecular Schrödinger equation consequently must be solved by wave functions that possess all these symmetries. This inherently couples the abstract symmetry groups with dynamical theories. A proper description of the symmetry of functions is given by the theory of representations which we review in the next section.

2.1.1 General Representation Theory

One important property of symmetry groups is the possible definition of isomorphic or homomorphic matrix groups which are called *irreducible representations* of the group. The representation matrices act on a vector space spanned by a set of functions. The action of any group element leaves this space invariant, i.e. if a representation of a group \mathbf{G} is spanned by n functions ϕ_n , the elements $g \in \mathbf{G}$ act on the functions by $g\phi_i = \sum_j c_j \phi_j$, where the c_j are constants. Specific linear combinations of the ϕ_i can therefore be used to construct common eigenfunctions of all elements in \mathbf{G} . If we consider a dynamical system described by some Hamiltonian, \hat{H} , and assume the group \mathbf{G} to be a proper symmetry group, the eigenfunctions of \hat{H} are equivalent (up to possible factors) to these combinations of the ϕ_i . Each irreducible representation provides a different set of eigenfunctions and consequently, the irreducible representations can be used to symmetry classify or label the eigenstates of the Hamiltonian. These labels are often referred to as the *quantum numbers* of the system since any time evolution operator, usually written as $\exp(-\frac{i}{\hbar} \hat{H} t)$, leaves the vector space of the irreducible representation invariant. One particular use of this symmetry classification is the block-diagonalization of the Hamiltonian matrix into the irreducible representations. If we consider a proper basis for writing \hat{H} in matrix form, a similarity transformation can be used to group the respective matrix elements into blocks defined by the irreducible representations. Subsequently, those blocks can be diagonalized separately in order to find the energies. The symmetry group \mathbf{G} prescribes that in this symmetry-adapted basis, no couplings between states of different irreducible representations can exist.

For further reading on the mathematical details of representation theory, we refer to, e.g., the textbooks of [18, 19] and the more historical work of [20].²

A **representation** is defined as a group of linear transformations on a vector space mimicking the very same multiplication behavior as the group it is representing. In the cases used here, it is therefore a matrix group **isomorphic** or **homomorphic** to the abstract group G of, e.g., symmetry operations. The former is defined by a one-to-one mapping of group elements to matrices and the latter allows for certain ambiguities. The vector space, however, is **invariant** under the applications of the group elements [18]. If one can find a vector subspace which is still invariant under G , the respective representation on this subspace is said to be a **sub-representation** of the original one. If no such subspace exists, the representation is called **irreducible**. Finite groups and semi-simple Lie groups, which are the objects of interest in the following, carry only completely reducible (finite) representations. This induces any representation to be describable as a **direct sum** of irreducible representations. For ordinary representation matrices, the sub-representations can be found by similarity transformations, where the matrices are decomposed into a **diagonal block structure**.

One way to describe the irreducible representations is by the characters (traces) of the respective matrices. Each group element hence gives rise to one such character. The set of characters unambiguously defines the representations and exhibits various very simple properties. First, different irreducible representations satisfy an orthogonality relation [20, 21]. In particular, if we denote the irreducible representations of a certain (finite) group by Γ_i , they fulfill

$$\sum_{R \in G} \chi^{\Gamma_i}[R] \chi^{\Gamma_j}[R]^* = |G| \delta_{ij}, \quad (2.1)$$

where the group G has $|G|$ elements denoted by R . χ represents the character of the respective representation. Second, every representation, Γ , can be written as a direct sum of irreducible representations Γ_i which is known as *complete reducibility* (see [18], p. 6)

$$\Gamma = \Gamma_1^{\oplus a_1} \oplus \Gamma_2^{\oplus a_2} \oplus \cdots \oplus \Gamma_k^{\oplus a_k} \equiv a_1 \Gamma_1 \oplus a_2 \Gamma_2 \oplus \cdots \oplus a_k \Gamma_k.$$

²An English translation was published in [21].

For the conveniently used matrix representations, the direct sum is, as usual, equivalent to a diagonal block structure, where the blocks represent the irreducible sub-representations. The character χ^{Γ} is therefore the sum of the characters of the irreducible representations.

Using the orthogonality property, the multiplicities a_j can be found by

$$a_j = \frac{1}{|G|} \sum_{R \in G} \chi^{\Gamma}[R] \chi^{\Gamma_j}[R]^*. \quad (2.2)$$

For the continuous groups, we use in the following, the above statements can be generalized by replacing the sums by integrals over the appropriate parameter space of the irreducible representations (see Part II of [18]).

Since the **character** is the trace of the representation matrix, it is a **class** function: If two group elements R and S can be transformed into each other by a similarity operation $R = T S T^{-1}$, where T is also a group element, they share the same character. Therefore, the **character tables** always show only the classes of the respective groups with a single representative element and the according characters of the irreducible representations. From the orthogonality of the irreducible representations of (2.1), one can directly infer that the number of classes equals the number of irreducible representations.

A First Example: The Rotation Group A single molecule in field-free space obviously has a rotational symmetry. Physical observables do not depend on rotations of an observer-fixed coordinate system. Therefore, the molecular Hamiltonian exhibits a symmetry group $\text{SO}(3)$ (or K (spatial) [14]), the group of all (orientation-preserving) rotations about an axis through the center of mass of the molecule. The eigenstates of the Hamiltonian, the molecular states, therefore span an irreducible representations of that group. From the theory of continuous groups, which we discuss in more detail in Chap. 6 of Part II, we know the irreducible representations to be labeled by the well-known angular momentum J , whereas there are $2J + 1$ functions of different projection quantum numbers, m , necessary to build the matrix equivalents for the elements of the rotation group. These functions are commonly known to be the spherical harmonics, Y_J^m , the representation matrices are the so-called Wigner-matrices, \mathcal{D}_J .

The eigenstates of the system's Hamiltonian can therefore be labeled by the J quantum number and exhibit a degeneracy of $2J + 1$. The characters of the Wigner matrices define the irreducible representation and are given by (see Sect. 6.1 of Part II and [9])

$$\chi_J(R^0) = 2J + 1, \quad \chi_J(R_v^\beta) = \frac{\sin((2J + 1)\beta/2)}{\sin(\beta/2)}.$$

Here, $R_{\mathbf{v}}^{\beta}$ is the rotation by an angle β about an axis, defined by the vector \mathbf{v} . These characters fulfill the integral form of the orthogonality relation for distinct J and hence they unambiguously define different irreducible representations of $\text{SO}(3)$.

2.1.2 Lie Groups and Permutation Groups

Two main types of groups will be discussed in this work: (i) Lie groups for the description of rotating systems including the more abstract “rotation” of nuclear spins; (ii) Permutation groups for nuclear spins but also for the symmetry of rotational and vibrational (ro-vibrational) states in molecules consisting of a finite number of constituents.

A real *Lie group* is a continuous group G , where both multiplication and inversion are smooth (differentiable) maps of the type $G \times G \rightarrow G$ [22]. More important for the following discussion is the fact that Lie groups define so-called *Lie algebras*: They consist of matrices, say, X , for which the matrix exponential $\exp(tX)$, where t is some constant, is an element of the respective underlying Lie group. The defining property for the elements of the Lie algebra is that their commutator $[X, Y] = XY - YX$ fulfills certain axioms [22]. The most obvious simplification of dealing with Lie algebras in comparison to the underlying Lie group is the finite number of elements.

Example 2.1 The already encountered rotation group $\text{SO}(3)$ is a Lie group. Representing the elements as matrices and the group product as usual matrix product can be used to straightforwardly verify the requirements for being a Lie group. The respective Lie algebra, conveniently denoted by lower case $\text{so}(3)$, is spanned by the three well-known infinitesimal operators of rotation, J_x, J_y, J_z , each rotating by an infinitesimal angle about the three orthogonal axes of some coordinate system. Therefore, every element of $\text{SO}(3)$ can be represented by the matrix exponential $\exp(\theta_i J_i)$, where i specifies the rotation axis and θ_i the respective angle. The elements of $\text{so}(3)$ fulfill the usual commutation relations $[J_i, J_j] = i\varepsilon_{ijk} J_k$, where ε_{ijk} is the Levi–Civita symbol.

Representation theory of Lie groups has shown that the irreducible representations of unitary, $U(d)$, as well as of orthogonal groups, $\text{SO}(d)$, can be labeled unambiguously by so-called highest weights. In general, a weight is defined by the eigenvalues of the simultaneous eigenfunctions of specific elements of the corresponding Lie algebra which span the so-called Cartan subalgebra. For a Cartan subalgebra consisting of n such operators,³ there are n corresponding weights λ_i . Conventionally, these weights are arranged such that $\lambda_1 \geq \lambda_2 \geq \dots \geq \lambda_n$.

³The elements of the Lie algebra are abstractly defined as operators. By choosing a suitable basis they correspond to matrices and we therefore use these terms equivalently.

The **Cartan subalgebra** is spanned by all elements H_i of the Lie algebra, whose commutator vanishes, i.e., $[H_i, H_j] = 0$. The commutator with all other operators is non-zero. Consequently, the Cartan subalgebra is **abelian** which is the general term for a group/algebra, where the consecutive application of two elements does not depend on the order. For the unitary groups $U(d)$, there are exactly d operators spanning the Cartan subalgebra, for $SO(2n + 1)$ and $SO(2n)$ there are n , respectively.

The other elements of the Lie algebra can change the weights. An irreducible representation is consequently spanned by functions of various weights. The highest such weight unambiguously defines the respective representation.

A weight $\lambda = \{\lambda_1, \lambda_2, \dots, \lambda_n\}$ is said to be **higher** than another $\xi = \{\xi_1, \xi_2, \dots, \xi_n\}$ if the difference $\lambda - \xi = \{\lambda_1 - \xi_1, \lambda_2 - \xi_2, \dots, \lambda_n - \xi_n\}$ is **positive**. A positive weight is defined by having a positive first non-vanishing component.

Especially for unitary groups, there exists an ingenious tool to graphically work with their irreducible representations, the so-called Young diagrammatic technique [23]. It extremely simplifies the calculations we perform in Chap. 3 for the spin symmetry of nuclei.

Young diagrams and tableaux

Irreducible representations of $U(d)$ are labeled by highest weights $\lambda_1 \geq \lambda_2 \geq \dots \geq \lambda_d$, where the λ_i are integers [22]. Therefore, they can be understood as a partition of the number $p = \sum_i \lambda_i$ into d parts. For example, an irreducible representation of highest weight $\lambda = \{2, 1\}$ is defining a partition of $p = 3$.

For a graphical depiction of the irreducible representation, these partitions are used to define so-called *Young diagrams*. A Young diagram is the composition of p boxes, defined by the partition λ , where the λ_i specify the number of boxes in the i th row.

For example, the irreducible representation with highest weight $\{2, 1\}$ of, e.g.,

$U(2)$, corresponds to the Young diagram of the shape .

In addition, the functions spanning this representation can be represented by so-called *Young tableaux*, which are numbered Young diagrams. For that, certain rules exist that can be found in the literature, e.g., in the textbook of [24], p. 334.

In order to understand the rules, consider each box as representing a single particle. Their collection indicates a product of the single-particle wave functions, where

distinct rows imply an antisymmetric product, whereas boxes in one row are simply multiplied. As a representation of the weights or quantum numbers of the respective group, the boxes get numbers.

In general, the highest weight state of $U(d)$ corresponds to a tableau, where all boxes of the i th row are numbered by a common integer i . The other states are found by inserting other numbers $j \leq d$. They must increase strongly for boxes in one column and increase weakly for those next to each other. Strong increment forbids duplicate numbers, whereas the weak variant allows them. These rules can be intuitively understood by noticing that an anti-symmetric combination of the same quantum numbers is indeed impossible. In our example of highest weight $\{2, 1\}$, we therefore get the following possible Young tableaux and hence linearly independent states spanning this representation by

$$\begin{array}{|c|c|} \hline 1 & 1 \\ \hline 2 & \\ \hline \end{array}, \quad \begin{array}{|c|c|} \hline 1 & 2 \\ \hline 2 & \\ \hline \end{array}.$$

In this rather intuitive way, the dimension of the respective irreducible representation can be found. In addition, in Chap. 3, we encounter an alternative dimension formula independent of the counting of the number of possible Young tableaux.

For further reading on the properties of Young tableaux and the respective irreducible representations of the according Lie groups, we refer to [18, 22, 25] and many other available textbooks on representation theory of Lie groups.

Permutation Groups In contrast to continuous groups, permutation groups have a finite number of elements. Nevertheless, one common element is the possibility to visualize the irreducible representations in terms of Young diagrams. In Chap. 3, we use this fact in order to explore an intimate connection of the unitary and the permutation group.

Permutation groups and in particular their combination with the inversion operation are one of the building blocks of modern group theory for molecules. It has been found that the geometric analysis of molecular structure and the related symmetry considerations are insufficient when it comes to describing the internal nuclear dynamics of molecules. Nevertheless, identical particle permutation and inversion symmetry must hold also for excited molecular states. It was one of the biggest successes in molecular group theory to show how these groups can be used to classify these states by the irreducible representations of the according permutation-inversion groups. The correlation to geometric symmetry is still given since the usual geometric *point groups* are found to be isomorphic to certain permutation-inversion groups [14]. As already introduced in the beginning of Sect. 2.1, the fact that the nuclear permutation-inversion group is a symmetry group of the molecular Hamiltonian induces the use of the irreducible representations of the group for a symmetry classification and labeling of the eigenstates of the molecular Hamiltonian. In the following we introduce the representation theory of permutation-inversion groups very briefly and refer to [14] for further information.⁴

⁴We refer here only to the exchange symmetry of identical nuclei since we do not deal with the electronic motion in any particular sense in the following chapters. However, the definitions of permutations, symmetric groups, etc., are indeed fully general.

A **permutation** is described abstractly by $(ijk\dots)$, whereas their products are noted by $(ij\dots)(kl\dots)$ [14]. As in [14], we exclusively use the N-convention, where permutations are defined to act on a set of numbers which, in our application, label indistinguishable particles by

$$(123)123 = 231; (132)123 = 312$$

The **length** of a permutation is the number of interchanged particles, i.e., the permutation (123) has length three, whereas the **transposition** (12) has length two. The **sign** of a permutation is given by the number of interchanged elements as well: If a permutation can be reconstructed from a product of an even number of transpositions, it is called even and its sign is defined to be positive. If an odd number of transpositions build a specific permutation, the sign is negative and the permutation is called odd. Furthermore, one defines so-called **generators** of the group, from which all other elements can be calculated by successive application. The group of possible permutations of a fixed set of indistinguishable particles, n , is called either the permutation group of n particles or the **symmetric group of degree n** , S_n . The order of such a permutation group, S_n , is the total number of elements given by $n!$.

Permutations and permutation products can be characterized by their length. A permutation $(123)(45)$ for example can be denoted by its *shape* as $\{32\}$. For a full characterization, one also includes the particles that are not exchanged by the specific permutation. If, e.g., a set of four particles is described in the symmetric group S_4 (see Example 2.2), the permutation (123) is written as $\{31\}$. Consequently, the neutral element of S_n is indicated as $\{1^n\}$ where we used the shorthand exponent notation (e.g. $\{1^2\} = \{11\}$). The elements of a general permutation group can be divided into classes with different shapes which can be straightforwardly calculated by the partition of the degree of the group. Since the number of classes equals the number of irreducible representations, these partitions are also used to characterize the latter in terms of, again, Young diagrams. In molecular theory, the labeling of irreducible representations is often slightly different, but a “translation” exists (see Example 2.2 and Chap. 3).

Like for unitary groups, Young tableaux can be set up from these partitions. However the numbering scheme differs slightly: Nothing changes with respect to distinct rows, but in a single row the numbers for the permutation group Young tableaux must also increase strongly. In addition, all integers up to the order of the group must be put in the boxes (see Example 2.2).

Example 2.2 Consider the group of permutations for four identical particles, S_4 . It consists of all permutations of these particles and we count $n! = 24$ of them. They are divided into five classes by the partitioning of the degree $n = 4$: E , (ij) , (ijk) , $(ij)(kl)$, $(ijkl)$, where $ijkl$ are all different. The sizes of the classes are given as 1, 6, 3, 8, 6 (see Table 2.1). Their irreducible representations are therefore labeled accordingly by $\{1^4\}$, $\{21^2\}$, $\{31\}$, $\{2^2\}$, $\{4\}$, where we use the exponent to shorten the

Table 2.1 Irreducible representations of the symmetric group of degree four S_4 . For each class of the group we list one representative element together with the number of elements in the class. The irreducible representations are labeled in the standard way of molecular theory [14] and by the according respective partition labels of representations theory

S_4	E	(12)	(12)(34)	(123)	(1234)
	1	6	3	8	6
$A_1 \{4\}$	1	1	1	1	-1
$A_2 \{1^4\}$	1	-1	1	1	1
$E \{2^2\}$	2	0	2	-1	0
$F_1 \{31\}$	3	1	-1	0	-1
$F_2 \{21^2\}$	3	-1	-1	0	1

notation, i.e. $\{1^2\} \equiv \{11\}$. In molecular theory these labels are more usually written as A_2 , F_2 , F_1 , E , A_1 (see Table 2.1). As an example for the Young tableaux, the $F_2 = \{21^2\}$ irreducible representation is depicted by

$$\begin{array}{|c|c|} \hline 1 & 2 \\ \hline 3 \\ \hline 4 \\ \hline \end{array}.$$

Since molecules are subjected to inversion symmetry, the permutation groups are conveniently extended to include the inversion operation and consequently all multiplications of permutations and inversion. For N identical nuclei, these groups are called *complete nuclear permutation-inversion groups* and are given by the product group $G_{CNPI} = S_N \times \{E, E^*\}$, where E^* is the inversion element. The number of elements, and hence also the number of irreducible representations grows faster than exponentially with the number of identical nuclei in the molecule. At this point, physics sets in to restrict the G_{CNPI} group to include only so-called *feasible* operations, thus obtaining the *molecular symmetry group*. We discuss them in particular in the next section. This concludes our introductory part on symmetry groups and general features of Lie and permutation groups and we now turn to a brief description of zero-order models in molecular theory. During the course of this work, more details on some of the concepts mentioned above will be discussed.

2.2 Zero-Order Models in Molecular Theory

After the more general, mathematical view on molecular symmetry, we now discuss some features of dynamical models for molecules. They are built on a few central assumptions leading to very simple zero-order models for the respective dynamics. In general, zero-order models are approximations of the according full Schrödinger equation, where all deviations from that model are considered to be comparably small. The latter can be incorporated by perturbation theory. This includes all kinds of deviations from the zero order model in a converging series with certain so-called

distortion or coupling constants and respective operator products. In difference to the perturbative approach, the variational approach to molecular dynamics uses the operator products in a more direct way. No assumption on the coupling constants is made and the Hamiltonian is set up in a matrix form, where the respective diagonalization determines the energies. However, the basis states for the Hamiltonian matrix are chosen again from particular zero-order models and all kinds of couplings are incorporated by choosing product basis states.

To introduce the zero-order models of traditional molecular theory, we discuss in the following section (i) the separation of different degrees of freedom, (ii) the molecular symmetry group restricting the nuclear motion and (iii) finally the zero-order models for nuclear vibration and rotation. The discussion of the nuclear vibrations is kept short since rotational degrees of freedom are the main focus of the present work. For more details on the models of molecular theory, we refer to the classic textbook of [26].

2.2.1 *The Separation of the Molecular Hamiltonian*

To start with, notice once again that the full many-body Hamiltonian for molecular dynamics can only be solved approximately. The main idea is to separate different types of fast and slow motions: At first, the electron mass is considerably smaller than the nuclear masses and one very conveniently uses the Born–Oppenheimer approximation [27], where the Coulomb interaction of nuclei and electrons is considered to depend parametrically on the coordinates of the nuclei. Hence one can successively solve the electronic Schrödinger equation by varying the nuclear configuration. The respective energies create a static potential energy surface for the motion of the nuclei. The electronic Schrödinger equation, however, is most likely not exactly solvable and once again certain approximations are used. A detailed description of this almost independent field of molecular ab-initio theory is beyond the scope of this work. For an introduction to this field we refer to, e.g., [28].

Once the electronic problem is approximately solved, the nuclear motion can be treated. On the potential energy surface, one can usually define numerous minima indicating different low-energy structures. The lowest one defines the equilibrium structure. If the molecule consists of a number of indistinguishable nuclei, the nuclear permutation symmetry (see Sect. 2.1) imposes a number of distinct such minima, differing by the numbering of the identical nuclei (see Fig. 2.1). The equilibrium structure can be altered by vibrational motion of the nuclei, whereas translation and overall rotational motion are (almost) structure preserving. Any collective translational motion can be neglected by assuming the molecular center of mass to be fixed relative to the observer.

The Molecular Symmetry Group The potential energy surface restricts the nuclear motion: Energy barriers between different minima influence the tunneling probability between the different structures. Consequently, the tunnel splitting of an energy

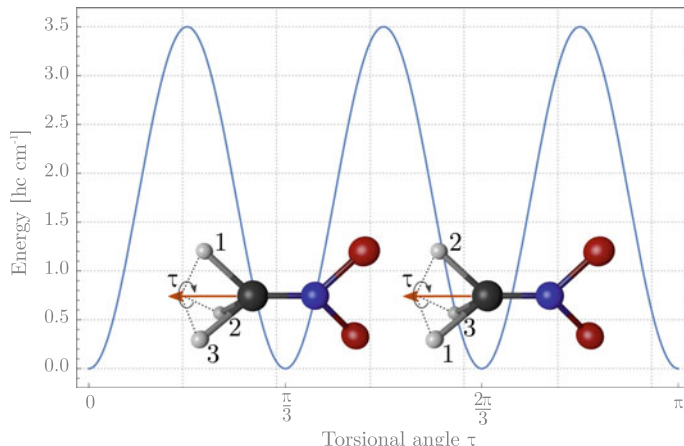


Fig. 2.1 The potential energy for a torsional motion of the methyl group, CH_3 , in nitromethane, CH_3NO_2 [29]. The respective angle indicates the relative orientation of the methyl group to the two oxygen nuclei. The indicated equilibrium structures differ only by the numbering of the three protons. It is hence an example of different equilibrium structures as well as of the possibility of tunneling. We return to a discussion of this molecule in Part II

level (see Fig. 2.2) becomes very small if the barrier is very large. Therefore, tunneling is possibly not resolvable in a resolution-limited spectroscopic experiment. If the respective minima differ in their numbering of identical nuclei, one calls the permutation-inversion element that interconverts these specific minima to be *unfeasible*. The elements of the complete nuclear permutation-inversion group that are *feasible* consequently form a subgroup, usually called *molecular symmetry group* [30]. In the molecular symmetry group, the nuclear states are characterized by their behavior under permutation and inversion which defines the according irreducible representation they can be labeled by.

Consequently, inter-conversions between particular structures could be observable only in high-resolution experiments. Lower resolutions would not resolve the tunneling, the states would be measured to be degenerate (see Fig. 2.2). Therefore, the definition of the molecular symmetry group strongly depends on the experimental conditions.

Example 2.3 The molecular symmetry group consists only of a subset of permutation-inversion operations. Especially in molecules consisting of a large number of identical nuclei, a thorough definition of the molecular symmetry group is essential. Otherwise, the order of the complete nuclear permutation-inversion group is exceedingly large. In a “simple” molecule like benzene, C_6H_6 , we already count 1036800 permutation- and permutation-inversion operations. Its molecular symmetry group, however, is predicted to be isomorphic to D_{6h} which consists of 24 elements only. This considerably simplifies all different kinds of symmetry considerations for that molecule [14].

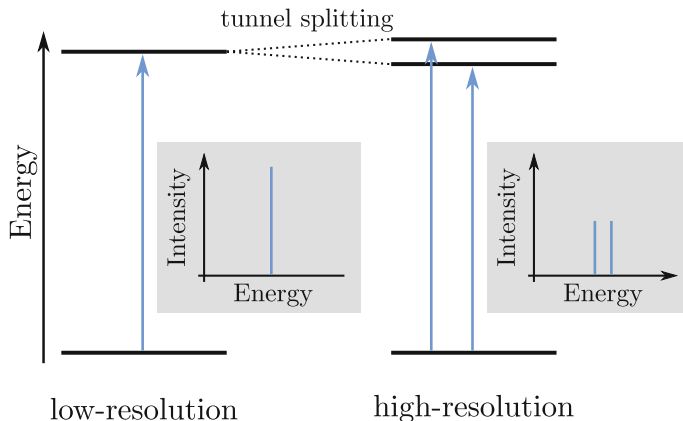


Fig. 2.2 Schematic of an energy term diagram with and without tunnel splitting of the excited state. In a high-resolution spectroscopic experiment, the splitting would be observable as a doubled line instead of a single line in the lower-resolution case. In the latter, the excited state would be doubly degenerate and hence the transition intensity would be larger than if the states split

The Separation of Nuclear Degrees of Freedom After having separated the electronic motion, the $3N - 3$ nuclear degrees of freedom⁵ for a molecule consisting of N atoms, are further subdivided into different parts. This is motivated by the different influences on the structure of the molecule. If we assume the nuclear vibrations to lead only to nuclear displacements that are small compared to the linear dimension of the total molecule, overall molecular rotation can still be treated as being that of an almost rigid body. Hence, again three degrees of freedom are counted for the overall rotational degrees of freedom, conventionally described by a change of the Euler angles, the angles indicating the orientation of the molecule relative to an observer. The remaining $3N - 6$ degrees of freedom are identified as nuclear vibrations. For linear molecules, however, the counting scheme is slightly different. There, only two rotational degrees of freedom exist and hence we count $3N - 5$ vibrational ones, respectively.

In total, we now separated the molecular dynamics – as a zero order approximation – into three different parts: (i) electronic motion creating the almost static potential energy surface, (ii) rotational and (iii) vibrational nuclear motions. In addition, as quantum objects, both nuclei and electrons possess spin quantum numbers. The spin is conveniently also assumed to not interact with the other degrees of freedom. The full molecular Hamiltonian therefore splits into those parts $H_{\text{full}} = H_{el} + H_{\text{vib}} + H_{\text{rot}} + H_{\text{nspin}}$, where the latter is considered to be trivial.

Example 2.4 Due to Pauli's principle, the electrons must behave totally anti-symmetric under permutations of negative sign. Their wave function must span the according irreducible representation of the electron permutation group called *sign representation*. Actually, all permutation groups of order $N > 1$ exhibit one trivial

⁵We have subtracted three degrees of freedom for the translational motion of the center of mass.

and one sign irreducible representation, differing in the sign of the character for the even permutations.

In zero order, the full *nuclear* wave function is therefore conventionally written as

$$\psi_{\text{tot}} = \psi_{\text{vib}} \psi_{\text{rot}} \psi_{\text{nspin}},$$

and the Schrödinger equation for the nuclear motion reads as

$$(H_{\text{vib}} + H_{\text{rot}} + H_{\text{nspin}}) \psi_{\text{tot}} = (E_{\text{vib}} + E_{\text{rot}}) \psi_{\text{vib}} \psi_{\text{rot}} \psi_{\text{nspin}}.$$

At this point, representation theory sets in: For a molecule consisting of a single nuclear species, permutation symmetry must be fulfilled and hence the irreducible representations of the respective symmetry group are spanned by the ψ_{tot} . Since the nuclei are of definite spin, the latter defines whether they follow the Fermi–Dirac or Bose–Einstein statistics for half-integer or integer spin particles (see, e.g., [14]). In particular, the total wave function must behave either as the sign or the trivial representation of the molecular symmetry group.

In consequence, the product of $\psi_{\text{vib}} \psi_{\text{rot}} \psi_{\text{nspin}}$ is restricted to span an explicit representation of the molecular symmetry group. Linking this statement to the more general discussion of representation theory in Sect. 2.1.1, we notice that instead of calculating the products of wave functions we can equivalently multiply the respective irreducible representations. In particular, the three parts of the total nuclear wave function span certain representations in the molecular symmetry group and in calculating the irreducible sub-representations of their product, we can determine if a certain combination of wave functions is allowed by Fermi–Dirac or Bose–Einstein statistics. Before the irreducible representation spanned by either of the parts can be calculated, the rotational and vibrational dynamics are usually treated in a more general way without restricting to certain permutation symmetry. In Chaps. 3 and 4 of Part I we discuss in addition the details of the nuclear spin part of the full wave function.

2.2.2 The Zero-Order Models for Nuclear Motion

For the vibrational part, the most convenient zero-order model is the harmonic oscillator. This is motivated by the potential energy surface which can locally be approximated as being quadratic in the respective vibrational, or normal coordinate. If the vibration is higher-dimensional, as, e.g., the two-dimensional bending vibration of a linear molecule, the model is extended to a two-dimensional harmonic oscillator (see, e.g., [31]).

Note 2.1 Molecular vibrations are described as collective motions of different nuclei. The respective **normal coordinates** are therefore linear combinations of the nuclear Cartesian coordinates relative to their equilibrium values. For non-linear molecules consisting of N nuclei, one usually defines $3N - 6$ vibrational degrees of freedom and according **normal modes**. The latter describe the vibrational motion in the respective normal coordinates, which are defined such that when the vibrational part of the molecular Hamiltonian is expanded to second order in this normal coordinate, no interaction to other normal modes exists. One famous example is the bending vibration of water, H_2O , described as a change in the bond angle of the oxygen-hydrogen bonds. The respective potential energy surface is approximated to be almost harmonic around the equilibrium bond angle of about 105° .

The zero-order model for molecular rotation is that of a rigid rotor without any applied external field. The molecular structure is assumed to be fixed and hence a moment of inertia tensor can be defined, usually transformed into diagonal form by using a body-fixed principal axis system. In general, all three principal moments of inertia $I_1 \leq I_2 \leq I_3$ are different, and the Hamiltonian is that of an asymmetric rigid rotor. Again, this is only solvable analytically in three symmetric limits, the spherical ($I_1 = I_2 = I_3$), the oblate ($I_1 = I_2 < I_3$), and the prolate ($I_1 < I_2 = I_3$) rotor. For the asymmetric rotor, the Hamiltonian is written as

$$\hat{H}_{\text{rot}} = A \hat{J}_x^2 + B \hat{J}_y^2 + C \hat{J}_z,$$

where the constants $(A = \frac{1}{2I_1}, B = \frac{1}{2I_2}, C = \frac{1}{2I_3})$ are called rotational constants.⁶ By using the angular momentum quantum number J , i.e. the eigenvalue of the total angular momentum $\hat{\mathbf{J}}^2 = \sum \hat{J}_i^2$, and its projection, k , onto the body-fixed principal axis of rotation,⁷ the energies for the symmetric rotor cases are found analytically [14]

$$E_{\text{rot}}^{(\text{prol})} = BJ(J+1) + (A-B)k^2, \quad E_{\text{rot}}^{(\text{obl})} = BJ(J+1) - (B-C)k^2.$$

The respective eigenfunctions are the well-known symmetric rotor functions [32]

$$|Jkm\rangle = \left(\frac{2J+1}{8\pi^2} \right)^{1/2} (\mathcal{D}_{mk}^J)^*(\theta, \phi, \chi). \quad (2.3)$$

The \mathcal{D}_{mk}^J are the matrix elements of the Wigner-matrices, defining a rotation with angular momentum J (see, e.g., [32] for more details). They depend on the three Euler angles, (θ, ϕ, χ) which define the relative orientation of the body-fixed axes

⁶Notice that we set $\hbar = 1$ for the moment.

⁷The principal axis of rotation for an oblate top is the molecule-fixed axis corresponding to the moment of inertia I_3 . For the prolate case, it is the axis of I_1 .

to an observer-fixed coordinate system. The spherical rotor energies can directly be read off from the symmetric rotor energies since all rotational constants are equal and no k quantum number is necessary.

The $|Jkm\rangle$ functions are also used for the numerical evaluation of the asymmetric rotor problem. The respective eigenfunctions are found to be linear combinations of fixed J but different k projection quantum numbers.

Note 2.2 Since the molecule is assumed to be in a field-free environment, the energies of the $|Jkm\rangle$ states are independent of the **magnetic quantum number** m , the angular momentum projection onto a space- or lab-fixed axis. The total number of those states for a single quantum number J is hence given as $(2J + 1)^2$. In terms of symmetry groups, these lab-fixed rotations are considered as a second rotation group. The full “rotation group” therefore is the product group $\text{SO}(3)_{\text{spatial}} \times \text{SO}(3)_{\text{mol}}$ (see Chap. 6 of Part II).

Having formulated a zero-order model for both the rotational and vibrational motion, the next natural step is to include their interaction. This is usually done in a perturbative way. The interaction is assumed to be described by explicit couplings of the respective angular momentum and vibrational operators, equipped with constants, indicating the respective interaction strength. With increasing order of the coupled operators, the interaction strength is assumed to decrease. In addition, similar higher order terms from centrifugal distortions of the rigid rotor model as well as anharmonic corrections for the vibrations are introduced. The respective constants can be predicted from ab-initio calculations and are conveniently refined in least-squares fittings to data obtained from spectroscopic measurements. For a large variety of molecules, these constants allow impressively accurate predictions of electromagnetic transitions also in energy ranges that have not been measured before.

Actually, one roughly distinguishes two different approaches for the perturbative treatment of ro-vibrational couplings and the respective constants: (i) The effective Hamiltonian approach, where each vibrational level is treated independently (see the classic work of [33]) and (ii) variational approaches, where the influence of vibrations is included by calculating Hamilton matrix elements of products of angular momentum and vibrational operators in a suitable product basis of rotational and vibrational basis functions (see [34, 35] for two examples). Both approaches have certain advantages, but due to increased computing power during the last years, the variational approach becomes more and more important especially in the realm of relatively hot molecules [36].

One application following from the knowledge of these constants is the prediction of molecular spectra in, e.g., interstellar space, where indeed the conditions are considerably different from those in laboratories. The precise knowledge of the constants is nevertheless used to extrapolate to the spectral regions where no laboratory data is available. For instance in hot molecular clouds, electromagnetic transitions including

large J values can be observed radio-astronomically. This has led to a large number of unambiguous identifications of molecules in different regions in space [37].

2.3 Connecting Dynamics and Group Theory – Outlook to This Work

After the introduction of general representation theory and zero-order models for the nuclear motion in molecules in the last two sections, Chap. 3 of this part and Chap. 6 of Part II focus explicitly on the connection of the dynamical models and representation theory.

To initiate these treatments, notice once again that the eigenfunctions of any Hamiltonian span the irreducible representations of its symmetry group. For the vibrational part of the wave function, the zero-order model is that of a d -dimensional harmonic oscillator. It is symmetric under the unitary group in d dimensions and the irreducible representations are labeled by their highest weights. In the most simple case of a one-dimensional harmonic oscillator, the eigenfunctions therefore get integer labels, the well-known vibrational quantum numbers n . Since we do not consider the vibrations in any detail in this work, we skip a thorough discussion. Instead, we focus especially in parts II and III on the rotational dynamics of molecules. The rigid rotor Hamiltonian for a spherical rotor ($I_1 = I_2 = I_3$) is symmetric with respect to the full group of rotations in three dimensions, $\text{SO}(3)$. This group and the respective representations are discussed in detail in Sect. 6.1 of Part II. There we encounter also the subgroup $\text{SO}(2) \subset \text{SO}(3)$ describing the symmetry group of the symmetric oblate or prolate rotors.

However, since a molecule consists of a finite number of constituents, the continuous groups for the vibrational and rotational motion are not sufficient to symmetry classify the wave functions. The permutation-inversion group or, more precisely, the molecular symmetry group is the, say, real symmetry group of the nuclear part of the Hamiltonian. Both, vibrational and rotational wave functions must therefore span representations in that group. This induces two-fold labels of the respective functions: They are labeled by the irreducible representation of the continuous group *and* by the irreducible representation labels of the finite molecular symmetry group. The exact behavior of the rotational functions under the application of the permutation-inversion operations is subject of Sect. 6.1 of Part II.

Note 2.3 In the separate treatment of vibrations and rotations, the full Hamiltonian then exhibits a **product symmetry group**. In the simple case of a one-dimensional harmonic oscillator and a spherical rotor, the group would be $\text{U}(1) \times \text{SO}(3)$. The states would therefore span a representation which is a definite product of the irreducible representations of the two individual groups.

In difference to perturbative models, where for each vibrational energy level a “new” effective rotational Hamiltonian is constructed, the variational approaches to molecular dynamics consider the coupled ro-vibrational Hamiltonian straightforwardly. The **basis states** for constructing a possibly very large Hamiltonian matrix are conveniently chosen again as the product states of decoupled vibrational and rotational states. However, the calculated eigenfunctions can span representations which are **linear combinations of products** of different irreducible representations, e.g., states of different vibrational quantum numbers might couple to a single rotational state. Consequently, the intuitive physical picture of the effective approach is lost and interpretation poses a considerable challenge.

Apart from the rotational and vibrational states, the nuclear spin part of the full molecular wave function has not been treated in detail yet. In the next chapter we actually perform a thorough symmetry analysis. We also introduce the zero-order model for nuclear spins there. Actually, the main assumption is that the energy of molecular states does not depend at all on the spins of the nuclei. Hence, the zero-order model is trivial and one has to care only of the respective symmetry group of spin in general. The latter again is found to be continuous but we also establish an intimate correlation to the finite molecular symmetry group.

In both, the following Chaps. 3 and 4 as well as in the whole Part II, representation theory is one of the main concepts. Also in the very last part (Part III) of the work, symmetry guides through the semi-classical description of ultrafast rotating molecules. The previous chapter therefore intended to lay the foundations for all of the upcoming discussions. For further reading we again refer to the textbooks of [14, 18, 19, 38].

Chapter 3

Schur–Weyl Duality in Molecules

Abstract Both, the intra-molecular dynamics of a single molecule and the inter-molecular dynamics of, e.g., reacting molecules, are strongly influenced by the symmetry of the respective nuclear spin states. Due to Pauli's exclusion principle it restricts the allowed ro-vibrational molecular states. In this chapter, the unification of the nuclear spin angular momentum symmetry and the permutational symmetry of the nuclei is shown. Traditional approaches to find these symmetries become very impracticable when it comes to molecules with a large number of identical nuclei or a large individual spin quantum number. With the Schur–Weyl duality theorem, this complication is solved, it actually provides a simple rule to find both symmetries in a coherent manner. Furthermore, the use of the duality theorem is simplified by using the ingenious technique of Young tableaux, which are graphical depictions of irreducible representations. With this new technique, a few examples of calculating the nuclear spin symmetries are shown, including the famous H_5^+ complex and its fully deuterated isotopologue, D_5^+ .

3.1 Nuclear Spin States in Molecules

In modern physics and chemistry dealing with many-body systems, identical-particle-permutation symmetry represents one of the most influential concepts. One cornerstone is the differentiation of particles by their intrinsic spin quantum number. Half-integral spin fermions obey the Fermi–Dirac statistics, i.e. they cannot occupy a common quantum state, whereas a collection of bosons (integer spin) is described by the Bose–Einstein statistics allowing them all to occupy the very same state. This fundamental difference is responsible, e.g., for magnetism in solids, where the repulsive force between electrons leads to a macroscopic alignment and certain response to any applied electric or magnetic field. There, the simplified spin-1/2 chain is sometimes described as “one of the crowning glories of many body physics” [39, p. 5] as it covers a wide range of physical phenomena in many-body physics concerned with spin–spin interaction. Regarding molecular dynamics, Fermi–Dirac/Bose–Einstein statistics is used to formulate selection rules for intra-molecular state-to-state transitions or, in the realm of reactive collisions, for inter-molecular dynamics.

As discussed in Sect. 2.2, molecular systems are conventionally described using the Born–Oppenheimer approximation, where the electronic motion is considered to be much faster than the nuclear motion and is approximated to create a fixed potential energy surface on which the nuclear motion takes place. The moving nuclei naturally carry a spin which makes them subject to similar forces as described in solid-state theory. However, the nuclear magnetic interaction, also termed *hyperfine effect*, is exceedingly small compared to, e.g., the energy of rotational transitions. Thus, a separation of the nuclear-spin wave function from the *motional* one is very intuitive. The motional part includes the rotational as well as the vibrational dynamics, i.e. it describes the ro-vibrational wave function.

Nevertheless, the importance of nuclear spin is hard to overestimate: By forming the total nuclear wave function from motional and nuclear spin parts, the latter is responsible for two important properties: First, various motional states have different so-called spin-statistical weights calculated from simple combinatorial arguments [14]. They represent the number of possible combinations of a single motional symmetry species with different nuclear spin wave functions such that the total wave function has the appropriate exchange symmetry dictated by Pauli’s principle [40, 41]. In particular, the spin-statistical weights manifest themselves in experimental spectra as intensities of state-to-state transitions and enable to perform a first tentative assignment of respective quantum numbers to the observed transitions. Second, the nuclear spin states are responsible for selection rules in experiments, since different nuclear spin configurations cannot be interchanged by electric dipole transitions usually observed in spectroscopic experiments. Thus, distinct spin configurations behave as independent chemical species. As such, they also influence the selection rules in reactions (see Chap. 4).

In addition to the distinct exchange behavior of bosons and fermions, spin is also interpreted as intrinsic angular momentum. Hence, nuclear spins are thought to couple to a total spin angular momentum, say, I_{tot} . The different allowed symmetry species of the motional wave function are often distinguished by the total spin quantum number of the associated nuclear spin wave function. The most prominent example is the hydrogen molecule, H_2 , where one conveniently separates ortho ($I_{\text{tot}} = 1$) and para ($I_{\text{tot}} = 0$) states [42]. Under usual experimental conditions total nuclear spin is conserved such that spin conversion is forbidden and no ortho-to-para conversion is observable. Only in experiments with strong inhomogeneous magnetic fields, spin conversion in an individual molecule can be observed.

States of different total spin are also naturally distinguished by their permutation symmetry, guiding us straightforwardly to the general question to be answered in this chapter:

Is there any one-to-one correspondence of total spin quantum number and the respective permutation symmetry of a molecular system?

Mainly there are two reasons for this question: First, the currently used method of finding all the nuclear spin configurations and the corresponding total spin quantum numbers (see Sect. 3.1.1) becomes extremely impracticable for molecules with a large number of identical nuclei and/or with identical nuclei of large individual spin. Second, permutation as well as rotational symmetry play a decisive role in reactions since correlating the symmetry of reactant and product states can be used to gain insight into the properties of the intermediately formed complex (see Chap. 4). Furthermore, they can be used to determine statistical state-to-state reaction rates depending only on the symmetry of the reaction's participants [43, 44]. Earlier attempts to find these rates were using exclusively the angular momentum property of nuclear spins, [44] but we find the correlation to the permutation symmetry to be particularly decisive in that kind of calculations.

We show the answer to the above stated question to be actually twofold: In a general sense there is a strict one-to-one correlation between a generalized spin quantum number and the respective permutation symmetry. Conversely, using the conventional spin quantum number I can lead to ambiguities in the exact correspondence to permutation symmetry species, which have been observed before [45].

The main concept we use to show the correspondence of spin and permutation symmetry is the Schur–Weyl duality theorem, a result from representation theory, which has been developed already in the 1900s [46, 47]. Its application is rather simple when using the Young diagrammatic technique also established in the beginning of the 20th century [23]. The latter is a graphical tool to work with representations suitable for both spin representations and permutation symmetry species (see Fig. 3.1) [14, 18, 24]. Schur–Weyl's duality theorem and the Young tableaus are used in various other contexts (for a recent review see, e.g., [48]), but, to our knowledge, have never been applied to the nuclear spin problem of molecular theory.

The rather mathematical ideas of the duality theorem and the Young diagrams are utilized to solve some ambiguity problems found in the work of [45] who considered in particular deuterated molecular species and their nuclear spin symmetries. Moreover, they can be applied to determine the spin rotational and permutation symmetry of arbitrary large molecules in a simple way. By applying them to problems concerning reactive collisions we show them to open up a new pathway for describing selection rules for such reactions. Formerly, these rules have been determined by different authors with distinct methods [43, 44], which we now show to be inherently coupled. The selection rules are of obvious importance in studying state-to-state transitions in very cold environments, where symmetry dictates the thermalization pathways for certain molecules.

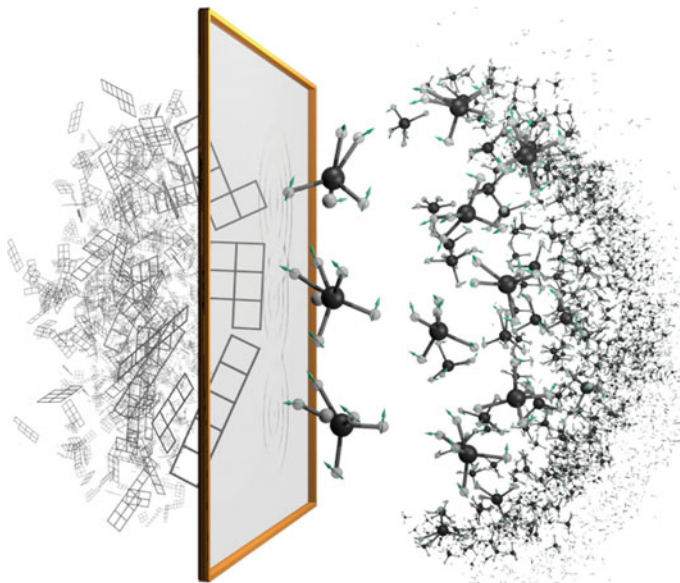
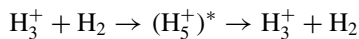


Fig. 3.1 Graphical depiction of the nuclear spin degrees of freedoms (*right*) in terms of the mathematical construct of Young tableaux (*left*). The different spin configurations are mirrored to a particular shape of diagram which simplifies the use of representation theory for the nuclear-spin permutational and rotational symmetry. The graphic is reproduced after [8]

In the following, we consider temperatures of a few Kelvin and hence only a few molecular states are populated in **thermal equilibrium**. In particular, the molecules are assumed to be in their vibrational and electronic ground state, while the first few J energy levels are occupied. To reach these low- J quantum states, the molecules must undergo various electromagnetic transitions, which we call the **thermalization pathway**. In usual **collisional cooling**, symmetry selection rules exist prohibiting certain such pathways. However, if the molecules collide and form an intermediate complex, other selection rules arise. This is the reason for the importance of **reactive collisions** in thermalization processes.

One primary example is the



reaction, which is believed to be the primary mechanism in the (spin-) cooling of molecular hydrogen in interstellar molecular clouds. We will enter the discussion of the application of the Schur–Weyl duality to reactive collisions in Chap. 4.

Conclusively, the use of Schur–Weyl’s duality theorem along with the Young diagrammatic technique for studying nuclear spin state symmetry represents a simple method to find the respective symmetry properties of molecular complexes of any size. It represents furthermore a suitable tool for studying selection rules in reactive collisions. While being a direct consequence of representation theory it is nevertheless rooted actually in the physical assumption of neglecting all spin-related influences to the total molecular energy. The results we present here are based on [8], however, we give more details on the underlying mathematical concepts, and in particular in Chap. 4 on the application to collisional dynamics.

3.1.1 *The Natural Way*

To answer the question of correspondence of total nuclear spin and permutation symmetry of the respective wave function, we start with a review of the most intuitive and fundamental method to obtain the respective quantum numbers or irreducible representations. One main law of nature is the indistinguishability of identical particles which implies Pauli’s principle [40, 41]: The exchange of two identical fermionic particles reverses the sign of the system’s total wave function, whereas it remains unaffected if two bosons are permuted. Considering molecules, interchanging two electrons therefore gives rise to a global change in the wave function’s sign, whereas it depends on the nature of the nuclei whether their permutation affects the total molecular wave function. In particular, the nuclear spins dictate whether an exchange of identical nuclei leads to a sign change in the nuclear wave function.

Molecules generally consist of several types of nuclei, their respective complete nuclear permutation group (cf. Chap. 2) is the product of symmetric groups S_N , where N is the number of identical nuclei. For the moment, we restrict ourselves to one species only, but the generalization to more species is straightforward. Quantum mechanics (see Sect. 2.1) cause the total nuclear wave function to be described as spanning a one-dimensional irreducible representation of the according symmetry group, here S_N . The only one-dimensional irreducible representations of the symmetric groups of $N > 1$ are the trivial symmetric one and an anti-symmetric (sign) representation, where the latter has a negative character for permutations of negative sign. The connection to the exchange theory of fermions or bosons induces that if the nuclei are all of integer spin, the total nuclear wave function must be described by the trivial totally symmetric irreducible representation, whereas a collection of fermionic nuclei dictates the wave function to behave as the sign representation. Straightforwardly, for molecules consisting of different nuclear species, the irreducible representation of the total nuclear wave function is defined as the product of sign and trivial representations for the combination of bosonic and fermionic nuclei respectively.

To be fully general, the inversion operation must be included if the full symmetry of the nuclear wave function is considered. This generates the complete nuclear permutation-inversion group [14, 30], which is formally the product group of $S_N \times \{E, E^*\}$, where E^* is the inversion operation. The number of irreducible representations of S_N thus gets doubled, i.e., a single irreducible representation of S_N is now replaced by two representations differing in their signs for operations involving the inversion. Physically, the response to the inversion operation signals the parity of the respective quantum state, which is not related to Pauli's principle. For a more thorough discussion of parity, we here refer to [14].

Furthermore, nuclear spins of a certain molecule are treated to be independent, usually their contribution to the total molecular energy is by far, i.e. many orders of magnitude, smaller than, e.g., the asymmetry splitting of a single rotational level. Therefore, the total nuclear wave function ψ_{tot} is approximately described as a product state of the form

$$\psi_{\text{tot}} = \psi_{\text{rovib}} \psi_{\text{nspin}}. \quad (3.1)$$

The symmetry of ψ_{tot} is dictated by Pauli's principle and parity. We call the respective symmetric or anti-symmetric irreducible representation $\Gamma_{\text{Pauli}}^{\pm}$, where the \pm superscript indicates the parity. The splitting of the wave function into two parts is thus expressed as

$$\Gamma_{\text{Pauli}} \supset \Gamma_{\text{rovib}} \otimes \Gamma_{\text{nspin}}, \quad (3.2)$$

where we omit the parity for convenience.¹ The above equation indicates that the product of the two wave functions can equivalently be described as a product of the respective representations. In addition, it prescribes which combinations are possible, since Γ_{Pauli} is restricted. The number of allowed combinations of a single ro-vibrational state with nuclear spin states defines the so-called spin-statistical weight for the respective state. The representation of the ro-vibrational part is usually described through according quantum numbers. In order to find the nuclear spin representation, we now focus on the nuclear spin part.

In addition to the permutation picture of the discussion of fermions and bosons, nuclear spin is also imagined as an intrinsic angular momentum and as such the combination of spins can be expressed as a coupling of angular momenta. As already introduced in Sect. 2.1 of this first part and discussed further in Chap. 6 of Part II, the angular momentum algebra allows to define irreducible representations of the rotation group SO(3). The spin is said to have a “rotational symmetry”. The respective irreducible representations are labeled by the spin angular momentum quantum number and are usually denoted as \mathcal{D}_I , where I is the spin and \mathcal{D} represents the Wigner-D-matrices of size $2I + 1$ [14, 21]. The coupling of angular momentum can be expressed by using the “almighty formula for addition of angular momentum” [44, p. 636], where the product of two Wigner-D-matrices results in a sum of matrices

¹Inversion does not act on the spin part of the nuclear wave function, which allows us to omit it for the discussion of the symmetry of this part of the full molecular wave function.

$$\mathcal{D}_{I_1} \otimes \mathcal{D}_{I_2} = \mathcal{D}_{I_1+I_2} \oplus \mathcal{D}_{I_1+I_2-1} \oplus \cdots \oplus \mathcal{D}_{|I_1-I_2|}. \quad (3.3)$$

Here, the I_j indicate the individual spin angular momentum quantum numbers of different nuclei. With this rule, all total angular momenta can be set up and therefore the rotational symmetry of the nuclear spin wave function of a molecule consisting of N identical nuclei is defined. However, the spin angular momentum picture is not related to Pauli's principle. Nevertheless, each nuclear spin wave function possesses simultaneously certain permutation and spin rotational symmetry. To simplify the notation, we here introduce a “joint” representation, written as

$$(\alpha X, \beta \mathcal{D}_I), \quad (3.4)$$

where X is the irreducible representation of the symmetric group and \mathcal{D}_I is the Wigner-D-matrix of spin I . The coefficients α and β indicate the respective multiplicity as a single irreducible representation X of the permutation group can be linked more than once to the same spin quantum number and vice versa. With this inclusion, the dimension of the joint representation is given by

$$\dim (\alpha X, \beta \mathcal{D}_I) = \alpha \dim X = \beta(2I + 1).$$

Straightforwardly, we define the addition of two joint representations as the usual direct sum of the respective parts

$$(\alpha_1 X_1, \beta_1 \mathcal{D}_{I_1}) \oplus (\alpha_2 X_2, \beta_2 \mathcal{D}_{I_2}) = (\alpha_1 X \oplus \alpha_2 X_2, \beta_1 \mathcal{D}_{I_1} \oplus \beta_2 \mathcal{D}_{I_2}).$$

The most natural way to find permutation and angular momentum symmetry of the nuclear spin wave function is to set up the respective joint representations by hand. This, say, pedestrian way is best explained by considering a system of N identical nuclei. Each of the nuclei carries a specific spin, say I . Thus, we can set up all possible spin configurations by adding up all individual spin vectors using (3.3). The nuclear spin states can be written in bra-ket notation as $|I, M_I\rangle$, where M_I is defined as the projection of the spin onto a fixed z -axis giving $2I + 1$ different values $M_I = -I, -I + 1, \dots, I - 1, I$. The number of all respective states is given by $(2I + 1)^N$. To set up all those spin configurations, we can write, e.g. for $I = 1/2$, the states as combinations of $|\uparrow\rangle \equiv |1/2, 1/2\rangle$ and $|\downarrow\rangle \equiv |1/2, -1/2\rangle$ states. The permutation symmetry thus can be determined by hand. This concept is best understood by studying certain examples like the hydrogen molecule.

Example 3.1 The hydrogen molecule H_2 consists of two fermionic nuclei, the total nuclear spin is hence either $I_{\text{tot}} = 1$ or $I_{\text{tot}} = 0$. The $I_{\text{tot}} = 1$ states are

$$|\uparrow\uparrow\rangle, \quad |\downarrow\downarrow\rangle, \quad \frac{1}{\sqrt{2}}(|\uparrow\downarrow\rangle + |\downarrow\uparrow\rangle).$$

The anti-symmetric combination has $I_{\text{tot}} = 0$ and is written as $\frac{1}{\sqrt{2}}(|\uparrow\downarrow\rangle - |\downarrow\uparrow\rangle)$. Remember that, e.g., $\hat{I}^2|\uparrow\downarrow\rangle = \sqrt{1(1+1)}|\uparrow\downarrow\rangle$, which defines the normalization prefactor in the last two wave functions. The permutation symmetry is obvious: The three $I_{\text{tot}} = 1$ states are symmetric, i.e. they transform each as the trivial representation of S_2 , whereas the $I_{\text{tot}} = 0$ state is anti-symmetric and is described by the sign representation. In molecular symmetry, one usually uses A for the trivial representation and B for the sign one, such that the permutation representation is $3A + B$. The joint representation is consequently given as

$$(3A, \mathcal{D}_1) \oplus (B, \mathcal{D}_0).$$

Obviously, for systems of larger N and especially larger individual spin quantum number, this method becomes increasingly difficult.

In order to circumvent the problem of large N , T. Oka [44] suggested a method based only on the coupling of angular momentum with the advantage of using of (3.3), which is rather simple and straightforward also for larger N and I . However, the disadvantage is that it completely omits the permutation symmetry which still has to be done by the above presented pedestrian way. Furthermore, particularly for deuterated species, Hugo [45] noted certain ambiguities in the relation of total spin quantum number and permutation symmetry. In the example of molecular hydrogen, Example 3.1, there is actually a one-to-one correspondence $X \leftrightarrow \mathcal{D}_I$ in the sense that to each permutation symmetry species there is one total spin quantum number. In more advanced examples, the author of [45] showed that this correspondence must be dropped, one spin quantum number can be associated with different permutation symmetries. One of the peculiar cases is presented in Example 3.2.

Example 3.2 The D_3 molecule consists of three identical bosonic deuterium nuclei with a spin of $I = 1$. By using (3.3), the total spin representation is calculated to be

$$\mathcal{D}_0 \oplus 3\mathcal{D}_1 \oplus 2\mathcal{D}_2 \oplus \mathcal{D}_3.$$

If we set up all the according $3^3 = 27$ spin functions, we find the permutation symmetry

$$10A_1 \oplus A_2 \oplus 8E$$

in the corresponding symmetric group S_3 , see Table 4.1. Thus, a one-to-one correspondence is impossible: Each of the three $I_{\text{tot}} = 1$ sets of states span the $A_1 \oplus E$ representation, the other spins are again in a one-to-one correspondence:

$$(A_2, \mathcal{D}_0) \oplus (3(A_1 \oplus E), 3\mathcal{D}_1) \oplus (5E, 2\mathcal{D}_2) \oplus (7A_1, \mathcal{D}_3).$$

In particular in the study of selection rules for reactions, such ambiguities can lead to an impossibility of defining symmetry correlations between reactant and product states. In the examples formulated in [44], these problems did not occur since only spin $I = 1/2$ was considered and the determined selection rules for the according reactions turned out to be equivalent to those calculated by using the pedestrian way years before by [43].

In the following sections, we will explain in detail the method we established in [8], which unifies the spin and permutation symmetry and solves the ambiguity problem in a mathematical elegant and still very practicable approach.

3.1.2 Unitary Symmetry

For the description of the unification of spin and permutation symmetry, we start with a detailed inspection of the symmetry of the nuclear spin itself. As discussed above, an initial assumption is the separation of all other degrees of freedom from the nuclear spin part, so that the individual spins are fully uncoupled. Considering a single spin I , the according states $|I, M_I\rangle$ span the respective Hilbert space, say, \mathcal{H} . The Hilbert space is in general spanned by all eigenfunctions of the system's Hamiltonian, which in this case only restricts the spin quantum number. Therefore, the $2I + 1$ states of different M_I are not distinct in energy and hence there is an intrinsic symmetry that can interchange them. The most general symmetry group for that purpose is the unitary group of dimension $d = 2I + 1$. It includes all unitary operations on the Hilbert space, i.e. for $U \in U(d)$, $U : \mathcal{H} \rightarrow \mathcal{H}$ with $U^*U = UU^* = E$, where E is the identity operation and U^* represents the adjoint of U . These operations preserve the probability amplitude of any wave function indicating that they are the most general symmetry operations in ordinary quantum mechanics.

Representation theory allows us to label irreducible representations of $U(d)$ by their highest weights ω , corresponding to a certain partition $\lambda(\omega)$ (see Sect. 2.1.2 and [19, 22, 49]). For $U(d)$, the partition $\lambda = \{\lambda_1, \lambda_2, \dots, \lambda_d\}$ is restricted to be [22]

$$\lambda_1 \geq \lambda_2 \geq \dots \geq \lambda_d \geq 0, \quad (3.5)$$

where the λ_i are all integers. A set of λ_i hence unambiguously defines an irreducible representation of the unitary group. The d dimensional irreducible representation is called the standard representation and is actually spanned by the $d = 2I + 1$ spin functions $|I, M_I\rangle$. The appropriate partition label is $\{1, 0, \dots, 0\}$, where one conventionally omits the zeros, so that one abbreviates it to $\{1\}$ for any dimension. To relate the labels of $U(d)$ to the common spin labels of the Wigner-D-matrices in $SO(3)$, we use that $SO(3) \subset U(d > 1)$ and hence the irreducible representations of the larger unitary group can be expressed in terms of the irreducible representations of $SO(3)$. These *branching rules* are standard results of representation theory and one can use, e.g., the SCHUR program [50] for their application. As an example, the $U(2)$ labels $\{\lambda_1, \lambda_2\}$ correspond to the representation of $I = (\lambda_1 - \lambda_2)/2$. In a

more physical interpretation, the branching reveals how the functions spanning the irreducible representation of $U(d)$ behave under rotations in usual three-dimensional space. This behavior expresses itself as irreducible representations of $SO(3)$, labeled by the common spin labels I . In general the branching is not in a one-to-one sense, i.e. an irreducible representation of the unitary group can be reducible in the $SO(3)$ group. For the d -dimensional $\{1\}$ representation, the branching is – as expected – always to the respective $I = (d - 1)/2$ irreducible representation of $SO(3)$.

If a group G_1 is a subgroup of, say, G_2 , the irreducible representations of both are connected via **branching rules**. Since the group G_1 can be obtained by erasing specific elements of G_2 , the irreducible representations of the latter naturally creates, most likely, reducible representations of the smaller group. For continuous groups, mathematical literature provides these rules based on the respective algebras, see, e.g., [51] for some examples. For finite groups, a corresponding scheme is reviewed in Sect. 4.1, where we consider particular examples of these **restricted** representations for permutation groups.

Conclusively, the single-particle spin wave function spans an irreducible representation of $U(2I + 1)$, which equivalently is described by the Wigner-D-matrices \mathcal{D}_I of $SO(3)$. Considering a collection of spins, as in a molecule, they couple to a specific total spin. This coupling can be expressed as the tensor product of the respective representations. Therefore, a collection of N nuclei of spin I span the tensor product representation

$$\underbrace{\{1\} \otimes \{1\} \otimes \dots \otimes \{1\}}_{N \text{ copies}} \quad (3.6)$$

on the respective product Hilbert space [24]

$$\mathcal{H}_d^N := \underbrace{\mathcal{H}_d \otimes \dots \otimes \mathcal{H}_d}_{N \text{ copies}}. \quad (3.7)$$

Any tensor product representation can be decomposed into a direct sum of irreducible representations, described by the Littlewood–Richardson coefficients [52] (for a modern review see, e.g., [19] or [18]). The most simple way to determine these coefficients uses the technique of Young diagrams already introduced briefly in Sect. 2.1.2.

Example 3.3 For better understanding take the H_2 molecule, where the two protons carry spin $I = 1/2$. Individually, they are hence described by the $\{1\}$ irreducible representation of $U(2)$, whereas their collective behavior under this group is characterized by the product representation, which we describe schematically by the Young diagrams

$$\left. \begin{aligned} \square \otimes \square &= \square \square \oplus \boxed{\square} \\ \{1\} \otimes \{1\} &= \{2\} \oplus \{11\} \end{aligned} \right\} \xrightarrow{\text{U(2) } \rightarrow \text{SO(3)}} I_{\text{tot}} = 1, 0,$$

where the second row indicates the $\{\lambda_1 \lambda_2\}$ labels of the irreducible representations of U(2). In addition, we used the simple branching rule $I_{\text{tot}} = (\lambda_1 - \lambda_2)/2$ for $\text{U}(2) \rightarrow \text{SO}(3)$. In terms of the numbered Young tableaux, a single box of U(2) can carry a number 1 or 2 and hence the product must be written as:

$$\left. \begin{aligned} \boxed{1} \otimes \boxed{1} &= \boxed{1} \boxed{1} \\ \boxed{1} \otimes \boxed{2} &= \boxed{1} \boxed{2} \oplus \boxed{\frac{1}{2}} \\ \boxed{2} \otimes \boxed{1} &= \emptyset \\ \boxed{2} \otimes \boxed{2} &= \boxed{2} \boxed{2} \end{aligned} \right\} = \underbrace{\boxed{1} \boxed{1} \oplus \boxed{1} \boxed{2} \oplus \boxed{2} \boxed{2}}_{=\{2\}} \oplus \boxed{\frac{1}{2}}_{=\{11\}}$$

Here, \emptyset indicates the product to be not compatible to the general rules of numbered Young tableaus in U(2). We can now directly infer from the number of diagrams of certain shape the branching to SO(3) since this number is simply the dimension of the SO(3) irreducible representation. With this method, we therefore have found the very same result as by using the pedestrian way in Example 3.1. Notice that the use of the numbered tableaus is not necessary since dimension formulas exist for the unnumbered Young diagrams. This method is fully generalizable and one must not write down all spin functions by hand.

Conclusively, a collection of particles with spin I , each described by the $\{1\}$ irreducible representation in $\text{U}(2I+1)$, forms a tensor product representation in that group. This tensor product can be decomposed into a direct sum of representations and is related to the common total spin quantum number by the branching of $\text{U}(2I+1) \rightarrow \text{SO}(3)$.

3.1.3 Permutation Symmetry

Exchanging identical nuclei obviously leads to another kind of symmetry in molecules. The finite group of permutations is a valid symmetry group and is usually called the complete nuclear permutation group (see Chap. 2). It is intimately connected to the Hilbert space of (3.7) since all single-particle Hilbert spaces are indistinguishable. Hence, the according functions spanning this product space must also span a certain representation of the symmetric group of N particles, S_N . The operations of S_N and $\text{U}(d)$ indeed commute since the permutation does not act on an individual spin but rather on the set of particles. This indicates the total symmetry group for the N particles of spin I to be the product group $\text{U}(d) \times S_N$.

Furthermore, this suggests composite, joint representations of the two groups to exist (cf. (3.4)). This is actually the subject of the Schur–Weyl duality theorem,

which we present in the next section. Before, we shortly review the properties of the permutation group for the nuclear spins.

In order to distinguish and label the irreducible representations, in standard mathematical textbooks like [18] or [19] but also in molecular theory publications, e.g. Sect. 9.4.5 of [14], Young diagrams are introduced for a graphical illustration of the irreducible representations. As we showed in Sect. 2.1.2, they are used in a very similar manner as for unitary groups. The respective labels in terms of partitions (λ) can be “translated” in the more common terminology of molecular symmetry,² like used in, e.g., [14]. Since there exists an overwhelmingly large variety of textbooks on the subject of Young diagrams for the symmetric group, we will not discuss them in every detail. Instead, we focus on a method to find the dimension of a certain irreducible representation, illustrated by a Young diagram. This will be used for some of the examples in the next sections.

In general, the dimension is given by the number of Young tableaus, which are distinguished by their numberings. However, this numbering and the respective counting becomes increasingly difficult for larger dimensional irreducible representations. To avoid these lengthy calculations, one conveniently defines the so-called *hook length* (cf. [24, p. 335]): Each box of a Young diagram gets a label (i, j) , where i is the row and j the column of the diagram. The hook length $H_{(i,j)}$ is defined as the number of boxes below and to the right of the (i, j) box. The dimension of an irreducible representation (λ) of S_N is then given as [53]

$$\dim(\lambda) = \frac{N!}{H^\lambda}, \quad (3.8)$$

where H^λ is the product of all hook lengths in the respective Young diagram, say, Y^λ and is hence given as

$$H^\lambda := \prod_{(i,j) \in Y^\lambda} H_{(i,j)}. \quad (3.9)$$

Actually, the hook length can also be used to define the dimension of an irreducible representation $\{\lambda\}$ in the unitary group $U(d)$. There, the dimension is given by

$$\dim\{\lambda\} = \frac{N_d^{\{\lambda\}}}{H^\lambda}, \quad (3.10)$$

where N_d is defined as

$$N_d^{\{\lambda\}} = \prod_{(i,j) \in Y^\lambda} (d - i + j).$$

With these simple formulas we can obtain the dimensions of an irreducible representation in a simple way. Notice that in both groups the dimension does not

²To avoid any confusion, we use parentheses () for the partitions of the permutation groups. For the unitary group we use curly brackets {} instead.

unambiguously define the irreducible representation. Various partitions can have the same dimension.

Example 3.4 Consider the symmetric group S_4 again as an example (see Example 2.2). We choose for illustration of the dimension formula of (3.8) the irreducible representation with the partition (31). The hook lengths (3.9) are best depicted in the non-standard Young tableau

4	2	1
1		

Therefore $H^{(31)} = 8$ and $N! = 24$, which results (3.8) in $\dim(31) = 3$.

We can also consider the {31} irreducible representation of $U(2)$ for the use of the dimension formula for the unitary groups. The hook length is calculated as in the case of the symmetric group. The values for $(d - i + j)$ are given by:

2	3	4
2		

and their product is $N_d^{\{31\}} = 24$, such that the dimension is $\dim\{31\} = 3$, which is supported by the branching to $SO(3)\{31\} \rightarrow J = 1$.

At the beginning of this section, we introduced the complete nuclear permutation group as the symmetry group of any molecule with a fixed number of identical particles. Although this symmetry is generally valid, we already encountered the fact that the electronic motion generates a potential energy surface, which can restrict the number of feasible permutation (-inversion) operations (see Sect. 2.2 and [30]). This restricted, molecular symmetry group is a proper subgroup of the complete nuclear permutation-inversion group. Therefore a discussion of the complete nuclear permutation group for the nuclear spins, where inversion is not acting, is totally general and we will focus on that for the moment. In Chap. 4, we will discuss in more detail subgroups of the full permutation-inversion groups.

Next, we turn to the discussion of the Schur–Weyl duality theorem, which states the correlation of the permutation symmetry and the unitary symmetry in systems of N particles of certain spin I .

3.2 Schur–Weyl Duality

The Schur–Weyl duality theorem is a result from representation theory, which in the case of the Hilbert space of (3.7) states which representations of $U(d)$ and of S_N are spanned by the set of states that span the according Hilbert space. Actually, Schur–Weyl duality is also adaptable for other pairs of symmetry groups but we here use only its version for $U(d) \times S_N$. For the correlated, joint representations, we use the notation introduced in Sect. 3.1.1, namely $(\alpha X, \beta \mathcal{D}_I)$, but now generalize it to $(\alpha(\lambda), \beta\{\lambda'\})$ for the partition labels of S_N and $U(d)$ respectively. The duality

theorem states that the space of (3.7) is spanned by functions also spanning the following direct sum of joint representations [46, 47]

$$\Gamma_d^{(N)} = \bigoplus_{\lambda \vdash N}^{\ell(\lambda) \leq d} ((\lambda), \{\lambda\}), \quad (3.11)$$

where $\lambda \vdash N$ denotes the partition λ of N and $\ell(\lambda) = p$ is the length or depth of the partition, counting the non-zero integers. Therefore the joint representation consists of a pair of the same partitions. A proof of this theorem is beyond the scope of this work. We refer to the textbook of [19] or other textbooks of representation theory.

The joint representation $((\lambda), \{\lambda\})$ is meant to include multiplicities, which are calculated by combining all (numbered) Young tableaus of the S_N partition with all of the $U(d)$. In particular, all of the $k = \dim \{\lambda\}$ diagrams have to be combined with each of the $l = \dim (\lambda)$ tableaux and vice versa. This straightforwardly gives the respective multiplicities α and β . In the next section, we will apply this theorem to some examples, where the dimensional analysis becomes clearer.

Conclusively, the Schur–Weyl duality induces a one-to-one correspondence of irreducible representations of S_N and $U(d)$. The partition labels of $U(d)$ can be called generalized spin quantum numbers, hence there exists an one-to-one correspondence of the symmetric group representations and the generalized spin quantum numbers. To correlate the latter to the usual spin labels, we need the according branching rules to $SO(3)$. This explains the possible loss of the one-to-one correspondence to the usual spin labels since one $U(d)$ label can correlate to several I labels of $SO(3)$. Nevertheless, with the Schur–Weyl duality, we can calculate the irreducible representations of any N and any d in a very simple way.

3.2.1 Application of the Duality Theorem

As a first example of applying the Schur–Weyl duality, take again the molecular hydrogen as in Examples 3.1 and 3.3. The according joint representation is given as

$$\begin{aligned} \Gamma_2^{(2)} &= ((2), \{2\}) \oplus ((11), \{11\}) = (\boxed{}, \boxed{}) \oplus \left(\boxed{}, \boxed{} \right) \\ &= (\underset{\uparrow\downarrow}{[1 \ 2]}, \underset{\downarrow\downarrow}{[1 \ 1]}) \oplus (\underset{\downarrow\downarrow}{[1 \ 2]}, \underset{\uparrow\downarrow}{[2 \ 2]}) \oplus (\underset{\uparrow\downarrow+\downarrow\uparrow}{[1 \ 2]}, \underset{\uparrow\downarrow}{[1 \ 2]}) \oplus \left(\underset{\uparrow\downarrow-\downarrow\uparrow}{\begin{array}{c|c} 1 & 1 \\ \hline 2 & 2 \end{array}} \right) \\ &= (3A, \mathcal{D}_1) \oplus (B, \mathcal{D}_0), \end{aligned}$$

where we indicated in addition the usual spin labels $\uparrow\downarrow$ for each joint irreducible representation. In the last step, we used the branching rule for $U(2) \rightarrow SO(3)$. Instead of using the numbered Young tableaus, the multiplicities can also directly be calculated by the dimension formulas of (3.8) and (3.10)

$$\dim(2) = 1, \dim\{2\} = 3 \quad \text{and} \quad \dim(11) = \dim\{11\} = 1$$

$$\Rightarrow \alpha_{(2)} = 3, \beta_{\{2\}} = \beta_{\{11\}} = \alpha_{(11)} = 1.$$

Two other examples are shown in Tables 3.1 and 3.2. The H_5^+ cation of Table 3.1 is particularly interesting in reactive collisions of the type $H_3^+ + H_2 \rightarrow (H_5^+)^* \rightarrow H_3^+ + H_2$. This reaction will be studied in more detail in Chap. 4. The intermediate H_5^+ complex consists of five fermionic protons and as such the respective symmetry group for the Schur–Weyl duality is $S_5 \times U(2)$. Therefore the branching to the usual spin labels of $SO(3)$ is straightforward and we show the joint representation in the last row of Table 3.1. The spin-angular momentum part of the joint representation has already been found by [44] using the angular momentum coupling scheme. However, with this scheme, no information on the permutation symmetry can be inferred. Indeed, the pedestrian way is capable of calculating both spin and permutation symmetry. Nevertheless, our method represents a mathematically rigorous and fast method to determine the respective symmetry labels and is of particular use for larger molecules, where the pedestrian way obviously becomes exceedingly lengthy.

As an example of larger individual spin, we choose the deuterated isotopologue of H_5^+ , namely D_5^+ , which is encountered in the same kind of reactions. Here the use of the duality becomes particularly apparent: The symmetry group is $S_5 \times U(3)$ and the branching to $SO(3)$ reveals the loss of the one-to-one correspondence of conventional spin quantum number and permutation symmetry. This is shown in the last row of Table 3.2, where the joint representation is indicated. From a permutation point of view, the A_1 representation is correlated to spins of $I_{\text{tot}} = 1, 3, 5$. In turn, from a spin perspective, the spin $I_{\text{tot}} = 1$ spans the permutation representation $3(A_1 \oplus G_1 \oplus H_1 \oplus H_2)$.

In both tables, we calculated the multiplicities α and β by using the respective dimension formulas for the Young diagrams to avoid the lengthy listing of all possible numbered tableaus.

3.3 Conclusion

In order to find a consistent theory for rotational *and* permutation symmetry of nuclear spin states in molecules, we utilize a rather formal mathematical result of representation theory, namely the Schur–Weyl duality theorem. It provides a prescription for combining irreducible representations of certain symmetry groups in an unambiguous way if the system’s Hamiltonian is subjected to the respective product symmetry group.

Considering independent nuclear spins in molecules in a field-free environment, these two symmetry groups are (i) the unitary group of dimension $d = 2I + 1$, where I is the nuclear spin, and (ii) the symmetric group of degree N , S_N , where N is the number of identical nuclei of that spin. The use of the unitary group formally generalizes the more common spin labels in the spatial rotation group $SO(3)$, which enables to straightforwardly use the duality theorem. The theorem states that in the product

Table 3.1 The nuclear spin symmetry of the H_5^+ ion in terms of Young diagrams, permutation group representations (λ) and the $\text{U}(2)$ unitary symmetry $\{\lambda\}$ for the composition of spin-1/2 nuclei. The last row shows the joint representation of permutation group and $\text{SO}(3)$ including all multiplicities. The common spin labels of $\text{SO}(3)$ are calculated by the branching $\text{U}(2) \rightarrow \text{SO}(3)$. The table is a slightly changed version of Table II in [8]

Young diagram	S_5		$\text{U}(2)$		
	(λ)	$\dim(\lambda)$	Label	$\{\lambda\}$	$\dim\{\lambda\}$
	(5)	1	A_1	{5}	6
	(4,1)	4	G_1	{41}	4
	(3,2)	5	H_1	{32}	2
$\text{H}_5^+: (6A_1, \mathcal{D}_{5/2}) \oplus (4G_1, 4\mathcal{D}_{3/2}) \oplus (2H_1, 5\mathcal{D}_{1/2})$					

Table 3.2 The nuclear spin symmetry of the D_5^+ ion, the fully deuterated isotopologue of H_5^+ (see Table 3.1). The deuterons carry a spin of $I = 1$, which induces the use of $\text{U}(3)$ as the unitary symmetry group. The labels are the same as in Table 3.1. The table is a slightly changed version of Table III in [8]

Young diagram	S_5		$\text{U}(3)$		
	(λ)	$\dim(\lambda)$	Label	$\{\lambda\}$	$\dim\{\lambda\}$
	(5)	1	A_1	{5}	21
	(41)	4	G_1	{41}	24
	(32)	5	H_1	{32}	15
	(311)	6	I	{311}	6
	(221)	5	H_2	{221}	3
$\text{D}_5^+: (21A_1, \{ \mathcal{D}_5 \oplus \mathcal{D}_3 \oplus \mathcal{D}_1 \}) \oplus (24G_1, 4\{ \mathcal{D}_4 \oplus \mathcal{D}_3 \oplus \mathcal{D}_2 \oplus \mathcal{D}_1 \})$ $\oplus (15H_1, 5\{ \mathcal{D}_3 \oplus \mathcal{D}_2 \oplus \mathcal{D}_1 \}) \oplus (6I, 6\{ \mathcal{D}_2 \oplus \mathcal{D}_0 \}) \oplus (3H_2, 5\mathcal{D}_1)$					

symmetry group $S_N \times U(d)$, the composite nuclear spin states span the representation defined in (3.11), which gives a one-to-one correspondence of the irreducible representations of unitary and symmetric group. This correspondence has not been obtained before, in particular [45] showed the correlation of $SO(3)$ and S_N labels to break down in cases, when individual nuclear spins of $I > 1/2$ are considered. By using the generalized unitary symmetry group we re-established the correspondence and in turn can explain its loss for the $SO(3)$ labels. The unitary groups always ($d > 1$) include the spatial rotations as a subgroup such that branching rules exist to correlate the usual I labels to the partition labels of $U(d)$. These branching rules shows the possibility that a single irreducible representation of $U(d)$ can decompose into a reducible representation of $SO(3)$, such that a single permutation symmetry is related to one of $U(d)$ but possibly to several $SO(3)$ representations, which explains the ambiguities found before. From a physical perspective, the $U(d)$ symmetry is motivated from the observation that spin is an intrinsic property of the nuclei and does not depend on the three-dimensional space of the observer, hence assuming an $SO(3)$ spatial rotation group does restrict the full symmetry group. For nuclear spin states that are not subjected to any kind of force, the most general probability amplitude conserving symmetry group is therefore the unitary group in d dimensions.

The main advantage of using the duality of (3.11) is the application to larger species and especially to larger individual spins. In particular, the technique of Young diagrams renders the Schur–Weyl method highly useful in difference to the pedestrian way, which until now was applied if both symmetry groups were considered. In particular, we resolved the problems found in [45], where the pedestrian way showed ambiguities in the relation of common spin labels and the according permutation symmetry.

In the next chapter we will explore furthermore the use of the Schur–Weyl theorem for reactive collisions, where different pathways for a single reaction are considered from a symmetry perspective. From the discussion in this chapter, especially the use of Young diagrams is expected to be very useful in studying these kinds of reactions.

Chapter 4

Reactive Collisions

Abstract In this chapter, the application of the Schur–Weyl theorem to reactive collisions is discussed. In particular, reactions involving hydrogen are discussed. The most famous among them is possibly the $\text{H}_3^+ + \text{H}_2$ reaction, which forms an intermediate H_5^+ complex, which subsequently dissociates again. The symmetry properties of the intermediate complex are discussed and are found to be crucial for the selection rules for state-to-state transitions in this prototypical reactive collision. The respective symmetry properties are results from the potential energy surface of the full system. In addition to selection rules, we also discuss statistical properties of the state-to-state transitions in these reactions. The most important result of the calculations is actually the possibility to gain insights into the intermediate symmetry properties from experiments on the initial and final states of the reactants.

In the opening of the preceding chapter, identical-particle permutation symmetry was introduced to be one of the main concepts in many-body physics and chemistry. In the case of single molecules we found the nuclear spin angular momentum symmetry and the respective permutation symmetry to be connected via the mathematical concept of the Schur–Weyl duality. In the introductory part to that chapter, we already mentioned two main implications of the nuclear spin states and their respective symmetry: (i) The ro-vibrational states of molecules get spin-statistical weights from the number of possible combinations to the nuclear spin states to fulfill Pauli’s exchange principle; (ii) Due to certain conservation rules, different nuclear spin states behave as distinct chemical species influencing chemical reaction pathways. These two aspects form the basis of the upcoming discussion.

In general, reactions of the type $A + BC \rightarrow AB + C$ are described via so-called rate equations describing the change of the concentrations, say $[X]$, in time [37]

$$-\frac{d[A]}{dt} = \frac{d[C]}{dt} = k(T) \cdot [A] \cdot [BC].$$

Here, $k(T)$ is the rate coefficient defining the speed of the reaction. In the present study, we will examine the influence of identical-particle permutation (and spin angular momentum) symmetry on this rate equation, whereas we do not enter the discussion of, e.g., temperature or energy dependence. As already indicated in Chap. 3, the symmetry of the nuclear spin states define distinct species of the same molecule.

They are characterized by their total nuclear spin and correlated permutation symmetry. The respective molecular states are products of the nuclear spin part, defining the species, and the ro-vibrational wave function.¹ We avoid here any dynamical treatment of the ro-vibrational states, we only assume them to be characterized by the irreducible representations of the nuclear permutation-inversion group of the respective molecules. In the second part of this work, especially in Chap. 6 of Part II, we discuss a method for this characterization particularly for pure rotational states. Consequently, we define the states of the reactants only by their permutation-inversion symmetry and their correlated spin wave function defining distinct species.

Due to the selection rules of radiative transitions, in particular the conservation of total spin angular momentum, the species are not inter-convertible by this type of transition. Actually, this is one reason for calling them distinct species. However, they can eventually be interchanged by reactions, where all nuclei are potentially exchanged in an intermediately formed complex before they again dissociate. Due to this *scrambling*, the nuclear spin species of one reactant can change if the spin of the reaction partner change accordingly.

The prototypical reaction is the thermoneutral $\text{H}_3^+ + \text{H}_2 \rightarrow \text{H}_2 + \text{H}_3^+$ reaction (see, e.g. [37, 43–45, 54–62]), which is of particular interest in, e.g., chemical networks of astrophysical models. It is thought to be the major mechanism in the cooling of molecular hydrogen in the interstellar medium. Usual radiative and collisional cooling of molecular hydrogen is not capable to convert H_2 into its global ground state of angular momentum $J = 0$ with spin $I = 0$ (*para-H*₂), although the $J = I = 1$ *ortho* state is about $E/k_B = 175\text{ K}$ higher in energy. Indeed, this energy difference is much larger than usual kinetic temperatures ($\sim 10\text{ K}$) in cold molecular clouds, which renders the ortho-to-para conversion highly important in the study of any kind of reaction in these environments. If the H_2 molecule collides with H_3^+ however, it can form a complex H_5^+ (see Fig. 4.1) before it dissociates again. The symmetry group of the complex is decisive if the protons are all scrambled and spin can be interchanged between the reaction partners. This statement is the starting point of the following discussion in which we partly reconsider what has been done in [43–45, 57] but add the possibility of various different intermediate symmetries to the discussion. This has been done partially also by [62] although there the main focus is on the spectroscopy of H_5^+ itself.

Conclusively, the symmetry of all participants in the reaction, including the intermediately formed complex influences (i) the possible state-to-state reaction pathways and (ii) give inherent probabilities to each of these ways. In order to incorporate all the different symmetries, we start the following chapter with a review on the topic of induced and subduced representations, where larger and smaller permutation groups are linked. This mathematical concept then is applied first – as a proof of principle – to the simple example of $\text{H}_2 + \text{H}^+ \rightarrow \text{H}_3^+ \rightarrow \text{H}^+ + \text{H}_2$. Afterwards, we discuss the famous reaction of $\text{H}_3^+ + \text{H}_2 \rightarrow \text{H}_2 + \text{H}_3^+$ mentioned above. In following the discussion of the preceding chapter, we will additionally discuss the implications of exchanging the protons by deuterons.

¹The molecules are assumed to be in their electronic ground state in the following discussion.

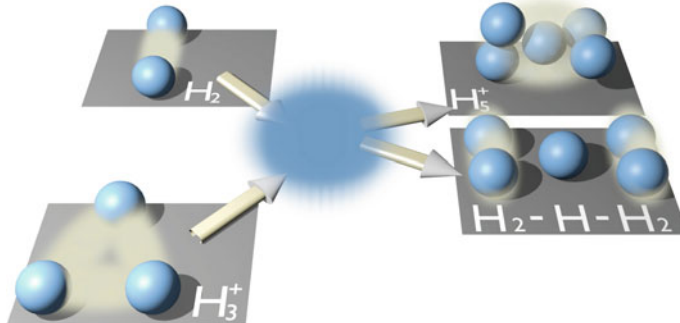


Fig. 4.1 Two reaction pathways for the famous $\text{H}_3^+ + \text{H}_2$ reaction. An intermediate complex is formed but there are two possibilities of its internal dynamics: (i) All protons might scramble (upper pathway) or (ii) only one proton is allowed to move between two subunits in a $\text{H}_2 - \text{H} - \text{H}_2$ complex

4.1 Representation Theory in Reactions of Small Molecules

4.1.1 Mathematical Preliminaries

To describe the symmetry properties of the formation of a molecular complex in a specific reaction, the main mathematical concept is that of induced representations. To start with, consider the molecular complex to be described by some molecular symmetry group G , while the reaction partners are jointly described by some group $H \subset G$. In G , the molecular states form an irreducible representation, Γ_G , which can be expressed in the smaller group by restriction. In particular, the restricted or *subduced* representation can now be reduced in terms of the irreducible representations of the smaller group H by using the standard reduction formula already introduced in Chap. 2, (2.2)

$$a_j = \frac{1}{|H|} \sum_{h \in H} \chi_G[h] \chi_H^{(j)}[h]^*, \quad (4.1)$$

where χ_G and $\chi_H^{(j)}$ are the characters of Γ_G and $\Gamma_H^{(j)}$ respectively. The latter denotes the j th irreducible representation of H and the factor a_j is its multiplicity in Γ_G . The subduced representation is conventionally written as $\Gamma_G \downarrow H$. Furthermore, the opposite situation might also happen, i.e. the molecular states of the subgroup H *induces* a certain representation in the larger group. For this, the Frobenius reciprocity theorem [63] states that the multiplicity of the irreducible representations Γ_H^j in the subduced representation, a_j , equals the multiplicity of the irreducible representation Γ_G in the induced representation $\Gamma_H^{(j)} \uparrow G$. From that one can also infer the characters of the induced representation (see, e.g., [18, 19])

Table 4.1 Irreducible representations of the symmetric group of degrees two and three, S_2 and S_3

S_2	E	(12)
A	1	1
B	1	-1

(a) Character table of S_2

S_3	E	(12)	(123)
A_1	1	1	1
A_2	1	-1	1
E	2	0	-1

(b) Character table of S_3

$$\chi_{ind}(g) = \frac{1}{|H|} \sum_{x \in G} \tilde{\chi}(x^{-1}gx) \quad \text{with } \tilde{\chi}(g) = \begin{cases} \chi_H(g) & g \in H \\ 0 & \text{else} \end{cases}, \quad (4.2)$$

where χ_H is the character in the group H , and $|H|$ is its order. With these characters, one can again find the decomposition into the irreducible representations by using the standard reduction formula.

Example 4.1 Consider the symmetric group of degree three $S_3 = G$ and its subgroup $S_2 = H$. The restricted, subduced representations of the irreducible ones of S_3 are found by using the reduction formula of (4.1) (see Table 4.1)

$$A_1 \downarrow S_2 = A; \quad A_2 \downarrow S_2 = B; \quad E \downarrow S_2 = A \oplus B$$

A bit more effort is needed to find the induced representation: For example, the induced characters for the A representation of S_2 are calculated to be:

$$\begin{aligned} \chi_A(E) &= \frac{1}{2} (\chi(EEE) + 3\chi((12)E(12)) + 2\chi((123)E(132))) = 3 \\ \chi_A((12)) &= \frac{1}{2} (\chi(E(12)E) + \chi((12)(12)(12)) + 0) = 1 \\ \chi_A((123)) &= \frac{1}{2} \cdot 0 = 0 \end{aligned}$$

In the first row, we only show one representative element of the classes in S_3 . In the other rows we only show the non-vanishing sum elements. Hence, the characters of the representation $A \uparrow S_3$ are $\{3, 1, 0\}$ for the classes of E , (12) , (123) respectively (see Table 4.1). From standard reduction we then obtain $A \uparrow S_3 = A_1 \oplus E$, which indeed can also be directly inferred from the Frobenius reciprocity theorem.

With these tools we can “follow” reaction paths in terms of state symmetries. In general, there will be no one-to-one correspondence between initial and final state symmetry since a single initial irreducible representation is much likely decomposed

at a certain step of the path. This eventually gives rise to a probability for a state-to-state reaction based on simple combinatorial arguments.

In the following, we consider reactions of the type $A + BC \rightarrow ABC \rightarrow AB + C$. An initial quantum state of one of the reactants undergoes certain transitions to states of the intermediately formed complex. In a second step it hence evolves in another state of the resulting molecules. We call this procedure state-to-state **reaction path**. In determining the irreducible representations spanned by the respective molecular states, we **follow** this path in terms of symmetry. This has to be seen in contrast to (chemical) reaction paths, where different products or intermediate complexes are formed.

4.1.2 Single Molecules

To start with, note once again that the total molecular wave function is usually separated into an electronic, a ro-vibrational and a nuclear spin part. For convenience, we consider all molecules here to be in their electronic ground state and to be anti-symmetric under the permutation of electrons. Therefore, we can restrict ourselves to the nuclear wave function $\psi = \psi_{\text{rovib}}\psi_{\text{nspin}}$. For fermionic nuclei, we require the representation of the molecular symmetry group spanned by this function to be the anti-symmetric one. With the Schur–Weyl duality, we can straightforwardly find the irreducible representations of the nuclear spin part. The ro-vibrational wave function hence must span the so-called *conjugated* irreducible representation (see, e.g., the classic textbook of [64]). By using the Young diagrams for the permutation symmetry of the nuclear spin part, they can be found by interchanging the number of rows with the number of columns.² For example, in a molecule with S_2 symmetry group, the nuclear spin wave function of $A \equiv (2)$ permutation symmetry couples to ro-vibrational states of $B \equiv (11)$ symmetry. In general, states of a certain angular momentum may decompose into several irreducible representations, which, if possible, individually couple to their spin counterpart. In the following, we give one textbook example of rotational states coupled to the nuclear spin wave functions.

Molecular Hydrogen H₂ The molecular symmetry group of H₂ is generally known as $D_{\infty h}(M) = S_2 \times \{E, E^*\}$, where E^* is the inversion operation (see Table 4.2). In the preceding chapter, we showed the nuclear spin states to span the joint representation $(3A, \mathcal{D}_1) \oplus (B, \mathcal{D}_0)$ in the product group $S_2 \times \text{SO}(3)$. Since the inversion operation does not act on spin states, we can calculate the nuclear spin permutation symmetry in the full $D_{\infty h}$ group by induction (see Table 4.2). We find $A \uparrow D_{\infty h} = \Sigma_g^+ \oplus \Sigma_u^-$, and $B \uparrow D_{\infty h} = \Sigma_g^- \oplus \Sigma_u^+$, leading to

²For bosonic nuclei, their spin states couple to ro-vibrational states of the same symmetry since their product is required to be totally symmetric under particle exchange.

Table 4.2 Character table of $D_{\infty h}(M)$ including the nuclear spin representation and the rotational state symmetry. The Pauli allowed representations are marked by $\Gamma_{\text{Pauli}}^{a/b}$. The table is reproduced partly from [14], Table A-18

$D_{\infty h}(M)$	E	(12)	$(E)^*$	(12)*	
Σ_g^+	1	1	1	1	
Σ_u^+	1	-1	1	-1	Γ_{Pauli}^a
Σ_g^-	1	-1	-1	1	Γ_{Pauli}^b
Σ_u^-	1	1	-1	-1	
Γ_{nspin}	8	4	0	0	$(3A + B) \uparrow$ $D_{\infty h}(M)$
\mathcal{D}_J	1	$(-1)^J$	$(-1)^J$	1	

Table 4.3 Nuclear spin weights g_{ns} for the rotational states (Table 4.2) of molecular hydrogen

Γ_{rovib}	Γ_{nspin}	Γ_{tot}	g_{ns}
Σ_g^+	Σ_u^+ / Σ_g^-	Σ_u^+ / Σ_g^-	1/1
Σ_g^-	Σ_u^- / Σ_g^+	Σ_u^- / Σ_g^+	3/3

$$\Gamma_{\text{nspin}} \uparrow D_{\infty h} = 3(\Sigma_g^+ + \Sigma_u^-) + (\Sigma_g^- + \Sigma_u^+).$$

In Table 4.2 we show the characters of the Γ_{nspin} representation for all the elements of $D_{\infty h}$.

Assuming molecular hydrogen to be in its vibrational and electronic ground state, the product of nuclear spin and overall rotational states must form the anti-symmetric representation in the molecular symmetry group. Since inversion has no effect in that respect, the anti-symmetric representations are Σ_u^+ and Σ_u^- .

For the rotational states, we notice that due to the linearity, the appropriate symmetry group is SO(2) describing the two rotational degrees of freedom. The permutation (12) and the inversion E^* both map onto a rotation by 180° and the respective character of the rotation matrix is $(-1)^J$ (see Table 4.2 and Chap. 6 of Part II for details on rotational state symmetries). Therefore, states of even angular momentum $J = 0, 2, 4, \dots$ are described by Σ_g^+ , whereas all odd- J states span the Σ_g^- representation. Therefore, the latter odd- J states couple to the nuclear spin states of Σ_u^- or Σ_g^+ symmetry to form the Pauli-allowed representations. Conversely, the even- J states form Pauli allowed products with Σ_u^+ or Σ_g^- (see Table 4.3). From the nuclear spin weights, we get the well-known 3:1 odd-to-even angular momentum state ratio. This is conventionally known as the ortho-to-para ratio since the odd- J states couple to the spin $I = 1$ states and are called ortho states, whereas the even- J states couple to $I = 0$ and are usually known as para states. Under normal conditions, i.e. thermal equilibrium etc., this 3 : 1 ratio gives the relative weight of the ortho and para states in a gas of H₂ molecules.

We did not use the notion of conjugated representations since in this case there are two Pauli-allowed representations. If we assume only the S_2 subgroup of the full

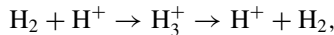
molecular symmetry group, where the total nuclear wave function must span the B representation, even- J states of A symmetry couple to their conjugate representation of B symmetry, while the odd- J states couple to nuclear spin states of A symmetry, respectively. Considering the number of possible couplings, we retrieve the 3 : 1 ratio of nuclear spin weights.

In general, ro-vibrational states couple to the nuclear spin states of a specific symmetry, such that the combined state $\psi_{\text{rovib}}\psi_{\text{nspin}}$ has the required exchange symmetry. The nuclear spin statistical weights, as the number of possible such couplings, can directly be read from the dimension of the nuclear spin representation of the state to which the particular ro-vibrational state couples.

The above example shows two main steps: (i) the use of the induced representations and (ii) the representation of the ro-vibrational states leading to the nuclear spin weights. If the hydrogen molecule reacts with another molecule, we start with either a Σ_g^+ state or a Σ_g^- state to find the state-dependent reaction rates. For other molecules, we can apply the very same method to find the symmetry and the nuclear spin weights of particular rotational or ro-vibrational states. From now on, we skip the calculations of the nuclear spin weights which can easily be done by using Schur–Weyl duality, but focus on the state-to-state transitions in reactions.

4.1.3 A First Example

The simplest reaction incorporating molecular hydrogen is its reaction with the hydrogen cation H^+ , see, e.g., the discussion in [65, 66]. The reactive collision is described as



where intermediately the H_3^+ complex is formed. This is our initial simple example of reactive collisions, where the two reaction partners first form a complex before they dissociate again. We simplify our further discussion to the permutation subgroups of the molecular symmetry group. The extension to include the inversion operations is straightforward as shown for the H_2 molecule. Here, the permutation groups of the reaction are $S_2 \times S_1 \rightarrow S_3 \rightarrow S_1 \times S_2$, where $S_1 = \{E\}$ is the trivial group containing only the identity element. Using the expressions for the induced and subduced representations (4.1) and (4.2) for the group chain

$$S_2 \times S_1 \subset S_3 \supset S_1 \times S_2,$$

we find the following chain of representations (cf. Table 4.1)

$$\begin{aligned} (A, A) &\rightarrow A_1 + E; & A_1 &\rightarrow (A, A); \\ (B, A) &\rightarrow A_2 + E; & A_2 &\rightarrow (A, B); \\ && E &\rightarrow (A, A) + (A, B). \end{aligned}$$

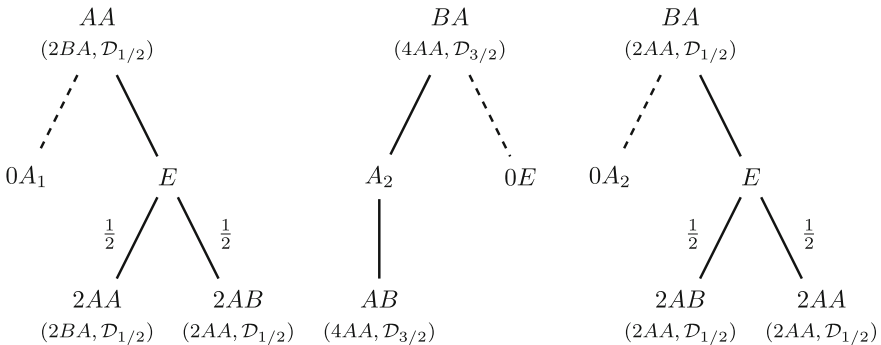


Fig. 4.2 Probabilities for state-to-state transitions in the reaction $H_2 + H^+ \rightarrow H^+ + H_2$. The dashed lines connect to a missing level of the intermediate H_3^+ complex

The nuclear spin weights for $H_2 + H^+$ are $g_{ns}(AA) = 2$, $g_{ns}(BA) = 6$, whereas for the H_3^+ ion they are calculated to be $g_{ns}(A_1) = 0$, $g_{ns}(A_2) = 4$, $g_{ns}(E) = 2$. Now we can set up probability chains for certain state-to-state reactions starting by a fixed initial combination of ro-vibrational and nuclear spin symmetry. The latter is important, since the total spin of the system, say I_{tot} , is conserved during the reaction, whereas the individual spin may get interchanged. This gives the three possible probability trees of Fig. 4.2, where the missing levels of the intermediate H_3^+ complex are included. In particular, H_3^+ spin symmetry dictates the ro-vibrational states to be only of A_2 and E symmetry. The E states couple to a total spin angular momentum of $I_{\text{tot}} = \frac{1}{2}$, whereas for A_2 the total nuclear spin is $I_{\text{tot}} = \frac{3}{2}$. The probability trees therefore suggest the following: If we were able to prepare the H_2 molecule in exactly one quantum state of, e.g., even J , it is described by the symmetric representation in S_2 , namely A . The reaction with the H^+ ion, where it first forms H_3^+ and then dissociates again, gives an equal probability to end in a state of the same symmetry and to change the symmetry to B . In particular this means that it is possible to induce a change of a para state into an ortho state.

Starting from an ortho state of B symmetry gives two possibilities to couple to a total spin: For the coupling to $I_{\text{tot}} = \frac{3}{2}$, there is only one reaction path possible, namely to the same symmetry, whereas for the coupling to $I_{\text{tot}} = \frac{1}{2}$ we find a probability $P(BA \rightarrow AB) = \frac{1}{2}$ and $P(BA \rightarrow AA) = \frac{1}{2}$.

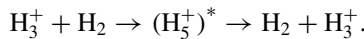
In a mixture of states, where one finds not only one particular quantum state but the usual 3:1 ortho-to-para ratio (normal H_2), these probabilities indeed have to be multiplied by the probability to find the respective initial state (see (4.3) below). Furthermore, an ortho- H_2 molecule can couple in two different ways to the H^+ ion. Thus, there exists a 1:2 ratio between the $I_{\text{tot}} = \frac{1}{2}$ and $I_{\text{tot}} = \frac{3}{2}$ states, inducing that for an ortho- H_2 state, there is a probability of $\frac{1}{3} \cdot \frac{1}{2} = \frac{1}{6}$ to undergo a change to a para state [65]. Here, $\frac{1}{3}$ is the probability to find a BA state of $I = 1/2$, whereas the factor of $\frac{1}{2}$ is the probability to get changed to a state of AA symmetry (see Fig. 4.2).

For calculating real reaction rates, we indeed need to consider the energetics of the particular reaction. We here want to avoid this discussion and refer, e.g., to the works of [65–67].

In conclusion we have shown here a first, well-established, example of state-to-state reaction rates only dependent on the nuclear spin symmetry and the correlated motional states. We found the intermediate complex, or, to be more precise, its symmetry, to be highly influential since due to its missing levels, certain pathways are rendered impossible. If any experimental results deviates from the calculated ratios, the symmetry of the intermediate complex might be different than assumed. Even without an energetic description, the symmetry-based state-to-state reaction rates therefore allow first predictions for the possible dynamical processes in the intermediate complex.

4.2 The $\text{H}_3^+ + \text{H}_2$ Reaction

After the initial example of the $\text{H}_2 + \text{H}^+$ reaction, we are now ready to discuss our main example: The famous reaction



It has encouraged a lot of also very recent theoretical and experimental studies (see, [43–45, 54–56, 58–62]) but still issues are unresolved in the exact reaction mechanism. In particular the corresponding reaction energy surface, including also the potential energy surface of the intermediate complex is still an object of intensive studies. In difference to the spectroscopically well-known H_3^+ ion, the H_5^+ molecule itself shows a lot of unusual features as it is an extremely floppy molecule exhibiting various large amplitude motions even in very low energy states [60, 68]. Postponing the discussion of this kind of dynamics to Part II, we focus here on the nuclear permutation-inversion symmetry only. As we already encountered in the introductory example of the previous section (Sect. 4.1.3), this is the decisive factor for state-to-state reaction rates.

For the reaction partners H_3^+ and H_2 , the situation is rather simple: By restricting the treatment again to the permutation subgroups of the molecular symmetry groups, the symmetry group of the $\text{H}_3^+ + \text{H}_2$ part of the reaction is given as the group product $S_3 \times S_2$, where the operations of S_3 commute with those of S_2 . The nuclear spin states span the representation $\{(4A_1, \mathcal{D}_{3/2}) \oplus (2E, 2\mathcal{D}_{1/2})\} \otimes \{(3A, \mathcal{D}_1) \oplus (B, \mathcal{D}_0)\}$. From this product we obtain seven distinct total nuclear spin symmetries

$$\begin{aligned} (4A_1, \mathcal{D}_{3/2}) \otimes (3A, \mathcal{D}_1) &= (6A_1A, \mathcal{D}_{5/2}) \oplus (4A_1A, \mathcal{D}_{3/2}) \oplus (2A_1A, \mathcal{D}_{1/2}), \\ (4A_1, \mathcal{D}_{3/2}) \otimes (B, \mathcal{D}_0) &= (4A_1B, \mathcal{D}_{3/2}), \\ (2E, 2\mathcal{D}_{1/2}) \otimes (3A, \mathcal{D}_1) &= (4EA, 2\mathcal{D}_{3/2}) \oplus (2EA, 2\mathcal{D}_{1/2}), \\ (2E, 2\mathcal{D}_{1/2}) \otimes (B, \mathcal{D}_0) &= (4EB, 2\mathcal{D}_{1/2}), \end{aligned}$$

Table 4.4 State-to-state transitions and their statistical probability in the reaction $\text{H}_3^+ + \text{H}_2 \rightarrow (\text{H}_5^+)^* \rightarrow \text{H}_2 + \text{H}_3^+$, where the intermediate complex has the full S_5 symmetry. The last column gives the probabilities for a state of Γ_{init} to end up in a certain final state of Γ_{final} symmetry

Γ_{init}		Γ_{int}		Γ_{final}		P
Γ_{rovib}	Γ_{nspin}	Γ_{rovib}	Γ_{nspin}	Γ_{rovib}	Γ_{nspin}	$[\Gamma_{\text{init}} \rightarrow \Gamma_{\text{final}}]$
A_2B	$(6A_1A, \mathcal{D}_{5/2})$	A_2	$(6A_1, \mathcal{D}_{5/2})$	A_2B	$(6A_1A, \mathcal{D}_{5/2})$	1
A_2B	$(4A_1A, \mathcal{D}_{3/2})$	G_2	$(4G_1, 4\mathcal{D}_{3/2})$	A_2B	$(4A_1A, \mathcal{D}_{3/2})$	1/4
				A_2A	$(4A_1B, \mathcal{D}_{3/2})$	1/4
				EB	$(4EA, 2\mathcal{D}_{3/2})$	2/4
A_2B	$(2A_1A, \mathcal{D}_{1/2})$	H_2	$(5H_1, 5\mathcal{D}_{1/2})$	A_2B	$(2A_1A, \mathcal{D}_{1/2})$	1/5
				EA	$(2EB, 2\mathcal{D}_{1/2})$	2/5
				EB	$(2EA, 2\mathcal{D}_{1/2})$	2/5
A_2A	$(4A_1B, \mathcal{D}_{3/2})$	G_2	$(4G_1, 4\mathcal{D}_{3/2})$	A_2B	$(4A_1A, \mathcal{D}_{3/2})$	1/4
				A_2A	$(4A_1B, \mathcal{D}_{3/2})$	1/4
				EB	$(4EA, 2\mathcal{D}_{3/2})$	2/4
EA	$(2EB, 2\mathcal{D}_{1/2})$	H_2	$(2H_1, 5\mathcal{D}_{1/2})$	A_2B	$(2A_1A, \mathcal{D}_{1/2})$	1/5
				EA	$(2EB, 2\mathcal{D}_{1/2})$	2/5
				EB	$(2EA, 2\mathcal{D}_{1/2})$	2/5
EB	$(4EA, 2\mathcal{D}_{3/2})$	G_2	$(4G_1, 4\mathcal{D}_{3/2})$	A_2B	$(4A_1A, \mathcal{D}_{3/2})$	1/4
				A_2A	$(4A_1B, \mathcal{D}_{3/2})$	1/4
				EB	$(4EA, 2\mathcal{D}_{3/2})$	2/4
EB	$(2EA, 2\mathcal{D}_{1/2})$	H_2	$(2H_1, 5\mathcal{D}_{1/2})$	A_2B	$(2A_1A, \mathcal{D}_{1/2})$	1/5
				EA	$(2EB, 2\mathcal{D}_{1/2})$	2/5
				EB	$(2EA, 2\mathcal{D}_{1/2})$	2/5

where the SO(3) part of the joint representation on the right hand side indicates the total nuclear spin I_{tot} . This total spin is the conserved quantity during the reaction. For the H_5^+ complex, we have already calculated the nuclear spin species in Table 3.1, from which the respective couplings of the ro-vibrational states are easily determined.

For following the reaction (see Sect. 4.1.1), we use the results of [45], in particular Table 2.12, where he calculated the induced and subduced representations for the $S_3 \times S_2 \subset S_5 \supset S_2 \times S_3$ group chain.³ The resulting probability trees can be calculated and we summarize them in Table 4.4.

If normal H_2 and H_3^+ are assumed, i.e. a mixture of the respective spin configurations, the probabilities for state-to-state reactions must be multiplied by the respective spin statistical weights, which can be read off from the dimension of the nuclear spin representation Γ_{nspin} . Notice that nuclear spin representations E are two-dimensional, such that the weight for, e.g., the ro-vibrational state EB is

³Actually, there are two minor mistakes in his table: $(EA) \uparrow S_5 = G_1 + H_1 + H_2 + I$ and $(EB) \uparrow S_5 = G_2 + H_1 + H_2 + I$. This can easily be verified by using Frobenius reciprocity theorem and (4.2).

$g_{\text{ns}}(EB) = \dim(4EA, 2\mathcal{D}_{3/2}) = 8$. The probability to find one specific reaction with fixed initial and final ro-vibrational and according nuclear spin representation is therefore calculated by

$$P = P[\Gamma_{\text{init}}]P[\Gamma_{\text{init}} \rightarrow \Gamma_{\text{final}}] = \frac{g_{\text{ns}}(\Gamma_{\text{init}})}{\sum g_{\text{ns}}} P[\Gamma_{\text{init}} \rightarrow \Gamma_{\text{final}}]. \quad (4.3)$$

In contrast to the work of [44], this probability is normalized. Omitting the denominator $\sum g_{\text{ns}}$ leads to his definition of branching ratios.

For example, by using (4.3), the conversion of A_2B coupled to $(4A_1A, \mathcal{D}_{3/2})$ to a final state of A_2A symmetry, correlated with $(4A_1B, \mathcal{D}_{3/2})$ is calculated to be $\frac{4}{32} \cdot \frac{1}{4} = \frac{1}{32}$ (see Fig. 4.3). This represents one example of a spin flip in this reaction, since in the final ro-vibrational state of the hydrogen molecule, the symmetry has changed, which simultaneously means a (relative) spin flip has happened. This is possible due to the conservation of the total nuclear spin, which allows the individual spins to change in the intermediately formed complex. In particular, the intermediate state of G_2 symmetry is fourfold degenerate ($\dim(G_2) = 4$) and therefore decomposes into

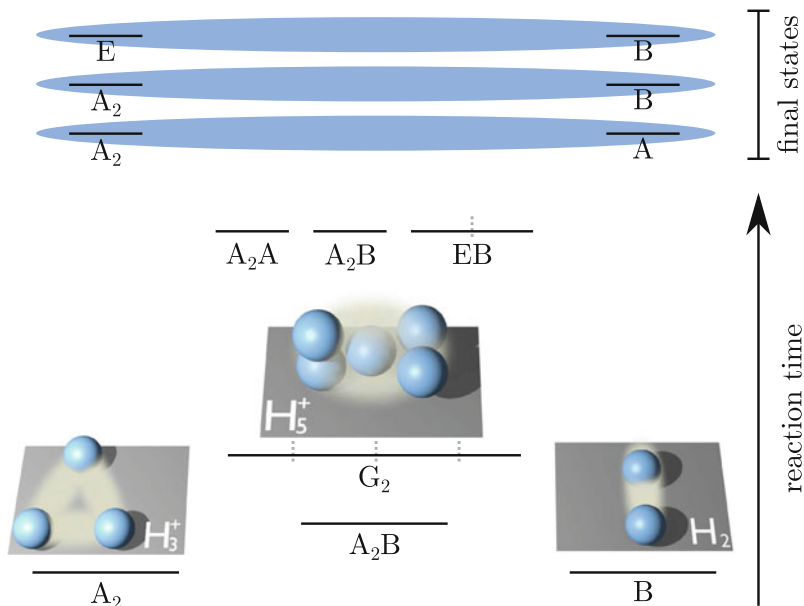


Fig. 4.3 One example of a state-to-state reaction in $\text{H}_3^+ + \text{H}_2 \rightarrow \text{H}_3^+ + \text{H}_2$. The formerly separated ro-vibrational states are combined to form the complex H_3^+ which dissociates eventually. Due to the possible full scrambling of the nuclei in the complex, the ortho state of H_2 (r.h.s.) can evolve to a para state of A symmetry. For the final dissociated states only the combinations marked in blue are possible. Note the degeneracies of G_2 and E , where especially the latter influences the probability to follow a specific path in this reaction (see Table 4.4)

four states in the dissociation process. Indeed, a single state is not decomposed but due to the degeneracy it has some probability to evolve into one of these four states.

Combining all the possibilities for ortho states of H_2 , we find an effective ortho-to-para conversion rate in this reaction of

$$P[\text{ortho-to-para H}_2] = P[\Gamma_{\text{rovib}}(\text{H}_2) = B \rightarrow \Gamma_{\text{rovib}}(\text{H}_2) = A] = 9/50.$$

The para-to-ortho conversion rate is calculated to be:

$$P[\text{para-to-ortho H}_2] = P[\Gamma_{\text{rovib}}(\text{H}_2) = A \rightarrow \Gamma_{\text{rovib}}(\text{H}_2) = B] = 9/50,$$

meeting the expectation of reversibility.

In [44], the author used a method relying on the spin angular momentum only, with which he calculated conversion rates for ro-vibrational states coupled to a specific spin angular momentum. Furthermore, he used the separated angular momenta of H_2 and H_3^+ as initial and final state. In particular, he calculated, e.g., the conversion rate of $(I(\text{H}_2), I(\text{H}_3^+)) = (\frac{3}{2}, 0)$ to $(\frac{3}{2}, 1)$ and found a value of 1. In our case, this corresponds to the transition of $\Gamma_{\text{rovib}} = A_2A \rightarrow A_2B$ because their coupling is exactly to $(4A_1B, \mathcal{D}_{3/2})$ and $(4A_1A, \mathcal{D}_{3/2})$ respectively. If we use the unnormalized probability, we get the value

$$g_{\text{ns}}(A_2A) \cdot P[\Gamma_{\text{rovib}} = A_2A \rightarrow A_2B] = 4 \cdot \frac{1}{4} = 1$$

and hence retrieve the value of [44].

In these reaction paths, we assumed the intermediate complex to have the full S_5 symmetry. Actually, the potential energy surface of the H_5^+ cation is an object of recent studies, where presumably there are potential energy barriers restricting this full symmetry group [54, 68]. To include this into the present discussion, we will give one example of a restricted symmetry group and follow the symmetry during this reaction in the respective group chain. This actually represents the main novelty of our approach for this reaction: We assume different intermediate symmetry, which is impossible in Okas approach, whereas also in [43], the author did not tackle such a problem although it would have been possible. However, combining this with the general Schur–Weyl duality approach, we are able to link all the states, i.e. ro-vibrational and nuclear spin states, of reactant, intermediate, and product molecules depending on the symmetry groups of the participants.

4.2.1 A Restricted Symmetry Group for the Intermediate Complex

In order to find the feasible operations for the molecular symmetry group of the intermediately formed complex H_5^+ , we assume the simplest possibility: The complex is formed from two H_2 units and a single central proton, which, if the complex

dissociates, forms an H_3^+ with either one of the two units. This picture might be oversimplified, other possible groups are discussed in [62], but we here present it as a proof-of-principle for the use of the state-to-state symmetries in this particular reaction.

The symmetry group for the described complex is the product group $S_2 \times S_2 \times S_1$, where the two S_2 groups describe the H_2 units at both sides of the central proton. In this group, the nuclear spin representations are given as

$$\begin{aligned} (3A, \mathcal{D}_1) \otimes (3A, \mathcal{D}_1) \otimes (2A, \mathcal{D}_{1/2}) &= (6AAA, \mathcal{D}_{5/2}) \oplus 2(4AAA, \mathcal{D}_{3/2}) \oplus \\ &\quad \oplus 2(2AAA, \mathcal{D}_{1/2}), \\ (3A, \mathcal{D}_1) \otimes (B, \mathcal{D}_0) \otimes (2A, \mathcal{D}_{1/2}) &= (4ABA, \mathcal{D}_{3/2}) \oplus (2ABA, \mathcal{D}_{1/2}), \\ (B, \mathcal{D}_0) \otimes (3A, \mathcal{D}_1) \otimes (2A, \mathcal{D}_{1/2}) &= (4BAA, \mathcal{D}_{3/2}) \oplus (2BAA, \mathcal{D}_{1/2}), \\ (B, \mathcal{D}_0) \otimes (B, \mathcal{D}_0) \otimes (2A, \mathcal{D}_{1/2}) &= (2BBA, \mathcal{D}_{1/2}). \end{aligned}$$

The intermediate symmetry group is a subgroup of the initial $S_3 \times S_2$ group and the subduced representations are given as [45]

$$\begin{aligned} A_1A &\rightarrow AAA; & A_1B &\rightarrow ABA; \\ A_2A &\rightarrow BAA; & A_2B &\rightarrow BBA; \\ EA &\rightarrow AAA \oplus BAA; & EB &\rightarrow ABA \oplus BBA. \end{aligned}$$

Notice the initial difference between states of ABA and BAA symmetry, motivated by the physical picture: The states of BAA symmetry are rooted in the decomposition of the H_3^+ ion, where $A_2 \downarrow S_2 = B$. Conversely, states of ABA symmetry originate from the B states of the initial H_2 molecule. However, after the complex has formed, the two H_2 units are indistinguishable and so are the two representations ABA and BAA . In the dissociation process, the central proton can bind to either one of the two intermediate H_2 units. Therefore a state of $ABA = BAA$ can either form a $A_1B \oplus EB$ or an $A_2A \oplus EA$ representation in the final $S_3 \times S_2$ symmetry group. This is the essence of this restricted symmetry group approach: In difference to the assumption of a full proton scrambling, there is only one single proton removed from the H_3^+ molecule. It possibly forms the final H_3^+ with either one of the subunits.

In conclusion, the Frobenius reciprocity must be used with caution since there are two possibilities to form $S_3 \times S_2$ out of $S_2 \times S_2 \times S_1$ and we find:

$$\begin{aligned} AAA &\rightarrow A_1A \oplus EA; & BBA &\rightarrow A_2B \oplus EB; \\ ABA &\rightarrow (A_1B \oplus EB) \oplus (A_2A \oplus EA); \\ BAA &\rightarrow (A_1B \oplus EB) \oplus (A_2A \oplus EA). \end{aligned}$$

Mathematically, these restricted or subduced representations result from the fact that the smaller $S_2 \times S_2 \times S_1$ is found twice in the $S_3 \times S_2$ group.

Table 4.5 State-to-state transitions and their statistical probability in the reaction $\text{H}_3^+ + \text{H}_2 \rightarrow (\text{H}_5^+)^* \rightarrow \text{H}_2 + \text{H}_3^+$, where the intermediate complex has a restricted $S_2 \times S_2 \times S_1$ symmetry

Γ_{init}		Γ_{int}		Γ_{final}		P
Γ_{rovib}	Γ_{nspin}	Γ_{rovib}	Γ_{nspin}	Γ_{rovib}	Γ_{nspin}	$[\Gamma_{\text{init}} \rightarrow \Gamma_{\text{final}}]$
A_2B	($6A_1A, \mathcal{D}_{5/2}$)	BBA	($6AAA, \mathcal{D}_{5/2}$)	A_2B	($6A_1A, \mathcal{D}_{5/2}$)	1
A_2B	(4 $A_1A, \mathcal{D}_{3/2}$)	BBA	(4 $AAA, 4\mathcal{D}_{3/2}$)	A_2B	($4A_1A, \mathcal{D}_{3/2}$)	1/3
				EB	($4EA, 2\mathcal{D}_{3/2}$)	2/3
A_2B	(2 $A_1A, \mathcal{D}_{1/2}$)	BBA	(2 $AAA, \mathcal{D}_{1/2}$)	A_2B	($2A_1A, \mathcal{D}_{1/2}$)	1/3
				EB	($2EA, 2\mathcal{D}_{1/2}$)	2/3
A_2A	(4 $A_1B, \mathcal{D}_{3/2}$)	BAA	(4 $ABA, \mathcal{D}_{3/2}$)	A_2A	($4A_1B, \mathcal{D}_{3/2}$)	1/3
				EB	($4EA, 2\mathcal{D}_{3/2}$)	2/3
EA	(2 $EB, 2\mathcal{D}_{1/2}$)	AAA	(2 $BBA, \mathcal{D}_{1/2}$)	EA	($2EB, 2\mathcal{D}_{1/2}$)	1/2
		BAA	(2 $ABA, \mathcal{D}_{1/2}$)	EA	($2EB, 2\mathcal{D}_{1/2}$)	1/4
				EB	($2EA, 2\mathcal{D}_{1/2}$)	1/4
EB	(4 $EA, 2\mathcal{D}_{3/2}$)	ABA	(4 $BAA, \mathcal{D}_{3/2}$)	EB	($4EA, 2\mathcal{D}_{3/2}$)	2/9
				A_2A	($4A_1B, \mathcal{D}_{3/2}$)	1/9
		BBA	2(4 $AAA, \mathcal{D}_{3/2}$)	EB	($4EA, 2\mathcal{D}_{3/2}$)	2/9
				A_2B	($4A_1A, \mathcal{D}_{3/2}$)	4/9
EB	(2 $EA, 2\mathcal{D}_{1/2}$)	ABA	(2 $BAA, \mathcal{D}_{1/2}$)	EB	($2EA, 2\mathcal{D}_{1/2}$)	1/3
				EB	($2EA, 2\mathcal{D}_{1/2}$)	4/9
		BBA	2(2 $AAA, \mathcal{D}_{1/2}$)	A_2B	($2A_1A, \mathcal{D}_{1/2}$)	2/9

With the nuclear spin symmetries and the induced/subduced representations, we can again set up the probability trees, which we summarize in Table 4.5.

In following the discussion of the full S_5 symmetry group of the intermediate H_5^+ complex and its implications for the ortho-to-para transitions in this a reaction, we can recalculate the ortho-to-para conversion rate in the case of the restricted symmetry group (see (4.3))

$$P[\text{ortho-to-para H}_2] = P[\Gamma_{\text{rovib}}(\text{H}_2) = B \rightarrow \Gamma_{\text{rovib}}(\text{H}_2) = A] = 4/135,$$

$$P[\text{para-to-ortho H}_2] = P[\Gamma_{\text{rovib}}(\text{H}_2) = A \rightarrow \Gamma_{\text{rovib}}(\text{H}_2) = B] = 11/90.$$

This shows the main difference between the restricted and the full symmetry group of the intermediate complex: (i) The rates for ortho-to-para and para-to-ortho conversion in the reaction differ, and (ii) they differ from the values calculated for the full symmetry group. A more appropriate comparison might be done in the future, we here only state these preliminary results. In conclusion, the two possible symmetries of the intermediate complex unambiguously induce different probabilities for certain state-to-state reactions. Indeed, the assumed symmetry group for the intermediate complex is very much simplified but also for more appropriate ones as defined in, e.g., [62], we expect a similar behavior.

4.2.2 Implications for Experiments

Even though more complete studies have to be done in the future, the main message of the preceding sections is clear: State-to-state reaction rates strongly depend on the molecular symmetry group of the intermediately formed complex. We have demonstrated an initial example for the reaction $\text{H}_3^+ + \text{H}_2 \rightarrow \text{H}_3^+ + \text{H}_2$, which is thought to represent one major cooling mechanism of molecular hydrogen in space. In this case, cooling is meant to be ortho-to-para cooling, and hence state-to-state reaction rates for this kind of transition are highly important. If the complex H_5^+ is formed in an intermediate step in the reaction, it is described by an appropriate symmetry group. We chose two simple examples for this group: (i) The full nuclear permutation group S_5 , where all nuclei scramble and can be interchanged, and (ii) a much smaller $S_2 \times S_2 \times S_1$ symmetry group, where only one proton is released from the H_3^+ molecule. The latter is conventionally thought to resemble a proton hop, which is one idea of a restricted symmetry group in the H_5^+ cation. With respect to ortho-to-para conversion rates, two important results have been found: (i) The rates depend on the intermediate symmetry group, and (ii) in the restricted group, ortho-to-para and para-to-ortho rates differ.

With these results we are still far from being able to provide predictions for real experiments. Energetics of the reaction and also other symmetry groups must be discussed towards this end. However, the trend is obvious: If the para-to-ortho ratio of molecular hydrogen can be measured in an experiment before and after a collisional reaction with H_3^+ , its possible change is directly correlated to the symmetry group of the intermediate complex. Analogously, the symmetry of the H_5^+ ion could be measured. This can provide information on the H_5^+ molecule even without any direct observation and furthermore yields more insight into the cooling process for molecular hydrogen in space. First experiments of this type already have been done using the reaction $\text{H}_3^+ + \text{O}_2 \rightleftharpoons \text{O}_2\text{H}^+ + \text{H}_2$, where the different nuclear spin states of H_3^+ have been shown to exhibit distinct reaction rates [69]. Potentially, this reaction could be used to test the H_3^+ state symmetry before and after a reaction with, e.g., para-hydrogen. However, an explicit discussion of the experiment and the required extensions is beyond the scope of this work.

In conclusion, together with an ideal state-resolved collision experiment of these two hydrogen species, our symmetry analysis can help in understanding the cooling mechanism of molecular hydrogen and it would lead to a better understanding of the H_5^+ molecule itself.

4.2.3 The Deuterated Version

In order to use the results of Chap. 3, we replace all the hydrogen atoms in the reaction $\text{H}_3^+ + \text{H}_2 \rightarrow \text{H}_3^+ + \text{H}_2$ by deuterons. The main reason is to show explicitly the implications of the larger spin angular momentum and the correlated use of the

unitary group for the symmetry of the spin state. This very preliminary work is a proof-of-principle study for using Schur–Weyl duality in reactive collisions and is by no means a complete analysis of deuterated versions of this famous reaction. The latter would include all kinds of reactants, such as HD, H₂D⁺, D₂H⁺, etc. Furthermore different symmetry groups should be considered and a similar behavior as in the previous section should be expected. Nevertheless, this is the first time that Schur–Weyl duality provides new results in the discussion of reactions which differ from the works of [43, 44]. The decisive difference is the use of unitary symmetry for the nuclear spin states instead of the spatial rotation symmetry. As we will see, this controls the reaction pathways in a rather explicit way.

For the permutation symmetry, we here consider the symmetry pathway

$$S_3 \times S_2 \subset S_5 \supset S_3 \times S_2$$

as done also for the non-deuterated reaction. Since we are now facing integer spin deuterons, the appropriate spin angular momentum symmetry group is U(3) and the possible nuclear spin symmetries are the following

$$\begin{aligned} (10A_1, \{3\}) \otimes (6A, \{2\}) &= (60A_1A, \{5\} \oplus \{41\} \oplus \{32\}), \\ (8E, 2\{21\}) \otimes (6A, \{2\}) &= (48EA, 2(\{41\} \oplus \{32\} \oplus \{31\} \oplus \{221\})), \\ (A_2, \{111\}) \otimes (6A, \{2\}) &= (6A_2A, \{311\}), \\ (A_1, \{3\}) \otimes (3B, \{11\}) &= (30A_1B, \{311\}), \\ (E, 2\{21\}) \otimes (3B, \{11\}) &= (24EB, 2(\{32\} \oplus \{311\} \oplus \{221\})), \\ (A_2, \{21\}) \otimes (3B, \{11\}) &= (3A_2B, \{221\}), \end{aligned}$$

where we used the notation of Chap. 3 of curly brackets {} for the partitions labeling the irreducible representations of U(3).

For the reaction, we assume that the nuclear spin symmetry in U(3) is conserved. This is a non-trivial statement since we have already seen that the branching to the more common SO(3) symmetry group of nuclear spins gives rise to certain ambiguities (Table 3.2). If we require the spin quantum number in SO(3) to be conserved, different state-to-state reactions become possible. For the moment, we here stick to the use of the Schur–Weyl duality and require that the largest possible symmetry group, namely the unitary group, is appropriate for the whole reaction process. However, in the future, this could be the starting point for further discussion.

Focusing on an intermediately formed D₅⁺ complex with full S₅ symmetry, we can calculate the probability trees as done in the previous sections. The results are shown in Table 4.6.

The results show in particular the use of the U(3) symmetry, whereas in a treatment with conserved SO(3) symmetry many more transitions would be possible. For example, an initial ro-vibrational state of A₂B symmetry couples in the unitary picture to a nuclear spin state of (21A₁A, {5}) symmetry. The only reaction path with conserved unitary symmetry is (see Table 4.6)

Table 4.6 State-to-state transitions and their statistical probability in the reaction $\text{D}_3^+ + \text{D}_2 \rightarrow (\text{D}_5^+)^* \rightarrow \text{D}_2 + \text{D}_3^+$, where the intermediate complex has the full S_5 symmetry group

Γ_{init}		Γ_{int}	Γ_{final}	P	I_{tot}
Γ_{rovib}	Γ_{nspin}	Γ_{rovib}	Γ_{rovib}	$[\Gamma_{\text{init}} \rightarrow \Gamma_{\text{final}}]$	
$A_1 A$	$(6A_2 B, \{221\})$	H_1	$A_1 A$	1/5	1
			$E A$	2/5	
			$E B$	2/5	
$A_2 B$	$(21A_1 A, \{5\})$	A_2	$A_2 B$	1	5,3,1
$A_2 B$	$(24A_1 A, \{41\})$	G_2	$A_2 B$	1/4	4,3,2,1
			$A_2 A$	1/4	
			$E B$	1/2	
$A_2 B$	$(15A_1 A, \{32\})$	H_2	$A_2 B$	1/5	3,2,1
			$E A$	2/5	
			$E B$	2/5	
$A_2 A$	$(24A_1 B, \{41\})$	G_2	$A_2 A$	1/4	4,3,2,1
			$A_2 B$	1/4	
			$E B$	1/2	
$A_2 A$	$(6A_1 B, \{311\})$	I	$A_2 A$	1/6	2,0
			$A_1 B$	1/6	
			$E A$	1/3	
			$E B$	1/3	
$E A$	$(15E B, 2\{32\})$	H_2	$E A$	2/5	3,2,1
			$A_2 B$	1/5	
			$E B$	2/5	
$E A$	$(6E B, 2\{311\})$	I	$E A$	1/3	2,0
			$A_2 A$	1/6	
			$A_1 B$	1/6	
			$E B$	1/3	
$E A$	$(3E B, 2\{221\})$	H_1	$E A$	2/5	1
			$A_1 A$	1/5	
			$E B$	2/5	
$A_1 B$	$(6A_2 A, \{311\})$	I	$A_1 B$	1/6	2,0
			$A_2 A$	1/6	
			$E A$	1/3	
			$E B$	1/3	
$E B$	$(24E A, 2\{41\})$	G_2	$E B$	1/2	4,3,2,1
			$A_2 A$	1/4	
			$A_2 B$	1/4	
$E B$	$(15E A, 2\{32\})$	H_2	$E B$	2/5	3,2,1
			$E A$	2/5	
			$A_2 B$	1/5	

(continued)

Table 4.6 (continued)

Γ_{init}		Γ_{int}	Γ_{final}	P	I_{tot}
Γ_{rovib}	Γ_{nspin}	Γ_{rovib}	Γ_{rovib}	[$\Gamma_{\text{init}} \rightarrow \Gamma_{\text{final}}$]	
EB	$(6EA, 2\{311\})$	I	EB	$1/3$	2,0
			A_1B	$1/6$	
			A_2A	$1/6$	
			EA	$1/3$	
EB	$(3EA, 2\{221\})$	H_1	EB	$2/5$	1
			A_1A	$1/5$	
			EA	$2/5$	



Using the branching rules to $\text{SO}(3)$, however, the initial state therefore couples to nuclear spin states of $I_{\text{tot}} = 5, 3, 1$. We could then use an initial state of, e.g., A_2B symmetry coupled to (A_1A, \mathcal{D}_3) . This state can induce A_2 , G_2 and H_2 symmetric states in S_5 since all can couple to nuclear spin states of $I = 3$. Therefore a large number of final states are possible. Consequently, the analogue to Table 4.6 would be exceedingly more difficult.

This provides another open question, which is not answered in this work: Is the underlying unitary symmetry essential for the conservation of spin angular momentum during the reaction? With experiments like the one described in Sect. 4.2.2, one can potentially resolve this issue in the future.

4.3 Discussion

Nuclear spin statistical weights are most conveniently used to determine so-called missing ro-vibrational energy levels or other properties of intra-molecular states. In Chap. 3, we have shown that they can be calculated straightforwardly from the Schur–Weyl duality theorem. Yet, their calculation was done in a pedestrian approach, where all possible spin configurations had to be considered. In difference to that, the Schur–Weyl theorem gives a prescription how to find the respective symmetries at once. This can be implemented into programs, where the hope is to establish an automated calculation of nuclear spin weights from only specifying the number of particles and their spins. This could, e.g., help in particular in the description of larger molecules and species with large individual nuclear spins. In particular interesting for future work is the combination of particles of different spin. Is there a simple way to treat the total spin quantum number in terms of the here discussed unitary symmetry groups? As an example, the H_2D^+ molecule must be described in a permutation symmetry group of S_2 and its unitary spin symmetry group would be $U(2) \times U(3)$.

Can we now define the total spin in $U(3)$ or in $U(2)$, or are we forced to determine first the correlation to the usual $SO(3)$ symmetry group to calculate the total spin quantum number. These questions should be answered in the future to make the duality theorem applicable also to molecules with distinguishable nuclei.

Apart from their importance in intra-molecular states, we demonstrated the influence of nuclear spin states in reaction dynamics: Different symmetries of the intermediately formed molecular complex in a reactive collision lead to distinct selection rules in state-to-state reactions. In particular, we used the famous $H_3^+ + H_2 \rightarrow H_2 + H_3^+$ reaction to show how the symmetry group of the intermediately formed H_3^+ complex influences the reaction. This molecular complex itself is subject of intense recent research [60–62], which we will partly discuss in Part II. There, the internal dynamics of this complex are studied, whereas in this part we focused on its symmetry.

State-to-state reaction rates, where one assumes a single initial quantum state and a number of potential final states, are particularly affected by the intermediate symmetry. Especially possible degenerate energy levels in the intermediate complex influence the probabilities for specific state-to-state transitions. Using the Schur-Weyl approach, we nevertheless restrain the total nuclear spin to remain constant during the whole reaction process. Regarding the above mentioned reaction, state-to-state reaction rates are highly important, since they give a purely statistical weight for ortho-to-para transitions in the reaction. Ortho states, i.e. H_2 molecular states with unit total nuclear spin, are usually not convertible to their para versions ($I_{\text{tot}} = 0$), because usual radiative transitions as well as collisions with other molecules are not capable to flip the internal spins. In a reaction with H_3^+ however, spin flips can occur. The respective probabilities however, depend on the symmetry group of the intermediately formed H_3^+ ion: If all nuclei can scramble, the possibility to do a spin-flip is much larger than if only one proton is allowed to be exchanged in the complex. This represents the novelty of our approach: State-to-state reaction rates are calculated based exclusively on the molecular symmetry group of reacting, intermediate, and product molecules. Together with an explicit treatment of the energetics in that reaction, we expect these rates to be a tracer of the intermediate complex and to provide more information on a possible ortho-to-para cooling mechanism in interstellar space. Furthermore, from spectroscopic experiments on these rates, one would be able to draw conclusions on the intermediate complex without studying it directly. Since the different symmetry groups for the intermediate complex are directly related to assumptions on the potential energy surface for the respective molecular complex, such experiments could help in understanding this potential energy surface, e.g., for H_3^+ [60–62], without investigating the molecule itself, which, due to the absence of any dipole moment, known to be difficult.

In treating the deuterated version of the reaction, we also demonstrated a major influence of Schur-Weyl duality in reactions with nuclei of larger spin quantum numbers. In contrast to more convenient treatments, where the spatial rotation group is assumed to describe the symmetry of nuclear spin properly, we use the more general unitary group to represent the full symmetry of the nuclear spin angular momentum. With this group, the possible pathways for ro-vibrational state-to-state transitions in

the exemplary reaction $D_3^+ + D_2 \rightarrow D_2 + D_3^+$ are studied and are actually restricted by the unitary symmetry. If the usual spatial symmetry would have been assumed, much more transitions are possible due to the fact that there is no one-to-one correspondence of nuclear spin permutation to spatial rotation symmetry for spins of $I \geq 1$ (see Chap. 3). This restriction of pathways will be of interest also for partially deuterated species, where one has to deal with distinguishable particles but still with a combined total spin quantum number and the combination of different unitary groups is one of the open questions at the moment.

In conclusion, we studied the use of symmetry groups in reactions with a small number of protons (or deuterons). The here presented results suggest (i) the importance of distinct symmetry group chains for reactions, and (ii) the use of the unitary symmetry group for the nuclear spin angular momentum. We expect that applying the used techniques to other molecules, and to other symmetry groups, will provide more detailed insights into state-to-state reactions without using dynamical studies, but relying on symmetry assumptions only. State resolved reaction experiments could be used to determine the exact reaction rates and by comparing these rates to the calculations, experimental results could provide clear evidence for, e.g., the symmetry of the intermediate complex.

Part II
Extremely Floppy Molecules

Chapter 5

Introducing Extreme Floppiness

Abstract Extremely floppy molecules are not describable by the traditional picture of a ball-and-stick molecular structure. Their ground state wave function is highly delocalized and a number of large amplitude motions makes it impossible to define a fixed equilibrium structure. In this chapter, the most basic properties of this class of molecules is introduced and an outlook on the following chapters is given, where a fundamentally new approach for describing the respective dynamics is developed.

In customary molecular theory, the many-particle Schrödinger equation is only solved approximately. First, the electrons are considered to be much faster than the nuclei so that their movement can be approximated to create a potential energy surface for the nuclear motion. This Born-Oppenheimer approximation is widely used and is particularly reasonable when it comes to cold molecules where only the lowest (nuclear) ro-vibrational energy levels are populated. For a description of the nuclear dynamics in cold molecules an additional approximation is most likely made: The electrons are considered to form almost stable bonds between the nuclei, implying a fixed geometrical structure of the molecule. Nuclear vibrations are consequently imagined to give rise to only small deformations of that structure, usually described by a harmonic oscillator model. With fixed relative nuclear positions, molecular rotation can be approximated as a rotation of a rigid body. In particular, this ball-and-stick picture gives rise to a zero-order model, where (rigid) rotations and (harmonic) vibrations are completely decoupled. Extending this model by including anharmonic as well as ro-vibrational coupling effects perturbatively can be used to describe spectra of all kinds of molecules with impressive accuracies (see also Chap. 2.2 of Part I).

However, not all molecules can be described by this rather simple ball-and-stick picture of perturbation theory. Vibrational motion displacing nuclei by distances that are comparable to the linear dimension of the full molecule implies that any perturbative treatment of the ro-vibrational coupling cannot converge. These large amplitude motions are subject of an immense number of theoretical and experimental studies and explicitly their interplay with other vibrational and rotational excitations is still far from being as accurately described as ro-vibrational couplings in molecules without large amplitude motion. Nevertheless, for many molecules a single such motion

can be identified: The ‘umbrella flipping’ motion in ammonia, NH_3 , the internal rotation of the methyl group (CH_3) in dimethyl ether, CH_3OCH_3 , or different motions in weakly bound cluster molecules. In these cases, the convenient and intuitive ball-and-stick picture can be maintained to a certain point and advanced models exist to describe these motions [70, 71].

In the following part, we consider extremely floppy molecules exhibiting numerous large amplitude motions, which “render moot the idea of a fixed equilibrium structure” [7, p. 1]. Other authors have also called such molecules “astructural” [60, p. 1] pointing out the impossibility to define a geometric structure. As such, these molecules are fundamental examples of quantum mechanics, since their behavior is by no means classical [72, 73]. Important examples of this class of molecules are some Hydrogen-bonded or van-der-Waals clusters, quasi-linear or -planar molecules, carbonium ions, as well as the famous H_5^+ cation (see, e.g., [37, 60, 68, 72, 74–76]). The maybe most prominent example, the “enfant terrible of molecular spectroscopy”([3], p. 1), is protonated methane, CH_5^+ . Even though the ro-vibrational spectrum of its parental methane molecule, CH_4 , is well-understood, the protonated version has been shown to behave differently from all molecules whose cold ro-vibrational spectrum has been measured [4, 77, 78]. Despite a vast variety of theoretical approaches to this single molecule (see, e.g., [9, 73, 79–81]), up to very recent results of [35], none of them was able to reproduce the experimental results of [4] with any degree of accuracy. However, unresolved issues remain as well in the recent results of [35]. Also extremely expensive calculations for the carbonium ion, H_5^+ , have been performed only recently and show very unusual features, where a convincing physical explanation is still missing [60, 68].

In the previous paragraph, the unusual features of extremely floppy molecules were boiled down to the property of having no fixed equilibrium structure. For the example of CH_5^+ , this is supported by many theoretical ab-initio studies, where the potential energy barriers are calculated to be extremely low compared to the zero-point energy of the ground vibrational state [82, 83]. Therefore the structure can only be defined as a vibrationally averaged quantity, which suggests a non-classical delocalization of the protons in CH_5^+ . They figuratively form a protonic cloud around the central carbon nucleus already in the vibrational ground state. This physical picture must cause the perturbation theory to fail completely, a zero-order separation of rotation and vibration cannot be established in any traditional sense.

Nevertheless, some of the essential ideas of molecular physics remain: For the molecular states, although not separable into rotational and vibrational part, we must be able to define an angular momentum quantum number, J . This is a very fundamental statement, motivated by the fact that any molecule is subjected to the usual spatial rotational symmetry and hence its wave functions must span the corresponding irreducible representations of the group of rotations, labeled by J . Therefore, one could argue that the use of well-known rotational basis functions coupled to a large number of vibrational states remains a well-defined starting point. In principle, this is done in [35], but the enormous number of coupled basis states leads to a loss of the meaning of the initial zero-order model. The advantage of zero-order models in general is hard to overestimate: They usually provide physical, intuitive

interpretations, they are linked to well-understood quantum mechanical operators, and their model Schrödinger equation is analytically solvable and relies only on a limited number of free parameters. With the calculations of [35], one can perhaps link some of the produced energies to the experimentally determined ones, and one can also give a J quantum number, but a detailed understanding in the sense of a physical picture is lost.

Another important point in examining the properties of extremely floppy molecules is their symmetry. Conveniently, elements of the molecular symmetry group (see Chap. 2.2 of Part I) are assumed to act on three distinct sets of coordinates describing vibrational-electronic (vibronic) motion, the rotation, and the nuclear spin, respectively [14]. Their separation is a direct consequence of the assumption of small-amplitude vibrations, so that rotations and vibrations of the nuclei are described by distinct parts of the molecular wave function. However, as discussed above, this separation of variables is unfeasible in the case of extremely floppy molecules. One main consequence in terms of symmetry is the impossibility of defining the action of the molecular symmetry group elements by using exclusively rotational coordinates. Especially for the example of CH_5^+ , the technique of finding equivalent rotations, established in the 1960s, [30] is impossible to apply due to fundamental mathematical reasons: The molecular symmetry group can be shown not to be isomorphic to a subgroup of the rotation group, hence usual rotational coordinates are not sufficient to describe the action of the permutation-inversion operations of the molecular symmetry group [9]. In [29, 35] this problem is avoided by restricting the full molecular symmetry group to certain smaller groups, for which the usual approach is possible. We discuss this particular symmetry feature in detail in Chap. 6.

In [6, 7] we proposed a fundamentally new approach for the dynamics of extremely floppy molecules, called *super-rotation*. It provides a zero-order model with a well-defined Hamilton operator and only one single free parameter. The according energy eigenvalues are known in closed form and we are able to interpret the respective dynamics in terms of a combined ro-vibrational motion. We will discuss this model in detail in the following part, including the very encouraging comparison with the experimental spectrum of CH_5^+ , where our model predicts almost all identified low energy states with an astonishing accuracy of a few wave numbers. In addition to the discussion of the dynamics in the model, we include a detailed symmetry analysis. This shows our approach to be capable of overcoming the problem of finding equivalent rotations for the full molecular symmetry group by including more degrees of freedom. Consequently, it induces a fundamentally new separation of variables.

In a concluding part, we also discuss other possible targets for our theory and necessary extensions of the super-rotor model. Furthermore, first ideas of linking our model to well-established models of single large-amplitude motions are also discussed. This comparison further facilitates this model opening up a new avenue for a more general description of internal dynamics in a large class of molecules; it is not limited to the single molecule CH_5^+ .

Chapter 6

Symmetry Beyond Perturbation Theory

Abstract In this chapter, the limits of traditional theories of molecular rotation are discussed. First, the basic ideas of angular momentum theory are introduced and in particular the technique of equivalent rotations is discussed, which is used to map the molecular symmetry group, i.e. the identical nuclear permutation/inversion operations, onto a subgroup of the rotation group, $\text{SO}(3)$. This procedure is shown to fail for permutation groups of more than four particles, which is demonstrated for a particular example and is explained by a rigorous mathematical statement.

6.1 Representation Theory of Molecular Rotation

Before we start a detailed discussion of the molecular super-rotation as a fundamentally new model of combined ro-vibrational motion for extremely floppy molecules, we first investigate the conventional three-dimensional rotation and its correlation to the permutation and inversion group of molecular symmetry. This discussion is based on a thorough understanding of the representation theory of the rotation group, which we describe in this upcoming chapter. The application to molecular dynamics is rooted in the common approximation of separating the ro-vibronic coordinates,. This approximation is usually motivated by the fact that the electronic motion is much faster than that of the nuclei and that nuclear vibrations are small compared to the linear dimension of the molecule. Furthermore, as indicated in Chap. 3 of Part I, the nuclear spin is usually considered to be decoupled from the spatial coordinates. This traditional approach of molecular dynamics can be used to symmetry classify the vibrational, rotational and nuclear spin wave functions separately in the molecular symmetry group. In the following, we show this to be possible if and only if the molecular symmetry group is isomorphic to a subgroup of the rotation group $\text{SO}(3)$. If it is not in the finite set of subgroups of $\text{SO}(3)$, the traditional approach fails. In Sect. 6.2 we demonstrate one respective example for this break-down of usual rotational theory for molecules. The presented results can be found in condensed form in [9] but we give more details in the upcoming chapter.

In order to describe the molecular rotation from a symmetry point of view, two main symmetry groups of the total molecular Hamiltonian have to be considered (see Sect. 2.1 of Part I): (i) Since the Hamiltonian is invariant under the overall rotation of the molecule, we identify the K (spatial) symmetry group, [14] which mathematically is equivalent to the special orthogonal group in three dimensions, $\text{SO}(3)$; [9] (ii) Since identical nuclei are indistinguishable, the complete nuclear permutation-inversion group, often restricted to the smaller molecular symmetry group (see Part I) is recognized as symmetry group.

As we showed in the first part of this work, symmetry groups are used to classify molecular states in terms of irreducible representations. Especially in Chap. 3 of Part I, we already discussed the permutation group representations for the nuclear spin part of the full molecular wave function. We showed them to be crucial in spectroscopic experiments, where Pauli's exclusion principle is used to identify missing levels or to perform tentative assignments of electromagnetic transitions.

In contrast to the finite permutation groups, the special orthogonal group is a continuous Lie group, which changes the respective representation theory. Before discussing its application to molecules, we first review some of the basic properties of the $\text{SO}(3)$ group and of $\text{SO}(N)$ groups in more general terms. We introduced some of these concepts already in Sect. 2.1.2 of Part I, we reconsider and further explain them here for convenience.

Short Excursion to Lie Theory Irreducible representations of special orthogonal groups are labeled by so-called highest weights [18, 19, 38]. For $\text{SO}(3)$, those weights are the eigenvalues of the \hat{J}_z operator, say m , which are bounded by the total angular momentum $m_{\max} = J$. Here, z is a fixed axis onto which \hat{J}_z projects the rotation (see Example 6.1 and Fig. 6.1a below). The quantum number J is the eigenvalue of the total angular momentum operator, defined as¹

$$\hat{J}^2 = \hat{J}_x^2 + \hat{J}_y^2 + \hat{J}_z^2. \quad (6.1)$$

J and therefore the highest weight label of the irreducible representations is a good quantum number since \hat{J}^2 commutes with the Hamiltonian. This (squared) total angular momentum operator commutes with all infinitesimal rotations, $[\hat{J}^2, \hat{j}_i] = 0$, and since we required the Hamiltonian to be invariant under all rotations in three-dimensional space, the eigenvalues of \hat{J}^2 are good quantum numbers.

In a more mathematical language, the \hat{J}^2 operator is the so-called Casimir operator of $\text{so}(3)$, the respective Lie-algebra of $\text{SO}(3)$, which is generated by the three infinitesimal rotations \hat{j}_i [18, 19, 38]. The \hat{J}_z operator is usually known as defining the Cartan subalgebra of the $\text{so}(3)$ algebra, i.e. it forms an abelian subalgebra, here consisting only of this single element, and has non-vanishing commutation relations to the other two operators. Those operators are very conveniently represented by their ladder equivalents, i.e.

¹See Chap. 2 for some general discussion of angular momentum and Part III for a semi-classical treatment.

$$\hat{J}_+ = \frac{1}{\sqrt{2}} (\hat{J}_x + i \hat{J}_y), \quad \hat{J}_- = \frac{1}{\sqrt{2}} (\hat{J}_x - i \hat{J}_y),$$

which raise or lower the m eigenvalue.

These definitions of ladder and projection operators is fully generalizable to any $\text{SO}(2n + 1)$ group: The $\text{so}(2n + 1)$ algebra is a semi-simple algebra [18] inducing that the elements can be grouped into the Cartan subalgebra consisting of elements we call H_i ($i = 1, \dots, n$), and ladder operators, E_α . For these groups, there are $l - n$ such ladder operators, where $l = 2n^2 + n$ is the number of generators of $\text{SO}(2n + 1)$. The commutation relations are in general (see [38, p. 61])

$$\begin{aligned} [H_i, H_k] &= 0, \quad [H_i, E_\alpha] = \alpha_i E_\alpha, \\ [E_\alpha, E_\beta] &= N_{\alpha\beta} E_{\alpha+\beta} \quad (\text{if } \alpha + \beta \neq 0), \\ [E_\alpha, E_{-\alpha}] &= \sum_i \alpha_i H_i. \end{aligned} \tag{6.2}$$

In these relations, the α_i span an n -dimensional so-called *root vector* or *root*. For each ladder operator, say E_α and E_β , there exists one such root vector. This induces the vector addition $\alpha + \beta$ in the usual Euclidean sense. Therefore, one can identify *simple*, linearly independent, root vectors, which define a basis of the full set of roots. Consequently, all other root vectors can be written as linear combinations of the simple roots.

For defining the irreducible representations of the group $\text{SO}(2n + 1)$, we can construct simultaneous eigenvectors of the H_i operators, which have certain so-called weights, defined by the components of the α . The respective α_i are conveniently chosen to be ordered, such that $\alpha_1 \geq \alpha_2 \geq \dots \geq \alpha_n$. The weight vectors themselves can also be ordered, where a weight α is said to be larger than another weight vector β if $\alpha - \beta$ is positive. A positive weight is defined by having a positive first non-vanishing component. The highest weight specifies unambiguously the irreducible representation since all other weights straightforwardly follow.

Conclusively, an irreducible representation of $\text{SO}(2n + 1)$ is unambiguously defined by the highest weight vector with n components, which are the eigenvalues of the H_i operators spanning the Cartan subalgebra. Actually, other schemes for the labeling exist, but the Cartan form is used throughout the present work [51].

In addition, one can generally construct n Casimir operators commuting with all the l generators of the algebra. For the $\text{so}(2n + 1)$ algebras, only Casimir operators of even power exist, i.e. the Casimir operators are constructed from a product of an even number of generators [22, 38].

For root vectors α, β, \dots one defines a usual scalar product

$$(\alpha, \beta) = \sum_j \alpha_j \beta_j,$$

which leads to **lengths** of individual roots and to **angles** between distinct roots. One can show that these lengths and angles are restricted to have specific values which leads to a **classification** of the semi-simple algebras [38]. Furthermore, they can be used to set up a **root vector diagram**, which is a graphical representation of the Lie algebra. In these root vector diagrams, one can additionally depict irreducible representations of the according Lie group. For that, one draws points on the respective α vectors to represent the weights. In Fig. 6.1 we show two examples of root vector diagrams.

Example 6.1 For the SO(3) group, the commutation relations can be easily checked and the E_α and H operators can be straightforwardly defined

$$\begin{aligned} [\hat{J}_z, \hat{J}_z] &= 0, & [\hat{J}_z, \hat{J}_\pm] &= \pm \hat{J}_\pm, \\ [\hat{J}_+, \hat{J}_-] &= \hat{J}_z. \end{aligned}$$

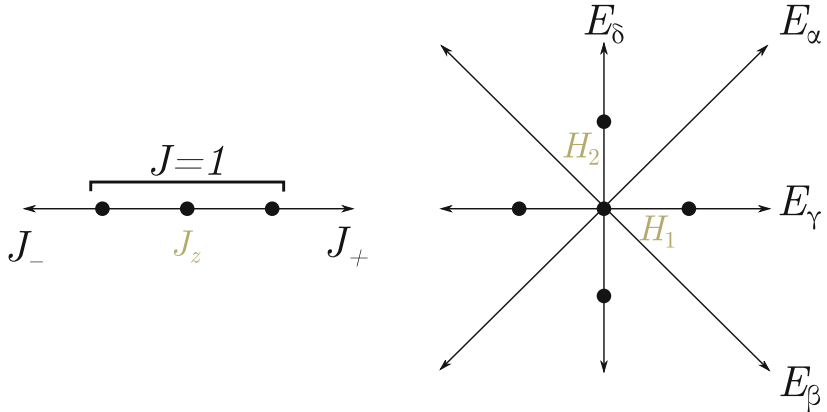
Therefore, $\alpha = +1$ and $\beta = -1 = -\alpha$, i.e. $E_\alpha = \hat{J}_+$, $E_\beta = E_{-\alpha} = \hat{J}_-$ and $H_1 = \hat{J}_z$. Since $n = 1$, there is one element of the Cartan subalgebra and $l - n = 2$ ladder operators. The highest weight is actually J , since the eigenvalues of J_z for the respective eigenfunctions of the rotations in three dimensions are defined to be $|m| \leq J$. In Fig. 6.1 we show the root vector diagram of so(3).

The quadratic Casimir operator of so(3), the only one existing, can be written as $C_2 = \hat{J}_x^2 + \hat{J}_y^2 + \hat{J}_z^2 = \hat{J}_+ \hat{J}_- + \hat{J}_- \hat{J}_+ + \hat{J}_z^2$ and therefore equals the total angular momentum operator.

Example 6.2 A second, more elaborate example is the group of five-dimensional rotations, SO(5), which we will use in Chap. 7 of this part. The corresponding Lie-algebra so(5) is generated by ten operators, $J_{ij} = -J_{ji}$ with $i > j = 1, \dots, 5$. The defining property is the commutation relation

$$[J_{ij}, J_{kl}] = i [\delta_{ik} J_{jl} - \delta_{il} J_{jk} - \delta_{jk} J_{il} + \delta_{jl} J_{ik}].$$

The Cartan subalgebra can be chosen to be spanned by $H_1 = J_{12}$ and $H_2 = J_{34}$ with $[H_1, H_2] = 0$ and four ladder operators can be derived to be [84]



(a) Root vector diagram for the $\text{so}(3)$ algebra. The three dots indicate the $J = 1$ representation, and the J_{\pm} operators potentially raise the projection quantum number, whereas the J_z operator does not affect this number. The respective root vector angle is trivially 90°

(b) Root vector diagram of the $\text{so}(5)$ algebra. The E operators are the generalized ladder operators and the H_i are the elements of the Cartan subalgebra and hence are projections onto the root vectors δ and γ . The angle between two root vectors is calculated to be $\varphi = 45^\circ$. The dots indicate the irreducible representation $[1, 0]$ with its five weights.

Fig. 6.1 Root vector diagrams of the $\text{so}(3)$ and $\text{so}(5)$ algebras. The ladder operators E and the Cartan subalgebra elements H are shown. The dots represent exemplary irreducible representations

$$\begin{aligned} E_\alpha &= \frac{1}{2}(J_{13} + i J_{23}) + \frac{i}{2}(J_{14} + i J_{24}), \\ E_\beta &= \frac{1}{2}(J_{13} + i J_{23}) - \frac{i}{2}(J_{14} + i J_{24}), \\ E_\gamma &= \frac{1}{\sqrt{2}}(J_{15} + i J_{25}), \\ E_\delta &= \frac{1}{\sqrt{2}}(J_{35} + i J_{45}). \end{aligned}$$

The commutation relations with H_i lead, see (6.2), to the roots $\alpha = (1, 1)$, $\beta = (1, -1)$, $\gamma = (1, 0)$, and $\delta = (0, 1)$.

The roots can be displayed in a root vector diagram (see Fig. 6.1b). In addition, an irreducible representation can be depicted in that diagram. For a highest weight $(1, 0)$ there are four weights, which are “smaller”, i.e. their difference has a first non-vanishing positive component

$$(1, 0) > (0, 0), \quad (1, 0) > (-1, 0), \quad (1, 0) > (0, 1), \quad (1, 0) > (0, -1),$$

which makes the irreducible representation five dimensional. In the root vector diagram in Fig. 6.1b, these weights are indicated on the axes of the respective ladder operators, e.g., the weight $(0, 1)$ is represented as a dot on the E_δ axis. Since the ladder operators E_γ and E_δ raises the eigenvalue of either H_1 or H_2 while the respective other one remains fixed, the H_i operators can be understood as projection operators onto the roots γ and δ .

In analogy to the three-dimensional case, we call the highest weight eigenvalues of H_1 and H_2 , $[n_1, n_2]$ with $n_1 \geq n_2$, generalized angular momentum quantum numbers. They unambiguously define the irreducible representations and are both either integer or half-integer [85].

The second-order Casimir operator, which will be discussed in greater detail in Chap. 7, and its eigenvalues for a certain $[n_1, n_2]$ irreducible representation are given as [22, 38]

$$\widehat{C}_2 = 1/2 \sum_{i < j} L_{ij}^2, \quad C_2 = 1/2 (n_1(n_1 + 3) + n_2(n_2 + 1)).$$

In addition to that, also a quartic Casimir operator exists, which can be represented by $\widehat{C}_4 = \sum_i^5 v_i^2$ with $v_m = \varepsilon^{ijklm} J_{ij} J_{kl}$, where the common Einsteins sum convention is used and ε^{ijklm} it the Levi-Civita symbol in five dimensions [86].

Properties of the Matrix Representations of SO(3) Irreducible representations of SO(3) are described by the Wigner-matrices \mathcal{D}_J , which are matrix representations in a suitable basis of spherical harmonics $Y_m^J(\theta, \phi)$ [21, 32, 87]. Elements of the rotation group are defined by an angle of rotation, say β , and a respective axis, \mathbf{v} . The characters of the irreducible representations however, depend only on the angle (and on the highest weight label J)

$$\chi_J(R^0) = 2J + 1, \quad \chi_J(R_v^\beta) = \frac{\sin((2J + 1)\beta/2)}{\sin(\beta/2)}. \quad (6.3)$$

An applied electric field induces a preferred lab-fixed axis and the full SO(3) symmetry is broken to $\text{SO}(2) \subset \text{SO}(3)$. The $2J + 1$ (degenerate) states of a single SO(3) representation split into $\mathcal{D}_J \downarrow \text{SO}(2)$, which are simply the one-dimensional SO(2) irreducible representations with the well-known magnetic quantum number m . The respective characters for a rotation by φ about the preferred axis are $e^{im\varphi}$.

Isomorphism of Rotations and Permutation-inversion Symmetry Groups The elements of the complete nuclear permutation-inversion group or the restricted molecular symmetry group affect three different types of coordinates: [14] (i) Electronic and nuclear vibrational coordinates, (ii) rotational coordinates, usually taken to be the three Euler angles specifying the orientation of a molecular fixed coordinate system relative to a lab- (or observer-) fixed one, and (iii) nuclear spin coordinates.

In the most convenient approach to molecular dynamics, these coordinates are initially considered to be (near-) separable. All couplings between motions described in different sets of coordinates, as, e.g., ro-vibrational or spin-orbit couplings, are treated perturbatively or as inducing off-diagonal matrix elements in a variational treatment. As outlined in Chap. 2, the perturbative approach to ro-vibrational dynamics is extremely successful for most molecular species.

Assuming the separation of variables to be valid, we can write the permutation-inversion operations g as a product $g = g_{\text{vibronic}} \circ g_{\text{rot}} \circ g_{\text{nspins}}$, where all three parts commute. In the following, we concentrate on the rotational part, the vibrational degrees of freedom are treated fully independently and we will not discuss their symmetry in any detail.

Focusing on the group of g_{rot} , the operators acting exclusively on the Euler angles, its elements can be found by using the equivalent rotation technique of Longuet-Higgins [30]. In general, the group of g_{rot} is a group of rotations describing how a molecule fixed axis system has to be rotated to “follow” a permutation-inversion operation on identical nuclei. The Longuet-Higgins [30] technique prescribes how such a permutation-inversion operation can be mapped to a respective rotation. Conventionally, this is done by a geometric analysis of a fixed molecular structure. In Chap. 8 however, we will show a matrix-based formulation of the equivalent rotations, which is generalizable to higher-dimensions.

The mathematical description of this translation of permutation-inversion group elements into rotational group elements is the mapping from the molecular symmetry group to a *subgroup* of the full group of rotations in a molecular fixed coordinate group, also termed \mathbf{K} (mol) in the book of [14]. If this mapping is possible, the molecular symmetry group is hence *isomorphic* to a subgroup of $\text{SO}(3)$, say $\mathbf{G}_{\text{ms}} \subset \text{SO}(3)$. The representations \mathcal{D}_J of the full rotation group therefore subduce a restricted representation $\mathcal{D}_J \downarrow \mathbf{G}_{\text{ms}}$ into the smaller group.²

Example 6.3 For an example of factorizing the molecular symmetry operations, we consider the water molecule (see [9]). Its molecular symmetry group is $\mathbf{C}_{2v}(\mathbf{M}) = \{E, (12), E^*. (12)^*\}$. Writing the elements as according products $g = g_{\text{vibronic}} \circ g_{\text{rot}} \circ g_{\text{nspins}}$, we find

$$\begin{aligned} E &= E R^0 p_0, \\ (12) &= C_{2x} R_x^\pi p_{12}, \\ E^* &= \sigma_{xz} R_y^\pi p_0, \\ (12)^* &= \sigma_{xy} R_z^\pi p_{12}. \end{aligned}$$

The group $\mathbf{D}_2 = \{R^0, R_x^\pi, R_y^\pi, R_z^\pi\}$ acts exclusively on the Euler angles and hence on the rotational degrees of freedom. It forms a subgroup of the molecule-fixed rotation group $\text{SO}(3)$. Due to the same multiplication behavior, \mathbf{D}_2 is isomorphic to $\mathbf{C}_{2v}(\mathbf{M})$, the permutation-inversion group. The elements of \mathbf{D}_2 are consequently

²See Sect. 4.1 for a description of the subduced representations in the case of finite groups. The generalization to continuous “parental” groups with finite subgroups is straightforward.

called *equivalent rotations* and are usually found by geometric analysis [30]. All other operations, e.g., C_{2x} , σ_{xz} etc., does not act on the Euler angles and are not further treated here.

Equivalently to the statement that elements of the molecular symmetry group are separable into three parts, the total molecular wave function can be written as a product

$$\psi_{\text{tot}} = \psi_{\text{vibronic}} \psi_{\text{rot}} \psi_{\text{nspin}}.$$

In particular, this demands the rotational states ψ_{rot} to span the representation $\mathcal{D}_J \downarrow G_{\text{ms}}$ in the molecular symmetry group. With this representation, missing pure rotational levels can be found by inspecting the product representation of $(\mathcal{D}_J \downarrow G_{\text{ms}}) \otimes \Gamma_{\text{nspin}}$ (see, e.g., Sect. 6.1.1). With this, certain dipole selection rules can be identified. The latter are already restricted by the $\text{SO}(3)$ group itself: Since a photon carries an angular momentum of $J = 1$, the electric dipole operator, describing the spectroscopic transitions most easily observed, spans the \mathcal{D}_1 representation of $\text{SO}(3)$. The product of initial and final representations, \mathcal{D}_{J_1} and \mathcal{D}_{J_2} , and the dipole representation are calculated from (3.3) of Part I, and leads to the well-known selection rule $\Delta J = \pm 1$.

The isomorphism between molecular symmetry group and rotational subgroup induces a fundamental question we answer in the upcoming chapter:

Are all molecular symmetry groups isomorphic to a subgroup of the special orthogonal group in three dimensions?

This question is of particular importance since the convenient separation of variables relies on an affirmative answer. If the zero-order model of separated rotational and vibrational degrees of freedom fails, fundamentally new methods must be developed, which is the initial idea of Chap. 7.

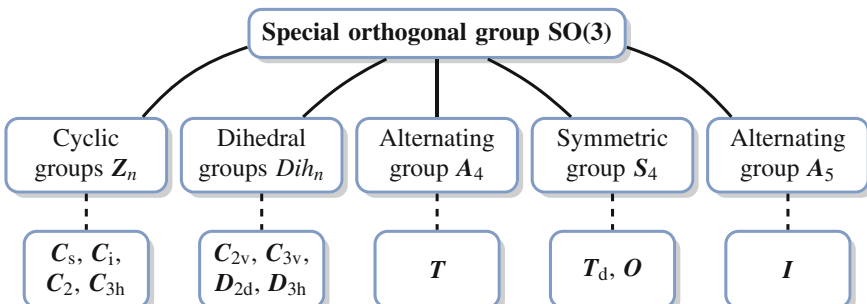


Fig. 6.2 Set of subgroups of the group of rotations in three dimensions. In the last row, examples of isomorphic molecular symmetry groups are shown. The graphic is reproduced after [9]

In order to answer the question raised above, we use again group theory since $\text{SO}(3)$ possesses a well-known finite set of subgroups (see Fig. 6.2). In this set, we find all common examples of molecular symmetry groups, however, there is no strict rule for this and some exceptions are already known: Products of $\text{SO}(3)$ subgroups can be found to be isomorphic to certain molecular symmetry groups, which signals the possibility of symmetry operations, reversing the handedness of the molecule-fixed coordinate system. This can be understood by noting that a product of two subgroups of $\text{SO}(3)$ is – if not a subgroup of $\text{SO}(3)$ – a subgroup of $\text{O}(3) = \text{SO}(3) \times \{E, E^*\}$, including the so-called *improper* rotations, defined by a negative determinant of their matrix representative. In addition, molecules with an odd number of electrons and a strong spin-orbit coupling are symmetric under so-called spin-double groups (see Chap. 18–1 of [14]) Such groups are isomorphic to subgroups of $\text{SU}(2)$, the special unitary group in two dimensions, which in turn is the double-cover group of $\text{SO}(3)$ [88].

For molecules of strong spin-orbit coupling and an odd number of electrons, the total angular momentum can be half-integral. The characters of the usual $\text{SO}(3)$ representation matrices, see (6.3), indicate that a rotation by $\theta + 2\pi$ possibly reverses the sign of the character of a rotation by θ :

$$\chi_J(\theta + 2\pi) = (-1)^{2J} \chi_J(\theta)$$

In the equivalent rotations for a specific molecular symmetry group however, one would consider a 2π rotation as being no rotation. Hence, all equivalent rotations with $\theta = 0$ would have two possible characters for half-integral J . To avoid the ambiguities, one introduces the $\text{SU}(2)$ group instead of the $\text{SO}(3)$ rotation group. There, a rotation by $\theta + 2\pi$ is explicitly distinguished from the rotation by θ . The molecular symmetry group elements are consequently also doubled to specifically fix those elements which map onto the 2π rotations. Each permutation-inversion element gets a “partner” element, which is correlated to a rotation by additional 2π . For example if the permutation (12) is mapped onto a rotation by $\theta = \pi$, it gets a partner, say $(12)'$, mapped onto $\theta = 3\pi$. This particularly fixes the respective characters of the irreducible representation for both operations and these **spin-double groups** are therefore isomorphic to subgroups of $\text{SU}(2)$ rather than $\text{SO}(3)$. For examples, see Chap. 18 of [14].

Apart from these two already known exceptions, which still are strongly related to the $\text{SO}(3)$ group itself, in Sect. 6.2, we discuss the very first example – to our knowledge – of a molecular symmetry group which is neither isomorphic to a subgroup of $\text{SO}(3)$, $\text{O}(3)$, nor $\text{SU}(2)$.

In conclusion, molecular symmetry groups need *not* to be isomorphic to subgroups of the rotational group $\text{SO}(3)$. Permutations of identical particles are not per se

isomorphic to a subgroup of the three-dimensional rotation group. As we show in Sect. 6.2 these permutations can act on different sets of molecular coordinates in a non-separable manner. Before we actually consider the non-SO(3) subgroups, we first discuss some details of the more usual molecular symmetry groups and their isomorphisms to the rotation group.

In the set of subgroups of SO(3), the cyclic as well as the dihedral groups are special in the sense that their elements can be reduced to two representative operators, either a rotation by β about a molecule-fixed z -axis, or a rotation by π about an axis in the xy plane, which encloses an angle α with the x axis. For molecules with symmetry groups isomorphic to a cyclic or a dihedral group, one usually assumes their rotation to be approximately described by a rigid symmetric rotor. Hence one can use the rigid rotor eigenfunctions $|Jkm\rangle$ as basis states for the solution of the molecular Schrödinger equation, including the perturbative treatment of couplings to other degrees of freedom.³ The action of the representative operators of the cyclic and dihedral group is given by [14]

$$R_z^\beta |Jkm\rangle = e^{ik\beta} |Jkm\rangle, \quad (6.4a)$$

$$R_\alpha^\pi |Jkm\rangle = (-1)^J e^{2ik\alpha} |J, -k, m\rangle. \quad (6.4b)$$

Therefore the \mathcal{D}_J representations, spanned by the $|Jkm\rangle$ functions for fixed J and $k = -J, \dots, J$, can be subdivided into a one-dimensional representation for $k = 0$ and two-dimensional pairs of $|J, |k|, m\rangle$ and $|J, -|k|, m\rangle$. The characters are given by (6.4).

Here, the m value is not required, it simply adds the overall dimensionality of $2J + 1$ of the lab-fixed rotation symmetry. More precisely, the molecular rotational symmetry is two-fold: [9] There is a $\text{SO}(3)_{\text{spatial}}$ group, where an applied external field could lift the degeneracy, and there is an $\text{SO}(3)_{\text{mol}}$ group, which contains the rotation group isomorphic to the molecular symmetry group. In [14], these groups are called \mathbf{K} (spatial) and \mathbf{K} (mol) respectively. Therefore the whole set of $(2J + 1)^2$ functions $|Jkm\rangle$, where k and m both range from $-J$ to J , spans the irreducible representations \mathcal{D}_J in $\text{SO}(3)_{\text{spatial}}$, and $\mathcal{D}_J \downarrow \mathbf{G}_{\text{ms}}$ in the molecular symmetry group.

The isomorphisms of molecular symmetry groups to the A_4 , A_5 or S_4 cannot be found by the equivalent rotation technique of [30]. However, the authors of [89] established a suitable approach for finding the respective isomorphisms. There, the splitting into $k = 0$ and $k \neq 0$ is impossible and the rotational representations simply restrict to $\mathcal{D}_J \downarrow \mathbf{G}_{\text{ms}}$.

At this point, a short note on linear molecules is appropriate: They are also viewed as rigid rotors, but they exhibit two distinct rotational axes only. Therefore, the molecular rotation group is defined to be $\text{SO}(2)$ and the respective irreducible

³Notice the synonymous use of separable “molecular coordinates”, “degrees of freedom” and “molecular wave function”. The degrees of freedom are usually used as an umbrella term for the molecular coordinates, whereas the molecular wave function shows a functional dependence on them. Therefore separating the molecular coordinates is equivalent to separating the degrees of freedom and to write the molecular wave function as a product.

Table 6.1 Permutation-inversion elements, their equivalent rotations of $D_{3h}(M)$, and the characters of the respective matrix representations of the representations spanned by symmetric top rotor functions. The last row displays the characters of the representation spanned by all k functions which is also found by restricting the related representation \mathcal{D}_J of SO(3) to the $D_{3h}(M)$ group by using (6.3). The table is reproduced after [9], TABLE I

$D_{3h}(M)$	E	(123)	(23)	E^*	$(123)^*$	$(23)^*$
equiv. rot	R^0	$R_z^{2\pi/3}$	$R_z^{\pi/2}$	R_z^{π}	$R_z^{5\pi/3}$	R_0^{π}
rot. angle	0	$2\pi/3$	π	π	$5\pi/3$	π
$ k > 0$	2	$2 \cos(\frac{2}{3}K\pi)$	0	$2(-1)^K$	$2 \cos(\frac{5}{3}K\pi)$	0
$k = 0$	1	1	$(-1)^J$	1	1	$(-1)^J$
\mathcal{D}_J	$2J+1$	$\frac{2}{\sqrt{3}} \sin(\frac{\pi}{3}(2J+1))$	$(-1)^J$	$(-1)^J$	$2 \sin(\frac{5\pi}{6}(2J+1))$	$(-1)^J$

representations are one-dimensional with character $e^{iJ\varphi}$, where J denotes the angular momentum quantum number restricted to two dimensions. In the molecular symmetry group therefore, the SO(2) representations subdue the representation $\mathcal{D}_J \downarrow \mathbf{G}_{ms}$. We already noticed one example in the discussion of molecular hydrogen in Sect. 4.1.2 of Part I. For the linear molecules the molecular symmetry groups are therefore isomorphic to subgroups of SO(2). In the rest of this chapter, we focus on non-linear molecules, but since $\text{SO}(2) \subset \text{SO}(3)$, the indications for the smaller two-dimensional rotation group are straightforward.

6.1.1 Example: The H_3^+ ion

The smallest, non-linear molecule is the triangular H_3^+ ion, which we already encountered in Chap. 4 of Part I. That part focused on its reaction with H_2 and computed the Pauli-allowed ro-vibrational states in the permutation group S_3 by using the Schur-Weyl duality of the first part of this work. However, these states were labeled only by the irreducible representations of the symmetric group (see Table 4.1 of Part I). With the isomorphism to a subgroup of SO(3) however, we are able to identify also the J, k labels of conventional rotational theory. For a full treatment, we here treat the complete nuclear permutation-inversion group $S_3 \times \{E, E^*\} \equiv D_{3h}(M)$, [14] whereas for the nuclear spin treatment, the permutation subgroup was sufficient. The number of irreducible representations of S_3 is doubled in $D_{3h}(M)$ and their symmetric or antisymmetric behavior under inversion is used to name them, e.g., A'_1 and A''_1 respectively (see Table 6.2). It is a textbook example of equivalent rotations and we only list them in Table 6.1, where we additionally show the $\mathcal{D}_J \downarrow D_{3h}(M)$, and the according $k = 0$ and $|k| > 0$ representations. In Table 6.2 we show the character table of $D_{3h}(M)$ together with the $J = 0$, $J = 1$, and $J = 2$ representations.

From the discussion of the nuclear spin states in Sect. 4.1 of Part I, we can calculate the $\Gamma_{n\text{spin}}$ representation of the $D_{3h}(M)$ group leading to the nuclear spin weights [14, 90]

Table 6.2 The character table of $D_{3h}(M)$ and the characters of the $J = 0, 1, 2$ representations of $\mathcal{D}_J \downarrow D_{3h}(M)$ calculated from Table 6.1

$D_{3h}(M)$	E 1	(123) 2	(23) 3	E^* 1	$(123)^*$ 2	$(23)^*$ 3
A'_1	1	1	1	1	1	1
A''_1	1	1	1	-1	-1	-1
A'_2	1	1	-1	1	1	-1
A''_2	1	1	-1	-1	-1	1
E'	2	-1	0	2	-1	0
E''	2	-1	0	-2	1	0
$J = 0$	1	1	1	1	1	1
$J = 1$	3	0	-1	-1	2	-1
$J = 2$	5	-1	1	1	1	1

$$g_{ns}(A'_2) = g_{ns}(A''_2) = 4, \quad g_{ns}(E') = g_{ns}(E'') = 2.$$

All other weight factors are zero. Therefore the $J = 0$ state is missing, whereas the $J = 1$ states of $A'_2 \oplus E''$ symmetry are present (see Table 6.2). The respective $J = 1$, $k = 0$ state has a nuclear spin weight of $g_{ns} = 4$ and the pair of $k = \pm 1$ states have $g_{ns} = 2$. In $J = 2$, the $k = 0$ level is missing, as it is for all even J states. The corresponding $k = 1, 2$ states are of E'' and E' with $g_{ns} = 2$ symmetry respectively.

This concludes the example of H_3^+ showing how the $SO(3)$ characters can be used to determine the symmetry of the rotational wave function in the molecular symmetry group, whenever G_{ms} is a subgroup of $SO(3)$.

With this restricted representation, we also notice one additional feature: The molecular rotational wave function ψ_{rot} must span an irreducible representation of the molecular symmetry group. Since the \mathcal{D}_J representations span certain reducible representation in the molecular symmetry group, conversely, they can be used to rewrite ψ_{rot} as linear combination of the respective $|Jkm\rangle$ functions. This is actually a validation of the use of the $|Jkm\rangle$ functions as (part of) the basis states for the solution of the full molecular Schrödinger equation for most molecules.

6.2 The Failure of the Subgroup Picture

In the previous paragraph, we justified the use of $|Jkm\rangle$ functions as rotational basis for the solution of the full molecular Schrödinger equation. This does not depend on the type of approach, whether it is a strict perturbative approach – as a Watson-type Hamiltonian [33] – or more advanced bend-rotation Hamiltonians recently used in high-level calculations [35]. However, in any numerical approach, the basis set size is limited by computing time, which possibly restricts the achievable accuracy.

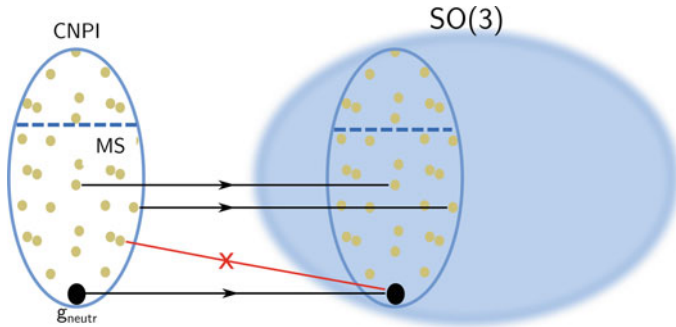


Fig. 6.3 Left Permutation-inversion elements of the complete nuclear permutation-inversion group (CNPI). The molecular symmetry group (MS) defines a subset of these elements, indicated by the dashed dividing line. The respective elements are mapped (black arrows) onto equivalent rotations which are elements of the rotation group $\text{SO}(3)$ (right hand side). Also there, the respective rotations for the full CNPI group and the MS subgroup are shown. We indicate the continuous group of rotations by the filled bluish area. Single spots represent the equivalent rotations on which the elements of the molecular symmetry group are mapped. To represent a proper isomorphism, only the neutral element of the molecular symmetry group is allowed to be mapped onto the neutral element of the rotation group. The red arrow indicates a forbidden mapping of a second MS group element onto the neutral element of the rotations

But as we already indicated, there is no strict rule forcing the molecular symmetry group to be representable by rotations of $\text{SO}(3)$. For that, the elements of a chosen molecular symmetry group must show a one-to-one correspondence to the rotations. In particular, there must be a three-dimensional corresponding map $\rho : G_{\text{ms}} \rightarrow \text{SO}(3)$ where the kernel of ρ , i.e. elements mapping onto the neutral element of the rotations, must be trivial. Hence, only neutral elements can map onto the neutral element of the rotations (see Fig. 6.3). Otherwise, the multiplication behavior of the rotations would differ from those of the permutation-inversion elements and no one-to-one correspondence could be established.

In general, any map from the molecular symmetry group to n -dimensional matrices is described as a possibly reducible n -dimensional representation. As indicated in Sect. 2.1 of Part I, these representations are decomposable into the irreducible representations of the group. Therefore we can use the dimensions of the irreducible representations as a first indication for identifying impossible mappings to the rotation group $\text{SO}(3)$. For example, the permutation group of five identical particles, S_5 , actually the permutation subgroup of the molecular symmetry group of the celebrated protonated methane, CH_5^+ , has irreducible representations with dimensions $\{1, 1, 4, 4, 5, 5, 6\}$. The two one-dimensional representations are the symmetric and the anti-symmetric one, so that the kernel of any three-dimensional map ρ would have a kernel equal to the full S_5 group or at least the alternating subgroup. Therefore, there is no possible isomorphism to a subgroup of $\text{SO}(3)$.

Hence, the S_5 group is the very first example of a molecular symmetry group that is not isomorphic to a subgroup of customary three-dimensional rotations. The strict

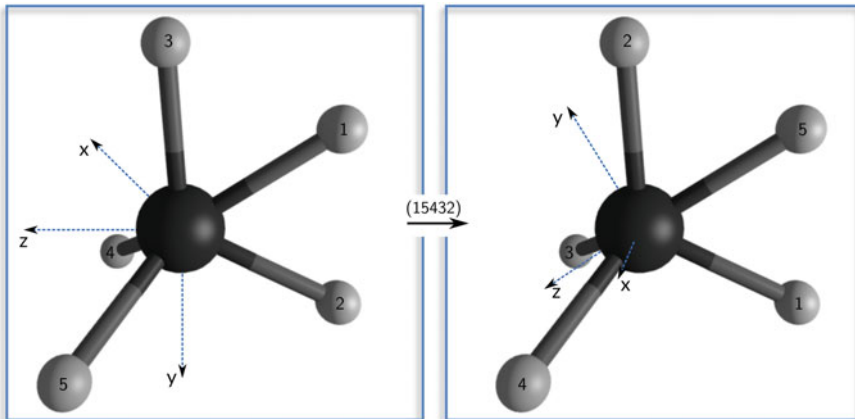


Fig. 6.4 Protonated methane with a molecule-fixed coordinate system defined in the text. *Left* Initial CH_5^+ in its C_3v structure, where protons (H_1, H_2, H_3) and the carbon nucleus are in the plane of the drawing, whereas protons 4 and 5 lies in a perpendicular plane. The x axis points inwards the drawing plane. *Right* Same molecule, where the symmetry operation (15432) has been applied. The same definition of the coordinate system is used and the x axis is now pointing outwards in the direction of the reader. The figure is reproduced after [9]

mathematical statement of the non-trivial kernel for any map to three-dimensional linear transformations is further supported by attempting to apply the equivalent rotation technique to a fixed CH_5^+ structure. This will be discussed in detail in Chap. 9.

Equivalent Rotations The equivalent rotation technique of [30] starts by defining a molecule-fixed coordinate system. First, we label the protons in an imagined fixed geometric structure by 1,...,5 (see Fig. 6.4). The y axis is chosen to be parallel to the $H_1 - H_2$ connecting line pointing towards H_2 . The carbon nucleus and these two protons define a plane, to which we define the x -axis to be perpendicular. Its direction is fixed by the vector $\mathbf{r}_{C1} \times \mathbf{r}_{C2}$, where the \mathbf{r}_{Ci} are defined as vectors starting at the C nucleus and ending at H_i . The z axis then is defined straightforwardly from the requirement of a right-handed system. The symmetry operation (15432) is performed and the coordinate system can be attached again (see right part of Fig. 6.4). We obtain a change in the coordinate system that cannot be described by either the rotation about a fixed z -axis nor by a mirror operation about an axis in the xy plane. In particular, the z -axis loses its “status” of a quantization axis. This result does not depend on the chosen numbering of the protons nor on the definition of the axis system as long as it is defined coherently for the molecule before and after the permutation [9].

Therefore, rotational wave functions of the form $|Jkm\rangle$ cannot be transformed in the conventional way of (6.4), since the two equivalent rotations are not sufficient to describe the rotation of the full coordinate system as shown in Fig. 6.4.

The lab-fixed $\text{SO}(3)_{\text{spatial}}$ group remains a proper symmetry group and J is still – as expected – a good quantum number. Consequently, also the magnetic quantum number m is still valid, but k cannot be defined in any way. Indeed, in the

discussion of asymmetric top molecules, it is well-established that k is not a good quantum number, but rather a “near”-quantum number (see 13.1.2 of [14]). It is used as an approximate labeling for the rotational states and, e.g., in pattern recognitions in spectroscopic experiments it has proven very helpful. In the case of the S_5 molecular symmetry group, our discussion indicates however, that the k label loses also the status of being a “near” quantum number, since no fixed quantization axis is definable.

In conclusion, the quantum labels J as the total angular momentum, its projection m on a lab-fixed axis, a parity label from spatial inversion and of course the labels of the symmetry group S_5 remain valid. More strikingly, the k label and, simultaneously, the vibrational labels are questionable since no separate treatment of the molecule-fixed rotation and nuclear vibration can be established. We will discuss this particular point and its physical meaning in Chap. 7.

Actually, the use of $\text{SO}(3)$ symmetric states was noticed to be insufficient already by [73]. The authors however only stated: “One must now note that the permutation groups S_n are not isomorphic to subgroups of the rotation group $\text{SO}(3)$ if $n > 4$.” ([73, p. 4230]). With our mathematical explanation, this statement is now set on a strict mathematical basis.

Subgroups of the Molecular Symmetry Group of CH_5^+ The break-down of the conventional approach is a strict mathematical consequence of the assumed permutation symmetry group. We assumed the total S_5 group, the group of permutations of five identical particles, to be valid molecular symmetry group. An example for such a symmetry group is CH_5^+ . However, the respective potential energy surface potentially induces certain barriers, such that a subgroup of the full S_5 group must be used. This has attracted a lot of interest in realm of ab-initio calculations, but recent calculations show that all barriers are low compared to the zero-point vibrational energy, such that the full group is appropriate. Nevertheless, a treatment of the subgroups is useful also with respect to possible other molecules, where conventional ro-vibrational separation might fail. One respective example is the H_5^+ ion, where recent ab-initio studies revealed that certain potential energy barriers exist which possibly restrict the complete nuclear permutation group. We will discuss it in a bit more detail in Chap. 10.

The subgroups of S_5 are shown in Fig. 6.5 and all of them turn out to be isomorphic to subgroups of the $\text{SO}(3)$ [or $\text{O}(3)$] group with the exception of the full group. Therefore, if any of the barriers is assumed to restrict the movement of the protons, such that not all permutations are feasible, the rotational – and hence also the vibrational – dynamics can be treated in a more conventional, separable, way (see, e.g., the discussion in [80]). This is actually the starting point of calculations recently done by T. Carrington and co-workers, [29, 35, 92] where one proton is assumed to be special such that the indistinguishability is lost. Consequently, the total symmetry group is restricted to a subgroup before the technique of induced representations is used to represent the calculated states in the proper, full group. For a more detailed study of the respective definition of coordinates, we here refer to our study in [9].

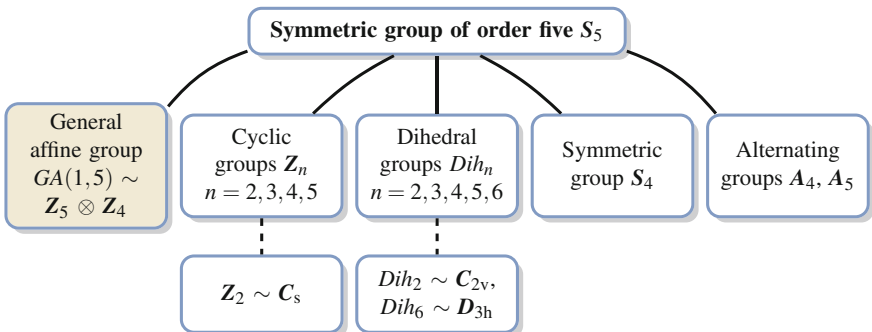


Fig. 6.5 Set of subgroups of the symmetric group of degree five up to conjugacy [91]. The last row indicates the groups used in [80], whereas [35] use the S_4 group. All shown subgroups are isomorphic to subgroups of $SO(3)$, except the group $GA(1, 5)$, which is a subgroup of $O(3)$. The graphic is reproduced after [9]

6.3 Concluding Remarks

In conclusion, from a purely mathematical point of view, we showed that the molecular symmetry group is not restricted to be isomorphic to a subgroup of $SO(3)$. The elements of the molecular symmetry group are permutations of identical particles and as such are not required to be representable in terms of rotations in conventional three-dimensional space. Nevertheless, the majority of molecular species are described by molecular symmetry groups which *are* isomorphic to subgroups of $SO(3)$. The extension to $O(3)$ and $SU(2)$ covers more molecules and is straightforward. Usually, the isomorphism is found by a technique invented in the 1960s, [30] where each symmetry element is mapped onto a rotation of a molecule-fixed coordinate system. Representation theory of $SO(3)$ subsequently can be used to determine the permutation-inversion symmetry of the rotational states. We demonstrated this for the textbook example of H_3^+ , where the molecular symmetry group is isomorphic to D_{3h} which is a proper subgroup of $SO(3)$.

However, we also considered a first example where $SO(3)$ is *not* sufficient to cover the full molecular symmetry group. The permutation group of five identical particles is not isomorphic to any subgroup of $SO(3)$, nor of $O(3)$ or $SU(2)$. This group has been shown to be the permutation subgroup of the molecular symmetry group of the famous CH_5^+ cation and hence our findings indicate that the discussion of rotational states for this molecule cannot be done in the conventional way. The latter assumes an initial separation of rotational and vibrational degrees of freedom, which now mathematically is ruled out. In the next chapter, however, we develop a fundamentally new physical model for extremely floppy molecules which circumvents the problem of rotation-vibration separation. This model is shown to overcome the isomorphism problem by using a larger *super*-rotation group involving a five-dimensional space.

Chapter 7

The Molecular Super-Rotor

Abstract In this chapter, the model of super-rotation is introduced. In this model, the internal and overall rotation of extremely floppy molecules is treated as indistinguishable and hence both are treated together in a higher-dimensional rotor model. In particular, by releasing the internal rotor axis and its angle, one is led to use a five-dimensional rotor approach. The energy expression of a five-dimensional rotor is discussed and compared to that of traditional internal rotor theories.

7.1 Large Amplitude Motion

As indicated in Chap. 5 of the present part, introducing large amplitude motions is the first step on a route away from the classical ball-and-stick picture of molecules. These motions are paradigmatic examples of quantum mechanics because they are mostly correlated to classically forbidden dynamics. One example is the famous umbrella flipping motion in the ammonia molecule, but also the (hindered) internal rotation of methyl groups in molecules like dimethyl ether, CH_3OCH_3 or nitromethane, CH_3NO_2 . One step beyond are the *extremely* floppy molecules, which exhibit a number of equivalent internal rotations, such that the physical picture of an (almost) freely moving internal rotor axis in addition to the correlated internal rotation emerges.

In order to establish a new theory on the dynamics of extremely floppy molecules, we start with a brief introduction to the theory of internal rotation. For more information, we here refer to [70] for a recent review and to the famous textbook of [26]. The main purpose of this section is to pave the way to the super-rotor model, developed in [7] and [6] and further discussed in Sect. 7.2.

The theory of internal rotation starts with the assumption of a substructure rotating with respect to a framework. In Fig. 7.1, we show the vibrational ground state of nitromethane, CH_3NO_2 , where the methyl group can rotate nearly freely relative to the NO_2 moiety (see also Fig. 2.1 of Part I on p. 14). The potential energy surface for such a motion of the substructure can be described approximately by a one-dimensional projection onto a single internal rotation axis. The respective angular coordinate is considered to be sufficient for the description of the internal dynamics.

All other degrees of freedom are assumed to be decoupled and hence can be described as frozen for the moment. In the very common case of internal rotation of a methyl group attached to such a framework, the internal rotation potential is described by a cosine-type function. It exhibits three equivalent minima, differing only in the numbering of the methyl group protons. For the motion in that potential two main limits exist: (i) in the high-barrier case, the internal rotation can be approximately described by a concerted small-amplitude vibration of the three protons of the methyl group and (ii) in the low-barrier case, they can rotate almost freely around the internal axis. In the intermediate regime, where the cosine form of the potential is crucial, the according Schrödinger equation can be transformed to Mathieu's equation [93]. In the almost free rotating limit, the internal rotor states are given as

$$U_{v\sigma}(\alpha) \propto e^{i(3k+\sigma)\alpha}, \quad (7.1)$$

where $\sigma = 0, \pm 1$ defines the permutation symmetry in the C_3 permutation group of the methyl group.¹ Here, $\sigma = 0$ spans the A representation, while $\sigma = \pm 1$ is a pair of functions spanning the two-dimensional E species. The unbound $3k + \sigma$ value corresponds to the angular momentum quantum number which is quantized on the axis of internal rotation (see next paragraph). The respective energies are given as

$$E_{v\sigma} = F(3k + \sigma)^2,$$

where $F \propto 1/I_{\text{red}}$ with the reduced moment of inertia I_{red} for the relative rotation of the methyl group and the framework. The value $3k + \sigma$ is not bounded and can take any integer value.

The principal torsional quantum number v becomes evident in the other limit, namely the high-barrier approximation, where the Hamiltonian is that of a harmonic oscillator. The according functions are well-known and the energy is given as

$$E_{v\sigma} = 3\sqrt{V_3 F}(v + 1/2),$$

where V_3 is the barrier height.

Symmetry of the Hamiltonian for Internal Rotation From a more general perspective, the free internal rotation limit of Mathieu's equation has an evident $SO(2)$ symmetry, and the harmonic oscillator is described by an $U(1)$ symmetry group. By substituting $p = 3k + \sigma$ we recover the usual highest weight label of $SO(2)$. In view of the discussion of Lie algebras in Sect. 6.1, we can shortly review the correlation of the two groups $U(1)$ and $SO(2)$. The unitary group can be described using the unitary Lie algebra $u(1)$. For general such algebras $u(n)$, there are n Casimir operators. Consequently, $u(1)$ has one linear Casimir operator producing eigenvalues v for irreducible representations labelled by v . These representations are spanned by the well-known one-dimensional harmonic oscillator functions.

¹The permutation group is $C_3 = \{E, (123), (132)\}$ and has a totally symmetric irreducible representation A and a two-dimensional one, say, E (see p. 578 of [26]).

The $\text{SO}(2)$ group is special since it is abelian and possesses a linear as well as a quadratic Casimir operator. The representations are labelled by p and a \pm index, indicating the handedness of rotation. Conventionally, physical models of free rotation in two dimensions does not depend on the handedness and hence the respective Hamiltonian is proportional to the second-order Casimir of the $\text{SO}(2)$ group only.

In fact, $\text{U}(1)$ and $\text{SO}(2)$ are isomorphic but their Lie algebras are different: The (one-dimensional) elements of $\text{u}(1)$ satisfy $X^\dagger = -X$, where X^\dagger indicates the conjugate transposed of X . In contrast, the elements of $\text{so}(2)$ must fulfill $X^T = -X$ and are expressed as two-dimensional real matrices. This difference induces also the difference in the Casimir invariants even though the elements of $\text{U}(1)$ can be mapped in a one-to-one fashion onto those of the rotation group $\text{SO}(2)$.

Include Overall Rotations The next step in the description of molecules exhibiting internal rotation is its combination with the overall rotation. For our purposes, we consider the case of free internal rotation since its interaction with the overall rotation will be the starting point for the super-rotor theory for extremely floppy molecules. There are different approaches to incorporate the different motions in one model but the main idea remains an initially decoupled system of internal and overall rotors. In all approaches, the basis states for further calculations are given as a product of rigid (overall) rotor states and the states of a decoupled internal rotor.

Example 7.1 Consider as an example a symmetric overall rotor ($A = B$) with an internal rotor, where the internal rotor axis is along the molecule-fixed z axis. The simplified Hamiltonian is given as (p. 609 of [26])

$$H = A(\hat{J}_x^2 + \hat{J}_y^2) + C\hat{J}_z^2 + F\hat{p}^2 - 2C\hat{p}\hat{J}_z,$$

where F is the reduced moment of inertia of the internal rotor $F \propto I_z/(I_\alpha(I_\alpha - I_z))$ and $C \propto 1/(I_z - I_\alpha)$. Here, I_α is the moment of inertia of the internal rotor. The eigenfunctions of the Hamiltonian are products of internal and overall rotor functions and can be written as $\psi = \psi_p |Jkm\rangle$, where the $|Jkm\rangle$ are the usual symmetric rotor eigenfunctions and the $\psi_p = e^{ipa}$ are the eigenfunctions of the free internal rotor. The energy is given as:

$$E = AJ(J+1) + (C - A)K^2 + Fm^2 - 2CmK.$$

The last term represents the direct coupling of the two motions, since the respective operators are coupled. The symmetry group of the Hamiltonian is $[\text{SO}(3) \supset \text{SO}(2)] \times \text{SO}(2)$, where the first part is the usual symmetry chain of a symmetric overall rotor, which has a preferred axis of rotation. In the interaction term of internal and overall rotation obviously the handedness of the particular rotation is decisive. Hence, the according product of the two linear Casimir operators has to be taken into account.

In very general terms, the Hamiltonian for the internal and overall rotation can be described by a symmetry group, which is a subgroup of the product group $\text{SO}(3)_{\text{overall}}$

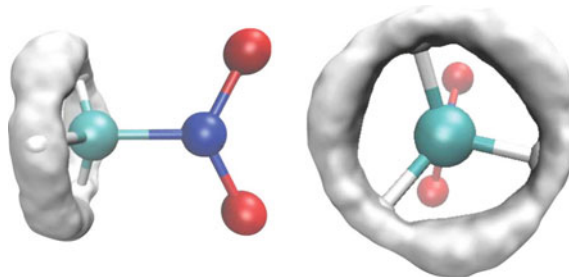


Fig. 7.1 The ground vibrational state wave function of nitromethane as calculated in [94]. The amplitude of the wave function is shown as an isosurface in gray and clearly shows the free internal rotation of the methyl group. Reprinted with permission from X. Wang et al., *The Journal of Physical Chemistry A*, American Chemical Society (ACS), 2015, 119, 11632–11640 ([94]). Copyright 2015 American Chemical Society

$\times \text{SO}(2)_{\text{internal}}$ (see Example 7.1). Therefore, the respective eigenstates are labelled by J and p , the quantum numbers of overall and internal angular momentum. For symmetric or asymmetric overall rotors, the k label will also be appropriate. In the following, we exclusively use the superior J label. As usual, the ground state level is assigned to $(J, p) = (0, 0)$. For most molecules, where the internal rotor subsystem is small compared to the framework, the internal rotation is much faster than the overall one and hence for each J level, many p levels exist nearby. In particular, the energy spacing of two internal rotor states is usually much smaller than those of two successive J states. The two states, $(J, p) = (1, 0)$ and $(0, 1)$ hence are central in the discussion of the internal rotation. Their difference is a first characteristic of the system.

Example 7.2 One example of almost free internal rotation is nitromethane, [94–96]. In this molecule, the V_3 constant is actually zero due to the two oxygen nuclei. The potential for the internal rotation is therefore best described by the next higher order term, i.e., $V(\alpha) = V_6 \cos 6\alpha + \dots$. In [94], the authors calculated a barrier height of $V_6 = 3.5 \text{ cm}^{-1}$, slightly higher than previous experimental values of $V_6 = 2.1 \text{ cm}^{-1}$ [95]. This value is much smaller than the vibrational zero-point energy and the respective ground vibrational wave function is calculated to be delocalized suggesting the methyl group to be an almost free internal rotor. We have indicated the internal rotor and overall rotational states schematically in the right side of Fig. 7.2. In Fig. 7.1 we show an illustration of the vibrational wave function for the ground vibrational state as calculated by [94], clearly showing the free internal rotor property of the methyl group. For comparison, see also Fig. 2.1 on p. 14.

The discussion presented here is undoubtedly incomplete and shows only a few general properties of the theoretical approach to describe internal rotation in molecules. There exists a large variety of studies on that subject, both experimental and

theoretical. However, the central idea of a zero-order model, consisting of a decoupled pair of internal and overall rotors persists in all of these studies, and is likewise the basis for our concept of super-rotation.

7.2 Super-Rotation

The central problem of applying conventional methods of large amplitude motions to extremely floppy molecules, where numerous internal rotations are present in an indistinguishable way, is the fixed internal rotor axis. In the case of nitromethane, we have encountered a single such axis, whereas dimethyl ether already exhibit two such axes. In the latter, they are spatially well-separated, so that again a decoupled zero-order model is appropriate. If this spatial separation is lost, as, e.g. in weakly bound molecular complexes,[71, 97] or in protonated methane, the whole concept of an initial separation of internal and overall rotation is questioned.

The super-rotation model overcomes this problem by inherently treating the two motions in a collective manner. In the following section, we review this fundamentally new zero-order model that we have developed in [7].

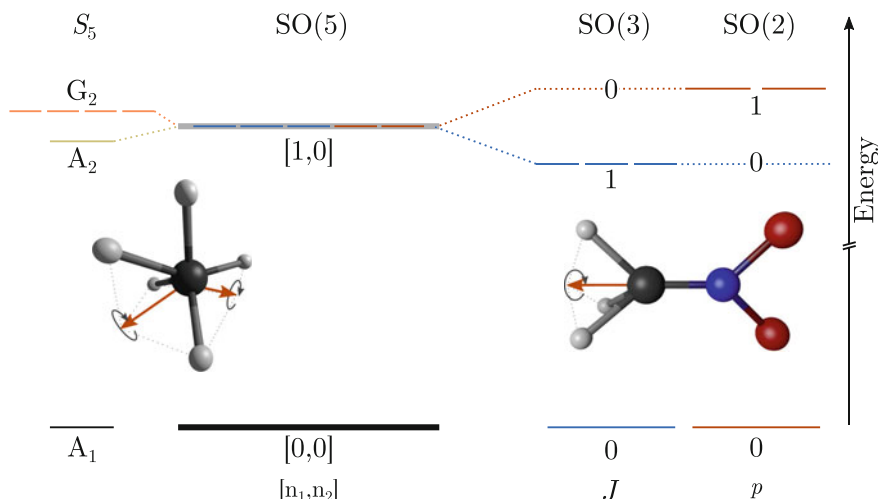


Fig. 7.2 The internal rotor state of $p = 1$ and the overall rotor state $J = 1$ (right) combine to a single five-fold degenerate state in the new super-rotor model (middle). This state is labelled by two fundamentally new quantum numbers $[n_1, n_2]$, defining the $\text{SO}(5)$ symmetric state. The primary example of almost free internal rotation is the nitromethane molecule (CH_3NO_2), whereas the super-rotor model is applied to protonated methane CH_5^+ , see Chap. 9. The respective decomposition of the super-rotor state in the molecular symmetry group of CH_5^+ is shown in the left part of the figure. The figure is reproduced after [7]

In order to establish a model combining internal and overall rotation, we introduce a *super* angular momentum (or super- j) vector, say, \mathbf{N} . It comprises all possible rotations in the molecule, namely the overall rotations about the three molecular-fixed axes and two rotations of the internal rotor, denoting its relative rotation either clockwise or anticlockwise. These five rotations equivalently describe a five-dimensional state, including the two $(J, p) = (1, 0)$ and $(0, 1)$ states (see Fig. 7.2). Conventionally, the three overall rotations can be described by the angular momentum operators $(\hat{J}_x, \hat{J}_y, \hat{J}_z)$ and their action on one of the $2J + 1 = 3$ states with total angular momentum $J = 1$ produces a linear combination of the others. Equivalently a right- or left-handed rotation of an internal rotor state, described by $\exp(\pm i\phi\hat{p})$, does not change the p quantum number of the respective state (see 7.1).

This five-dimensional state however, opens up new possibilites for the exchange of angular momentum. In a separate treatment, angular momentum cannot be transferred between the internally rotating top and the full molecule. In particular, changing the J quantum number induces no change in p and vice versa. The respective operators commute and hence there is no operator lowering J and simultaneously raising p . Eventually, this is possible in the five-dimensional state. If the states $(J, p) = (1, 0)$ and $(0, 1)$ are degenerated as required (see Fig. 7.2), there exist operators “shifting” the $(1, 0)$ to the $(0, 1)$ state, which is equivalent to a shift of the angular momentum from the overall rotor to the internal one. More precisely, there exists a fundamentally new type of rotation, transforming the super- j vector components into each other without changing $|\mathbf{N}|$.

These rotations actually form the special orthogonal group in five dimensions, $\text{SO}(5)$, and hence can be described by ten generalized angular momentum operators (see Sect. 6.1, where the Lie theory for $\text{SO}(2n + 1)$ is discussed). Since the product group $\text{SO}(3) \times \text{SO}(2)$ is a proper subgroup of $\text{SO}(5)$, the four generators of the usual internal and overall rotations are naturally included. However, other subgroups exist, and other forms of representing the ten generators are available [51].

The identification of $\text{SO}(5)$ as the symmetry group of the super-rotor theory, where the internal and overall rotations explained above are indistinguishable, obviously has far-reaching consequences. The Hamiltonian must be proportional to the Casimir operators of $\text{SO}(5)$ and the corresponding eigenfunctions span irreducible representations, which are labelled by *two* quantum numbers (see Sect. 6.1). These highest weight labels, say, $[n_1, n_2]$ can be used to calculate the respective eigenvalues of the Casimir operators, which therefore give an energy expression for an $\text{SO}(5)$ invariant model. They are conventionally chosen to be ordered, such that $n_1 \geq n_2$. The quadratic Casimir operator of $\text{SO}(5)$ is given as (see Example 6.2)

$$\widehat{C}_2 = \frac{1}{2} \sum_{i < j=1}^5 \hat{J}_{ij}^2, \quad (7.2)$$

where the $\hat{J}_{ij} = -\hat{J}_{ji}$ are the ten generalized angular momentum operators, defined to fulfill the commutation relation

$$[\hat{J}_{ij}, \hat{J}_{kl}] = i \left[\delta_{ik}\hat{J}_{jl} - \delta_{il}\hat{J}_{jk} - \delta_{jk}\hat{J}_{il} + \delta_{jl}\hat{J}_{ik} \right].$$

7.2.1 The Energy Expression

The super-rotor model starts with the assumption of indistinguishable internal and overall rotation, leading straightforwardly to a required five-dimensional rotation symmetry group, SO(5). The according Casimir operator is invariant under all the rotations and hence is proportional to the Hamiltonian of the model. In a zero-order approximation, we use only the second-order Casimir operator and we obtain the energies of the super-rotor as [22, 38, 47, 85, 98]

$$E(n_1, n_2) = \frac{B}{2} \{n_1(n_1 + 3) + n_2(n_2 + 1)\}. \quad (7.3)$$

This is the most remarkable result from the unification of internal and overall rotation: Their joint treatment results in a very simple analytical energy expression with a single adjustable parameter. Higher order contributions as, e.g., the quartic Casimir operator, potentially lead to more parameters. In Chap. 9 however, we describe the comparison to recent experimental observations, demonstrating surprising accuracy even in this zero-order approximation.

In order to understand the adjustable parameter B , all of the \hat{J}_{ij} can be equipped with generalized rotational constants, i.e. the Hamiltonian can be written as

$$H_{asym} = \sum_{b < a, c < d=1}^5 \hat{J}_{ab} \frac{1}{2\chi_{abcd}} \hat{J}_{cd}, \quad (7.4)$$

which in principle resembles an asymmetric rigid five-dimensional rotor, where the χ tensor represents the generalized moments of inertia. By using the subgroup $SO(3) \subset SO(5)$, three of the \hat{J}_{ab} operators can be expressed as the conventional generators of three-dimensional rotations, $\{\hat{J}_x, \hat{J}_y, \hat{J}_z\}$, whereas the others form an octupole tensor in $SO(3)$. Choosing the moments of inertia carefully, we can therefore retrieve the usual rotational Hamiltonian in three dimensions and recognize the B constant as equivalent to that of a spherical conventional rotor. Eventually, this can be used for a first guess of the parameter when it comes to assigning spectroscopically determined transitions (see Chap. 9). The comparison to known Hamiltonians of more traditional models will reappear in Chap. 10, where we discuss in particular the connection to internal rotor models like that shown in Example 7.1.

Another remarkable feature of the energy for the super-rotor model is its independence of the conventional angular momentum J . However, J must be a good quantum number, since space is isotropic and an overall rotational symmetry holds. This is ensured by the fact that $SO(3)$, the group of spatial rotations, is naturally included in the (larger) $SO(5)$ symmetry group. Again, this suggests that the super-rotor model enlarges the three rotational degrees of freedom to five, now including two that were previously thought to be of vibrational nature (the internal rotor ones). Straightforwardly this leads to a new, say, counting scheme for the degrees of freedom which we discuss in the next paragraph.

Conclusively, the conjunction of internal and overall rotor states to a combined theory has led us to the formulation of a simple, analytical energy expression with a single adjustable parameter. The quantum numbers of the new model are $[n_1, n_2]$ defining the energy as well as the highest weights of the irreducible representations the according states span.

7.2.2 Degrees of Freedom

In conventional molecular theory, the $3N$ nuclear degrees of freedom are separated into (i) three overall translational, (ii) three rotational, and (iii) $3N - 6$ vibrational ones. One exception is known: If a molecule is linear, only two rotational and consequently $3N - 5$ vibrational degrees of freedom are present. With the arguments of the preceding part, the new super-rotor model includes the internal rotor degrees of freedom (two for the handedness of the relative motion) into a generalized rotation treatment. Therefore, the $3N$ nuclear degrees of freedom can again be separated into (i) three overall translational, (ii) five generalized rotational, and (iii) $3N - 8$ vibrational ones. Again, we hence used the well-known strategy of identifying *collective* degrees of freedom for the dynamics of extremely floppy molecules, where usual models reach their limits.

Consequently, in a zero-order model, vibrational modes are described separately and their respective energies add to the ones of the generalized rotor model of (7.3). By analogy to traditional rotation, the energy differences of vibrational states are naturally larger than those of two adjacent super-rotor states.

If the two additional rotor degrees of freedom are restricted again to be of vibrational nature, where a single internal rotor axis is fixed, we expect the energies to follow a correlation diagram from the limit of completely free internal rotor axis ($\text{SO}(5)$) to fixed internal rotation ($\text{SO}(3) \times \text{SO}(2)$). This correlation qualitatively resembles that of the linear-to-bent correlation diagram in, e.g., triatomic molecular species, as described algebraically in [31] and particularly in Sect. 17.5 of [14]. The exact course of the correlation in case of the $\text{SO}(5) \rightarrow \text{SO}(3) \times \text{SO}(2)$ symmetries is not yet determined, the control parameter still needs further discussion (see Chap. 10).

After having formulated a collective description of internal and overall rotation in the super-rotor model, the corresponding states are described in detail in the following chapter. In particular, we focus on their symmetry in molecular symmetry groups, which is needed to use this model for understanding experimental spectra of extremely floppy molecules. Furthermore, a representation of the states in a basis of well-known symmetric rotor functions is shown. For that, we use ideas of nuclear physics where models of $\text{SO}(5)$ symmetry are used to describe collective nuclear excitations.

Chapter 8

Super-Rotor States and Their Symmetry

Abstract The super-rotor model is discussed in more detail. The respective states of SO(5) symmetry are discussed by relating the model to well-known models of nuclear theories. Furthermore, branching rules for the correlation of these states to well-known states with an ordinary angular momentum quantum number are discussed. These rules follow from the fact that the symmetry group SO(5) incorporates SO(3), the group of three-dimensional rotations, as a proper subgroup. Furthermore, a new technique to find equivalent rotations of permutation/inversion operations is discussed. With this generalization of the well-known Longuet–Higgins method, also the limits, which were discussed in Chap. 6 are overcome. It is now possible to map the elements of the permutation group of five identical particles to rotations in five dimensions. With this, Pauli’s principle can also be applied to the super-rotor states.

8.1 Five-Dimensional Rotor States

In the previous chapter we introduced the concept of super-rotation with which we combine the internal rotation about a free internal rotor axis and the overall rotation of a molecule. The model exhibits an unusual symmetry, which can be interpreted as that of a five-dimensional rigid rotor. Up to now, the discussion was done coordinate-free, and algebraic properties of the SO(5) group were used to formulate the Hamiltonian and the related energy eigenvalues in terms of the highest-weight labels of the irreducible representations of SO(5).

However, for an extension of the model to higher-orders in the generalized angular momentum operators, or for an incorporation of interactions with vibrations, one needs specific coordinate-dependent wave functions. For their definition, we utilize results from nuclear physics, where the five-dimensional rotor, established to describe the nuclear collective model, is one of the building blocks of the interacting boson model (see, e.g., [24, 99–101]). In particular, the collective nuclear model describes the nucleus in a fluid-like picture, where the five independent quadrupole degrees of freedom of the nuclear mass distribution form the configuration space for the dynamical treatment. The quadrupole moments can be written in spherical

coordinates specifying three usual Euler angles and two shape parameters, (β, γ) . Three main limits exist: $(\beta = 0, \gamma)$ defines a spherical shape, $(\beta > 0, \gamma = 0)$ a prolate spheroid, and $\beta > 0, \gamma = \pi/3$ an oblate spheroid [24]. In the spherical coordinates, the coordinate β represents the generalized radius of a four-sphere defined by the other four angular coordinates including the γ shape variable. The Laplacian of the dynamics in five dimensions can be expressed in these coordinates as [24]

$$\nabla^2 = \frac{1}{\beta^4} \frac{\partial}{\partial \beta} \beta^4 \frac{\partial}{\partial \beta} - \frac{\widehat{C}_2(\text{SO}(5))}{\beta^2}, \quad (8.1)$$

where the quadratic Casimir operator of $\text{SO}(5)$ describes the angular dependent part. It can be expressed in the respective coordinates as

$$\widehat{C}_2(\text{SO}(5)) = -\frac{1}{\sin 3\gamma} \frac{\partial}{\partial \gamma} \sin 3\gamma \frac{\partial}{\partial \gamma} + \sum_{k=1}^3 \frac{\hat{J}_k^2}{4 \sin^2(\gamma - 2\pi k/3)}, \quad (8.2)$$

where the \hat{J}_k represent the conventional operators of three-dimensional angular momentum theory.

In the case where the β coordinate is assumed to be fixed to some non-zero value β_0 , the so-called Wilets–Jeans sub-model of the collective model is appropriate. It assumes, as a further simplification, no potential in all four angular coordinates. Therefore, the Hamiltonian is proportional to the Casimir operator with an adjustable parameter depending in particular on the value of β_0 [102]

$$H_{\text{WJ}} = \frac{\hbar^2}{2M\beta_0^2} \widehat{C}_2(\text{SO}(5)).$$

In the realm of nuclear physics, the initial assumption of a liquid drop is justified if the nucleons are imagined to be a “soup” of bosonic indistinguishable particles. Consequently, the $\text{SO}(5)$ states solving the appropriate Schrödinger equation must be symmetric under imagined particle permutation. This is the case only for the irreducible representations of $[n_1 = v, n_2 = 0]$ weights. These so-called one-row irreducible representations therefore are the central objects in the Bohr collective models. For extended versions of the interacting boson model, also other irreducible representations are used but for simplicity we consider the $[v, 0]$ states only.

The weight v is conventionally called the *seniority* of the according state and the Wilets–Jeans model can be expressed in terms of this quantum number (see (7.3)) as

$$E_v = \frac{\hbar^2}{2M\beta_0^2} v(v+3).$$

The eigenstates of certain seniority can be expressed in a basis of symmetric rotor states, which is mathematically expressed through the subgroup $\text{SO}(3) \subset \text{SO}(5)$. The respective basis states are called generalized spherical harmonics, $\mathcal{Y}_{v\alpha Jm}$. They

satisfy the following eigenvalue equations [85]

$$\begin{aligned}\hat{C}_2 \mathcal{Y}_{v\alpha Jm} &= \frac{1}{2}v(v+3)\mathcal{Y}_{v\alpha Jm}, \\ \hat{\mathbf{J}}^2 \mathcal{Y}_{v\alpha Jm} &= J(J+1)\mathcal{Y}_{v\alpha Jm}, \\ \hat{\mathbf{J}}_z \mathcal{Y}_{v\alpha Jm} &= m\mathcal{Y}_{v\alpha JM}.\end{aligned}$$

The additional index α signals the possibility of multiple representations of identical J in one $\text{SO}(5)$ irreducible representation [103].

In contrast to the spherical harmonics in three dimensions, the five-dimensional equivalents are not known in closed analytical form. Nevertheless, one can determine them in an orthogonalization procedure or in a vector coherent state theory [104, 105]. To represent them in a known basis, we use symmetric rotor functions depending on the three usual Euler angles $\Omega = \{\theta, \phi, \chi\}$

$$\xi_{KM}^{(J)}(\Omega) := \left(\frac{2J+1}{16\pi^2(1+\delta_{K0})} \right)^{1/2} [\mathcal{D}_{KM}^J(\Omega) + (-1)^J \mathcal{D}_{-KM}^J(\Omega)],$$

where the \mathcal{D}_{KM}^J terms represent the matrix entries of the J th matrix representation of $\text{SO}(3)$. In addition, one defines polynomials $F_K^s(\gamma)$ of $\sin \gamma$ and $\cos \gamma$. The first few F functions are given as [104]

$$\begin{aligned}F_0^{[1000]}(\gamma) &= \cos \gamma, & F_2^{[1000]}(\gamma) &= \sin \gamma, \\ F_0^{[0100]}(\gamma) &= \cos 2\gamma, & F_2^{[0100]}(\gamma) &= -\sin 2\gamma, \\ F_0^{[0010]}(\gamma) &= \cos 3\gamma, \\ F_0^{[0001]}(\gamma) &= 0, & F_2^{[0001]}(\gamma) &= \sin 3\gamma.\end{aligned}$$

Their labels $s = [s_1, s_2, s_3, s_4]$ are non-negative integers and we combine them to NtJ labels by [104]

$$t = s_3, \quad N = 2s_2 + 2s_4, \quad J = 2s_1 + 2s_2 + 3s_4, \quad s_4 = 0, \text{ or } 1.$$

With these definitions, one can define monomials $\Phi_{NtJ}(\gamma, \Omega)$ as

$$\Phi_{NtJ}(\gamma, \Omega) = \sum_{K \geq 0}^{\text{even}} F_K^s(\gamma) \xi_{KJ}^{(J)}(\Omega),$$

and form the generalized spherical harmonics. The first few are given by

$$\mathcal{Y}_{1122} \propto \Phi_{102}, \quad \mathcal{Y}_{2122} \propto \Phi_{202}, \quad \mathcal{Y}_{4122} \propto \Phi_{412} - \Phi_{202}.$$

Using the orthogonality relation of the spherical harmonics, one can find the higher harmonics analogously [104].

Example 8.1 The symmetric rotor eigenfunctions $|Jkm\rangle$ (see (2.3) of Part I) in the conventional theory of three-dimensional rotations are also of product form. The $k = 0$ functions are proportional to the well-known spherical harmonics Y_{Jm} . In a very simplified notation, they can be written as

$$Y_{Jm} \propto f(J, m) P_J^m(\cos(\theta)) \cdot e^{im\varphi},$$

where $f(J, m)$ is a function depending only on the two quantum number J and m . The P_J^m are the ordinary Legendre polynomials and θ and φ are two of the three Euler angles (for more details, see [32]). Therefore, their construction is comparable to that of the generalized five-dimensional spherical harmonics of the previous paragraph.

As a superposition of symmetric rotor functions, these spherical harmonics resemble – at least partly – the eigenfunctions of the internal rotor, where the overall rotor states, $|Jkm\rangle$, are combined with e^{ika} (see Example 7.1). In the application of the SO(5) theory to molecules (see [6]), the γ variable can hence be interpreted as the internal rotor angle. As in the nuclear Wilets–Jeans model, this variable is assumed to be unbounded in the super-rotor model, whereas the variable β is assigned to a vibrational coordinate, frozen in the zero-order model considered here. However, the SO(5) spherical harmonics define specific combinations of the usual internal rotor functions, i.e. trigonometric functions, together with combinations of SO(3) invariant states. Surprisingly, the latter are allowed to have distinct J quantum numbers, which is impossible in the rigid overall rotor treatment of traditional approaches. However, SO(3) symmetry is still ensured. A single degenerate energy level of the SO(5) theory possibly combines different J states. However, a three-dimensional rotation cannot alter J but transforms states in the subset of super-rotor states with a particular J quantum number. Mathematically, the connection of the SO(5) irreducible representations with that of SO(3) is prescribed by the branching $\text{SO}(5) \downarrow \text{SO}(3)$. Its exact calculation is rather lengthy, we here refer to [24, 48] for further information. We only summarize the results in Table 8.1, where we also include the branching to the $\text{SO}(3) \times \text{SO}(2)$ subgroup of SO(5), which we used in the preceding chapter to introduce the combined treatment of overall [SO(3)] and internal [SO(2)] rotation.¹

For further development of the super-rotor theory, the SO(5) spherical harmonics can be used to determine possible deviations from the zero-order model: (i) Couplings to other degrees of freedom can be calculated; (ii) In order to account for deviations from the completely flat potential in the internal rotor axis change and respective angle, the coordinates, β and γ , must be used when a potential energy surface is

¹Both subgroups are different and so are the branchings. This suggests that the decoupling of the super-rotation into internal and overall rotation is somewhat different to the treatment in terms of one single rotating object. We discuss this feature in Chap. 10. For now, the SO(3) subgroup is used to express the SO(5) states in a known basis of rigid rotor functions.

Table 8.1 Branching of the super-rotor states with symmetry group SO(5) to the subgroups SO(3) and SO(3) \times SO(2). The branching rules are given in [48, 85, 106]. We used the numerical program SCHUR for the calculations [50]. The \pm superscript marks the two states of a single SO(2) irreducible representation. The superscript $(\cdot)^2$ indicates that a single SO(3) \times SO(2) representation of the respective subgroup occurs twice in one SO(5) representation

SO(5)	SO(3)	SO(3) \times SO(2)
$[n_1, n_2]$	J	(J, p)
$[0, 0]$	0	$(0, 0)$
$[1, 0]$	2	$(1, 0); (0, 1^\pm)$
$[1, 1]$	$3; 1$	$(1, 1^\pm); (1, 0); (0, 0)$
$[2, 0]$	$4; 2$	$(2, 0); (1, 1^\pm); (0, 2^\pm); (0, 0)$
$[2, 1]$	$5; 4; 3; 2; 1$	$(2, 0); (2, 1^\pm); (2, 0); (1, 2^\pm); (1, 1^\pm); (1, 0)^2; (0, 1^\pm)$
$[2, 2]$	$6; 4; 3; 2; 0$	$(2, 2^\pm); (2, 1^\pm); (2, 0); (1, 1^\pm); (1, 0); (0, 0)$
$[3, 0]$	$6; 4; 3; 0$	$(3, 0); (2, 1^\pm); (1, 2^\pm); (1, 0); (0, 3^\pm); (0, 1^\pm)$
$[3, 1]$	$7; 6; 5^2 4; 3^2; 2; 1$	$(3, 1^\pm); (3, 0); (2, 2^\pm); (2, 1^\pm); (2, 0)^2;$ $(1, 3^\pm); (1, 2^\pm); (1, 1^\pm)^2; (1, 0); (0, 2^\pm); (0, 0)$

defined; (iii) Higher order terms in the generalized angular momentum operators, i.e. generalized centrifugal distortion effects, can be described.

In conclusion, we used the results of nuclear physics, in particular of the Bohr collective model, to express the $[v, 0]$ eigenfunctions of the super-rotor model in terms of generalized rotational coordinates. Further functions with $n_2 \neq 0$ can be determined by other methods, [48, 104] but the details are beyond the scope of this work.

The comparison to conventional internal rotor theory suggests an intuitive interpretation of the additional angular coordinate, which will be supported further in the application to protonated methane in Chap. 9, where particular internal rotations can be assigned to an effective change in this particular coordinate.

8.1.1 Parity and Dipole Selection Rules

In traditional molecular theory, parity conservation is one of the concepts to identify selection rules for electromagnetic transitions. The usually observed dipole transitions change the parity and hence the lower and upper state connected by a transition must be of opposite parity. From the definition of the Euler angles in the description of rotational molecular states of total angular momentum J , the parity is calculated to be $\pi(|Jkm\rangle) = (-1)^J$.

In a five-dimensional rotor, parity is a more complicated issue. Naively, we can invert all the five coordinates of the underlying configuration space and determine the correlated five-dimensional parity. In nuclear physics, the parity is calculated to be $\pi(|[n_1, n_2]\rangle) = (-1)^{n_1+n_2}$, [107] which depends on the generalized angular

momentum quantum numbers only. However, in the branching rules of $\text{SO}(5) \rightarrow \text{SO}(3)$, see Table 8.1, we observe that three-dimensional rotor states of different parities are potentially combined in a single state of $[n_1, n_2]$ generalized angular momentum quantum numbers. The five-dimensional parity hence does not equal the three-dimensional one.

The electric dipole operator is crucial for the conventionally observed electromagnetic transitions. It has a definite (negative) three-dimensional parity. But how is its parity defined in five dimensions? Or do we have to stick to the three-dimensional parity and use the branching rules summarized in Table 8.1 to identify selection rules? These questions are left open for further discussion.

In addition to parity, the dipole moment operator also is said to carry an angular momentum of $J = 1$. Therefore, its symmetry under the rotations of $\text{SO}(3)$ is resembled by the irreducible representation \mathcal{D}_1 leading to the customary selection rules of dipole transitions $\Delta J = \pm 1$. However, in the super-rotor theory, a five-dimensional symmetry of the dipole moment operator must be considered. As it principally describes an electromagnetic transition under the absorption or emission of a photon which naturally carries a three-dimensional angular momentum of $J = 1$, we expect the branching of $\text{SO}(5)$ to $\text{SO}(3)$ again to be decisive. As a first intuitive guess for the symmetry of the dipole operator under the five-dimensional rotations, we hence identify the $[1, 1]$ irreducible representation as the one with lowest generalized angular momentum quantum numbers that restricts to $J = 1$ in $\text{SO}(3)$. However, many irreducible representation with higher $[n_1, n_2]$ quantum numbers exist that also include the conventional $J = 1$ angular momentum. This would induce some sort of ordering in the sense that the dipole transitions described by a dipole moment of $[1, 1]$ symmetry would be stronger than those of, e.g., $[2, 1]$. However, these are at the moment only speculations, the exact symmetry of the dipole moment operator under five-dimensional rotation is not yet determined in a fully convincing way.

In conclusion, dipole selection rules as well as parity in the super-rotor theory are not yet determined. In the here presented work we perform the first steps in developing this theory and due to the early stage in this process, we think open questions are very natural and that their formulation is crucial for the next steps.

8.2 Permutation-Inversion Symmetry

After having defined the Hamiltonian of the super-rotor model in a coordinate-free way, we specified a possible choice of coordinates in the last section. The solutions of the according zero-order Schrödinger equation were also discussed and the coordinates have been interpreted in terms of the usual three Euler angles and one internal rotation angular coordinate.

In this section, we review a method to find the permutation-inversion symmetry of the states of the super-rotor model (see [6]). This is of particular importance for the application to experimental results, since permutation-inversion symmetry of states lead to missing levels and particular selection rules for electromagnetic transitions

(see Part I). We first show a general treatment, which we exemplary apply to the case of the molecular symmetry group of protonated methane. This already prepares the discussion of the next chapter, where we show the application of the super-rotor model for this prototypical example of extremely floppy molecules.

To start with, consider a molecule consisting of N identical nuclei (see Sect. 2.1.2 of Part I). Hence, the complete nuclear permutation group is the symmetric group of degree N , S_N . Molecules consisting of different types of nuclei are consequently described by a product of symmetric groups, and the following discussion is easily generalized to this case. Permutations of N nuclei are conveniently written as $(ijk\dots)$, whereas permutation products are consequently represented as $(ij\dots)(kl\dots)$ [14].

The spatial Cartesian coordinates of the N nuclei define a $3N$ dimensional vector, which can be used to construct a matrix representation of the nuclear permutations. If a permutation $(ij\dots)$ is applied to a molecule, the nucleus j will occupy the coordinates (x_i, y_i, z_i) , which were the initial coordinates of nucleus i . Therefore, finding a representative matrix $\mathbf{D}[P]$ for the permutation $(ij\dots)$ is straightforward.

In more mathematical terms, the $\mathbf{D}[P]$ matrices are Kronecker products of three dimensional unit matrices (for the Cartesian coordinates) with permutation matrices, i.e. more abstract matrices permuting the according set of indices. From the properties of the latter, the $3N$ -dimensional matrices are found to be orthogonal with determinant $+1$ and -1 for even and odd permutations, respectively. The set of matrices for all permutations of S_N form a representation of that group.

To find the characters of this representation, we can use the fact that the matrices $\mathbf{D}[P]$ form a subgroup of the group $O(3N)$. Characters of $O(3N)$ are determined by the eigenvalues of the matrices. Since the elements of $O(3N)$ are defined to be orthogonal and to have unit absolute determinant, their eigenvalues are calculated by

$$\begin{aligned} O(2\ell+1) : & \{D, e^{\pm i\theta_1}, e^{\pm i\theta_2}, \dots, e^{\pm i\theta_\ell}\}, \\ O(2\ell) : & \{e^{\pm i\theta_1}, e^{\pm i\theta_2}, \dots, e^{\pm i\theta_\ell}\}, \end{aligned} \quad (8.3)$$

where D can be ± 1 for a positive/negative determinant. Using Lie theory, the ℓ eigenvalues are intimately connected to the ℓ operators, denoted by H in the preceding chapter, spanning the Cartan subalgebra of commuting operators in $so(n)$. In the well-known case of $SO(3)$, the eigenvalues are known to be customary rotation angles (see (6.3)). Each rotation in three-dimensional space can be expressed by a single rotation axis and an angle θ , see the detailed discussion in Chap. 6 of the present part.

In cases where the conventional theory is applicable, we find the permutation matrices $\mathbf{D}[P]$ to have only two non-redundant eigenvalues $e^{\pm i\theta_p}$ (in addition to the trivial eigenvalue D). These eigenvalues and the corresponding, say, eigen-angle are straightforwardly connected to the equivalent rotation angle found geometrically (see Chap. 6). For even permutations, they are equivalent, whereas for odd permutations, the negative determinant of $\mathbf{D}[P]$ must be taken into account. The geometrically found angles are conveniently chosen to describe a handedness-conserving rotation, such that their representative matrix is an element of $SO(3)$. Therefore, for odd

permutations, the determinant of $\mathbf{D}[P]$ has to be changed accordingly, which, in case of an odd dimensionality ($3N$), can be done by simply multiplying the matrix by -1 . If the dimension $3N$ is even, one can simply add an extra ghost particle, which adds three dimensions to the matrix but whose position is assumed to be fixed for all permutations.²

For the matrices $\mathbf{D}[P]$ of the groups S_N with $N \leq 4$ this technique can be used to determine the values of the equivalent rotation angles in a coordinate-free way, where no geometry has to be assumed at any point.

For the molecular symmetry groups of almost all molecules, we must include inversion operations into the discussion. In the usual Longuet–Higgins approach, no difference is made and the respective rotation angles are determined geometrically. In our approach, we use the multiplication properties of permutations. For pure permutations, the multiplication of a certain permutation P by itself produces the identity operation after n_P times. For including the inversion operation, we notice all the permutations P and P' , to be accompanied by respective permutation-inversion operations $P^* = PE^*$ and $(P')^* = P'E^*$, where E^* is the inversion operation satisfying $E^*E^* = E$. The multiplication $P^*(P')^*$ is therefore equivalent to PP' and the respective $3N$ dimensional matrices have the corresponding multiplication properties. With this, the angles θ_{P^*} can be found analogously to the pure permutation case.

In conclusion, this method resembles an alternative way to find the complete set of rotation angles of the rotation group isomorphic to any of the standard molecular symmetry groups. Also for the cases of spherical molecules with exceptional symmetry groups like methane with symmetry group T_d , this method is applicable and a special treatment as done in [89] is unnecessary.

The most interesting use of this method, however, is its application to molecular symmetry groups, where the conventional Longuet–Higgins approach fails, see Sect. 6.2. The first such group is the permutation group of five identical particles, which we discuss in detail in the following section.

8.2.1 The Permutation Group of Five Identical Particles

Using the method of constructing $3N$ dimensional permutation matrices, we have shown how non-redundant eigenvalues leading to the well-known equivalent rotation angles of [30] emerge. These angles are used (see Chap. 6) to classify the rotational states in the molecular symmetry group. The rotational states are solutions of the zero-order rigid rotor theory, where the Hamiltonian is assumed to have a full $SO(3)$ symmetry group. However, as we demonstrated before, this assumption cannot hold for extremely floppy molecules, instead we developed a theory based on an $SO(5)$ symmetry group. As indicated in (8.3), the $SO(5)$ group has two non-trivial

²The dimension $3N$ is indeed only odd, if the number of nuclei is odd and is even if N is even, respectively.

eigenvalues and respective eigen-angles (θ_1, θ_2). By analogy with the conventional three-dimensional treatment, we therefore assign to each molecular symmetry group element *two* angles to find the representation of the five-dimensional rotor states in the molecular symmetry group.

For the S_5 group, these two angles can be found by the program described above, where the 15-dimensional matrices of all permutations of five identical particles exhibit four non-redundant and non-trivial eigenvalues and consequently two eigen-angles. In particular the matrices for the simultaneous permutation of all five particles cannot be represented by only one such angle (see Fig. 6.4). The corresponding angles are summarized in Table 8.3. This isomorphism $S_5 \simeq SO(5)$ is not unique, [25] but due to our assumptions for the multiplication behavior and the conserved handedness, our method resembles the physical meaning of the permutations in the application to molecules.

In order to find the restricted representations of the super-rotor states in the S_5 group, the characters of the respective generalized rotations must be used. By using the eigen-angles (θ_1, θ_2), the characters $\chi_{[n_1, n_2]}$ are known to be [47, 108]

$$\chi_{[n_1, n_2]}(R) = \frac{\det \left[t_j^{n_k - k + 5/2} - t_j^{-(n_k - k + 5/2)} \right]}{\det \left[t_j^{5/2 - k} - t_j^{-(5/2 - k)} \right]}, \quad (8.4)$$

where $t_j = e^{\pm i\theta_j}$. The indices jk define two-dimensional matrices A_{jk} of which the determinants are taken.

With (8.4), the $SO(5)$ representations spanned by the super-rotor states with quantum numbers $[n_1, n_2]$ can be restricted to the S_5 group. In Table 8.3, we show the characters of the first few states and in Table 8.4 their respective reduction in the irreducible representations of S_5 (see also Table 8.2).

The character for the identity operation is the dimension of the irreducible representation and can be calculated by [85]

Table 8.2 Irreducible representations of the symmetric group of degree five S_5 . For each class of the group, we list one representative element together with the number of elements in the class. The table is reproduced after [14, p. 200]

S_5	E	(12)	(12)(34)	(123)	(123)(45)	(1234)	(12345)
	1	10	15	20	20	30	24
A_1	1	1	1	1	1	1	1
A_2	1	-1	1	1	-1	-1	1
G_1	4	2	0	1	-1	0	-1
G_2	4	-2	0	1	1	0	-1
H_1	5	1	1	-1	1	-1	0
H_2	5	-1	1	-1	-1	1	0
I	6	0	-2	0	0	0	1

Table 8.3 The equivalent rotations of the permutations of S_5 in the five-dimensional rotation group SO(5). The strategy for finding the *two* angles is described in the text. Selected restricted representations $\text{SO}(5) \downarrow S_5$ and their characters are also shown, labeled by their generalized angular momentum quantum numbers $[n_1, n_2]$. Their reduction in the irreducible representations of S_5 (see Table 8.2) is shown in Table 8.4

Class	E	(12)	(12)(34)	(123)	(123)(45)	(1234)	(12345)
Partition	1	10	15	20	20	30	24
(θ_1, θ_2) [n_1, n_2]	(0,0)	(π, π)	$(0, \pi)$	$(0, 2\pi/3)$	$(\pi/3, \pi)$	$(\pi/2, \pi)$	$(\frac{2\pi}{5}, \frac{4\pi}{5})$
[0, 0]	1	1	1	1	1	1	1
[1, 0]	5	-3	1	2	0	-1	0
[1, 1]	10	2	-2	1	-1	0	0
[2, 0]	14	6	2	2	0	0	-1
[2, 1]	35	-5	-1	-1	1	1	0
[2, 2]	35	3	3	-4	0	-1	0
[3, 0]	30	-10	2	3	-1	0	0

Table 8.4 Reduction of the representations of the first few states of the super-rotor model in the S_5 permutation group (see Tables 8.2 and 8.3)

$[n_1, n_2]$	$[n_1, n_2] \downarrow S_5$
[0, 0]	A_1
[1, 0]	$A_2 \oplus G_2$
[1, 1]	$G_1 \oplus I$
[2, 0]	$A_1 \oplus 2G_1 \oplus H_1$
[2, 1]	$2G_2 \oplus H_1 \oplus 2H_2 \oplus 2I$
[2, 2]	$G_1 \oplus 3H_1 \oplus 2H_2 \oplus I$
[3, 0]	$2A_2 \oplus 3G_2 \oplus 2H_2 \oplus I$

$$\dim([n_1, n_2]) = \frac{1}{6}(3 + 2n_1)(1 + n_1 - n_2)(2 + n_1 + n_2)(1 + 2n_2) \quad (8.5)$$

The equivalent rotations in three dimensions are connected to a physical picture of rotations relative to the lab-fixed axis system. In the five-dimensional picture presented here, this intuitive picture is lost. However, the SO(5) theory of super-rotations is built on the assumption that internal and overall rotations are inter-correlated. Consequently, we interpret the two eigen-angles of representative matrices of SO(5) as one angle of overall rotation and one of the internal-rotation equivalent. This is shown in particular when we consider protonated methane as a molecule exhibiting the full S_5 permutation symmetry group (Chap. 9).

8.3 Conclusion

In the present chapter, we showed the functional behavior of the super-rotor states for the case $n_2 = 0$, which has been established in nuclear physics for the characterization of quadrupole moments of rotating and vibrating single nuclei. They are expressed as generalized spherical harmonics depending on four angular variables describing the four-dimensional sphere on which the five-dimensional rotational motion takes place.

The parity of these states presents an open question at the moment. Likewise, the symmetry of the electric dipole moment in five-dimensional space is not yet fully understood. However, we think the early stage in the development of the super-rotor theory provides a valid excuse for these open but nevertheless important questions.

In contrast to the parity problem, we are able to find the permutation-inversion symmetry of the super-rotor states. For that, we developed a generalized procedure to find the isomorphism between the molecular symmetry group and the rotation group. Conventionally this is done by using a geometrical approach, developed in 1960s, [30] but we have developed a coordinate-free approach to find the respective rotations, which simultaneously overcomes the limits of the convenient approach for groups that are not isomorphic to subgroups of $\text{SO}(3)$, see Chap. 6. In particular, our method allows us to find equivalent five-dimensional rotations in cases where the $\text{SO}(3)$ group is insufficient.

The first example of groups where the convenient approach fails is the permutation group of five identical particles³ where we showed the permutations to be representable in terms of five-dimensional rotation matrices. Those matrices are representatives of elements of the $\text{SO}(5)$ group of the super-rotor model developed in Chap. 7. Consequently, the states of the $\text{SO}(5)$ theory span certain reducible representations in the S_5 group, which we use in the next section for the application of the super-rotor model to protonated methane, which actually exhibits the full S_5 molecular symmetry group.

Nevertheless, the method presented here is not at all limited to the application to $\text{SO}(5)$ -symmetry theories. We showed its application to conventional three-dimensional rotations and standard molecular symmetry groups but also other $\text{SO}(N)$ groups are possible. Since already in five dimensions intuition is very limited, the physical grasps of higher dimensional rotation groups have not been possible so far.

³One could think that the permutation group of *five* particles is embedded in the *five* dimensional rotation group due to the number of particles. This is not the case, the group S_4 is, e.g., isomorphic to a subgroup of $\text{SO}(3)$. The number five appears coincidentally in both groups.

Chapter 9

Protonated Methane

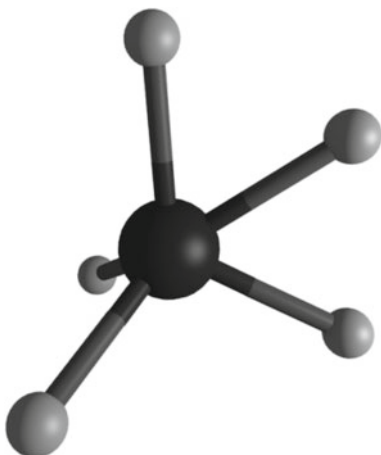
Abstract In this chapter, the success of the super-rotor theory in explaining the experimental spectrum of protonated methane is shown. This prototype of extremely floppy molecules has not been described by any traditional theory for a long time, with the introduction of the super-rotor model, however, a fundamentally new model for the internal motion has been established. With the help of traditional rotor theory, one can establish predictions for the energies in the vibrational ground state of protonated methane, which actually agrees very favourable with the experimental values. Certain discrepancies are also discussed but due to the zero-order type of the super-rotor model, the agreement is however astonishing.

9.1 The Molecule

In contrast to its parental molecule, methane (CH_4) the protonated version, CH_5^+ , precludes a definition of a fixed molecular structure and hence poses a considerable challenge for molecular theory as well as experimental spectroscopy. The extra proton causes a three-center-two-electron bond inducing an extremely floppy molecular complex. The minimum energy structure is calculated to be of C_s symmetry and is shown in Fig. 9.1. It can be subdivided into a CH_3 tripod and an CH_2 unit. However, recent ab-initio calculations have demonstrated that there are 120 equivalent global minima on the potential energy surface and that the energy of the ground ro-vibrational state exceeds all the barriers between those minima [83, 109, 110]. As in the example of nitromethane (see Example 7.1), these calculations suggest that the protons undergo internal rotations or “bendings” already in the ground vibrational state. Only their relative distance to the central carbon nucleus is calculated to be almost fixed in that ground state. The isosurface for the ground state wave functions of the protons is consequently an almost spherical cloud around the central carbon atom. Any interpretation in terms of a fixed geometric structure is therefore impossible and CH_5^+ is thus a prototypical example of extremely floppy molecules. As such it is of very general interest in the physics and chemistry of small molecules.

Protonated methane is one of the cornerstones for determining reaction pathways of carbon chemistry, which makes it highly relevant in astrophysics as well as in the

Fig. 9.1 Protonated methane in its C_s structure (see also Fig. 6.4). The electronic bonds must be shared by two protons simultaneously, so that this fixed geometric structure is not a valid physical picture but the molecule is better seen as in a superposition state (see text)



chemistry of plasmas. It was first found in mass spectra in the 1950s, [111] and a first infrared spectrum has been recorded about the turn of the new millennium [77, 78, 109]. Very recently, [4] recorded ro-vibrational transitions at nominal temperatures of 10 and 4 K, which enabled the authors to determine for the first time sets of ground vibrational states.

Due to its importance and its puzzling behavior, protonated methane has received tremendous attention in the last decades and an enormous number of theoretical studies have been performed (see, e.g., [9, 35, 73, 80, 112] and references therein). Surprisingly none of these studies has succeeded in providing a fully convincing assignment of the energy levels determined experimentally by [4]. Only the most recent high-level calculations of [35] predicted energy levels which are comparable to the values found in the experiments.

One of the most discussed features of CH_5^+ is its potential energy surface. Recent ab-initio calculations however, have shown that it must be assumed to be almost flat compared to the ground vibrational state energy. In particular, the “bending” motion of the five protons is nearly free and hence the molecular symmetry group of protonated methane is the complete nuclear permutation-inversion symmetry group of five identical particles, namely

$$G_{240} = S_5 \times E, E^*.$$

For other examples of extremely floppy molecules, as, e.g., H_5^+ , it is still an open question which molecular symmetry group is appropriate. Some barriers, for instance the barrier to internal rotation of the H_3^+ subunit, are calculated to be comparable to the vibrational ground state energy [60].

By assuming the G_{240} group as appropriate for the description of ro-vibrational states of protonated methane, Pauli’s exclusion principle restricts the symmetries of the full molecular wave function. With the results of Chap. 3 of Part I, explicitly

Table 3.1, we identify three allowed ro-vibrational symmetries, namely A_2 , G_2 , and H_2 in the permutation subgroup of G_{240} . For each of the three symmetry species, there exists a certain number of coupled nuclear spin wave functions leading to nuclear spin weights of $6 : 4 : 2$. The A_2 levels correspond to a single spin representation of $I = 5/2$, whereas G_2 correlates with four $I = 3/2$ representations and H_2 with five of $I = 1/2$. Therefore the number of states will follow the ratio $1 : 4 : 5$ (see Supplementary Material to [4]). In extending the S_5 group to G_{240} , the states get an extra label \pm , indicating their behavior under inversion. Since the latter has no influence on the spin states, the above considerations remain valid for both \pm species.

In Chap. 6 of the present chapter and [9] we have identified one important reason for the failure of traditional approaches applied to the CH_5^+ molecule: The molecular symmetry group of protonated methane is not in the set of subgroups of $\text{SO}(3)$, the spatial rotation group. This leads to the impossibility of applying the usual zero-order approach of molecular rotation, namely the rigid rotor treatment.

The realization of the inapplicability of $\text{SO}(3)$ as the embedding symmetry has been the starting point for the development of the super-rotor theory (see Chap. 7 and [6, 7]) with which we introduced a fundamentally new concept of combining internal and overall rotation into a collective motion. We already anticipated that protonated methane is the perfect target molecule to test this theory. In the following chapter, we discuss the application of the super-rotor theory in detail and show a surprisingly accurate agreement of the predicted levels with experiment. The value of the (adjusted) generalized rotational constant is – as expected – almost equal to the calculated three-dimensional, rigid rotor, constant obtained in earlier ab-initio calculations.

Our model is of zeroth order, hence the accuracy is very limited. However, the underlying physical picture is of fundamentally new character. It opens up a new view on extremely floppy molecules and we hope that further refinements of the theory can improve its accuracy. This and possible other target molecules are discussed in Chap. 10.

9.2 The Experiment

In this section, we present some details on the experimental work on CH_5^+ , done recently by [4]. Although this was not part of the presented work, we find it reasonable to shortly review some details particularly of how the authors of [4, 15] obtained the low-energy structure from the experimental spectrum.

In the work of [4], two different methods of action spectroscopy were used to determine the experimental spectrum of protonated methane: In both cases, a few thousand mass-selected CH_5^+ ions were stored in a 22-pole trap. The first method relies on so-called laser-induced reactions (LIR), [78] where a tunable infrared laser induces a reaction with an appropriately chosen gas. In this case, the reaction $\text{CH}_5^+ + \text{CO}_2 \rightarrow \text{CH}_4 + \text{OCOH}^+$ was selected. The reactant CO_2 and the target molecule CH_5^+ were provided together with a helium buffer gas to the 22-pole trap in

a pulsed mode. This enables to reach a nominal temperature of about 10 K. The reaction product OCOH^+ was studied in a mass-selective way. The number of the product ions is recorded in dependence of the laser frequency, which represents a straightforward method to find the infrared transitions of the ions. The second method uses the inhibition of complex growth by shining a laser onto the target molecule (LIICG) [2]. Here, the attachment of helium is hindered if the laser frequency matches that of a molecular transition. Due to multiple collisions of the CH_3^+ with the helium buffer gas, the nominal ion temperature is close to that of helium, i.e. 4 K.

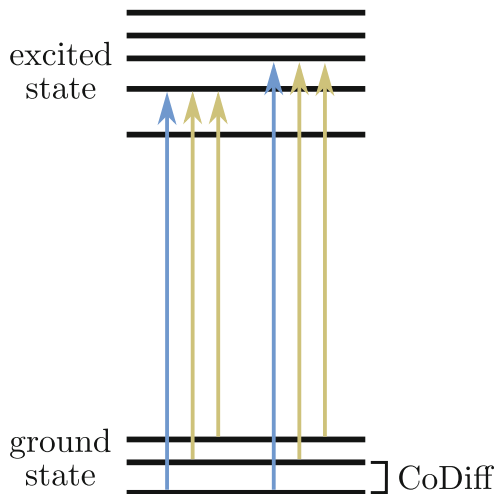
The use of an optical parametric oscillator with a narrow frequency band and a frequency comb for recording the frequency allows for accuracies of the measured transitions of better than 1 MHz [113]. As expected, the spectrum is very dense and 2879 lines have been recorded in the range of $2886\text{--}3116\text{ cm}^{-1}$ by using the LIR method. The LIICG approach still resolves 185 lines, where the reduction is a result of the further cooling.

From the high-resolution spectrum, the authors calculate differences between the observed transitions, so-called *combination differences*. In general, transitions connect two states, an upper level and a lower one. If we stick for the moment to the customary notion of vibrational and rotational states, the upper level is interpreted as an excited vibrational state while the lower one is the respective ground state. In the case of infrared transitions in the range mentioned above, the upper levels are assigned to CH-stretching vibrations of the CH_3 tripod [78]. If two transitions share the same upper level, their difference equals that of two respective levels in the lower vibrational state (see Fig. 9.2). Since, in contrast to the limited number of lower states, one assumes plenty of upper states, many differences of the exact same value are expected to appear in a histogram of combination differences. Differences of transitions not sharing the same upper (or lower) level would appear as a background in such a combination difference spectrum. Initially, one cannot distinguish between combination differences which have either the same upper or the same lower level. Hence, one compares the combination difference spectrum for the 10 K experiment to the lower temperature one, where only the lowest state is assumed to be populated. Using this comparison, one can identify those transitions which root in the lower vibrational state (see Fig. 9.2). This knowledge can therefore be used to calculate an energy level diagram of the vibrational ground state. In addition to this method, the more recent work of S. Brackertz [15] has shown an advanced statistical method based exclusively on the 10 K combination difference spectrum to further elucidate the energy level diagram.

In conclusion, this method allows to set up a ground vibrational energy level diagram. Assuming a conventional rotational energy level pattern, one would assign these levels to certain angular momentum quantum numbers. However, the experimentally determined level structure does not show the regularity of the usual rotational energies found more rigid molecules. In particular, no definite rotational constant could be fitted since the levels could not be labeled by any J quantum number.

In contrast to the questionable assignment of angular momentum quantum numbers, a rather convincing assignment to the irreducible representations of the molec-

Fig. 9.2 Schematics of an energy level diagram of ground and excited vibrational states connected by infrared transitions. The difference of the shown transitions (ground state CoDiff) of the same upper level reveal the ground state level structure, which is not directly observable. The blue colored transitions appear only in a low-temperature experiment where solely the absolute ground state is populated, whereas the other are apparent also in spectra of higher temperature. The graphics is adopted from [4]



ular symmetry group was possible. For that, the authors used a statistical approach: Two transitions of the same upper level must be of the same permutation-inversion symmetry since dipole selection rules prescribes only $A_2^\pm \leftrightarrow A_2^\mp$, $G_2^\pm \leftrightarrow G_2^\mp$, and $H_2^\pm \leftrightarrow H_2^\mp$ transitions. Therefore in total six distinct sets of lower states are expected to appear in the combination difference spectrum. With the help of the nuclear spin statistical weights for the different levels (1 : 4 : 5) the authors calculated the weights for the respective combination differences (1 : 16 : 25). This is used to identify two sets of levels with G_2 and H_2 symmetry, respectively. Recently, S. Brackertz [15] revealed two more distinct sets of levels by using advanced statistical methods in the analysis of the combination difference spectrum. These additional sets were not yet assigned to any symmetry species. However, from the statistical weights most probably these levels belong to the complementary G_2^\pm or H_2^\pm symmetry depending on what irreducible representation the previously found levels are assigned to.

9.3 The Model

As explained in detail in Chap. 7, the super-rotor model represents a new model of combined internal and overall rotation. These motions are assumed to be responsible for the low-energy states found in the combination difference spectrum in [4, 15]. The super-rotor states replace the customary rotational energy levels that would have been assigned if the molecule would be treated in a more traditional approach. In our zero-order model, the remaining $3N - 8 = 10$ vibrational modes are decoupled from the super-rotation and hence the energy in the respective vibrational ground state is given by (7.3)

$$E(n_1, n_2) = \frac{B}{2} \{n_1(n_1 + 3) + n_2(n_2 + 1)\},$$

Fig. 9.3 Schematic view on the (123) permutation in protonated methane in its global minimum structure ($C_s(I)$ symmetry, see Fig. 9.1). The protons four and five are *left* in fixed positions and the permutation can be equivalently described by a five-dimensional rotation with angles $(0, 2\pi/3)$, see Table 8.3. The second angle therefore can be interpreted as the internal rotation about the axis labeled by R_γ

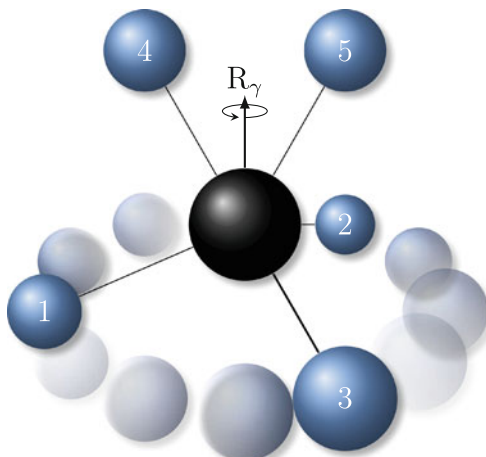


Table 9.1 The first few Pauli-allowed states of the super-rotor model in the S_5 symmetry group of protonated methane

$[n_1, n_2]$	$[n_1, n_2] \downarrow S_5$
$[0, 0]$	—
$[1, 0]$	$A_2 \oplus G_2$
$[1, 1]$	—
$[2, 0]$	—
$[2, 1]$	$2G_2 \oplus 2H_2$
$[2, 2]$	$2H_2$
$[3, 0]$	$2A_2 \oplus 3G_2 \oplus 2H_2$

where $[n_1, n_2]$ are the generalized angular momentum quantum numbers of the underlying $SO(5)$ symmetry.

In addition to the energies of the states with quantum numbers $[n_1, n_2]$, in Chap. 8 we showed their respective symmetry in the permutation group S_5 (see Table 8.4). With an assumed $C_s(I)$ global minimum structure, an intuitive interpretation of the two eigen-angles of $SO(5)$ rotations becomes possible. In Fig. 9.3 we show the example of the permutation (123), where we found the equivalent rotations to be $(0, 2\pi/3)$. This exactly recovers the angles of an internal rotation of the three protons while protons four and five are left fixed. This once more induces the combination of internal and overall rotation in the super-rotor model, where these motions are treated indistinguishably.

For transparency, we show in Table 9.1 the first few Pauli-allowed super-rotor states in the S_5 group with their respective quantum numbers. For low $[n_1, n_2]$, Pauli's principle dictates some states to be completely missing, whereas as $[n_1, n_2]$ grows, the dimension of the irreducible representations increases (see (8.5)) and there are no missing energy levels. In the zero-order model, the possibly different representations of S_5 in a single super-rotor state are degenerate due to the assumed

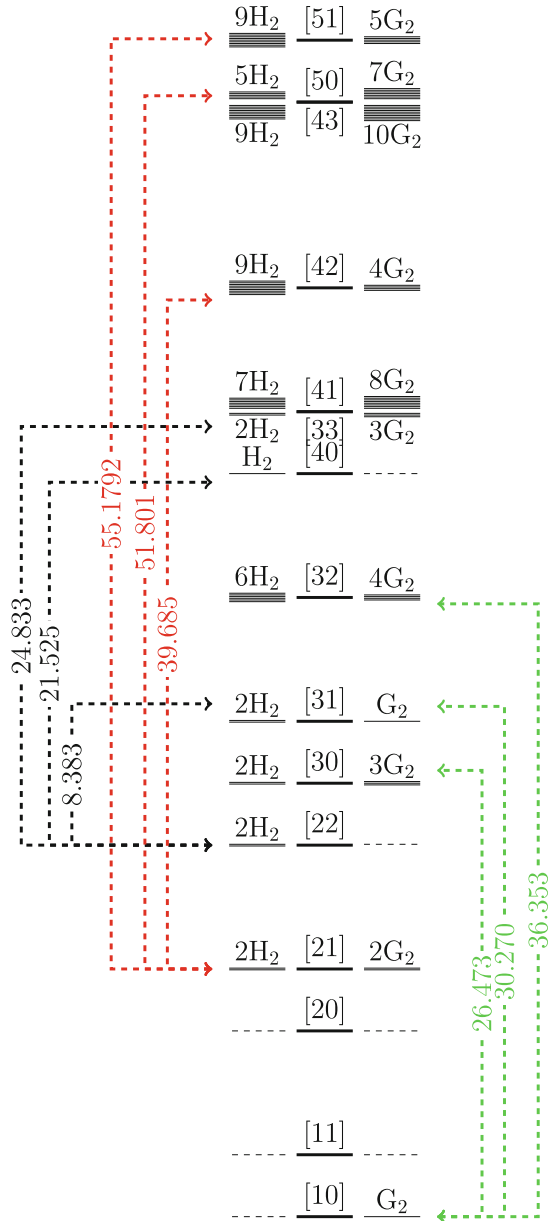


Fig. 9.4 Energy term diagram of the lowest states of protonated methane following (7.3) as a result of the super-rotor model. Three experimentally observed sets of combination differences (*dashed arrows*) are assigned to the ro-vibrational states with different symmetries. The latter were found by using the equivalent rotation technique shown in Chap. 8 and are shown to the left and right to the central super-rotor states labeled by the generalized angular momentum quantum number $[n_1, n_2]$ of the SO(5) theory. The figure is reproduced from [7]. States of A_2 symmetry are not shown since one does not expect them to contribute much to the experimental combination difference spectrum

Table 9.2 Comparison of the experimentally observed combination differences indicating energies in the vibrational ground state of protonated methane with the super-rotor model. The values marked with * were found very recently by S. Brackertz [15] and have been assigned to a new set of levels. Also in that work, the doubly marked energy was added to the set named set 2 in [4]. The two super-rotor states of generalized angular momentum [4, 3] and [5, 0] are degenerate, hence an unambiguous assignment is impossible. The table is reproduced after [7], Supplementary Material

Symmetry S_5	Exp. CoDiffs [cm ⁻¹]	Present work [cm ⁻¹]	Assignment SO(5)
G_2	26.47252	25.71	[1,0] - [3,0]
	30.26984	29.38	[1,0] - [3,1]
	36.35280	36.73	[1,0] - [3,2]
H_2	39.68499	40.41	[2,1] - [4,2]
	47.32219	—	—
	51.80126	51.42	[2,1] - [4,3]([5,0])
	55.17916**	55.10	[2,1] - [5,1]
H_2	8.38325*	7.35	[2,2] - [3,1]
	21.52476*	22.04	[2,2] - [4,0]
	24.83280*	25.7124	[2,2] - [3,3]

completely flat potential energy surface for the internal rotation angle and axis. In a more realistic treatment (see Chap. 10), the states of different symmetries in S_5 will split (see left part of Fig. 7.2), but we expect their energy difference to be small compared to the energy difference of two adjacent super-rotor states.

The generalized rotational constant B of the model was shown to equal the rigid rotor constant if the molecule is considered to have a fixed geometry. This value has been calculated in different ab-initio calculations to be $B_0 = 3.87 \text{ cm}^{-1}$, [80, 81] which we used as a first guess for the parameter in the super-rotor model. With this initial value it was possible to assign the experimentally observed energy levels and to fit the B constant to a value of $B = 3.67 \text{ cm}^{-1}$, close to the ab-initio value. The results are shown in Table 9.2 and Fig. 9.4. In particular, we show in Fig. 9.4 the super-rotor states with the respective S_5 symmetries and their corresponding degeneracies. For instance, the state [3, 0] induces the representations $2H_2$ and $3G_2$ of the permutation subgroup of G_{240} . Since parity is yet an open issue, the \pm labels of the full permutation-inversion group could not be assigned and we stick to the S_5 group as the relevant molecular symmetry group. For convenience, we do not show the A_2 levels in Fig. 9.4, since they are always degenerate with the G_2 levels (see Table 9.1).

Three of the four sets of levels determined from the experimental combination differences can be assigned rather unambiguously by the super-rotor model. In particular, the two sets found in [4] appear as G_2 and H_2 sets in the predictions. As expected from cooling the CH_5^+ to about 4 K, the related combination differences all originate in the lowest energy state of the respective symmetry. The third assigned set of level roots in the next higher energy level and is therefore assigned to H_2 symmetry. Consequently, this leads to a tentative distinction of the H_2 representations in the

state of [2, 1] and [2, 2] quantum numbers since no combination difference combines the two sets. Hence, one of these sets is assigned to H_2^+ in \mathbf{G}_{240} , whereas the other must have H_2 symmetry. Yet, these two are not distinguishable in the current status of the super-rotor model. Furthermore, in addition to its small assumed number in the combination difference, levels of A_2 symmetry appear only in degenerate pairs with G_2 levels, such that their unambiguous identification is very challenging at this state of the predictions.

The super-rotor model with the energies of (7.3) is of zero-order type and provides one single adjustable parameter. In that respect the accuracy of the predicted energies of about 1 cm^{-1} is astonishing and encourages further development of the theory. Clearly, many unassigned experimentally observed levels remain but also theory predicts many more energies.

9.4 The Discussion

The results of Table 9.2 are very promising and represent the first assignments ever of energies *and* symmetries consistent with the experimental values. Nevertheless, the super-rotor theory is in an infancy stage in the description of protonated methane. We think its development is the first big step towards the understanding of the dynamics in extremely floppy molecules like CH_5^+ . However, many new and unexpected questions arise. For example, one main question is the assignment of conventional angular momentum to the super-rotor states of protonated methane. The super-rotor states comprise possibly more than one angular momentum and so do the \mathbf{G}_{240} states. Since they are not representable in $\text{SO}(3)$, the irreducible representations of \mathbf{G}_{240} lack a one-to-one correspondence to the J quantum number. At the moment, a direct correlation of several J states to one \mathbf{G}_{240} symmetry is not possible since parts of the J states in a single super-rotor state could be forbidden by Pauli's principle.

Furthermore, a fourth set of combination differences in the spectrum of CH_5^+ needs to be assigned. For that, one idea is to thoroughly include the splitting of the super-rotor states into the \mathbf{G}_{240} states already indicated schematically in Fig. 9.4. In the super-rotor model, a totally flat potential was assumed but the ab-initio calculations show 120 minima suggesting at least some potential energy barriers. Although the zero-point vibrational energy is much larger than the barriers, they certainly will split the super-rotor energies. The respective splitting is assumed to be much smaller than the difference between two adjacent $[n_1, n_2]$ states, nevertheless they could be responsible especially for very small combination differences like the yet unassigned value of 5.46036 cm^{-1} [4, 15]. Also the unassigned level at 47.32 cm^{-1} of H_2 symmetry, see Table 9.2, is possibly explained by such a splitting.

In order to find the influences of potential energy barriers, one has to set up a potential energy surface in terms of the rotational coordinates of the super-rotor model and study its influence on the respective energies. With the generalized spherical harmonics, this task should in principle be possible, however, we leave it open for further studies.

In addition, the experimental combination differences and their assignment to the super-rotor states clearly suggest the existence of selection rules for the observed electric dipole transitions (see Sect. 8.1.1). However, from this small number of unambiguously identified differences, it remains impossible to formulate such a selection rule only from the observations. Also there, further studies of the underlying physical principle of dipole transitions in the five-dimensional configuration space of the model are needed.

From the experimental values, S. Brackertz [15] has determined the structure of the vibrationally excited levels, hence an assignment of those energies should be possible. However, in that particular spectral region, certainly more than a single vibrational mode is present. The multiple vibrational modes will strongly interact and their particular influence on the super-rotor states is also far from being understood.

In conclusion, we present here the first steps towards an understanding of protonated methane, the “enfant terrible” ([3], p. 1) of molecular spectroscopy. While some features of the molecule were known from theoretical considerations, we interpreted the dynamics in a completely new model, namely a combined internal and overall rotational, super-rotor model. Most astonishingly, the majority of the experimental energy levels of protonated methane follow the very simple algebraic energy expression of the model for this five-dimensional super-rotor. Even if many unsolved issues persist, we think we have opened up an avenue to a fundamentally new understanding in the dynamics of CH_5^+ and consequently of extremely floppy molecules in general. Further refinements and in particular additional applications to other “astructural” ([60], p. 1) molecules are certainly needed to improve the model. In the following chapter, we give a first outlook on these issues, we name a few possible targets for further work, and develop ideas for going beyond the zero order model are presented.

Chapter 10

Refinements and Further Applications

Abstract In this last chapter of the part on the super-rotor theory, future work is anticipated: The extension to higher orders in the generalized angular momentum operators as well as the introduction of an asymmetric five-dimensional rotor. This can be used in applications to other molecules than protonated methane and some examples are discussed.

10.1 Beyond Zero-Order

In the previous chapters, we proposed the five-dimensional super-rotor model for a description of combined internal and overall rotations in extremely floppy molecules. For the prototypical example of protonated methane, we have shown a good agreement of the predictions of our zero-order model with recent experimental results. Nevertheless, going beyond zeroth order, where the five-dimensional rotor is described by only one generalized rotational constant, is mandatory, although not straightforward. We present here two possible approaches for an extension of this model: (i) Generalized moments of inertia can help in understanding the link to conventional theories and describe much more accurately the molecule itself; (ii) Higher-order terms as an expression of non-rigidity can be used to further develop the model. The latter can also be used for the couplings to purely vibrational motions.

10.1.1 Generalized Moments of Inertia

Comparing the super-rotor theory with traditional rotational theory, the model presented here is at a stage comparable to that of a spherical rigid rotor. In general, molecules do not behave as rigid spherical rotors and thus extremely floppy molecules described by the five-dimensional rotor theory will in general be not “super-spherical”. As in the case of well-known symmetric rotors, asymmetry terms must be taken into account to improve the accuracy of the predictions and to render the model applicable to more molecules. Therefore, the introduction of generalized rotational

constants, or, equivalently, of a generalized moment of inertia tensor, is the next obvious step.

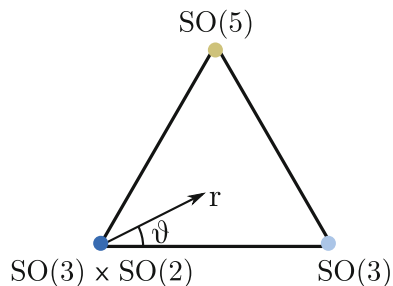
In (7.4), we already showed the generalized moment of inertia tensor and used it subsequently to describe the subgroup chain $\text{SO}(3) \subset \text{SO}(5)$ implying an understanding of the B -constant of the five-dimensional theory. Additionally, we also anticipated the use of possibly different generalized rotational constants for linking the super-rotor model to more traditional models of angular momentum theory. This can be done by identifying four of the ten generalized angular momentum operators \hat{J}_{ij} as the generators of the subgroup $\text{SO}(3) \times \text{SO}(2)$. In particular, we can introduce three different moments of inertia, one for the $\text{SO}(3)$ generators, one for the generator of $\text{SO}(2)$ and a last one for the remaining six of $\text{SO}(5)$, which we treat collectively. If the last one is set to zero, we therefore end up with the well-known model of internal rotation of a, here spherical, rigid rotor. By introducing three distinct moments of inertia for the $\text{SO}(3)$ generators we can extend this model to an asymmetric overall rotor with internal rotation (see Example 10.1).

By using Racah's method of subalgebra chains (see, e.g., [51]), the states of the full $\text{SO}(5)$ symmetry can be represented in the smaller $\text{SO}(3) \times \text{SO}(2)$ group. We already showed this correlation in Table 8.1. This can be used to set up a correlation diagram of $\text{SO}(5)$ symmetric states: Under variation of the appropriate moments of inertia, we cause the well-known states of internal rotor theory to appear. Since the two limits are known, the obvious question to answer is about the interpretation of the correlation parameter.

In customary molecular theory, we encounter correlation diagrams when discussing linear-to-bent transitions of few-atomic molecules [14, 31]. In that case, the according parameter is identified as the equilibrium bond angle describing the minimum on the potential energy surface (see in particular Fig. 17-7 in [14]). In the case of extremely floppy molecules, we assume the internal rotor angle and axis to be completely free, hence a parameter describing the level of restriction of the motion of this axis could control the transition to conventional internal rotors with a totally fixed axis. However, regarding the six remaining generalized angular momentum operators, possibly more than only one such parameter must be defined and the correlation diagram is replaced by a multidimensional correlation surface. The CH_5^+ molecule would be located at the one edge of the correlation diagram since its dynamics follow the $\text{SO}(5)$ symmetric model in good approximation. On the other edge, we expect, e.g., the nitromethane molecule, which exhibits a free internal rotation with fixed internal rotor axis.

In addition, the ten generalized moments of inertia can be used to restrict the model straightforwardly to the subgroup $\text{SO}(3) \subset \text{SO}(5)$, which we interpret as the case where all the internal rotation is frozen at once. In contrast, first restricting the internal rotor axis and then the internal rotor angle also leads to a conventional $\text{SO}(3)$ rotor. This would be described in the group chain $\text{SO}(3) \subset \text{SO}(3) \times \text{SO}(2) \subset \text{SO}(5)$. Therefore, a triangular picture of conventional limits of the super-rotor theory emerges (see Fig. 10.1): At the top of the triangle, the full $\text{SO}(5)$ symmetry is assumed where all the moments of inertia are equal. On the left side, the internal rotor (fixed internal rotor axis) subgroup is shown, and on the right side, the three-

Fig. 10.1 Triangle of limits of the super-rotor theory ($\text{SO}(5)$). The $\text{SO}(3)$ limit is that of a standard spherical rotor, whereas with the symmetry group $\text{SO}(3) \times \text{SO}(2)$ one describes a decoupled internal rotation in a spherical rotor



dimensional rotor without internal rotation is located. All three limits can be reached by manipulating the generalized moments of inertia in a very specific way.

Example 10.1 The internal rotor subgroup $\text{SO}(3) \times \text{SO}(2) \subset \text{SO}(5)$ can be reached by using the generalized moments of inertia and the Hamiltonian of (7.4). The Lie algebra of $\text{SO}(5)$ allows us to identify ten generators of five-dimensional rotations and by using Racah's rule for subalgebra chains, [51] it facilitates the identification of the four generators of the algebra of $\text{SO}(3) \times \text{SO}(2)$. If we use the notion of Example 6.2 on p. 74, the $\text{SO}(3) \times \text{SO}(2)$ operators (J_{\pm}, J_z, p) are found to be (see (6.2))

$$\begin{aligned} J_{\pm} &= E_{\pm\beta}, \quad \Rightarrow [E_{\beta}, E_{-\beta}] = H_1 - H_2, \quad \Rightarrow J_z = (H_1 - H_2) \\ p &= H_1 + H_2, \quad \Rightarrow [p, J_{\pm}] = [p, J_z] = 0. \end{aligned}$$

By choosing the moments of inertia of (7.4) carefully we can hence recover the Hamiltonian for internal rotation of Example 7.1. The exact definition of the respective constants in terms of the moments of inertia is rather lengthy and we skip it here.

In Fig. 10.1 we also introduce two parameters, ϑ and r , to indicate the “position” of a real molecule in this triangle. We expect these two parameters to be defined in terms of some combinations of generalized moments of inertia. Furthermore, we indicate three examples of molecules in the figure: The dot on the top of the triangle (goldish color, $(r, \vartheta) = (1, \pi/3)$) represents protonated methane, the dot in the left lower corner (dark blue color, $(0, 0)$) is the example of nitromethane, discussed in Example 7.2. In addition, in the lower right corner (light blue color, $(1, 0)$), the dot indicates a standard spherical rotor, as, e.g., sulfur dioxide (see Part III) usually described without the need of internal rotation.

Motivated by the fact that in customary rotational theories, the limiting cases of spherical, prolate, or oblate rotors are also only approximations and more realistic models are somewhere in between these limits, a proper description of real molecules in the super-rotor theory is also expected to be “located” somewhere in the triangle of Fig. 10.1. For instance, the water dimer represents a molecule, where the relative

orientation and respective rotation could be interpreted as internal rotation. The weak interaction between the two monomers could fix the internal rotation axis up to certain point but potentially does not fully constrain it. Therefore it is potentially described by a model in between the three limits discussed above. However, these are only the first steps towards a full description of the influences of the generalized moments of inertia, we expect future studies to recover more of the respective dynamics and to unravel more of the underlying physics.

As one more step, the view on results from nuclear physics can possibly help in understanding the triangle of Fig. 10.1. There, a so-called “symmetry triangle of equilibrium nuclear structure” ([100], p. 21) is used to show three limits of the interacting boson model, namely the Wilets–Jeans model of SO(5) symmetry, a vibrator model of U(5) symmetry and a prolate rotor, described in SU(3) [100]. These different limits are also obtained by varying certain structural parameters, analogous to the idea of generalized moments of inertia. Although the limits have different symmetries, the general method is probably adaptable to the theory of molecules. In that regard note that especially the correlation diagram of $\text{SO}(5) \leftrightarrow \text{U}(5)$ resembles the correlation diagram of the linear-to-bent transition of molecular physics (compare p. 210 of [24] and p. 635 of [14]). This point certainly needs further discussion since the initial assumption of the respective Bohr model of nuclear physics is a nucleus that is approximated by a liquid drop model and hence differs considerably from the initial molecular ball-and-stick model leading to the liner-to-bent correlation diagram.

10.1.2 Higher-Order Terms

As in the case of Watson’s Hamiltonian for conventional rotors, [33] see Parts I and III, the exclusive use of second order operators in the Hamiltonian of the super-rotor limits its applicability. Again symmetry helps increasing the order of the model: As already anticipated in Chaps. 6 and 7, there is a fourth order Casimir operator, which is invariant under all rotations in five dimensions. It is constructed from a sum of products of four generalized angular momentum operators and hence is central in the discussion of a next-order term in a model for super-rotation (see Example 6.2 on p. 74). Its eigenvalues for the states of generalized angular momentum $[n_1, n_2]$ are given as [22]

$$C_4 = (n_1(n_1 + 3)(n_1(n_1 + 3) + 3) - n_2 + 2n_2^3 + n_2^4).$$

In adding them to the zero-order Hamiltonian, the energy expression enlarges to

$$\begin{aligned} E_{[n_1, n_2]} &= \frac{B}{2} \{n_1(n_1 + 3) + n_2(n_2 + 1)\} + \\ &+ C \{n_1(n_1 + 3)(n_1(n_1 + 3) + 3) - n_2 + 2n_2^3 + n_2^4\} \end{aligned} \quad (10.1)$$

This induces, e.g., a lifting of the degeneracies of states with different quantum numbers, as [4, 3] and [5, 0]. However, a first try to fit also the second parameter C to the experimental values of protonated methane showed that the best fit C -value is almost zero and hence has no remarkable influence on the accuracy. Most likely, other molecules have different B and C parameters and $C > 0$ possibly influences the energy spectrum considerably.

As shown in the preceding section, the introduction of generalized moments of inertia can be used to define an asymmetric five-dimensional rotor. Consequently, one can also introduce certain fourth-order constants, analogous to the distortion constants usually named τ for the conventional three-dimensional distortable rotor [26]. Obviously, the number of these constants is much higher than in the traditional approach. In customary rotational theory, one defines 81 such constants but their number can be reduced due to certain symmetry constraints in the application to particular molecules. In the five-dimensional rotor case, we count 625 possible combinations of four generalized angular momentum operators, hence the number is by far larger than in the three-dimensional case. Again symmetry restrictions can possibly help to reduce the number of the generalized distortion constants and to determine them from experimental spectra.

In addition, with the introduction of higher order terms and in view of the results of Chap. 8, also a variational approach to the super-rotor dynamics seems to be within reach.

In conclusion, the zero-order model of the super-rotor can be enlarged in a perturbation series, where higher order operators can be included as well as according expansion constants. The number of these constants is, as the number of generalized moments of inertia, much higher than in the conventional three-dimensional case, however for fitting purposes, they might be essential. A variational approach might also be possible although nothing has been done towards that direction so far.

10.2 Additional Target Molecules

Protonated methane, studied in particular in Chap. 9, represents only the tip of the iceberg of extremely floppy molecules. A large variety of such molecules exist, where the idea of a fixed geometrical structure must be abandoned [68, 71, 72] and traditional approaches provide only very limited insights in the complicated ro-vibrational dynamics.

The first prominent example is H_5^+ where, in contrast to CH_5^+ , no central atom is present. It is the first of the H_n^+ family which shows an “astructural” behavior, [60, 68] indicating the loss of the meaning of a fixed equilibrium structure. In difference to the CH_5^+ molecule, no low-energy levels are yet determined experimentally but very recent expensive quantum chemical calculations were performed to predict ro-vibrational energies near the zero-point vibrational energy. The results are very remarkable as they exhibit a so-called “negative rotational increment” ([60], p. 4), indicating that the energies do not increase with J as they do in more regular

molecules. From ab-initio calculations however, the potential energy surface is predicted to restrict the motion of the five protons, such that the molecular symmetry group is not the full group G_{240} . Still, the relative rotation of two H_2 subunits is calculated to be almost free. For an application of the super-rotor theory, this implies the need of the generalized moments of inertia, a single parameter could be insufficient for fitting the respective energies and the full $SO(5)$ symmetry must be assumed to be broken. Since the recent calculations of [68] were performed for states of $J \leq 3$, an explicit comparison is not yet possible. The calculated energies clearly show that higher J quantum states can have smaller energies, hence a low-energy comparison would not be very meaningful.

The decreasing of energy with increasing angular momentum however, is a strong sign for an underlying super-rotational dynamics. The angular momentum content in the $[n_1, n_2]$ states does not follow a strong increasing scheme. In particular from the branching rules of $SO(5) \downarrow SO(3)$ (see Table 8.1), we know that the state, e.g., $[1, 1]$ already includes $J = 3$. From $SO(5) \downarrow [SO(3) \times SO(2)]$, the states $[1, 0]$ and $[1, 1]$ both include a $(J, p) = (1, 0)$ state. This induces the irregular behavior of the rotational energies to be potentially explained by the degeneracies of the $SO(5)$ symmetric states. However, more detailed comparisons and calculations are needed to support the above statements and to test the super-rotor model also on the H_5^+ molecule.

In general, all kinds of small clusters where weak van-der-Waals or hydrogen mediated bonds induce almost free relative torsions of the subunits building the cluster. One other example is the benzene dimer, recently studied theoretically and experimentally [71, 114]. There, the combination of particular internal rotations and overall rotation into a lower-dimensional treatment can be used to explain certain features of the experimental spectrum. This is again a strong sign for the super-rotor theory to be able to explain the dynamics from a more fundamental point of view. The coupling of the different internal motions is intrinsically done by our approach and the simple analytical energies could be used for further analysis of the spectrum.

Another object of current investigation is the H_3^+ -He complex, where ab-initio calculations show that the wave function of the helium nucleus is delocalized in the plane of the three protons but first calculations also show small potential energy barriers to another structure, where the helium nucleus would be at the top of a pyramidal structure. This is a strong indication towards a treatment in the sense of the super-rotor theory since the internal rotation, which would be usually bound to be in-plane) would get more flexible from the possibility that the Helium also possibly exits the plane spanned by the protons. Here, advanced quantum chemical calculations and experiments are on the way and the comparison to the super-rotor theory seems to be obvious.

In all these target complexes, namely H_5^+ , the benzene dimer, and the H_3^+ -He complex, we expect our zero-order model to be too restrictive to recover the full dynamics of the respective molecule. The internal axis, which we considered to be totally free in CH_5^+ , must be (at least partially) confined in these systems, leading to symmetry-breaking terms in the super-rotor Hamiltonian. Therefore, we expect these molecules to be described somewhere in the triangle of Fig. 10.1. Nevertheless,

regarding the super-rotor theory as the starting point of a perturbative approach, our model provides fundamentally new insights into the dynamics of these kinds of molecules.

Another field of application of the five-dimensional rotor theory can be seen in the vibrationally excited states of all kinds of molecules exhibiting internal rotor dynamics. Whenever the vibrational excitation is exceeding the potential energy barriers hindering the internal rotation, the assumption of a free such motion becomes meaningful. Consequently, a decoupling from the overall rotation becomes questionable and the super-rotor approach can help in understanding the according ro-vibrational spectrum. For that, however, we need a thorough investigation of the influence of other vibrational modes onto the super-rotor states. In particular, coupling terms of generalized angular momentum and vibrational operators must be included in the full Hamiltonian. Vibrational modes of dimensions $d > 1$ are especially interesting in this regard since they carry a generalized angular momentum and hence couple in a very specific way to the \hat{J}_{ij} operators of the super-rotor model. This is analogous to the case of conventional higher-dimensional vibrations, where one usually defines a so-called vibrational angular momentum to simplify the respective couplings to the overall rotations. One well-known example is the doubly degenerate bending vibration in linear molecules, where the two dimensions of the vibration leads to the definition of an angular momentum quantum number also for the vibrational states [14].

10.3 Concluding Remarks

With the super-rotor model, we have found a description of combined indistinguishable internal and overall rotational motions in extremely floppy molecules, where the internal rotation is totally free in its rotation angle and axis. We have shown the symmetry properties of this approach and used Lie theory to formulate a simple analytical energy expression for this fundamentally new type of ro-vibrational motion. It can be mapped onto that of a five-dimensional rigid rotor, which has been used in different parts of physics before, but has never been applied to molecular problems [24, 98, 115].

In a very first application, we used protonated methane as the target molecule. We showed the symmetry of the five-dimensional rotor to overcome the problem of representing ro-vibrational states in the full molecular symmetry group of protonated methane, G_{240} [9]. The latter is not isomorphic to a subgroup of $SO(3)$ – in difference to all other known molecular symmetry groups – and hence all attempts to assign unambiguously an angular momentum quantum number to the states in G_{240} must fail. With the larger $SO(5)$ symmetry group of the super-rotor model, we are able to assign generalized angular momentum quantum numbers, specifying also the energy of the five-dimensional rotor, to the states of G_{240} . In all honesty, we must admit that we used the permutation subgroup S_5 for that analysis only, but also for that group all traditional approaches fail for the same reasons and we expect the extension to

the full group to be rather simple once the coordinates of the five-dimensional rotor are fully understood.

With these symmetry considerations, we were able to identify missing levels in the super-rotor theory and the assignment of the generalized angular momentum quantum numbers to the experimentally determined low-energy states [4] became possible [7]. We used the assignment to fit the single free parameter of the model and found it to be – as expected – close to the rotational constant of a rigid three-dimensional rotor previously calculated by traditional ab-initio theory. The fitted energies agree favorably with the experimental values, we achieve accuracies of about one wave number. However, we were not able to fit all observed low-energy states, in particular one set of states, presumably of different parity, remained unassigned. This could be explained by the assumed completely flat potential energy surface for the motion of the five protons. The super-rotor model poses no restrictions at all on the internal rotor axis and angle. An inclusion of such constraints most likely leads to certain splittings into the states of different symmetries in the molecular symmetry group.

The current status of the super-rotation model can be seen analogous to the stage of describing non-rigid asymmetric rotors as rigid spherical molecules. With the inclusion of asymmetry terms as well as higher order terms, we expect the model to (i) become more accurate for the application to protonated methane but also (ii) to become a versatile tool in studying complicated internal dynamics in other extremely floppy molecular complexes, like H_5^+ , and van-der-Waals or hydrogen-bonded clusters. For that, we provided at least first steps using again symmetry: Lie theory is used to show how traditional approaches of describing internal rotational dynamics are naturally included in the super rotor model, and we expect many molecules, as, e.g., the water dimer, to be described in between the limits of a super-rotor and a rotor with fixed internal rotation axis.

Apart from the rather mathematical view on the inclusion of traditional models in the super-rotor approach, further studies are expected to show how the five-dimensional model influences the ball-and-stick picture of customary molecular theory. The comparison to nuclear physics, where the respective $\text{SO}(5)$ symmetry is interpreted as that a liquid drop model, suggests that the traditional view on molecules as structured matter potentially should be reconsidered thoroughly.

In conclusion, we developed a model of ro-vibrational motion in extremely floppy molecules, which exhibit, in the current zero-order stage, a very simple analytic energy expression with a single free parameter. It explains both qualitatively and quantitatively the complicated low-energy dynamics of the prototypical CH_5^+ ion, where traditional approaches reach their absolute limits. We have opened the first door to a new understanding of correlated, or collective, internal and overall rotational dynamics, where certainly many of the open questions presented here can be answered in future studies.

Part III

**Semi-classical Approach to Rotational
Dynamics**

Chapter 11

Ultrafast Rotation

Abstract For large angular momentum quantum numbers, a classical description of molecular rotation should be almost as good as quantum mechanical models. This is the starting point for this chapter, where a semi-classical method for the calculation of large angular momentum states in small molecules is discussed. Here, a classical description in terms of the angular momentum vector is extended by a quantization procedure, where path-integral methods are used. This combined method is known for a few decades but we apply it here to a totally quantum mechanical description of vibrational states using a variational approach. The chapter starts with an introduction of path integral methods in general and the formulation of the semi-classical approach to molecular rotation. The latter is also accompanied by a description of how a variational approach to vibrational dynamics can be used to create the rotational energy surface, the starting point for the semi-classical treatment.

11.1 Introduction

The majority of theoretical and experimental work on molecular physics is concerned with the inter- and intra-molecular dynamics at low temperatures. There, a few molecular states are sufficient to describe motion and interactions of single – or small ensembles of – molecules. The respective states are well-separated which facilitates the use of spectroscopic tools to examine the dynamics or the general molecular parameters as equilibrium structure or reaction rates. From a theoretical point of view, the low number of involved states is essential for quantum calculations to reach a level of accuracy comparable to the precision of high-resolution experiments. For the majority of molecular species, these calculations have been shown to successfully predict the experimental results. Whenever the density of states grows, computations become more challenging and common conventional models may fail. One primary example is the study of higher temperatures, where a large number of excited molecular states are populated and the number of states in a certain energy range increases. To obtain converged results, quantum chemical calculations are faced with the problem of their initial basis set size. Many different approaches to

deal with this exist in the literature, but still computations remain very expensive [34, 116–124].

In the following, we concentrate on highly excited rotational states, where different recent theoretical studies have shown their significance for, e.g., chemical reactivity, collisional dynamics, and rotational cooling or trapping [125–132]. Parallel to that, current developments of experimental techniques have successfully shown the possibility to study molecules at very high rotational states, where conventional experimental methods encounter major difficulties [125, 133].

As we presented in short in [16], the main idea of the present work is to treat the rotational dynamics at high speed by using ideas of classical mechanics to simplify the calculation and to improve the understanding of the related dynamics. This approach originates from the intuitive picture that an increasing angular velocity renders classical mechanics a very suitable tool in describing rotational dynamics at high speed. In a classical description, the energy “states” by definition describe a continuum, i.e. the density of state becomes a continuous (rising) function of the energy. However, since experiments can still resolve quantized energies also for these energetically high-lying states, we must attach a certain quantization procedure to extend our approach and to render it comparable to experimental results. The corresponding theoretical framework has been set up already in the 1970s and 1980s [134–136], but with few exceptions [136–141] the results have been – possibly because of the advent of larger computation facilities – overlooked by most spectroscopists. Conversely, one main ingredient of this *semi-classical* approach is used frequently to qualitatively explain certain features of experimental spectra: The concept of the rotational energy surface (RES) explains qualitatively, e.g., the so-called rotational level clustering [142–146]. The complete semi-classical approach is capable also of quantitatively predicting experimental spectra.

In the following, we will show how the almost 40 years-old approach is modernized by (i) reformulating it in the language of path integrals and, more importantly, by (ii) attaching it to a state-of-the-art computer program TROVE [34]. The latter is used to generate the rotational energy surface for the semi-classical analysis. It utilizes a variational approach [34, 116, 119, 147, 148] to solve the according vibrational problem, which differs from, e.g., the effective Hamiltonian approach of Watson [33]. In contrast to the latter, the variational approach is not limited to a single vibrational level and in principle can be used to solve the full rotation-vibrational problem even up to very high rotational excitations [149]. However, this method is, especially in the regime of ultrafast rotations, computationally expensive and the attachment of a semi-classical approach generates a versatile tool in studying these fast rotational dynamics in a less time-consuming and at the same time more intuitive way. This is one of the most important novelties of the presented semi-classical method. We use a variational approach to generate a rotational energy surface which yet was done – to our knowledge – exclusively by effective Watson-type methods.

The semi-classical approach is presented as described in [16] but in an extended, more educational way and we compare it quantitatively with other approaches for a test-molecule, namely sulfur dioxide SO₂, and discuss discrepancies and accuracies. Conclusively, reconsidering this semi-classical approach in the realm of modern

computation techniques such as TROVE is beneficial since it supports a better understanding and reduces the computation time for the dynamics of ultrafast rotations.

As in the other two parts of this work the semi-classical approach uses techniques of – in the first place – separated fields of theoretical physics. This is shown mainly in the reformulation in terms of path integrals, where the central ideas are adopted from chaos theory. Built from first principles, this approach actually reveals an intuitive picture of ultrafast rotational dynamics. As one of the “first principles”, molecular symmetry again plays a major role, showing once more the need of a detailed understanding of the fundamental symmetry properties for molecular dynamics.

In the next section, we introduce the theory of path integrals in general before entering the discussion of the rotational energy surface in detail in Sect. 11.3. In linking the two parts in Sect. 11.3.2, we find quantization conditions for the respective paths on that surface. Since the definition of the rotational energy surface is done classically, we call the full approach *semi-classical*.

11.2 The Gutzwiller Trace Formula

Before we enter the regime of this semi-classical approach to rotational dynamics, we review the theory of path integrals and the classical theory of motion to set the stage for the Gutzwiller trace formula of the semi-classical density of states. Readers familiar with the concept of path integrals and the respective semi-classical approximation may skip this chapter. We only introduce the basic ideas and show a few derivations, for more details we refer to the textbooks of [150, 151].

The central object is the propagator of an initial state, say, $|q_i\rangle$ to certain final state $|q_f\rangle$

$$K(q_i, q_f, t) = \langle q_f | \exp\left(-\frac{i}{\hbar} \hat{H}t\right) | q_i \rangle, \quad (11.1)$$

where the time evolution operator includes the Hamiltonian \hat{H} of the respective system, the (positive) time $t > 0$, and Planck’s reduced constant \hbar , which we, from now on, set to one for convenience. As a physical observable, $|K(q_i, q_f, t)|^2$ is the probability to find a particle after time t at a position q_f which initially, at $t = 0$, has been at q_i . The Fourier-transform of this propagator is given by the Green function

$$G(q_i, q_f, E) = i \int_0^\infty dt K(q_i, q_f, t) \exp(iEt) = \langle q_f | \frac{1}{E - \hat{H}} | q_i \rangle. \quad (11.2)$$

Thus, poles of the Green function signals quantized energy of any system described by the Hamiltonian \hat{H} . In order to evaluate these poles, the propagator itself is reformulated in terms of a path integral, which is “the ideal starting point for semi-classical calculations” ([151, p. 262]).

The propagator To evaluate the propagator in detail, we start with dividing the time for propagating from the initial to the final state into $N \gg 1$ small time steps of

size $\tau = t/N$. Since the time evolution operator $U(t) = \exp(-i\hat{H}t)$ satisfies $U(t) = [U(\tau)]^N$, the propagator can be written in a series of multiplications

$$K(q_i, q_f, t) = \langle q_f | [U(\tau)]^N | q_i \rangle. \quad (11.3)$$

To keep the notation simple, we consider a Hamiltonian of the form

$$\hat{H} = \frac{p^2}{2m} + V(q), \quad (11.4)$$

where p is the momentum, and q the position operator. As usual, m is the mass of the respective particle. By introducing an error of order $\mathcal{O}(\tau^2)$, we can simplify the time evolution operator to be

$$U(\tau) = \int d\tilde{p} \int d\tilde{q} |\tilde{q}\rangle \langle \tilde{q}| \exp\left(-i\tau\left(\frac{\tilde{p}^2}{2m} + V(\tilde{q})\right)\right) |\tilde{p}\rangle \langle \tilde{p}| + \mathcal{O}(\tau^2),$$

where the (\tilde{p}, \tilde{q}) are the eigenvalues of the respective operators and the $(|\tilde{p}\rangle, |\tilde{q}\rangle)$ are the corresponding eigenstates. Remember, that the eigenstates build a complete (continuous) basis system, such that, e.g., the integral $\int d\tilde{p} |\tilde{p}\rangle \langle \tilde{p}|$ is the identity operator. The approximate feature of the above equation originates from the need to factorize the exponential, such that the momentum and position operators can be evaluated separately, $\exp(-i\hat{H}t) = \exp\left(-i\tau\frac{\hat{p}^2}{2m}\right) \exp(-i\tau\hat{V}) + \mathcal{O}(\tau^2)$, whereafter we can introduce the basis functions and then sort the parts to get to the above final result.

Inserting this evolution operator into the (11.3) at each time step and noticing that $\langle q|p\rangle = e^{ip\cdot q}/\sqrt{2\pi}$, one arrives at

$$K(q_i, q_f, t) \simeq \int_{\substack{q_N=q_f \\ q_0=q_i}} \prod_{n=1}^{N-1} dq_n \prod_{n=1}^N \frac{dp_n}{2\pi} e^{-i\tau \sum_{n=0}^N \left(V(q_n) + \frac{p_n^2}{2m} - p_{n+1} \frac{q_{n+1}-q_n}{\tau} \right)}.$$

Here, p_n, q_n are the eigenvalues of $\hat{p}|p_n\rangle$ and $\hat{q}|q_n\rangle$ at the n th time step. Next, we take the continuum limit $N \rightarrow \infty$ while keeping $t = N\tau$ fixed. This changes the exponent in two ways: (i) the sum converges into an integral over time t' bounded by zero and t and (ii) the last term changes into a conventional time derivative \dot{q} . Finally, we simplify the expression by defining the integration measure:

$$\lim_{N \rightarrow \infty} \int_{\substack{q_N=q_f \\ q_0=q_i}} \prod_{n=1}^{N-1} dq_n \prod_{n=1}^N \frac{dp_n}{2\pi} \equiv \int_{q(t)=q_f, q(0)=q_i} Dx.$$

In conclusion, we arrive at the general formulation of the path integral:

$$K(q_i, q_f, t) = \int_{\substack{q(t)=q_f \\ q(0)=q_i}} Dx \exp \left(i \int_0^t dt' \{ p \dot{q} - H(p, q) \} \right) \quad (11.5a)$$

$$K(q_i, q_f, t) = \int_{\substack{q(t)=q_f \\ q(0)=q_i}} Dq \exp \left(i \int_0^t dt' L(q, \dot{q}) \right). \quad (11.5b)$$

The second equation is a result from a Gaussian integration of the momentum part which is possible if the kinetic energy part is quadratic in p . The resulting exponential factor L is the Lagrangian $L = m\dot{q}^2 - V(q)$. The functional measure in (11.5b) is only q -dependent and is defined as $Dq = \lim_{N \rightarrow \infty} \left(\frac{Nm}{2\pi i\hbar}\right)^{N/2} \prod_{n=1}^{N-1} dq_n$.

The two equations of (11.5) show the main result of the path integral formalism. A quantum mechanical object, namely the probability to end in certain state $|q_f\rangle$ when starting in $|q_i\rangle$, is expressed as an integral over all possible paths in phase space (p, q) , which is defined by the Hamilton function of the system. Each path, starting at q_i and ending at q_f is therefore weighted by the *classical* action of the system. This actually does not contradict the quantum feature of the propagator since the integral takes *all* connecting paths into account and not only the classically allowed ones. Actually, since the weight of the individual paths is the corresponding action, the classical paths always have the highest weight. To understand this, we have to remember some properties of classical mechanics.

A (classical) particle's path must be a solution of the corresponding equations of motion. Usually, the total energy of a classical system is described by a Hamilton function $H = T + U$ with a kinetic part T and some potential energy term U . Accordingly, the Lagrangian is given by $L = T - U$, and furthermore, the *action* is defined as the time integral $S = \int_0^t dt' L(q, \dot{q})$ over the Lagrangian. Here, (q, \dot{q}) represents the set of all relevant coordinates and their time derivatives. Hamilton's extremal principle states that the paths, say $q(t)$, the particle actually follows in a real system, extremize the action, i.e. $\delta S[q(t)] = 0$, where δ is the functional derivative

$$\delta S[q(t)] = \lim_{\varepsilon \rightarrow 0} (S[q(t) + \varepsilon] - S[q(t)]) \quad (11.6)$$

Actually, the action is extremal if and only if $q(t)$ satisfies Lagrange's equation of motion

$$\frac{d}{dt} (\partial_{\dot{q}(t)} L) - \partial_q L = 0 \quad (11.7)$$

Example 11.1 For an example of how the Lagrange equations of motion are connected to usual Newton's equations, we consider a mass fixed to a spring. The force of that spring is equivalently described by a potential of $U = \frac{1}{2}kx^2$, where x is the displacement from the relaxed length. Since $p = m\dot{q}$, the full Lagrangian reads as $L = \frac{1}{2}m\dot{q}^2 - \frac{1}{2}kq^2$. Performing the derivatives of (11.7) leads to $m\ddot{q} + kq = 0$ which equals the well-known Newton equation for the spring.

If a path $q(t)$ therefore satisfies this equation, it is said to be the classical path and in that respect is the only one possible in traditional classical mechanics. Thus, classical mechanics is recovered in the path integral formalism, if only the paths solving (11.7) are permitted.

In a semi-classical theory, we want to include in addition to these extremal paths also those which are “near” the extremal. In order to do so, we perform a stationary phase approximation, where the stationary phase is exactly this extremal path. Again, we here refer to [150], where this approximation is described in detail in the third chapter. In short, it utilizes a Taylor expansion to second order in the exponent of (11.5b), whereafter a Gaussian integration (the second order term is quadratic) is performed. Applying this to the path integral of (11.5) formally yields:

$$K(q_i, q_f, t) \simeq \sum_i e^{-iS[q_{cl}^{(i)}]} \det\left(\frac{\hat{A}_i}{2\pi}\right)^{1/2} \quad \text{with} \quad \hat{A}_i = i \frac{\partial^2 S[q]}{\partial q_f \partial q_i} \Big|_{q=q_{cl}^{(i)}}. \quad (11.8)$$

The sum is taken over all classical solutions of (11.7), namely the $q_{cl}^{(i)}$ connecting initial and final points q_i and q_f . Note the operator nature of \hat{A} and the corresponding definition of the determinant as the multiplication of the respective eigenvalues. With this, we finally arrived at the semi-classical approximation of the propagator $K(q_i, q_f, t)$.

The density of states To correlate the path integral formalism to experimental spectra, we need to evaluate the density of states of the respective system. It is given by

$$\rho(E) = \text{tr}\delta(E - \hat{H}) = \sum_a \delta(E - E_a), \quad (11.9)$$

where the $\{E_a\}$ are the energies (eigenvalues) of the Hamiltonian \hat{H} . From Dirac’s identity $\lim_{\epsilon \rightarrow 0} \frac{1}{x+ie} = -i\pi\delta(x) + \mathcal{P}\frac{1}{x}$, where \mathcal{P} indicates the principal value, we can infer the density of states to be identical to the trace of the Green function of (11.2)

$$\rho(E) = -\frac{1}{\pi} \text{Im} \text{tr}(G(E)) = \frac{1}{\pi} \text{Re} \int dq \int dt \{K(q, q, t) \exp(iEt)\}. \quad (11.10)$$

This is an integral over all paths that connect the same initial and final point. Inserting the semi-classical approximation of (11.8) and performing a stationary phase approximations for both, t and q , leads to the so-called Gutzwiller trace formula: [152]

$$\rho(E) \simeq \frac{1}{\pi\hbar} \text{Re} \sum_a T_a \sum_n \frac{e^{-in\pi/2\nu_p}}{\sqrt{|1 - M_p^n|}} e^{inS_a(E)/\hbar}. \quad (11.11)$$

Here, $S_a(E) = \oint pdq$ is the action for the complete, closed path. In the derivation of this equation, the paths connecting the same initial and final point are actually found

to be *periodic* in the sense that they also have the same initial and final momentum. Hence the sum has to be taken over all periodic paths labeled by a in the above equation. Moreover, one such path can be followed repeatedly n times, explaining the second sum in the above equation. Furthermore, T_a is the time for one of such closed trajectories, M_p^n is the monodromy matrix, which signals the stability of a path. Since we will focus on one-dimensional paths only, we can omit this factor. Conversely, the ν_p is a topological index, also called Maslov index, which in the one-dimensional case simply counts the number of turning points of the respective path, where $p(q) = 2m\sqrt{E - V(q)} = 0$. It is analogous to the phase change of a quantum mechanics wave function at a potential wall.

A closer look to the derivation of Gutzwiller's trace formula reveals that paths of zero lengths are excluded. Nevertheless, they contribute to the density of states by adding a smooth part ρ_0 to (11.11). It can be calculated formally by

$$\rho_0(E) = \int dp dq \delta(E - H(p, q)),$$

where $H(p, q)$ is the Hamilton function of the system. As such, ρ_0 describes the part of the phase space which a classical particle with an energy E can access. Obviously, this varies only smoothly with the energy, whereas the part described in (11.11) oscillates with energy (For details see, e.g., the textbook of [151, p. 287 et seq.]). In conclusion, the density of states in a semi-classical approximation can be written as

$$\rho(E) \simeq \rho_0(E) + \frac{1}{\pi\hbar} \operatorname{Re} \sum_a T_a \sum_n e^{in(S_a(E)/\hbar - \nu_p\pi/2)}. \quad (11.12)$$

Example 11.2 Consider again the harmonic oscillator of Example 11.1. The action for a closed path is hence given by

$$S_E = \oint pdq = 2 \int_{q_-}^{q_+} \sqrt{2m(E - \frac{1}{2}kq^2)} dq = E\sqrt{\frac{m}{k}} \cdot 2\pi,$$

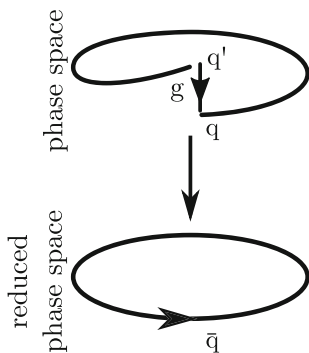
where $q_{\pm} = \pm\sqrt{2E/k}$ are the turning points of the harmonic potential. Therefore, the Maslov index is given by $\nu_p = 2$ and the oscillatory part of the density of states shows a geometric series in the sum over the repetitions n of certain path a , leading to

$$\rho_{\text{osc}}(E) \simeq \frac{1}{\pi\hbar} \operatorname{Re} \sum_a T_a \frac{e^{i(S_a(E)/\hbar - \pi)}}{1 - e^{i(S_a(E)/\hbar - \pi)}} = -\frac{1}{\pi\hbar} \operatorname{Re} \sum_a T_a \frac{e^{iS_a(E)/\hbar}}{1 + e^{iS_a(E)/\hbar}}$$

Obviously, the poles of the density of states are now at $S_a(E) = (2n + 1)\pi\hbar$, such that with the action of the harmonic oscillator, we retrieve the well-known WKB-quantization condition

$$E_n = \sqrt{\frac{k}{m}}\hbar(n + 1/2).$$

Fig. 11.1 A closed path from q to $gq' = q$, which in the reduced phase space maps onto a closed path from \bar{q} to itself (Figure reproduced after [153])



In conclusion, we used the semi-classical approximation to find quantization conditions for the harmonic oscillator. As expected, the time T_a is shown to have no influence on the quantization conditions. In this example, the semi-classical quantization conditions exactly recover the full quantum mechanical solution. In more advanced applications however, they lead to only approximate correspondence.

Symmetry projected density of states As introduced in Chap. 2 of Part I, molecules exhibit various symmetries. In particular, the molecular states are labeled by the irreducible representations of the complete nuclear permutation-inversion symmetry group. In order to find a semi-classical description also respecting the particular symmetry of the molecule, we must characterize the respective paths in the density of states by their symmetries.

To start with, recall that symmetry operations are defined as elements $g \in G$ with vanishing commutator $[\hat{H}, g]$. The eigenstates of \hat{H} can be labeled by the irreducible representations of the symmetry group G . The quantum mechanical projection operator onto the subspace of states, transforming according to a certain irreducible representation, is defined as

$$P_m = \frac{d_m}{|G|} \sum_{g \in G} \chi_m(g) U^\dagger(g), \quad (11.13)$$

where $U|q\rangle = |g q\rangle$. For a discussion of symmetry projections in continuous symmetry groups, we refer to [153]. We focus on the case of discrete symmetries, described by finite symmetry groups. In the above equation, m labels the d_m -dimensional irreducible representation of G with characters χ_m . Applying this to the states in the definition of the quantum propagator $K(q_i, q_f, t)$ leads to the symmetry projected Green function

$$G_m(q_i, q_f, E) = \frac{d_m}{|G|} \sum_{g \in G} \chi_m(g) G(q_i, gq_f, E).$$

It describes paths of symmetry m connecting q_i and q_f , where the energy is fixed to E . In the semi-classical approximation, this Green function then reads as

$$G_m(q_i, q_f, E) = \frac{d_m}{|G|} \sum_{g \in G} \chi_m(g) \sum_{j, gq', q} \det \left(\frac{\hat{A}_j}{2\pi} \right)^{1/2} e^{-iS_j},$$

where S_j is the action of the j th path connecting the points q and gq' . To apply Gutzwiller's trace formula here, we use results of [154], in particular the notion of reduced phase space. In the reduced phase space, two points q and gq are mapped onto the same point \bar{q} . With this, the trajectory in usual phase space that connects q and gq' corresponds to one in reduced phase space, which connects \bar{q} and \bar{q}' .

Taking the trace in the derivation of the density of states leads to $\bar{q} = \bar{q}'$ (see Fig. 11.1), and an integration over the whole phase space with $\int dq = |G| \int d\bar{q}$. Using Gutzwiller's trace formula, the symmetry projected, semi-classical density of states is given by

$$\rho_m(E) \simeq -\text{Re} \frac{d_m}{\pi} \sum_{\alpha} \frac{T_{\alpha}}{|K_{\alpha}|} e^{iv_{\alpha}} \chi_m(g_{\alpha}) e^{iS_{\alpha}}. \quad (11.14)$$

Since we are interested in paths of finite length, we omit the smooth part of the density of states. For convenience, we also omit the sum over the repetitions. Again, only periodic trajectories α are taken into account, which induces the g_{α} to be the identity operator of the respective symmetry group. The factor $|K_{\alpha}|$ is the order of the subgroup $K_{\alpha} \subset G$, which leaves trajectories invariant that are exactly at the boundary of the symmetry reduced phase space. Mostly, this factor is trivial but examples and details on its derivation can be found in [154]. Indeed, a sum over all irreducible representations of the symmetry group recovers the full oscillatory part of the density of states of (11.11).

This concludes the introductory part on the general semi-classical density of states, which was first introduced by [152]. The symmetry projected version for discrete symmetry groups was found by [154] and we will use this for our further studies. Actually, the (oscillatory) density of states will be shown to have certain poles, indicating quantized energy levels (see (11.2) and Example 11.2) in the case of the rotational dynamics. In order to find these poles, we now proceed to the discussion of the classical rotational dynamics that we need for the application of the above semi-classical theory.

11.3 The Rotational Energy Surface

In Part I, we already introduced the Hamiltonian for the quantum mechanical description of molecular rotation. In order to establish a semi-classical theory, where the dynamics are dominantly described by the classical motion, we here briefly present the classical description of molecular rotation. By using the correspondence principle, first formulated by [155], both descriptions can actually be transformed into each other. After having formulated the classical theory, we will use this correspondence in order to connect it to the variational approach of TROVE, [34] which usually employs a fully quantum method.

To start with, we suppose the molecular rotation to be separated from all other degrees of freedom and to be described by the kinetic energy of a free rigid rotor. The classical angular momentum of a rigid body is given by $\mathbf{J} = \mathbf{I} \cdot \boldsymbol{\omega}$, where \mathbf{I} is the conventional moment of inertia tensor, and $\boldsymbol{\omega}$ the angular velocity with components

$$\begin{aligned}\omega_1 &= \dot{\phi} \sin \theta \sin \psi + \dot{\theta} \cos \psi, \\ \omega_2 &= \dot{\phi} \sin \theta \cos \psi - \dot{\theta} \sin \psi, \\ \omega_3 &= \dot{\phi} \cos \theta - \dot{\psi},\end{aligned}\tag{11.15}$$

where the angles (ϕ, θ, ψ) are the usual Euler angles. In a molecule-fixed, principal axis system, where the non-diagonal elements of \mathbf{I} vanish, the kinetic energy of the rotor is given by

$$T = \frac{1}{2} (I_1 \omega_1^2 + I_2 \omega_2^2 + I_3 \omega_3^2) = L.\tag{11.16}$$

We assume furthermore, that the potential energy is independent of the angles, such that the Lagrangian L consists of the kinetic energy term only. Calculating the according equations of motion of (11.7) for the different angular coordinates and their time derivatives leads to

$$\begin{aligned}I_1 \dot{\omega}_1 + \omega_2 \omega_3 (I_3 - I_2) &= 0, \\ I_2 \dot{\omega}_2 + \omega_1 \omega_3 (I_1 - I_3) &= 0, \\ I_3 \dot{\omega}_3 + \omega_1 \omega_2 (I_2 - I_1) &= 0.\end{aligned}\tag{11.17}$$

Example 11.3 For calculating the equations of motion, the Euler angles are taken to be the generalized coordinates q and \dot{q} as their time derivatives. We can hence, e.g., calculate the Lagrange equation of motion for the ψ -coordinate:

$$\begin{aligned}\frac{\partial L}{\partial \dot{\psi}} &= I_3 \omega_3 \frac{\partial \omega_3}{\partial \dot{\psi}} = I_3 \omega_3 \\ \frac{\partial L}{\partial \psi} &= I_1 \underbrace{\omega_1}_{=\omega_2} \frac{\partial \omega_1}{\partial \psi} + I_2 \omega_2 \underbrace{\frac{\partial \omega_2}{\partial \psi}}_{=-\omega_1} = I_1 \omega_1 \omega_2 - I_2 \omega_1 \omega_2 \\ \frac{d}{dt} \frac{\partial L}{\partial \dot{\psi}} - \frac{\partial L}{\partial \psi} &= I_3 \dot{\omega}_3 + \omega_1 \omega_2 (I_2 - I_1) = 0,\end{aligned}$$

where we used (11.15). The other equations of (11.17) can be calculated analogously.

By changing to the more convenient formulation in terms of the angular momentum \mathbf{J} and by multiplying the first equation of (11.17) by J_x , the second by J_y , and the third by J_z , we can straightforwardly show the equations of motion to induce conservation of angular momentum:

$$J_x \frac{dJ_x}{dt} + J_y \frac{dJ_y}{dt} + J_z \frac{dJ_z}{dt} = 0 \Rightarrow J_x^2 + J_y^2 + J_z^2 \equiv J^2 = \text{const.}$$

Simultaneously, the kinetic energy

$$E_{\text{rot}} = \frac{1}{2} (J_x^2/I_1 + J_y^2/I_2 + J_z^2/I_3) \quad (11.18)$$

is the second conserved quantity. If we consider the three-dimensional space spanned by \mathbf{J} , (11.18) represents an ellipsoid with the three principal axes E_{rot}/I_1 , E_{rot}/I_2 , and E_{rot}/I_3 . However, since total angular momentum is conserved, $J^2 = \text{const.}$, the solutions of the classical equations of motion must lie on the intersection of that ellipsoid and a sphere of constant radius. Conventionally, one uses rotational constants $A = \frac{1}{2I_1}$, $B = \frac{1}{2I_2}$, $C = \frac{1}{2I_3}$ instead of the moments of inertia.

Angular momentum conservation can also be used to represent the classical solutions in a slightly different way as it was first done by [136]: The constant total angular momentum is used to define spherical polar coordinates with

$$\begin{aligned}J_x &= |\mathbf{J}| \sin \theta \cos \phi \\ J_y &= |\mathbf{J}| \sin \theta \sin \phi \\ J_z &= |\mathbf{J}| \cos \theta.\end{aligned} \quad (11.19)$$

In these polar coordinates energy appears as a sphere of constant radius, whereas the right hand side of (11.18) defines a so-called *rotational energy surface* which topologically varies for different moment of inertia tensors. Due to the two constants of motion, energy and angular momentum, paths are described by the intersection of the energy sphere and the rotational energy surface.

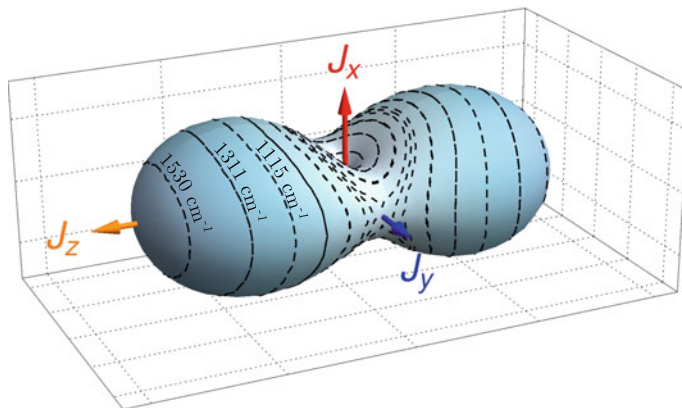


Fig. 11.2 Rotational energy surface for an asymmetric top molecule with rotational constants ($A = 8 \text{ cm}^{-1}$, $B = 14 \text{ cm}^{-1}$, $C = 23 \text{ cm}^{-1}$) near those of the water molecule H_2O . The total angular momentum quantum number has been set to $J = 10$ and we used (11.18) and (11.19) to represent the classical rotational energy in a spherical plot for fixed J . In order to better show the topology, we subtracted the minimal energy $E_{\min} = AJ(J+1)$ from the rotational energies of (11.18). The dashed curves indicate the intersections to different constant energies; They show the classical paths in J -space for the energies found by the quantization method shown in Sect. 11.3.2. The colored arrows indicate the different rotational axes

Semi-classical rotational energy surface At this point, we enter the *semi-classical* regime: Quantum mechanics dictates total angular momentum to be quantized, and applied to the symmetric rotor wave functions (see Sect. 2.2 of Part I) the respective eigenvalue is given by $\hat{\mathbf{J}}^2|\mathbf{J}m\rangle = J(J+1)|\mathbf{J}m\rangle$. In order to establish a semi-classical theory, the length of the J -vector (11.19) is set to $|\mathbf{J}| = \sqrt{J(J+1)}$. Since J is conserved, each J defines a distinct rotational energy surface as defined by (11.18).

A classical solution of quantized angular momentum J can be found by the intersection with a constant energy sphere. The \mathbf{J} vector of fixed length follows that path, hence describing the classical rotation of the real molecule (relative to a fixed space-fixed coordinate system) at certain energy. Notice that these paths are always closed around a certain axis indicating mainly two effects: (i) These paths are actually described by Gutzwiller's formula, where only closed paths contribute to the density of states; (ii) They close around a certain axis but the projection to this axis is not stable throughout the full rotation. In particular, we cannot define a J_z to be a constant of the motion in asymmetric rotors [26]. The axis around which the path closes, actually changes at a certain energy called *separatrix* by [136].

The representation of the classical rotational energy in terms of a surface with fixed quantized angular momentum is used fairly frequently to describe molecules exhibiting so-called *rotational clustering* (For some examples, see [140, 145, 156–158]). It describes the phenomenon of an increasing number of nearly degenerate states when the angular momentum quantum number is increased (For an example of four-fold clustering see in particular [158]). It can be explained by a topological

change of the rotational energy surface for increasing angular momentum quantum number. Already from the very simple example of the asymmetric top molecule in Fig. 11.2, we can imply that the actual energies will be doubly degenerate, since there are two closed paths for a single energy indicating the two possible directions of rotation (right or left-handed). In our zero-order model of molecular rotation, where we assumed a rigid rotor, no centrifugal distortion was included. Therefore, no topological change is expected for any angular momentum quantum number. In a more appropriate model, the distortion may lead to a change of the number of extrema, and the according degeneracy of the energy levels.

Before turning to the discussion of more appropriate methods to define the rotational energy surface for a given molecule, we focus first on the parametrization of the paths on the surface. These are subsequently used to apply Gutzwiller's formula to molecular rotation for finding the corresponding density of states and, if certain conditions are fulfilled, quantized energy levels.

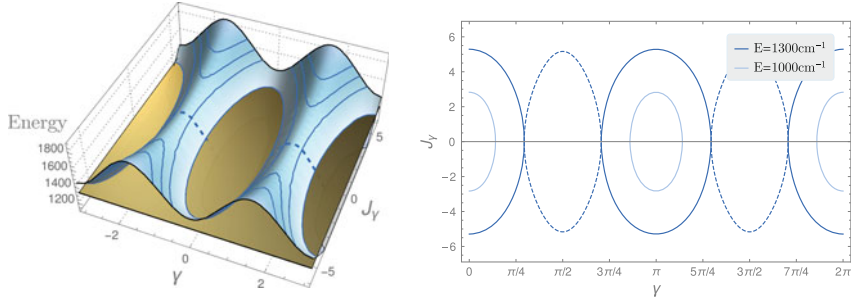
11.3.1 The Paths on the Rotational Energy Surface

The previously defined rotational energy surface is “simple” in the sense that their maxima and minima are well-separated. In Fig. 11.2 we observe that the intersection of a constant energy sphere and the rotational energy surface defines a line which closes around a single axis. In this case, the path can therefore be characterized by that axis. In topologically different surfaces, paths potentially change their respective enclosed axis. For the moment, we stick to the more simple case in order to present a proof-of-principle study of the semi-classical method.

A path with one encircled axis is thus best described by a projection on the perpendicular plane, i.e. if the path closes around J_x , the plane spanned by J_z and J_y . Hence we can parametrize it in terms of a coordinate, say, $q = \gamma$ and conjugated momentum $p = J_\gamma \equiv |\mathbf{J}| \cos \theta = J_z$ (see (11.19)). The respective action is defined as the integral $S_a(E) = \int J_\gamma d\gamma$. Accordingly, turning points are the angles at which J_γ vanishes. In this formulation, the rotation is similar to the motion of a particle in certain potential; If we take the simple Hamilton function of (11.18), and use the definition of the J_γ , the energy now reads as [136]

$$E = A(|\mathbf{J}|^2 - J_\gamma^2) \cos^2 \gamma + B(|\mathbf{J}|^2 - J_\gamma^2) \sin^2 \gamma + CJ_\gamma^2 \equiv H_J(J_\gamma, \gamma),$$

where $H_J(J_\gamma, \gamma)$ denotes the Hamilton function of fixed angular momentum J . Solving this for J_γ determines action and respective turning points of a path at fixed energy. By analogy to the spherical plot of the rotational energy surface in Fig. 11.2, we can set up two other plots, helping to understand the paths: First, a three-dimensional plot of the energy versus J_γ and γ highlights the analogy to a conventional potential energy surface (Fig. 11.3a); Second, a two-dimensional phase-space picture shows the paths themselves for fixed energies (Fig. 11.3b). The projection on paths closing



(a) Projection onto the J_y, γ plane: The intersection with the constant energy plane defines the paths.

(b) Phase space picture for two different energy paths. For the larger energy, the tunneling path is also shown.

Fig. 11.3 The rotational energy surface projection for $J_z = J_y$. Paths of different energies are shown in both pictures. The *dashed lines* represent the tunneling paths between the respective classical paths. The rotational constants have been chosen as in Fig. 11.2. The action of a single path is defined as the area it encloses

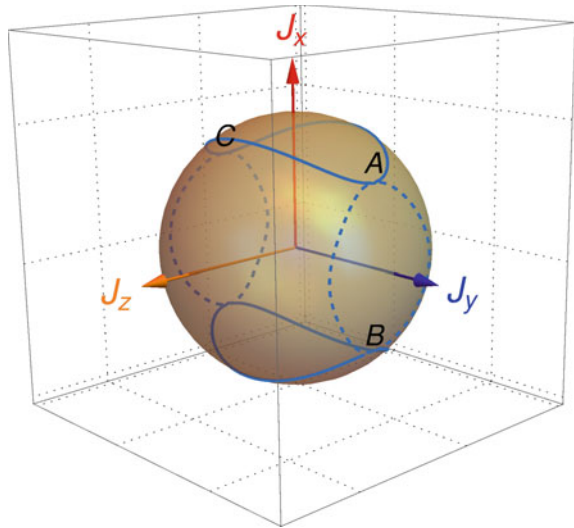
around the J_z vector follows straightforwardly by redefining the polar coordinates, i.e. $p = J_x = |J| \cos \bar{\theta}$ and $q = \bar{\gamma}$.

In order to find the separatrix energy, indicating the change of the quantization axis, the turning points have to be calculated. Exactly at E_{sep} , independent on the chosen quantization axis, the distance of the two respective turning points is π . For the Hamilton function of (11.18), it is found to be $E_{\text{sep}} = BJ(J + 1)$ [141, 159].

Tunneling paths – The non-classical contributions The projections of the rotational energy surface in Fig. 11.3 in particular show the analogy to a particle subjected to certain potential. From a quantum mechanical point of view, at each classical turning point, the particle has certain probability to tunnel through the potential barrier. Here, tunneling induces a change in the handedness of the rotation. The “particle” defines the angular momentum vector \mathbf{J} and if it tunnels through a barrier, its sign gets reversed. The barrier height depends on the distance to the separatrix energy E_{sep} , it vanishes for $E = E_{\text{sep}}$. Since tunneling always connects paths of identical energy, a change of the principal axis of rotation, i.e. the axis around which the path closes, cannot be induced by a tunneling event.

In the path integral formalism, tunneling paths are described by using a Wick-rotation to imaginary time, where the momentum, here J_y , becomes imaginary. This introduces an effective inversion of the potential, such that tunneling becomes a “classical” motion in the Wick-rotated potential [150]. Consequently, the paths are determined by the imaginary solution of $E = H(J_y, \gamma)$ (Examples of these paths are shown in Fig. 11.3). Therefore, the action also becomes imaginary, such that the tunneling paths cause – as expected from conventional quantum mechanics – an exponential damping factor in the propagator. Following the results of [136, 138, 160], and in particular [17], a path can either be reflected or transmitted at a certain turning point. There, the action is described in terms of reflection and transition amplitudes r and t [17, 160]

Fig. 11.4 The classical (solid) and tunneling (dashed) path in a spherical plot on the constant energy surface (cf. Fig. 11.2). A classical path ($A \rightarrow C$) can be followed, if one rotates the sphere by π about the J_x axis. The tunneling path ($A \rightarrow B$) is followed by rotating by π about J_y



$$r = \frac{e^{i\delta}}{\left(1 + e^{-2\tilde{S}_E}\right)}, \quad t = \frac{-i(-1)^J e^{-\tilde{S}_E} e^{i\delta}}{\left(1 + e^{-2\tilde{S}_E}\right)}, \quad (11.20)$$

$$\delta = \arg \Gamma \left(\frac{1}{2} + i \frac{\tilde{S}_E}{\pi} \right) - \frac{\tilde{S}_E}{\pi} \left(\ln \left| \frac{\tilde{S}_E}{\pi} \right| - 1 \right). \quad (11.21)$$

Here, we introduced \tilde{S}_E for the action of the tunneling path and the definition already includes the phase change and the Maslov index: In the limit of $\tilde{S}_E \rightarrow \infty$, i.e. infinite barrier height, the transition amplitude retrieves the Maslov factor and reflection goes to unity.

In order to describe a full path in the semi-classical density of states of (11.14), we identify three different parts: (i) A classical part weighted by the usual action e^{iS_E} , (ii) a reflection weighted by r , (iii) a tunneling part weighted by t . Indeed, in a single path, each of these parts can occur different times: [17]. If n is the total number of times, the path is tunneling through one potential energy barrier, and a_i is the number of classical paths between the, say, i th and $(i+1)$ th tunneling, the number of reflections is given by $a_i - 1$. At the end of the path, a_n , i.e. a_i for $i = n$, is the number of times the classical part is followed after the last tunneling. With these parameters, each path is uniquely defined by

$$(n, a_i), \quad \text{where } n \geq 0, \quad a_i > 0 \quad \text{for } i = 0, \dots, n-1 \quad \text{and } a_n \geq 0.$$

Therefore, the combination of reflection and transmission amplitude and the classical part reads as

$$r^{(a_0-1)+\dots+(a_{n-1}-1)+a_n} t^n e^{i(a_0+\dots+a_n)S_E}$$

However, in the symmetry projected density of states (11.14), we encounter $\chi_m(g)$, the character of a symmetry element g , which, for a closed path, must indeed be the identity but, at the same time, g is also described as a product of specific symmetry group elements. By projecting the density of states onto a certain irreducible representation, one hence identifies paths satisfying exactly the required symmetry. In order to describe the path by such symmetry elements, we can use – as a primary example – the asymmetric rotor, where the symmetry group is $C_{2v}(M)$. Using the isomorphism of the permutation-inversion group to equivalent rotations, [30] we can unambiguously identify a certain rotation for the classical part of the full path and another for the tunneling one (see Fig. 11.4). Since the axis around which the path closes changes with energy, also the corresponding parametrization in terms of rotation operation changes. In case of the projection to the $p = J_z, q = \gamma$ variables, the classical part is characterized by a rotation by π around the x -axis, R_x^π , while the tunneling path is followed by a rotation about the y -axis. Equivalently, the higher energy path closing around J_z is characterized by a classical path followed by a rotation about J_z and a tunneling path, again parametrized by R_y^π . In the first two rows of Table 11.1 we show both quantization axes and the corresponding parametrization in terms of the rotation operators and the respective permutation-inversion symmetry elements.

For the example of an asymmetric top molecule, this concludes the discussion of parameterizing the paths. We have shown a path to be composed of tunneling and classical parts. It can be represented as a sequence of classical action weights and tunneling and reflection amplitudes. Equivalently, we can follow the paths by applying certain rotations, which are elements of the symmetry group of the respective Hamiltonian. Both ideas are generalizable to other molecular Hamiltonians with different symmetries (see in particular [17] for an example of octahedral symmetry). Furthermore, we are not restricted to the order of approximation in the rotational Energy of (11.18). Any Hamiltonian including angular momentum operators can be translated to a Hamilton function and the respective paths on the rotational energy surface can be generated. In Sect. 11.3.3 we therefore introduce two different approaches for a more precise molecular rotational energy and the respective surface.

However, before improving the accuracy of the rotational energy surface we introduce the quantization method to find rotational energies comparable to full quantum results and experimental findings.

11.3.2 The Quantization Conditions

In the semi-classical approximation of the density of states (11.12), the oscillatory part shows poles at certain energies if the action fulfills particular quantization conditions (cf. Example 11.2). The poles of the symmetry projected version of the density of states therefore indicate the energies of quantum states of a well-defined symmetry. To find these poles, we can now rewrite the symmetry projected density of states in terms of the parametrized paths of the previous section (cf. (14) of [17])

Table 11.1 The parametrization of real (ω) and tunneling (τ) path in terms of the symmetry operations of $C_{2v}(M)$ and the related quantization conditions for the different quantization axes and symmetry species. To fulfill the conditions, they have to be zero for $n \in \mathbb{Z}$. The table is reproduced from [16]

	J_x -quantization	J_z -quantization
ω	$(12)^* \hat{=} R_x^\pi$	$E^* \hat{=} R_z^\pi$
τ	$(12) \hat{=} R_y^\pi$	$(12) \hat{=} R_y^\pi$
A_1	$\delta + S - (-1)^J \tan^{-1} e^{\tilde{S}_E} - 2n\pi$	$\delta + S - (-1)^J \tan^{-1} e^{\tilde{S}_E} - 2n\pi$
A_2	$\delta + S - (-1)^J \tan^{-1} e^{\tilde{S}_E} - (2n+1)\pi$	$\delta + S - (-1)^J \tan^{-1} e^{\tilde{S}_E} - (2n+1)\pi$
B_1	$\delta + S + (-1)^J \tan^{-1} e^{\tilde{S}_E} - 2n\pi$	$\delta + S + (-1)^J \tan^{-1} e^{\tilde{S}_E} - (2n+1)\pi$
B_2	$\delta + S + (-1)^J \tan^{-1} e^{\tilde{S}_E} - (2n+1)\pi$	$\delta + S + (-1)^J \tan^{-1} e^{\tilde{S}_E} - 2n\pi$

$$\rho_{\text{osc}}(E) \simeq \text{Re} \frac{d_m}{|G|} \sum_{n=0}^{\infty} \sum_{a_i=1}^{\infty} \sum_{a_n=0}^{\infty} \chi(\omega^{a_0} \tau \omega^{a_1} \cdots \tau \omega^{a_n}) r^{-n} t^n (re^{iS_E})^{a_0+\cdots+a_n}, \quad (11.22)$$

where $0 \leq i < n$ and $\omega(\tau)$ represent the symmetry operation for the classical (tunneling) path respectively. A thorough discussion of this formula and the slight differences to (11.14) has been done in [17, 139, 154].

However, the sums over n and the a_i are geometric series leading to the simpler formula (cf. (15) of [17]):

$$\rho_{\text{osc}}(E) \propto \frac{d_m}{|G|} \text{tr} \left\{ (e^{-iS_E} D_m^\dagger(\omega) - r \mathbb{1}_m - t D_m(\tau))^{-1} \cdot e^{iS_E} D_m(\omega) \right\},$$

where the $D_m(\kappa)$ are the representation matrices of the m th irreducible representation for the symmetry element $\kappa = \omega, \tau$. For convenience, we included $\mathbb{1}$ as the identity matrix of dimension d_m . The density of states in this semi-classical approximation, where the tunneling paths are particularly included therefore has poles at

$$\det(e^{-iS_E} D_m^\dagger(\omega) - r \mathbb{1}_m - t D_m(\tau)) = 0. \quad (11.23)$$

In the case of the $C_{2v}(M)$ symmetry of an asymmetric top molecule, the irreducible representations are all one-dimensional and the respective ω and τ parametrization leads to the quantization conditions shown in Table 11.1. The respective irreducible representations are shown in Table 11.2. Notice the general validity of the above quantization condition: It depends neither on the form of the model Hamiltonian nor on the symmetry group. The only assumption is that the symmetry group is finite and therefore the real and tunneling paths can be parametrized in a finite number of symmetry elements.

Conclusively, we found rather easy formulas for determining semi-classical energies for the different symmetry species of the $C_{2v}(M)$ symmetry group for an asymmetric rotor described by an Hamilton function H_J , see (11.18). The energies depend

Table 11.2 Character table of $C_{2v}(M)$ including the equivalent rotations for the choice of the z -axis to be the axis of largest moment of inertia (III^r convention)

$C_{2v}(M)$	E	(12)	$(E)^*$	$(12)^*$
	R_0	R_x^π	R_z^π	R_y^π
A_1	1	1	1	1
A_2	1	1	-1	-1
B_1	1	-1	-1	1
B_2	1	-1	1	-1

in particular on the chosen quantization axis, which is defined by the separatrix energy $E_{\text{sep}} = BJ(J + 1)$. For $E < E_{\text{sep}}$ the J_x quantization is appropriate, whereas the J_z axis is used for $E > E_{\text{sep}}$. The found energies compare very favorably to the full quantum calculations for an easy Hamiltonian as the asymmetric top rotor Hamiltonian used here. A comparison is shown in Fig. 11.5; the deviation of the semi-classical values from those of the quantum calculation is of the order of a few wave numbers and is largest close to E_{sep} . The symmetry species are also consistently calculated by both methods. Indeed, the computing time is not yet an argument for using the semi-classical approach, nevertheless, it provides an alternative and rather accurate method to determine energy levels of an asymmetric top molecule. In addition, it allows for an interpretation in terms of a classical rotation path since each energy can unambiguously assigned to a single path on the rotational energy surface (see Fig. 11.2).

However, up to this point, the presented approach is almost identical to the one, the authors of [17, 136, 138] used about 25 years ago. In the next section, we therefore extend this approach to a more accurate version, where essentially the construction of the rotational energy surface is improved.

11.3.3 Two Approaches to Generate the Rotational Energy Surface

In this section we introduce two distinct methods to generate the rotational energy surface which is the essential element of the semi-classical method described previously. The first method uses a perturbative treatment of the non-rigidity influence on the rotational energy (see, e.g., textbooks like [26]). It separately describes the rotational energy for each vibrational state in an effective Hamiltonian, [33] expressed as a power series in the angular momentum operators. It is predominantly used to determine centrifugal distortion constants, i.e. the expansion coefficients of the Taylor-like series. Conventionally, these constants are found by least-squares fitting to experimental spectroscopic data and are subsequently used for predictions of state-to-state transitions in other spectral regions. However, an extrapolation to very high rota-

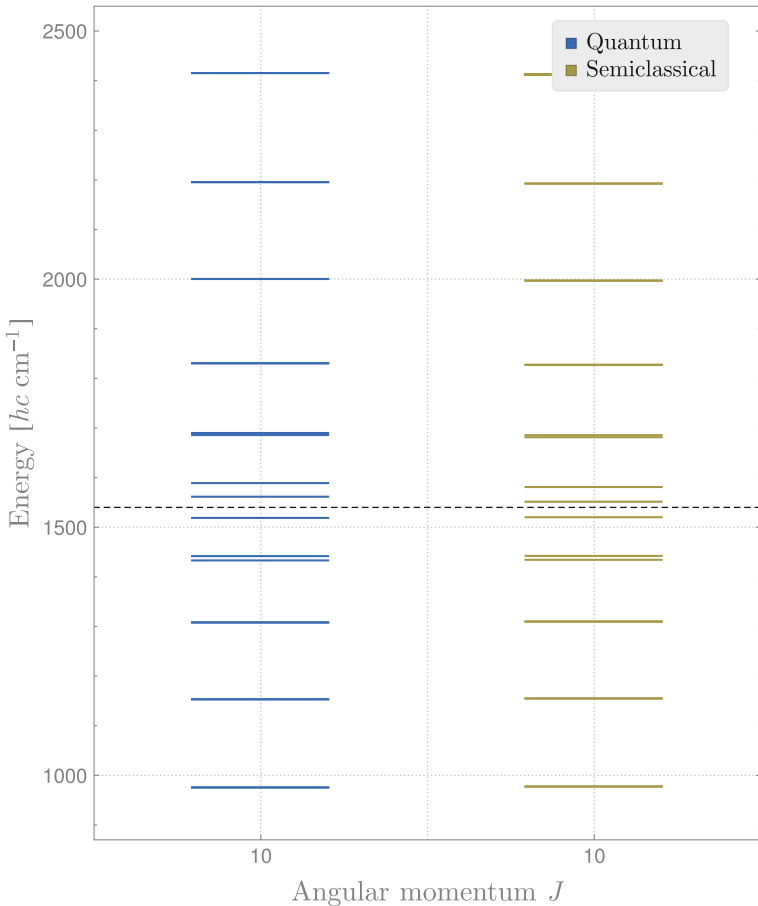


Fig. 11.5 Comparison of full quantum mechanical solution of the rotational problem for an asymmetric rotor with rotational constants as in Fig. 11.2 to the semi-classical energies found by using the quantization conditions of Table 11.1. For convenience, we show both separated although they are calculated at the same angular momentum quantum number. The *dashed line* indicates E_{sep} , the energy at which the quantization axis changes

tional excitation is intrinsically problematic since higher-order angular momentum operators become increasingly important.

In contrast to that, the variational approach, as implemented in, e.g., the program TROVE [34], is in general applicable to any excitation. It relies on ab-initio or spectroscopically refined potential energy surfaces and solves the total ro-vibrational Schrödinger equation by diagonalizing the appropriate Hamiltonian matrix using a proper ro-vibrational basis set. Recent developments have shown the variational approach to reach high-resolution spectroscopic accuracy [34, 116, 119, 147, 148]. However, for highly excited states, the basis set size is the crucial limiting factor.

Different techniques have been used to reduce the basis set size [34, 116–120], but still the computation time and storage capacity remains a formidable factor in calculations of highly excited molecular states.

In using the semi-classical approach for the molecular rotation, computation time is reduced by factors: In the full variational treatment, calculations for the rotational states scale with $(2J + 1)^3$, whereas the semi-classical computation time is (almost) linear in J .

The starting point for applying the semi-classical approach is the generation of the rotational energy surface. In the Watson Hamiltonian it is defined by substituting the angular momentum operators by their classical analogues of (11.19). After fixing the quantization axes, we can implement a numerical routine to find the energies meeting the quantization conditions (see Fig. 11.6).¹ Note that this is not restricted to any molecular symmetry or structure. For the use of the variational approach, we also substitute the angular momentum operators with their classical analogues in the full ro-vibrational Hamiltonian. For a certain choice of quantization axis, the vibrational Schrödinger equation is solved on a grid of (p, q) points respectively. This actually retains a fully quantum mechanical solution of the vibrational problem for each point in rotational phase space. With a suitable vibrational basis set, TROVE therefore provides proper rotational energy surfaces for several vibrational states. Notice that one drawback of using this grid-based procedure is the (yet) unknown dependence on the grid fineness and the prior choice of the quantization axis. Regarding computation time, generating the rotational energy surface in the Watson-type approach indeed is negligible. In the TROVE approach, it depends mostly on the efficiency of the vibrational calculations. However it is not limited by the amount of available spectroscopic data and is able to cover different vibrational modes at once.

In conclusion, we have formulated a semi-classical model for molecular rotation, which is – inspired by works done about 20 years ago – attached to the modern variational approach to quantum mechanical models. The semi-classical method is based on a path-integral formalism, where the density of states exhibit quantized energies, if the paths fulfill certain quantization conditions calculated from the rotational energy surface. Thus, the essential ingredient is the rotational energy surface which can be calculated quantum mechanically by the TROVE program. An alternative approach to define the rotational energy surface utilizes the effective Hamiltonian approach to molecular rotation, using spectroscopically determined constants.

With both approaches, the resulting quantized energies can be compared to full quantum calculations (Fig. 11.5). One major benefit is that the computing time of the semi-classical approach does depend only linearly on the angular momentum quantum number. This, and the intrinsic assumption of classical dynamics to dominate at large J quantum numbers, renders this approach in particular important for studying

¹We include the code of the routine in the electronic version of this work. In order to be fully transparent, we include also the TROVE-generated files of the rotational energy surfaces used in Chap. 12.

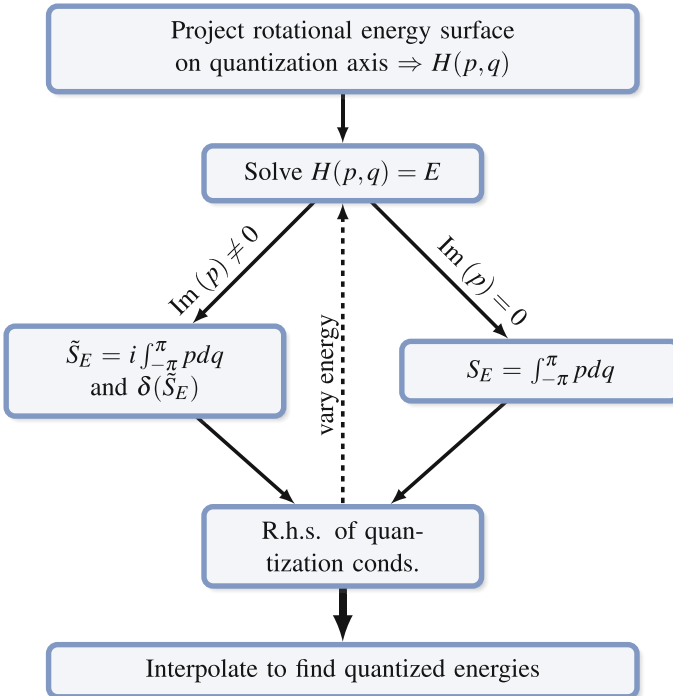


Fig. 11.6 Schematic view on the numerical approach to find the quantized energies using the semi-classical method described in the text. A very similar scheme is used also for attaching it to the TROVE program. The quantization conditions are given in Table 11.1

high-lying rotational excitations. In the next chapter, we will use this approach for a proof-of-principle study, namely by applying it to the sulfur dioxide molecule. Furthermore, an outlook on possible improvements especially in the attachment to the TROVE routine is also made at the end of the following chapter.

Chapter 12

Application to Sulfur Dioxide

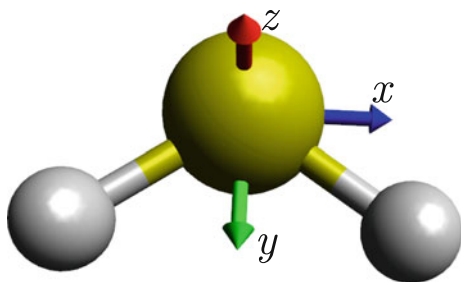
Abstract A first proof-of-principle example for the semi-classical calculations of highly excited rotational levels is shown in this chapter. In particular, the sulfur dioxide molecule is used since it has been already described extensively in the literature and also states of large angular momentum quantum numbers J are well-known. The comparison of the semi-classical treatment to the full quantum mechanical values for $J > 40$ shows a good agreement. Also calculations for excited vibrational states, where the variational approach is used to calculate the rotational energy surface, are shown to be possible with the semi-classical method.

12.1 The Molecule

In order to demonstrate the applicability of the semi-classical method developed in Chap. 11, we apply it to a test molecule which fulfills certain requirements: (i) It does not exhibit any rotational clustering, i.e. the topology of the rotational energy surface should not vary considerably for any value of the angular momentum; (ii) There are enough experimental data available up to a large angular momentum quantum numbers; (iii) Variational calculations have been performed, in particular for vibrationally excited states, s.t. we can test the semi-classical approach also for those states. These requirements are chosen in order to render the semi-classical calculations comparable to full quantum computations. They are no generic restrictions of the approach.

One molecule meeting these demands is sulfur dioxide, SO_2 (see Fig. 12.1). By using terahertz spectroscopy, pure rotational transitions have been studied for the vibrational ground state up to transitions involving $J = 92$ and for the first excited bend vibrational state up to $J = 81$ [161]. In particular, the spectroscopic parameters have been fitted and can be used for the effective Hamiltonian approach. In [162], the variational approach including a purely ab-initio potential energy surface has been shown to reproduce the experimental data up to $J = 80$ for the ground vibrational state with a root-mean-square error of less than 0.02 cm^{-1} . This approach can then be used to determine also excited vibrational states without the necessity to fit new spectroscopic constants.

Fig. 12.1 The equilibrium structure of sulfur dioxide with an attached molecule-fixed coordinate system (xyz) which also define the axes of rotations used for the semi-classical approach described in the text. The figure is reproduced after [16]



Sulfur dioxide, despite being of fundamental importance as a small asymmetric molecule, is found in various surroundings, ranging from the interstellar medium to earths atmosphere, where it is believed to be an important pollutant. In the former, SO₂ is observed with high column densities in particular in star-forming regions, and is thought to act as a molecular coolant [161]. For the present study, a discussion of its importance or role in any of these surroundings is beyond the scope, our goal is to use the semi-classical approach to find the energies of highly excited rotational states and to compare them to the previous theoretical work. The used spectroscopic data can be found in the Cologne Database for Molecular Spectroscopy [163] and the according spectroscopic constants are listed in [161].

Conceptually, sulfur dioxide is described as an asymmetric rotor with $3N - 6 = 3$ vibrational modes. They are usually separated into a symmetric and an anti-symmetric stretching mode and an additional bending one. We will show calculations for the ground vibrational state and the first excited state of the bending vibration, called ν_2 in the following. The zero-point energy is calculated to be $E_0 = 1535.633 \text{ cm}^{-1}$, whereas the $\nu_2, J = 0$ level is at $E_{\nu_2} = 517.9 \text{ cm}^{-1}$ above the ground state [161, 162]. The molecular symmetry group is $C_{2v}(M)$ and according to Fermi–Dirac statistics for the nuclear spins, levels of B_1 and B_2 symmetry are forbidden [14]. In the following, we nevertheless calculate all molecular symmetry species, i.e. we ignore the restrictions from Pauli’s exclusion principle for the moment.

12.2 The Comparison

As already indicated in the previous chapter, applying the semi-classical approach to molecules described by a Watson-type Hamiltonian, starts by substituting the angular momentum operators ($\hat{J}_x, \hat{J}_y, \hat{J}_z$) by their classical analogues while fixing the length to the quantized value $|J| = \sqrt{J(J+1)}$. We choose $J = 40$, which is relatively large but still in a very well-described range of quantum mechanical approaches. The rotational energy surface is hence defined by the spectroscopic constants $A, B, C, \Delta_K, \Delta_J, \dots$ and the total angular momentum $J = 40$. To find the quantized energies, we project the respective rotational energy surface onto the two axes identical to those of the rigid asymmetric top in the previous chapter. Subsequently, we numerically solve the

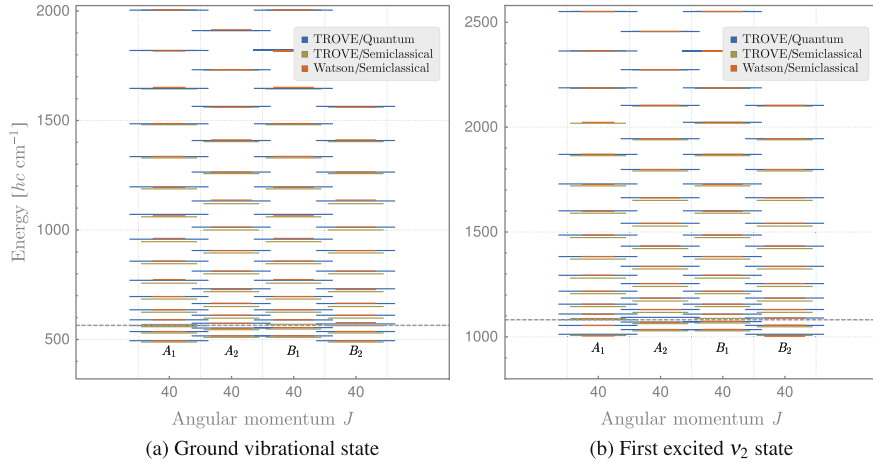


Fig. 12.2 Graphical comparison of the semi-classical approach to exact quantum calculations for two different vibrational states. For convenience the energy range covers only a fraction of the total energy range of the $J = 40$ states. In order to show the different symmetry species, we show them separated at one common angular momentum quantum number. The *dashed line* indicates the change of the quantization axis in both calculations respectively. The graphics is reproduced from [16]

equation $H(p, q) = E$ for a number of energies, ranging from $E_{\max} = CJ(J + 1)$ to $E_{\min} = AJ(J + 1)$, and calculate the respective action between the classical turning points, where $p = 0$. In particular, we include the imaginary solutions to define tunneling paths and their respective action (see Fig. 11.6). With this, the quantization conditions of Table 11.1 can be checked by interpolating between the calculated energies. The results are shown in Table 12.1 and Fig. 12.2.

These comparisons show a very good agreement with the pure quantum calculations provided by TROVE [164]. The root-mean-square deviation $RMS = \sqrt{\frac{1}{n} \sum_{i=1}^n (E_i^{SC} - E_i^{QM})^2}$ for the different symmetry species is in the range of a few wave numbers (Table 12.2). To compare how these residuals depend on the angular momentum quantum number, we calculated in addition the relative root-mean-square deviation, defined as

$$\text{relRMS} = \sqrt{\frac{1}{n} \sum_{i=1}^n ((E_i^{SC} - E_i^{QM})/E_i^{SC})^2}.$$

As shown in Fig. 12.3, this value shows the expected behavior, namely it decreases with increasing angular momentum.

With this, we showed the semi-classical approach to be a very suitable tool if applied to the effective Hamiltonian approach. However, it depends strongly on the accuracy of the experimentally determined spectroscopic constants. In the case of

Table 12.1 The A_1 rotational ($J = 40$) energies for SO_2 as calculated by a fully quantum method [162] and the semi-classical approach using the effective Hamiltonian approach with constants of [161] or the TROVE approach. The other symmetry species show very similar deviations or accuracies and are plotted in Fig. 12.2. All values are shown in [cm^{-1}]

Full quantum	Watson/Semi-classical	TROVE/Semi-classical
492.665	492.477	497.46
534.347	534.472	538.635
561.866	562.301	567.493
588.094	588.549	577.894
633.885	634.531	633.777
694.372	694.299	693.862
768.512	771.893	766.469
855.947	856.087	855.265
956.406	960.039	955.774
1069.64	1063.12	1069.52
1195.39	1192.72	1197.11
1333.4	1334.34	1338.43
1483.4	1484.53	1490.16
1645.1	1649.85	1653.48
1818.22	1815.77	1829.28
2002.47	2003.78	2013.95
2197.57	2194.87	2210.2
2403.22	2405.05	2418.02
2619.32	2621.26	2635.03
2845.03	2844.29	2861.21
3081.59	3081.85	3091.12

the well-studied SO_2 molecule, this accuracy is very high and therefore the effective approach very successful. Nevertheless, in order to apply the semi-classical method to molecules that are less well-known, we now turn to the discussion of the attachment to the TROVE approach.

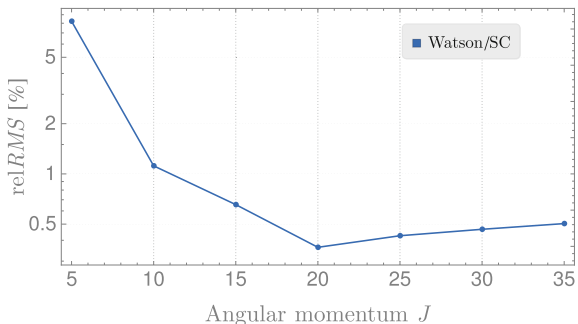
The TROVE/Semi-classical approach. The TROVE routine generates, if changed accordingly, a rotational energy surface for each angular momentum and vibrational quantum number. Hence, the generation is independent on any measured spectroscopic constants but uses ab-initio calculations.¹ Since we already know the two projection axes, we can let TROVE calculate the rotational energy surface on a grid of (p, q) for both projections. This defines the action integrals and we can – as in the effective Hamiltonian approach – check the quantization conditions by interpolating the respective functions between different energies. This interpolation is used

¹ Actually, the ab-initio potential energy surfaces are mostly refined by using measured spectra, but nevertheless do not principally depend on experiments.

Table 12.2 Root-mean-square deviation of the different semi-classical calculations to the exact quantum values. The last column, marked with an asterisk, was calculated by referencing the semi-classical energies to the exact quantum calculations of the ground state

State	Symmetry	Watson/SC [cm ⁻¹]	TROVE/SC [cm ⁻¹]	TROVE/SC* [cm ⁻¹]
GS	A_1	2.4	7.5	
	A_2	2.7	8.6	
	B_1	2.5	8.2	
	B_2	3.0	8.5	
ν_2	A_1	2.6	8.1	0.6
	A_2	0.8	8.9	0.5
	B_1	1.3	8.5	0.5
	B_2	2.0	8.8	0.5

Fig. 12.3 Relative root-mean-square deviation of the Watson/Semi-classical approach for different angular momentum quantum numbers in the vibrational ground state of SO₂



to smoothen the grid calculations and to avoid a too strong dependence of the results on the grid's fineness.

With this procedure, the ground vibrational state energies can be straightforwardly calculated. For the excited vibrational state ν_2 , the TROVE generated rotational energy surface is defined relative to the vibrational ground state. Hence, calculating the energies on that surface produces relative energy values. By relating them to their semi-classical analogues in the ground state, full semi-classical results are obtained. However, by relating them to quantum calculations of the ground state, the accuracy of the ν_2 states is heavily enhanced. The root-mean-square deviation to exact quantum calculations of the vibrational excited then reduces to below 1 cm⁻¹ (see Table 12.2). In Fig. 12.4 we show the absolute deviations for the different vibrational states compared to the Watson-type approach.

One clear indication of the dependence of the vibrational excited semi-classical rotational energies to them in the ground state is the similar shape of the respective deviation. This obviously induces the correction by the quantum values to lead to much more accurate results in the excited states.

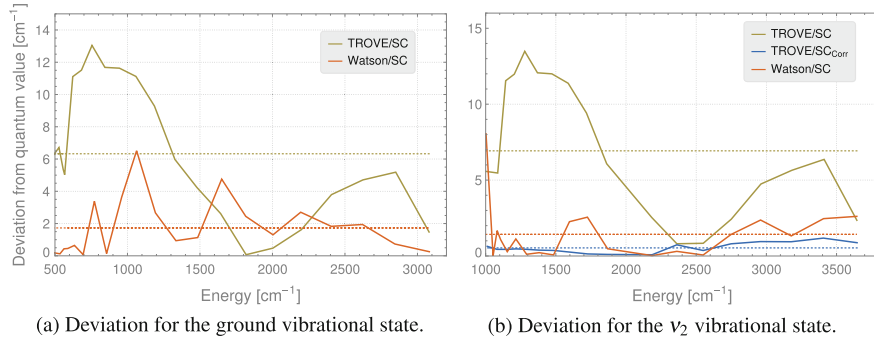


Fig. 12.4 Absolute deviation of the different methods for calculating the semi-classical energies for $J = 40$ and symmetry A_1 in the vibrational ground state and the first excited v_2 level. The TROVE/SC_{Corr} levels are further explained in the text, they are corrected by the exact quantum values of the ground state. The *dashed lines* are the mean deviation. Figure 12.4a is reproduced after [16]

In conclusion, the TROVE method to generate the rotational energy surface and the corresponding semi-classical energies are shown to have a similar level of agreement as the Watson-type approach. This is true also for the vibrationally excited state, where the effective Hamiltonian method needs to fit new spectroscopic constants. Therefore, the attachment of the semi-classical method to the TROVE program seems to be very promising and further studies are expected to show more accurate results.

Chapter 13

Discussion

Abstract In this chapter, the semi-classical approach to rotational dynamics in small molecules is shortly discussed. In particular, the application to the TROVE variational approach to calculate the rotational energy surface is considered and improvements and generalizations are discussed.

13.1 The TROVE - Generated Rotational Energy Surface

In the preceding chapter we showed the effective Hamiltonian approach to very successfully predict energy levels also if the Hamiltonian is changed into a Hamilton function by substituting the angular momentum operators by their classical counterparts. We argued that this Watson-type method is limited by the available spectroscopic data and hence a semi-classical method relying on ab-initio calculations is favored especially for molecules where experiments are not yet done as accurately as for our test molecule sulfur dioxide. One such model using an ab-initio potential energy surface is the TROVE program [34], which we used to generate rotational energy surfaces by solving the vibrational problem in a fully quantum manner. This is one of the main new features of our approach: The rotational energy surface is generated using a fully quantum treatment of the underlying vibrations. To the best of our knowledge, this has not been done before. We showed the results of the quantized semi-classical rotational energies to be comparable to the exact quantum values with deviations of a few wave numbers. One major benefit of using the variational approach of TROVE is that calculations for higher excited vibrational states do neither require any new measurements nor new effective spectroscopic parameters as in the case of the Watson-type approach. Furthermore, the application to more exotic molecules is possible within the TROVE approach, whereas spectroscopic constants are most likely not very well-defined for molecules with, e.g., large ro-vibrational couplings or non-rigidities.

Technically, the TROVE generated rotational energy surface of the excited ν_2 state depend particularly on the energies of the ground state calculations. In a fully self-consistent semi-classical approach we therefore corrected the quantized energy levels of the ν_2 states by their semi-classical counterparts in the ground state. Comparing

the v_2 rotational levels to the exact quantum levels now show a very similar deviation scheme as the ground state ones. Correcting the vibrationally excited states by their quantum counterparts in the vibrational ground state therefore removes this error propagation and the results are of exceptional accuracy. At this point, further studies are needed: Is this result reproducible also for other vibrationally excited states? Is there a reason for this behavior already in the generation of the rotational energy surface in the TROVE program? How about very-large-angular-momentum states?

The latter point refers to the very start of the discussion on ultrafast rotations: Is it possible to use this semi-classical approach, if attached to the variational method of TROVE, to predict the rotational levels of large J quantum numbers? In principle we showed that indeed it is possible to reproduce – up to a few wave numbers – exact quantum results. This should be true also for much higher J . In using the exact energies of the vibrational ground state as reference for vibrationally excited states, it is even possible to reach better accuracies, but this could not always be feasible since for higher J , the ground state levels are almost as computationally problematic as they are for excited states. Thus, the self-consistent semi-classical method should in principle be the better choice if one reaches angular momentum quantum numbers that have not been characterized in the ground state.

Technically, the results can be improved by refining the grid in the TROVE calculations. The exact dependence of the energies on this grid fineness has not yet been studied in much detail. First results on that suggests no significant influence of refining the grid. Most likely, the interpolation in the numerical semi-classical routine is sufficient to compensate grid effects to certain level.

Conclusively, a more thorough understanding of the generation of the rotational energy surface in the variational approach is needed to complete the present study of applying the semi-classical quantization method to molecules with large angular momentum quantum numbers. The current approach is only a first step towards a faster but still accurate calculation of ultrafast rotational states. We have shown a prototypical example of a rather simple molecule, where the rotational dynamics is – at least in the vibrational ground state – very straightforward. Hence, in a next step one would need to include molecules, where the rotational dynamics is more challenging to describe, e.g., where rotational clustering appears.

13.2 Generalization of the Approach

The rotational clustering phenomenon is the first on the list of generalizations of the semi-classical approach. As angular momentum (or vibrational excitation) increases, the rotational energy surface can change topologically. This possibly leads to a redefinition of the quantization axes and the according (p, q) pair of classical variables in the semi-classical calculations. The respective axes are defined by the global minima or maxima on the (non-projected) rotational energy surface and hence we think a numerical identification in the process of generating the projected rotational energy surface is needed. In the Watson-type approach, this can easily be implemented, while

the TROVE calculations yet rely on an initial choice of the according axes. However, there seems to be no principal reason for this being impracticable to implement also in the variational method.

Another next step is to consider transitions of states from one path to another on a single or even between different rotational energy surfaces. With this, electromagnetic transition intensities could be calculated essential for the comparison with experiments.

A further generalization is the inclusion of different rotational energy surfaces: If rotational and vibrational degrees of freedom are non-separable by means of strong coupling [165], including the vibrational influence on the particular rotation could be used to define a multidimensional surface. Since the trace formula of Gutzwiller (11.11) is valid for any dimension and chaos theory in particular deals with higher-dimensional versions of it [151], it could still be used to define quantization conditions. Furthermore, the parametrization of the paths should still be possible in terms of symmetry elements, since they remain valid also if rotations and vibrations are not separable. Actually, a first step towards the inclusion of vibrations could be to couple the rotational energy surfaces calculated individually for distinct vibrational states by defining a, say, rotational energy multi-surface, where J is still constant and the respective surfaces are straightforwardly superimposed. This would not increase the dimensionality but implies a change of the shape of the surface. However, if the change between surfaces of distinct vibrational states is also done in a semi-classical way, the degrees of freedom are increased. Thus, transitions between the different surfaces could then be treated as an additional dimension and again tunneling and classical paths could be identified leading to the necessity of reconsidering the whole semi-classical procedure. A first step on this route would be to calculate first distinct rotational energy surfaces for distinct, but energetically comparable, vibrational energy states. These distinct surfaces potentially interact in some way if the vibrational states are coupled which would lead to properties like avoided crossings. In non-interacting vibrational states, however, the surfaces may penetrate each other. These two different situations have to be studied in detail in the future, especially by focussing on their implication on the rotational energy states. In a next step, the higher-dimensional surfaces, where the interaction is treated in a more implicite way, could lead to an even better understanding of the ro-vibrational coupling at large angular momentum.

Finally, the semi-classical method has been shown to be able to predict quantized rotational energy levels at high rotational quantum numbers with an accuracy of a few wave numbers which is encouraging for further studies. In addition, the semi-classical approach depicts a rather intuitive model since it relies on classical dynamics: The paths correlated to the quantized energies all can be represented on the rotational energy surface and hence can be interpreted as classical rotations. Therefore, this model not only reduces computation time but also allows for a very convenient interpretation of molecular dynamics at large angular momentum.

Chapter 14

New Ideas for Solving Old Problems – A Conclusion

Abstract This chapter concludes the book. A brief description of the results and the open questions is done and future studies are anticipated.

Modern spectroscopy investigates molecules with incredible accuracy. For example, state-resolved collision spectroscopy as well as the study of ultrafast rotational dynamics has become possible due to advanced experimental techniques developed in the last few decades. Furthermore, action spectroscopy has unraveled parts of the dynamics of the “enfant terrible” ([3], p. 1) protonated methane, a prototypical example of a simple molecule where even the usually well-understood, ro-vibrational dynamics in the ground vibrational state are not describable in terms of traditional models.

As well as experiments are always trying to recover theoretical predictions, they also attempt to push these theories to their limits when it comes to explaining the according experimental results. Especially in the example of protonated methane, the experiments were done with astonishing accuracy, while it was assumed that “theoretical understanding [...] will take at least a few more decades” ([3], p. 1). In all three parts of this work we tried to overcome the barriers of traditional theory by using new ideas especially on symmetry aspects of the respective models.

In Part I we used group theory for symmetry considerations of the nuclear spin wave function of molecules. In particular, we identified the unitary symmetry group for the nuclear spin angular momentum as one of the symmetries of the wave function. It is intimately connected to the usual permutation symmetry of identical nuclei. Their correlation is formulated in the mathematical Schur–Weyl theorem. It provides a one-to-one correspondence of the irreducible representations of the nuclear permutation symmetry group and those of the unitary spin angular momentum group. Using the ingenious Young diagrammatic technique, the Schur–Weyl theorem can also be used to simplify the calculations of nuclear spin statistical weights especially in larger molecules and nuclei with arbitrary individual spins. In addition, we proposed the first steps towards a statistical approach for state-to-state reaction rates in certain reactive collisions. We showed them to depend in particular on the symmetry group of the intermediately formed complex and showed how state-resolving experiments of such reactions could help in understanding possible dynamical processes in this complex.

Even though the statistical method does not include any energetic treatment of the reaction, first indications for experiments were found and some selection rules were formulated rigorously for a number of examples. We noticed the unitary symmetry group of the nuclear spin to induce certain such rules which are entirely different from more traditional theories, where the standard spatial rotation group is assumed as the symmetry of nuclear spins. Also here, state-resolved experiments are now required to check the selection rules.

In the second part, we showed the extremely floppy molecules to be pathological examples of molecular theory, where traditional approaches reach their absolute limits. The customary idea of a fixed geometric equilibrium structure cannot be established and hence all traditional approaches encounter serious problems. In these molecules, the internal and overall rotations are indistinguishable which we use as a starting point for developing a fundamentally new theory for the ro-vibrational dynamics in this class of molecules. The respective degrees of freedom are now distinguished into 3 translational, $3N - 8$ vibrational, and five generalized rotational ones. The latter are used to establish a super-rotor model, where the two internal rotation degrees of freedom and the usual three overall ones are treated collectively. Even though the complexity of traditional models of internal rotations increase strongly with the inclusion of the overall motion, our combined treatment provides a simple analytic energy expression. More astonishingly, the energy depends – as a zero-order approximation – on only one free parameter. In addition, the super-rotor model also overcomes certain symmetry related limits of traditional theories. We have shown the group of five identical particles to be indescribable in terms of equivalent three-dimensional rotations. However, with the five super-rotation degrees of freedom, we are now able to find such equivalent rotations and to label the super-rotor states also in this particular finite symmetry group.

As a first application, we explicitly show the protonated methane molecule to be described within the super-rotor model. It actually is the prototype of extreme floppiness, and a large variety of previous approaches have been unsuccessful to comprehensively explain the recent experimental results of [4]. With only one free parameter, the super-rotor model agrees very favorably with the low-energy states found in these experiments. We were able to assign the levels and to fit the parameter, obtaining a value in good agreement with ab-initio theory, where the parameter was originally thought to be the conventional rotational constant of an almost spherical CH_5^+ molecule.

With the introduction of a completely new model for the dynamics of extremely floppy molecules, we showed a number of open questions to arise. By refining the model in terms of including couplings, higher order terms, etc., we hope to answer these questions and render it applicable also to various types of other examples of this extraordinary class of molecules. In conclusion, the super-rotor implies a fundamentally new view on the ro-vibrational dynamics in floppy molecules.

In the last part, we showed how path-integral based semi-classical methods help in understanding and predicting rotational dynamics at high speed. Also there, conventional methods tend to reach certain limits due to the huge number of involved quantum states. Starting from a so-called rotational energy surface, on which a classical

rotation is described, we were able to refine ideas from the 1990s and to numerically determine (quantized) rotational energy levels for a test-molecule. These energies correspond to certain paths on the surface and are defined by symmetry. The rotational energy surface, however, is usually defined by spectroscopic constants, whereas we showed the use of a variational approach to the vibrational part of the molecular Schrödinger equation to be possibly more accurate and more reliable. Once again, a number of questions are still unsolved also regarding this semi-classical approach, but the results, especially – as expected – for high energies, are very encouraging to further develop this method.

In all three parts, the combining element is the use of fundamental symmetry principles to overcome limits of traditional molecular theory. This is encouraging for future studies since still the potential of applying the rich variety of mathematical results on symmetry groups to the problems of molecular physics and chemistry is far from being exhausted. We hope to initiate further studies on all the different subjects of this work certainly revealing new problems but also most likely solving some old ones.

References

1. M. Quack, F. Merkt (eds.), *Handbook of High-resolution Spectroscopy* (Wiley, 2011). doi:[10.1002/9780470749593](https://doi.org/10.1002/9780470749593)
2. O. Asvany, S. Brünken, L. Kluge, S. Schlemmer, Appl. Phy. B **114**(1–2), 203 (2013). doi:[10.1007/s00340-013-5684-y](https://doi.org/10.1007/s00340-013-5684-y)
3. T. Oka, Science **347**(6228), 1313 (2015). doi:[10.1126/science.aaa6935](https://doi.org/10.1126/science.aaa6935)
4. O. Asvany, K.M.T. Yamada, S. Brünken, A. Potapov, S. Schlemmer, Science **347**(6228), 1346 (2015). doi:[10.1126/science.aaa3304](https://doi.org/10.1126/science.aaa3304)
5. H. Schmiedt, Molecular symmetry, super-rotation, and semi-classical motion. Ph.D. thesis, University of Cologne (2017)
6. H. Schmiedt, P. Jensen, S. Schlemmer, Chem. Phys. Lett. **672**, 3446 (2017). doi:[10.1016/j.cplett.2017.01.045](https://doi.org/10.1016/j.cplett.2017.01.045)
7. H. Schmiedt, P. Jensen, S. Schlemmer, Phys. Rev. Lett. **117**, 223002 (2016). doi:[10.1103/PhysRevLett.117.223002](https://doi.org/10.1103/PhysRevLett.117.223002)
8. H. Schmiedt, P. Jensen, S. Schlemmer, J. Chem. Phys. **145**(7), 074301 (2016). doi:[10.1063/1.4960956](https://doi.org/10.1063/1.4960956)
9. H. Schmiedt, S. Schlemmer, P. Jensen, J. Chem. Phys. **143**(15), 154302 (2015). doi:[10.1063/1.4933001](https://doi.org/10.1063/1.4933001)
10. J.C.J. Koelemeij, B. Roth, A. Wicht, I. Ernsting, S. Schiller, Phys. Rev. Lett. **98**(17) (2007). doi:[10.1103/physrevlett.98.173002](https://doi.org/10.1103/physrevlett.98.173002)
11. P. Jusko, O. Asvany, A.C. Wallerstein, S. Brnken, S. Schlemmer, Phys. Rev. Lett. **112**(25) (2014). doi:[10.1103/physrevlett.112.253005](https://doi.org/10.1103/physrevlett.112.253005)
12. J. Cami, J. Bernard-Salas, E. Peeters, S.E. Malek, Science **329**(5996), 11801182 (2010). doi:[10.1126/science.1192035](https://doi.org/10.1126/science.1192035)
13. B. Zuckerman, B.E. Turner, D.R. Johnson, F.J. Lovas, N. Fourikis, P. Palmer, M. Morris, A.E. Lilley, J.A. Ball, F.O. Clark, Astrophys. J. **196**, L99 (1975). doi:[10.1086/181753](https://doi.org/10.1086/181753)
14. P.R. Bunker, P. Jensen, *Molecular Symmetry and Spectroscopy* (NRC Research Press, 2006), <http://books.google.de/books?id=FZEI7VmjNyMC>
15. S. Brackertz. Analyse komplexer Molekülspektren. Diploma thesis, University of Cologne (2016)
16. H. Schmiedt, S. Schlemmer, S.N. Yurchenko, A. Yachmenev, P. Jensen, Phys. Chem. Chem. Phys. **19**(3), 18471856 (2017). doi:[10.1039/c6cp05589c](https://doi.org/10.1039/c6cp05589c)
17. J.M. Robbins, S.C. Creagh, R.G. Littlejohn, Phys. Rev. A **41**(11), 6052 (1990). doi:[10.1103/PhysRevA.41.6052](https://doi.org/10.1103/PhysRevA.41.6052)

18. W. Fulton, J. Harris, Representation theory: a first course, in *Graduate Texts in Mathematics*, vol. 129, 9th edn., (Springer Science + Business Media, New York, 2004)
19. R. Goodman, N.R. Wallach, Symmetry, Representations, and Invariants (Springer, New York (2009). doi:[10.1007/978-0-387-79852-3](https://doi.org/10.1007/978-0-387-79852-3)
20. E.P. Wigner, *Gruppentheorie und ihre Anwendung auf die Quantenmechanik der Atomspektren*. Die Wissenschaft; 85 (Vieweg, Braunschweig, 1931)
21. E.P. Wigner, *Group theory and its application to the quantum mechanics of atomic spectra*, exp. and impr. ed., edn. Pure and applied physics; 5 (Academic Press, New York, 1962)
22. F. Iachello, *Lie Algebras and Applications*, vol. 891, 2nd edn., Lecture Notes in Physics (Springer, Berlin, 2015). doi:[10.1007/978-3-662-44494-8](https://doi.org/10.1007/978-3-662-44494-8)
23. A. Young, *The Collected Papers of Alfred Young: 1873–1940*, vol. 21 (Mathematical Expositions (University of Toronto Press, Toronto, 1977)
24. D.J. Rowe, J.L. Wood, *Foundational Models* (Singapore, Fundamentals of Nuclear Models (World Scientific, 2010)
25. B.G. Wybourne, Int. J. Q. Chem. **7**(6), 1117 (1973). doi:[10.1002/qua.560070608](https://doi.org/10.1002/qua.560070608)
26. W. Gordy, R.L. Cook, *Techniques of Chemistry. Microwave Molecular Spectra* (vol. 18) (Wiley-Interscience, 1984), <http://www.amazon.com/Techniques-Chemistry-Microwave-Molecular-Spectra/dp/0471086819?SubscriptionId=0JYN1NVW651KCA56C102&tag=techkie-20&linkCode=xm2&camp=2025&creative=165953&creativeASIN=0471086819>
27. M. Born, R. Oppenheimer, Annalen der Physik **389**(20), 457484 (1927). doi:[10.1002/andp.19273892002](https://doi.org/10.1002/andp.19273892002)
28. D. Marx, J. Hutter, in *Modern Methods and Algorithms of Quantum Chemistry, NIC*, vol. 1, ed. by J. Grotendorst (John von Neumann Institute for Computing, Jülich, 2000), pp. 301–449
29. X. Wang, T. Carrington, in *AIP Conference Proceedings, Spectroscopy of Molecular Ions in the Laboratory and in Space*, vol. 1642 (Eighteenth International Conference of Computational Methods in Sciences and Engineering, Kos, Greece, 2015), vol. 1642, pp. 336–337. doi:[10.1063/1.4906687](https://doi.org/10.1063/1.4906687)
30. H.C. Longuet-Higgins, Mol. Phys. **6**(5), 445 (1963). doi:[10.1080/00268976300100501](https://doi.org/10.1080/00268976300100501)
31. F. Iachello, F. Pérez-Bernal, P.H. Vaccaro, Chem. Phys. Lett. **375**(3–4), 309 (2003). doi:[10.1016/s0009-2614\(03\)00851-0](https://doi.org/10.1016/s0009-2614(03)00851-0)
32. R.N. Zare, *Angular Momentum: Understanding Spatial Aspects in Chemistry and Physics*. George Fisher Baker non-resident lectureship in chemistry at Cornell University (Wiley, 1988), <http://books.google.de/books?id=kDQ31MBZxioC>
33. J.K.G. Watson, J. Chem. Phys. **46**(5), 1935 (1967). doi:[10.1063/1.1840957](https://doi.org/10.1063/1.1840957)
34. S.N. Yurchenko, W. Thiel, P. Jensen, J. Mol. Spectrosc. **245**(2), 126 (2007). doi:[10.1016/j.jms.2007.07.009](https://doi.org/10.1016/j.jms.2007.07.009), <http://linkinghub.elsevier.com/retrieve/pii/S002228520700207X>
35. X.G. Wang, T. Carrington, J. Chem. Phys. **144**(20), 204304 (2016). doi:[10.1063/1.4948549](https://doi.org/10.1063/1.4948549)
36. O.L. Polyansky, Science **277**(5324), 346 (1997). doi:[10.1126/science.277.5324.346](https://doi.org/10.1126/science.277.5324.346)
37. S. Schlemmer, H. Mutschke, T. Giesen, C. Jäger (eds.), *Laboratory Astrochemistry* (Wiley-VCH Verlag GmbH & Co. KGaA, Weinheim, Germany, 2014). doi:[10.1002/9783527653133](https://doi.org/10.1002/9783527653133)
38. B.G. Wybourne, *Classical Groups for physicists* (Wiley, New York, 1974)
39. J. Parkinson, D.J.J. Farnell, *An Introduction to Quantum Spin Systems*, vol. 816, Lecture Notes in Physics (Springer, Berlin, 2010). doi:[10.1007/978-3-642-13290-2](https://doi.org/10.1007/978-3-642-13290-2)
40. W. Pauli, Z. Physik **31**(1), 765 (1925). doi:[10.1007/bf02980631](https://doi.org/10.1007/bf02980631)
41. P.A.M. Dirac, Proc. R. Soc. A: Math. Phys. Eng. Sci. **112**(762), 661 (1926). doi:[10.1098/rspa.1926.0133](https://doi.org/10.1098/rspa.1926.0133)
42. E. Bartholomé, Berichte der Bunsengesellschaft für physikalische Chemie **41**(11), 812 (1935). doi:[10.1002/bbpc.19350411130](https://doi.org/10.1002/bbpc.19350411130)
43. M. Quack, Mol. Phys. **34**(2), 477 (1977). doi:[10.1080/00268977700101861](https://doi.org/10.1080/00268977700101861)
44. T. Oka, J. Mol. Spectrosc. **228**(2 SPEC. ISS.), 635 (2004). doi:[10.1016/j.jms.2004.08.015](https://doi.org/10.1016/j.jms.2004.08.015)
45. E. Hugo, The H_3^+ +H₂ isotopic system Origin of deuterium astrochemistry. Ph.D. thesis, Universität zu Köln (2008)
46. I. Schur, Ueber eine Klasse von Matrizen, die sich einer gegebenen Matrix zuordnen lassen. Ph.D. thesis, Friedrichs-Wilhelms-Universität zu Berlin (1901)

47. H. Weyl, *The Classical Groups: Their Invariants and Representations*, vol. 1. Princeton Mathematical Series, 2nd edn. (Princeton University Press, Princeton, 1946)
48. D.J. Rowe, M.J. Carvalho, J. Repka, Rev. Mod. Phys. **84**(2), 711 (2012). doi:[10.1103/revmodphys.84.711](https://doi.org/10.1103/revmodphys.84.711)
49. A. Savage, *Geometric Representation Theory and Extended Affine Lie Algebras*. (American Mathematical Society, 2011), <http://bookstore.ams.org/fic-59>
50. B.G. Wybourne, Euromath Bull. **2**, 145 (1996), <http://www.fizyka.umk.pl/~bgw/schur.pdf>
51. M.A. Caprio, K.D. Sviratcheva, A.E. McCoy, J. Math. Phys. **51**(9) (2010). doi:[10.1063/1.3445529](https://doi.org/10.1063/1.3445529)
52. D.E. Littlewood, A.R. Richardson, Philos. Trans. R. Soc. A: Math. Phys. Eng. Sci. **233**(721–730), 99 (1934). doi:[10.1098/rsta.1934.0015](https://doi.org/10.1098/rsta.1934.0015)
53. J.S. Frame, G.d.B. Robinson, R.M. Thrall, Canad. J. Math. **6**, 316 (1954). doi:[10.4153/cjm-1954-030-1](https://doi.org/10.4153/cjm-1954-030-1)
54. Z. Xie, B.J. Braams, J.M. Bowman, J. Chem. Phys. **122**(22), 224307 (2005). doi:[10.1063/1.1927529](https://doi.org/10.1063/1.1927529)
55. K. Park, J.C. Light, J. Chem. Phys. **126**(4), 044305 (2007). doi:[10.1063/1.2430711](https://doi.org/10.1063/1.2430711)
56. E. Hugo, O. Asvany, S. Schlemmer, J. Chem. Phys. **130**(16), 164302 (2009). doi:[10.1063/1.3089422](https://doi.org/10.1063/1.3089422)
57. K.N. Crabtree, B.A. Tom, B.J. McCall, J. Chem. Phys. **134**(19), 194310 (2011). doi:[10.1063/1.3587245](https://doi.org/10.1063/1.3587245)
58. K.N. Crabtree, C.A. Kauffman, B.A. Tom, E. Becka, B.A. McGuire, B.J. McCall, J. Chem. Phys. **134**(19), 194311 (2011). doi:[10.1063/1.3587246](https://doi.org/10.1063/1.3587246)
59. S. Gómez-Carrasco, L. González-Sánchez, A. Aguado, C. Sanz-Sanz, A. Zanchet, O. Roncero, J. Chem. Phys. **137**(9), 094303 (2012). doi:[10.1063/1.4747548](https://doi.org/10.1063/1.4747548)
60. C. Fábri, J. Sarka, A.G. Császár, J. Chem. Phys. **140**(5), 051101 (2014). doi:[10.1063/1.4864360](https://doi.org/10.1063/1.4864360)
61. Z. Lin, A.B. McCoy, J. Phys. Chem. A **119**(50), 12109 (2015). doi:[10.1021/acs.jpca.5b05774](https://doi.org/10.1021/acs.jpca.5b05774)
62. Z. Lin, J. Mol. Spectrosc. **324**, 36 (2016). doi:[10.1016/j.jms.2016.04.007](https://doi.org/10.1016/j.jms.2016.04.007)
63. G. Frobenius, Sber. preuss. Akad. Wiss, 501–515 (1889)
64. M. Hamermesh, *Group Theory and Its Application to Physical Problems* (Reading, Addison-Wesley Series in Physics (Addison-Wesley, 1962)
65. D. Gerlich, J. Chem. Phys. **92**(4), 2377 (1990). doi:[10.1063/1.457980](https://doi.org/10.1063/1.457980)
66. F. Lique, P. Honvault, A. Faure, J. Chem. Phys. **137**(15), 154303 (2012). doi:[10.1063/1.4758791](https://doi.org/10.1063/1.4758791)
67. T.P. Grozdanov, R. McCarroll, J. Phys. Chem. A **116**(18), 4569 (2012). doi:[10.1021/jp210992g](https://doi.org/10.1021/jp210992g)
68. J. Sarka, A.G. Császár, J. Chem. Phys. **144**(15), 154309 (2016). doi:[10.1063/1.4946808](https://doi.org/10.1063/1.4946808)
69. L. Kluge, S. Gartner, S. Brunken, O. Asvany, D. Gerlich, S. Schlemmer, Philos. Trans. R. Soc. A: Math. Phys. Eng. Sci. **370**(1978), 5041 (2012). doi:[10.1098/rsta.2012.0170](https://doi.org/10.1098/rsta.2012.0170)
70. I. Kleiner, J. Mol. Spectrosc. **260**(1), 1 (2010). doi:[10.1016/j.jms.2009.12.011](https://doi.org/10.1016/j.jms.2009.12.011)
71. M. Schnell, U. Erlekam, P.R. Bunker, G. von Helden, J.U. Grabow, G. Meijer, A. van der Avoird, Phys. Chem. Chem. Phys. **15**(25), 10207 (2013). doi:[10.1039/c3cp51181b](https://doi.org/10.1039/c3cp51181b)
72. Z. Bacic, J.C. Light, Ann. Rev. Phys. Chem. **40**(1), 469 (1989). doi:[10.1146/annurev.pc.40.100189.002345](https://doi.org/10.1146/annurev.pc.40.100189.002345)
73. R. Wodraszka, U. Manthe, J. Phys. Chem. Lett. **6**(21), 4229 (2015). doi:[10.1021/acs.jpclett.5b01869](https://doi.org/10.1021/acs.jpclett.5b01869)
74. J.O. Richardson, C. Perez, S. Lobsiger, A.A. Reid, B. Temelso, G.C. Shields, Z. Kisiel, D.J. Wales, B.H. Pate, S.C. Althorpe, Science **351**(6279), 1310 (2016). doi:[10.1126/science.aae0012](https://doi.org/10.1126/science.aae0012)
75. A.C. Legon, Chem. Rev. **80**(3), 231 (1980). doi:[10.1021/cr60325a002](https://doi.org/10.1021/cr60325a002)
76. R.J. Saykally, Science **239**(4836), 157 (1988). doi:[10.1126/science.239.4836.157](https://doi.org/10.1126/science.239.4836.157)
77. E.T. White, Science **284**(5411), 135 (1999). doi:[10.1126/science.284.5411.135](https://doi.org/10.1126/science.284.5411.135)
78. O. Asvany, Science **309**(5738), 1219 (2005). doi:[10.1126/science.1113729](https://doi.org/10.1126/science.1113729)

79. G.A. Olah, N. Hartz, G. Rasul, G.K.S. Prakash, J. Am. Chem. Soc. **117**(4), 1336 (1995). doi:[10.1021/ja00109a018](https://doi.org/10.1021/ja00109a018)
80. P.R. Bunker, B. Ostojić, S. Yurchenko, J. Mol. Struct. **695–696**, 253 (2004). doi:[10.1016/j.molstruc.2003.12.020](https://doi.org/10.1016/j.molstruc.2003.12.020)
81. L.M. Johnson, A.B. McCoy, J. Phys. Chem. A **110**(26), 8213 (2006). doi:[10.1021/jp061675c](https://doi.org/10.1021/jp061675c)
82. A.L.L. East, M. Kolbuszewski, P.R. Bunker, J. Phys. Chem. A **101**(36), 6746 (1997). doi:[10.1021/jp9704628](https://doi.org/10.1021/jp9704628)
83. Z. Jin, B.J. Braams, J.M. Bowman, J. Phys. Chem. A **110**(4), 1569 (2006). doi:[10.1021/jp0538480](https://doi.org/10.1021/jp0538480)
84. E.J. Weinberg, *Classical Solutions in Quantum Field Theory: Solitons and Instantons in High Energy Physics*, online edn. Cambridge monographs on mathematical physics (Cambridge University Press, Cambridge, UK, 2012), <http://lib.myilibrary.com/detail.asp?id=395091>
85. S.A. Williams, N. Kemmer, S.A. Williams, J. Math. Phys. **9**(8), 1230 (1968). doi:[10.1063/1.1664704](https://doi.org/10.1063/1.1664704)
86. R. Gilmore, *Lie Groups, Physics, and Geometry: An Introduction for Physicists, Engineers and Chemists* (Cambridge University Press, 2008), <https://books.google.de/books?id=MHExMkMFzvcC>
87. L.D. Landau, E.M. Lifšic, *Course of Theoretical Physics*, vol. 3, 3rd edn. (Butterworth-Heinemann, Oxford, 1998)
88. T. Damhus, MATCH Commun. Math. Comput. Chem. **16**, 21 (1984)
89. P.R. Bunker, P. Jensen, Mol. Phys. **97**(1–2), 255 (1999). doi:[10.1080/00268979909482827](https://doi.org/10.1080/00268979909482827)
90. P.R. Bunker, P. Jensen, *Fundamentals of Molecular Symmetry*. Series in Chemical Physics (Taylor & Francis, 2004), [http://books.google.de/books?id=jhIrUtaNiwC](https://books.google.de/books?id=jhIrUtaNiwC)
91. D. Samaila, IOSR J. Math. **8**(3), 87 (2013). doi:[10.9790/5728-0838793](https://doi.org/10.9790/5728-0838793)
92. X.G. Wang, T. Carrington, J. Chem. Phys. **129**(23), 234102 (2008). doi:[10.1063/1.3027825](https://doi.org/10.1063/1.3027825)
93. É. Mathieu, J. de Mathématiques Pures et Appliquées, 137–203 (1868), <http://eudml.org/doc/234720>
94. X. Wang, S. Carter, J.M. Bowman, J. Phys. Chem. A **119**(47), 11632 (2015). doi:[10.1021/acs.jpca.5b09816](https://doi.org/10.1021/acs.jpca.5b09816)
95. E. Tannenbaum, R.J. Myers, W.D. Gwinn, J. Chem. Phys. **25**(1), 42 (1956). doi:[10.1063/1.1742845](https://doi.org/10.1063/1.1742845)
96. F. Rohart, J. Mol. Spectrosc. **57**(2), 301 (1975). doi:[10.1016/0022-2852\(75\)90033-8](https://doi.org/10.1016/0022-2852(75)90033-8)
97. L. Dore, R.C. Cohen, C.A. Schmuttenmaer, K.L. Busarow, M.J. Elrod, J.G. Loeser, R.J. Saykally, J. Chem. Phys. **100**(2), 863 (1994). doi:[10.1063/1.466569](https://doi.org/10.1063/1.466569), <http://www.scopus.com/scopus/inward/record.url?eid=2-s2.0-0001426292&partnerID=40>
98. S.C. Zhang, Science **294**(5543), 823 (2001). doi:[10.1126/science.294.5543.823](https://doi.org/10.1126/science.294.5543.823)
99. D. Rowe, Prog. Particle Nuclear Phys. **37**, 265 (1996). doi:[10.1016/0146-6410\(96\)00058-0](https://doi.org/10.1016/0146-6410(96)00058-0)
100. J. Jolie, R.F. Casten, Nuclear Phys. News **15**(1), 20 (2005). doi:[10.1080/10506890500454584](https://doi.org/10.1080/10506890500454584)
101. A. Frank, P. Van Isacker, J. Jolie, Symmetries in atomic nuclei, in Springer Tracts in Modern Physics (Springer, New York (2009)). doi:[10.1007/978-0-387-87495-1](https://doi.org/10.1007/978-0-387-87495-1)
102. L. Wilets, M. Jean, Phys. Rev. **102**(3), 788 (1956). doi:[10.1103/PhysRev.102.788](https://doi.org/10.1103/PhysRev.102.788)
103. H. De Meyer, G. Vandén, J. Van Berghe, P. der Jeugt, De Wilde, J. Math. Phys. **26**(5), 2124 (1985). doi:[10.1063/1.526834](https://doi.org/10.1063/1.526834)
104. D.J. Rowe, Nuclear. Phys. A **735**(3–4), 372 (2004). doi:[10.1016/j.nuclphysa.2004.02.018](https://doi.org/10.1016/j.nuclphysa.2004.02.018)
105. P.S. Turner, D.J. Rowe, Nuclear. Phys. A **756**(3–4), 333 (2005). doi:[10.1016/j.nuclphysa.2005.04.003](https://doi.org/10.1016/j.nuclphysa.2005.04.003)
106. N. Kemmer, J. Math. Phys. **9**(8), 1224 (1968). doi:[10.1063/1.1664703](https://doi.org/10.1063/1.1664703)
107. N. Pietralla, P. von Brentano, A. Gelberg, T. Otsuka, A. Richter, N. Smirnova, I. Wiedenhöver, Phys. Rev. C **58**(1), 191 (1998). doi:[10.1103/physrevc.58.191](https://doi.org/10.1103/physrevc.58.191)
108. A.B. Balantekin, P. Cassak, J. Math. Phys. **43**(1), 604 (2002). doi:[10.1063/1.1418014](https://doi.org/10.1063/1.1418014)
109. X. Huang, Science **311**(5757), 60 (2006). doi:[10.1126/science.1121166](https://doi.org/10.1126/science.1121166)
110. P. Kumar, D. Marx, Phys. Chem. Chem. Phys. **8**(5), 573 (2006). doi:[10.1039/b513089c](https://doi.org/10.1039/b513089c)
111. V. Tal’roze, A. Lyubimova, Dokl. Akad. Nauk. SSSR **86**, 909 (1952)

112. A.S. Petit, J.E. Ford, A.B. McCoy, *J. Phys. Chem. A* **118**(35), 7206 (2014). doi:[10.1021/jp408821a](https://doi.org/10.1021/jp408821a)
113. O. Asvany, J. Krieg, S. Schlemmer, *Rev. Sci. Instr.* **83**, 093110 (2012)
114. M. Schnell, P.R. Bunker, G. von Helden, J.U. Grabow, G. Meijer, A. van der Avoird, *J. Phys. Chem. A* **117**(50), 13775 (2013). doi:[10.1021/jp408076q](https://doi.org/10.1021/jp408076q)
115. S.C. Zhang, *Science* **275**(5303), 1089 (1997). doi:[10.1126/science.275.5303.1089](https://doi.org/10.1126/science.275.5303.1089)
116. A. Yachmenev, S.N. Yurchenko, *J. Chem. Phys.* **143**(1), 014105 (2015). doi:[10.1063/1.4923039](https://doi.org/10.1063/1.4923039)
117. S. Carter, N. Handy, *Comput. Phys. Commun.* **51**(1–2), 49 (1988). doi:[10.1016/0010-4655\(88\)90061-6](https://doi.org/10.1016/0010-4655(88)90061-6)
118. M.J. Bramley, N.C. Handy, *J. Chem. Phys.* **98**(2), 1378 (1993). doi:[10.1063/1.464305](https://doi.org/10.1063/1.464305)
119. M.H. Beck, A. Jäckle, G.A. Worth, H.D. Meyer, *Phys. Rep.* **324**(1), 1 (2000). doi:[10.1016/S0370-1573\(99\)00047-2](https://doi.org/10.1016/S0370-1573(99)00047-2)
120. H.D. Meyer, G.A. Worth, *Theor. Chem. Acc.* **109**(5), 251 (2003). doi:[10.1007/s00214-003-0439-1](https://doi.org/10.1007/s00214-003-0439-1)
121. J.K. Cullum, R.A. Willoughby, *Lanczos Algorithms for Large Symmetric Eigenvalue Computations*, vol. 1 (Society for Industrial and Applied Mathematics, 2002). doi:[10.1137/1.9780898719192](https://doi.org/10.1137/1.9780898719192)
122. D. Neuhauser, *J. Chem. Phys.* **93**(4), 2611 (1990). doi:[10.1063/1.458900](https://doi.org/10.1063/1.458900)
123. V.A. Mandelshtam, H.S. Taylor, *J. Chem. Phys.* **102**(19), 7390 (1995). doi:[10.1063/1.469051](https://doi.org/10.1063/1.469051)
124. S.W. Huang, T. Carrington, *Chem. Phys. Lett.* **312**(2–4), 311 (1999). doi:[10.1016/S0009-2614\(99\)00889-1](https://doi.org/10.1016/S0009-2614(99)00889-1)
125. D.M. Villeneuve, S.A. Aseyev, P. Dietrich, M. Spanner, M.Y. Ivanov, P.B. Corkum, *Phys. Rev. Lett.* **85**(3), 542 (2000). doi:[10.1103/PhysRevLett.85.542](https://doi.org/10.1103/PhysRevLett.85.542)
126. R. Hasbani, B. Ostojić, P.R. Bunker, M.Yu. Ivanov, *J. Chem. Phys.* **116**(24), 10636 (2002). doi:[10.1063/1.1478696](https://doi.org/10.1063/1.1478696)
127. R. Forrey, N. Balakrishnan, A. Dalgarno, M. Haggerty, E. Heller, *Phys. Rev. Lett.* **82**(13), 2657 (1999). doi:[10.1103/PhysRevLett.82.2657](https://doi.org/10.1103/PhysRevLett.82.2657)
128. R. Forrey, N. Balakrishnan, A. Dalgarno, M. Haggerty, E. Heller, *Phys. Rev. A* **64**(2), 1 (2001). doi:[10.1103/PhysRevA.64.022706](https://doi.org/10.1103/PhysRevA.64.022706)
129. K. Tilford, M. Hoster, P.M. Florian, R.C. Forrey, *Phys. Rev. A* **69**(5), 052705 (2004). doi:[10.1103/PhysRevA.69.052705](https://doi.org/10.1103/PhysRevA.69.052705)
130. U. Steinitz, Y. Prior, I.S. Averbukh, *Phys. Rev. Lett.* **109**(3), 033001 (2012). doi:[10.1103/PhysRevLett.109.033001](https://doi.org/10.1103/PhysRevLett.109.033001)
131. R.C. Forrey, *Phys. Rev. A* **63**(5), 051403 (2001). doi:[10.1103/PhysRevA.63.051403](https://doi.org/10.1103/PhysRevA.63.051403)
132. R.C. Forrey, *Phys. Rev. A* **66**, 23411 (2002). doi:[10.1103/PhysRevA.66.023411](https://doi.org/10.1103/PhysRevA.66.023411)
133. J. Karczmarek, J. Wright, P. Corkum, M. Ivanov, *Phys. Rev. Lett.* **82**(17), 3420 (1999). doi:[10.1103/PhysRevLett.82.3420](https://doi.org/10.1103/PhysRevLett.82.3420)
134. W.G. Harter, C.W. Patterson, *Phys. Rev. Lett.* **38**(5), 224 (1977). doi:[10.1103/PhysRevLett.38.224](https://doi.org/10.1103/PhysRevLett.38.224)
135. W.G. Harter, C.W. Patterson, *J. Chem. Phys.* **66**(11), 4872 (1977). doi:[10.1063/1.433825](https://doi.org/10.1063/1.433825)
136. W.G. Harter, C.W. Patterson, *J. Chem. Phys.* **80**(9), 4241 (1984). doi:[10.1063/1.447255](https://doi.org/10.1063/1.447255)
137. S.D.S. Augustin, W. Miller, *J. Chem. Phys.* **61**(8), 3155 (1974). doi:[10.1063/1.1682471](https://doi.org/10.1063/1.1682471)
138. S.M. Colwell, N.C. Handy, W.H. Miller, *J. Chem. Phys.* **68**(2), 745 (1978). doi:[10.1063/1.435747](https://doi.org/10.1063/1.435747)
139. J.M. Robbins, S.C. Creagh, R.G. Littlejohn, *Phys. Rev. A* **39**(6), 2838 (1989). doi:[10.1103/PhysRevA.39.2838](https://doi.org/10.1103/PhysRevA.39.2838)
140. B.I. Zhilinskii, B. Zhilinskií, *Phys. Rep.* **341**(1–6), 85 (2001). doi:[10.1016/S0370-1573\(00\)00089-2](https://doi.org/10.1016/S0370-1573(00)00089-2)
141. A. Faure, L. Wiesenfeld, *J. Chem. Phys.* **121**(14), 6771 (2004). doi:[10.1063/1.1792613](https://doi.org/10.1063/1.1792613)
142. D.A. Sadovskii, B.I. Zhilinskii, J.P. Champion, G. Pierre, *J. Chem. Phys.* **92**(3), 1523 (1990). doi:[10.1063/1.458083](https://doi.org/10.1063/1.458083)
143. V. Krivtsun, D. Sadovskii, B. Zhilinskii, *J. Mol. Spectrosc.* **139**(1), 126 (1990). doi:[10.1016/0022-2852\(90\)90246-M](https://doi.org/10.1016/0022-2852(90)90246-M)

144. I. Pavlichenkov, B. Zhilinskii, Ann. Phys. **184**(1), 1 (1988). doi:[10.1016/0003-4916\(88\)90268-0](https://doi.org/10.1016/0003-4916(88)90268-0)
145. I. Kozin, P. Jensen, J. Mol. Spectrosc. **161**(1), 186 (1993). doi:[10.1006/jmsp.1993.1226](https://doi.org/10.1006/jmsp.1993.1226), <http://linkinghub.elsevier.com/retrieve/pii/S0022285283712269>
146. I. Kozin, S. Belov, O. Polyansky, M. Tretyakov, J. Mol. Spectrosc. **152**(1), 13 (1992). doi:[10.1016/0022-2852\(92\)90112-2](https://doi.org/10.1016/0022-2852(92)90112-2)
147. J.M. Bowman, S. Carter, X. Huang, Int. Rev. Phys. Chem. **22**(3), 533 (2003). doi:[10.1080/0144235031000124163](https://doi.org/10.1080/0144235031000124163)
148. E. Mátyus, G. Czakó, A.G. Császár, J. Chem. Phys. **130**(13), 134112 (2009). doi:[10.1063/1.3076742](https://doi.org/10.1063/1.3076742)
149. O.L. Polyansky, I.N. Kozin, R.I. Ovsyannikov, P. Małyszek, J. Koput, J. Tennyson, S.N. Yurchenko, J. Phys. Chem. A **117**(32), 7367 (2013). doi:[10.1021/jp401216g](https://doi.org/10.1021/jp401216g)
150. A. Altland, B.D. Simons, *Condensed Matter Field Theory*. Cambridge books online (Cambridge University Press, 2010), <http://books.google.de/books?id=GpF0Pgo8CqAC>
151. H.J. Stöckmann, *Quantum Chaos - An introduction*, repr. edn. (Cambridge University Press, Cambridge, 2000), www.cambridge.org/9780521592840
152. M.C. Gutzwiller, J. Math. Phys. **12**(3), 343 (1971). doi:[10.1063/1.1665596](https://doi.org/10.1063/1.1665596)
153. S.C. Creagh, J. Phys. A: Math. General **26**(1), 95 (1993). doi:[10.1088/0305-4470/26/1/013](https://doi.org/10.1088/0305-4470/26/1/013), <http://stacks.iop.org/0305-4470/26/i=1/a=013?key=crossref.d656defcff6affd4613d601d7a4ea017>
154. J.M. Robbins, Phys. Rev. A **40**(4), 2128 (1989). doi:[10.1103/PhysRevA.40.2128](https://doi.org/10.1103/PhysRevA.40.2128)
155. N. Bohr, Zeitschrift für Physik **2**(5), 423 (1920). doi:[10.1007/BF01329978](https://doi.org/10.1007/BF01329978)
156. I. Pavlichenkov, B. Zhilinskii, Chem. Phys. **100**(3), 339 (1985). doi:[10.1016/0301-0104\(85\)87060-9](https://doi.org/10.1016/0301-0104(85)87060-9)
157. S.V. Petrov, B.M. Kozlovskii, J. Mol. Spectrosc. **243**(2), 245 (2007). doi:[10.1016/j.jms.2007.04.001](https://doi.org/10.1016/j.jms.2007.04.001)
158. S.N. Yurchenko, R.I. Ovsyannikov, W. Thiel, P. Jensen, J. Mol. Spectrosc. **256**(1), 119 (2009). doi:[10.1016/j.jms.2009.03.001](https://doi.org/10.1016/j.jms.2009.03.001)
159. J.H. Frederick, G.M. McClelland, J. Chem. Phys. **84**(2), 876 (1986). doi:[10.1063/1.450533](https://doi.org/10.1063/1.450533), <http://scitation.aip.org/content/aip/journal/jcp/84/2/10.1063/1.450533>
160. M.V. Berry, K.E. Mount, Rep. Prog. Phys. **35**(1), 315 (1972). doi:[10.1088/0034-4885/35/1/306](https://doi.org/10.1088/0034-4885/35/1/306)
161. H.S.P. Müller, S. Brünken, J. Mol. Spectrosc. **232**(2), 213 (2005). doi:[10.1016/j.jms.2005.04.010](https://doi.org/10.1016/j.jms.2005.04.010)
162. X. Huang, D.W. Schwenke, T.J. Lee, J. Chem. Phys. **140**, 114311 (2014). doi:[10.1063/1.4868327](https://doi.org/10.1063/1.4868327)
163. H.S. Müller, F. Schlöder, J. Stutzki, G. Winnewisser, J. Mol. Struct. **742**(1), 215 (2005). doi:[10.1016/j.molstruc.2005.01.027](https://doi.org/10.1016/j.molstruc.2005.01.027)
164. S.N. Yurchenko, Private communications (2015)
165. S.N. Yurchenko, W. Thiel, P. Jensen, J. Mol. Spectrosc. **240**(2), 174 (2006). doi:[10.1016/j.jms.2006.10.002](https://doi.org/10.1016/j.jms.2006.10.002)

Index

A

Action, 131
Action spectroscopy, 109
Angular momentum, 13, 32, 72, 137
 conservation, 137
 super-, 92

B

Ball-and-stick model, 4, 67, 87, 120
Barrier height, 88, 90
Bending vibration, 150
Benzene dimer, 122
Born-Oppenheimer approximation, 19, 67
Branching rule, 35, 98, 99, 122

C

Casimir operator, 72
 fourth order, 120
SO(2), 89
SO(3), 74
SO(5), 76
U(1), 88
Combination differences, 110, 114
Correlation diagram, 118

D

Density of states, 132
 symmetry projected, 135, 142
Deuterons, 60

E

Equations of motion, 131, 136
Equivalent rotations, 69, 81, 84, 102, 142
Euler angles, 136
Extremely floppy molecules, 4, 68, 91, 121, 160

F

Frobenius reciprocity theorem, 47, 54, 57

G

Green function, 129
Gutzwiller trace formula, 132

H

Hamilton extremal principle, 131
Hamiltonian
 effective, 24, 128, 155
 Watson, 146, 150
Hook length, 38

L

Ladder operator, 73
Lagrangian, 131
Large amplitude motion, 67–69, 87
Lie algebra, 14, 72
Lie group, 14, 72

M

Magnetic quantum number, 76

- Maslov index, 141
 Molecular hydrogen, 46, 49
 Molecular symmetry, 5
 Moments of inertia
 generalized, 93, 118
- N**
 Nitromethane, 87, 107
 Nuclear degrees of freedom, 21, 94
- O**
 Ortho-to-para conversion, 52, 53, 56, 58, 59
- P**
 Parity, 99, 105
 five-dimensional, 100
 Partition, 35
 Path integral, 128–130, 160
 Pauli principle, 28, 31, 33, 45, 108, 150
 Permutation group, 16, 37, 41, 83, 85, 86, 101, 103, 105
 G_{240} , 108, 109
 S_5 , 109, 112
 Permutation group complete nuclear permutation inversion group, 76
 Perturbation theory, 18, 144
 Potential energy surface, 19, 56
 protonated methane, 107
 Projection operator, 73, 134
 Propagator, 129
 Protonated methane, 68, 83, 85, 91, 101, 107, 159
- Q**
 Quadrupole degrees of freedom, 95
 Quantization conditions, 134, 142, 151
- R**
 Rate equation, 45
 Reaction path, 46, 48, 49
 Reactive collisions, 30, 41, 51
 Reflection amplitude, 140
 Representation, 12
 character, 13
 character, $\text{SO}(5)$, 103
 dimension, 38
 dimension, $\text{SO}(5)$, 103
 induced, 47
 irreducible, 12, 25, 73, 134
- subduced, 47
 tensor product, 36
 Root vector, 73, 74
- Rotation group
 internal, 90
 overall, 90
 $\text{SO}(2n+1)$, 73
 $\text{SO}(3)$, 13, 32, 43, 68, 71, 74
 $\text{SO}(5)$, 74, 86, 92, 95, 105
 Rotational clustering, 128, 138, 156
 Rotational energy multi-surface, 157
 Rotational energy surface, 128, 137, 146, 153, 155, 160
- S**
 Schur-Weyl duality, 5, 29, 40, 41, 49, 60, 159
 Selection rules, 5, 46, 100, 111, 116
 Semi-classical approach, 128
 Seniority, 96
 Special unitary group $\text{SU}(2)$, 79
 Spectroscopic parameters, 149
 Spherical harmonics, 76, 97
 generalized, 96, 98
 State-to-state reaction rate, 53, 59, 63
 State-to-state transitions, 51, 52, 61
 Stationary phase approximation, 132
 Sulfur dioxide, SO_2 , 149
 Super-rotation, 4, 69
 Super-rotor, 95, 116, 117, 160
 energies, 93, 111
 states, 96, 100, 103, 105
 symmetry, 92
 Symmetry group, 11
- T**
 Thermal equilibrium, 30
 Three-center-two-electron bond, 107
 Transition amplitude, 140
 TROVE, 128, 145, 153, 155
 Tunneling paths, 140
 22-pole ion trap, 109
- U**
 Ultrafast rotations, 5
 Unitary group, 35, 41, 60, 64
- V**
 Variational approach, 19, 24, 26, 128, 145

W

Weight highest, 15, 35, 73, 76

Weights

spin-statistical, 5, 28, 32, 45, 51, 52, 62,
111

Wick rotation, 140

Wigner-D matrix, 33, 97

Wilets-Jeans model, 96, 120

Y

Young tableaux, 29, 36

Z

Zero-order model, 68, 69, 117